

**CHARACTERISATION OF HUMAN
SINGLE-STRANDED DNA-BINDING
PROTEIN 1 (hSSB1) REGULATION
BY POST-TRANSLATIONAL
MODIFICATIONS**

Nicholas William Ashton

BAppSc, BBiomedSc (Hons)

Submitted in fulfilment of the requirements for the degree of
Doctor of Philosophy

School of Biomedical Science
Faculty of Health
Queensland University of Technology
2016

Keywords

Human single-stranded DNA-binding protein 1 (hSSB1), nucleic acid-binding protein 2 (NABP2), OB-fold containing protein 2B (OBFC2B), sensor of single-stranded DNA complex subunit B (SOSS-B1), ubiquitination, replication stress, homologous recombination, phosphorylation, DNA-dependent protein kinase (DNA-PK), PPP-family protein phosphatases, integrator complex subunit 3 (INTS3), chromatin remodelling

Abstract

Genome stability is a central aspect of cellular homeostasis and is facilitated by numerous protein networks that repair DNA damage and maintain chromosomal integrity. Human single-stranded DNA-binding protein 1 (hSSB1) is a protein with known roles in the repair of double-strand DNA breaks and oxidative lesions, as well as the stabilisation and restart of stalled replication forks. In response to these insults, hSSB1 associates with chromatin to promote cell cycle checkpoint signalling, as well as the localisation of other proteins directly required for DNA repair. The physiological relevance of these roles is highlighted by the hypersensitivity of hSSB1-depleted cells to DNA damaging agents, including ionising radiation, oxidative compounds and the chemotherapeutics camptothecin and hydroxyurea.

The detection of damaged DNA by hSSB1 is facilitated by its evolutionarily conserved oligonucleotide/oligosaccharide-binding fold, which may bind directly to single-stranded DNA exposed at sites of DNA damage, as well as to poly ADP-ribose and double-stranded DNA containing oxidised guanine nucleotides. In addition, functionality of hSSB1 most likely requires association with other components of the sensor of single-stranded DNA protein complex.

Previous studies have indicated that hSSB1 may also be regulated by post-translational modifications. This includes phosphorylation of threonine residue 117, which may promote DNA repair signalling in response to double-strand DNA-break formation. In addition, hSSB1 may be degraded by poly-ubiquitination mediated targeting to the proteasome. Acetylation of hSSB1 lysine 94 has also recently been characterised and may promote hSSB1 protein accumulation following DNA damage. In this project, the characterisation of hSSB1 post-translational modifications was further explored with the aim of uncovering novel regulatory mechanisms.

In the first results chapter of this thesis, the poly-ubiquitination of hSSB1 was demonstrated by a nickel agarose pull-down of hexa-histidine-tagged ubiquitin, followed by immunoblotting of eluted proteins. As likely residues of ubiquitination

were initially unclear, site-directed mutagenesis was used to prepare hSSB1 constructs where each lysine residue was individually mutated to arginine. The disruption of no single lysine residue could however prevent hSSB1 ubiquitination and so further constructs were prepared containing multiple lysine to arginine mutations. Only the complete removal of lysine residues was however able to prevent ubiquitination of exogenously expressed 3x FLAG hSSB1, suggesting that each lysine residue of the protein may be ubiquitinated. Indeed, even the 3x FLAG epitope tag was found to be ubiquitinated under conditions where all other lysine residues were disrupted. As part of this work, mass spectrometry was also employed to analyse immunoprecipitated hSSB1 from cells treated with or without the replication inhibitor, hydroxyurea. In doing so, numerous potentially phosphorylated serine and threonine residues were detected, including serine residue 134 (S134).

The phosphorylation of hSSB1 S134 was further explored in the second data chapter and included the validation of a novel phospho-specific antibody, raised against a phosphorylated S134 peptide. Using this antibody, phosphorylation of immunoprecipitated endogenous hSSB1 was observed, as well as of transiently over-expressed hSSB1, which was enhanced following hydroxyurea treatment. Specificity of the antibody was confirmed by expression of a S134A phosphomutant, treatment of whole cell lysates with lambda phosphatase and by use of a phosphorylated peptide to block antigen recognition by the antibody. Phosphorylation of hSSB1 S134 was also observed following replication inhibition with aphidicolin and camptothecin. An increase in hSSB1 S134 phosphorylation was however not observed following ionising radiation exposure and the formation of double-strand DNA breaks. The functional importance of hSSB1 S134 phosphorylation was demonstrated by the inability of exogenously expressed S134A hSSB1 to rescue cells from the hydroxyurea and aphidicolin sensitivity caused by hSSB1 depletion, as assessed by clonogenic survival assays.

hSSB1 S134 is part of a serine-glutamine (SQ) motif, a common substrate of the major DNA repair PI3K-like kinases, ataxia telangiectasia mutated (ATM), ataxia telangiectasia and Rad3 related (ATR) and DNA-dependent protein kinase (DNA-PK). To explore if one of these kinases may phosphorylate S134, specific chemical inhibitors against each enzyme were employed. Although the inhibition of ATM and

ATR caused a small decrease in phosphorylation of hSSB1, this was almost completely reduced following inhibition of DNA-PK. In addition, an ~90% reduction in S134 phosphorylation was observed following depletion of the DNA-PK catalytic subunit (DNA-PKcs) from cells. DNA-PKcs also co-immunoprecipitated with hSSB1 from whole cell lysates and purified DNA-PK was able to phosphorylate hSSB1 S134 *in vitro*.

As PPP-family serine/threonine protein phosphatases are involved in the dephosphorylation of numerous DNA damage repair proteins, cells were also treated with chemical inhibitors against these proteins and their effect on hSSB1 S134 phosphorylation assessed. Strikingly, the inhibition of these enzymes resulted in a dramatic increase in S134 phosphorylation within minutes of treatment, which was comparable with 20 hours of hydroxyurea exposure. Phosphatase inhibitor induced phosphorylation was however predominantly suppressed by the co-inhibition of DNA-PK. Together these data suggest that in undamaged cells, S134 phosphorylation is dynamically regulated by DNA-PK and PPP-family phosphatases.

hSSB1 has previously been suggested to associate with stalled replication forks. It was therefore interesting to consider that S134 phosphorylation may alter hSSB1 binding to such substrates. To test this, electrophoretic mobility shift assays were performed using WT or S134E phosphomimetic hSSB1 and either ssDNA or a fork junction substrate. While WT and S134E hSSB1 bound ssDNA similarly, a significant reduction in fork junction binding was observed for the S134E mutant. These data therefore suggest that S134 phosphorylation may regulate the DNA-binding function of hSSB1.

Despite these advancements in understanding the regulation of hSSB1 following replication inhibition, the role of hSSB1 at sites of stalled replication forks remains unclear. To further elucidate these functions, mass spectrometry was used to detect proteins that may associate with chromatin-bound hSSB1. Unexpectedly, numerous chromatin-remodelling complexes were identified, including each component of the NuRD and WICH remodelling complexes. The detection of numerous of these components was further validated by immunoblotting of hSSB1-associating proteins.

The data presented in this thesis provide novel insight into the regulation of hSSB1 by post-translational modifications, as well as suggest a number of additional proteins with which hSSB1 may associate. These findings thereby contribute to a greater understanding of hSSB1 biology, the continued characterisation of which will be important for a full understanding of eukaryotic genome stability maintenance.

Table of Contents

Keywords.....	i
Abstract.....	ii
Table of Contents	v
List of Figures.....	viii
List of Tables.....	i
List of Abbreviations.....	i
Statement of Original Authorship	vi
Publications	vii
Acknowledgements	ix
Chapter 1: Introduction, Literature Review and Contextualisation of the Research Project.....	11
1.1 Genomic stability.....	11
1.2 Oxidative base excision repair.....	11
1.3 DNA replication and replication stress.....	16
1.3.1 Stabilisation and restart of uncoupled replication forks.....	17
1.4 Double-strand DNA break repair	21
1.4.1 Repair of double-strand DNA breaks by homologous recombination.....	21
1.5 Human single-stranded DNA-binding protein 1 (hSSB1).....	28
1.6 Post-translational regulation of hSSB1	30
1.7 Study aims	32
Chapter 2: Materials and Methods.....	33
2.1 <i>E. coli</i> strains and preparation of chemically competent cells	33
2.2 Plasmids and site-directed mutagenesis	34
2.3 Cell culture reagents, cell lines and transfections	39
2.4 Induction of genotoxic stress and other cell treatments	40
2.5 Clonogenic survival assays and statistical analysis.....	41
2.6 Preparation of whole cell lysates, polyacrylamide gel electrophoresis (PAGE) and immunoblotting	42
2.7 Immunoprecipitation	46
2.8 Subcellular fractionation	47
2.9 Mass spectrometry and data analysis	47
2.10 Poly-ubiquitination assay using hexa-His-tagged ubiquitin.....	49
2.11 Protein purification.....	50
2.12 <i>In vitro</i> DNA-PK kinase assays.....	51
2.13 One dimensional nuclear magnetic resonance spectroscopy (1D-NMR).....	51
2.14 Electrophoretic mobility shift assays (EMSA).....	51

2.15 pS/T-Reader protein domain array.....	52
Chapter 3: Identification of hSSB1 Post-Translational Modifications	53
3.1 Introduction.....	53
3.2 Results.....	56
3.2.1 Poly-ubiquitinated hSSB1 may be detected following nickel agarose pull-down of hexa-histidine tagged ubiquitin	56
3.2.2 The disruption of hSSB1 poly-ubiquitination requires the complete removal of lysine residues.....	60
3.2.3 The N-terminal 3x FLAG tag of hSSB1 may be modified.....	65
3.2.4 Mass spectrometric analysis of immunoprecipitated 3x FLAG hSSB1	69
3.4 Discussion.....	76
Chapter 4: Regulation of hSSB1 in the Response to Replication Stress	81
4.1 Introduction.....	81
4.2 Results.....	84
4.2.1 Detection of phosphorylated hSSB1 by mass spectrometry.....	84
4.2.2 S134A hSSB1 is unable to rescue cells from the hydroxyurea and aphidicolin-sensitivity caused by hSSB1 depletion	87
4.2.3 hSSB1 is phosphorylated at serine residue 134 (S134).....	92
4.2.4 hSSB1 S134 phosphorylation is mediated by the DNA-dependent protein kinase.....	98
4.2.5 hSSB1 S134 may not be phosphorylated in response to double-strand DNA break formation.....	103
4.2.6 S134 hSSB1 is suppressed by PPP-family protein phosphatases.....	107
4.2.7 Enzymatic regulation of hSSB1 phosphorylation is mediated similarly in HeLa and U-2 OS cells.....	113
4.2.8 hSSB1 may be phosphorylated at S134 independently of PAR- or DNA-binding.....	117
4.2.9 hSSB1-INTS3 binding promotes clonogenic survival of cells in response to replication stress.....	121
4.2.10 A phosphorylated S134 peptide does not interact with pS/T reader proteins.....	126
4.2.11 Multiple SQ/TQ motifs are found in the SSB1 C-terminus of animal species.....	131
4.2.12 S134 phosphorylation may not affect hSSB1 protein half-life or poly-ubiquitination.....	135
4.2.13 Phosphorylation of hSSB1 S134 may alter the affinity of hSSB1 for replication fork junctions.....	140
4.2.14 hSSB1 may associate with proteins involved in chromatin remodelling, RNA metabolism, DNA repair and numerous other functions	145
4.4 Discussion.....	153
Chapter 5: General Discussion and Concluding Remarks.....	165
References	173
Appendix A	221

List of Figures

Figure 1.1 hSSB1 post-translational modifications may occur at numerous residues	32
Figure 2.1 Site directed mutagenesis (SDM) approaches described in section 2.2.....	38
Figure 3.1 hSSB1 is poly-ubiquitinated at an unidentified residue.....	59
Figure 3.2 The disruption of hSSB1 poly-ubiquitination requires the complete removal of lysine residues	63
Figure 3.3 The N-terminal FLAG tag may be modified	66
Figure 3.4 Mass spectrometric analysis of immunoprecipitated 3x FLAG hSSB1	72
Figure 4.1 Detection of phosphorylated hSSB1 by mass spectrometry	86
Figure 4.2 Cells expressing S134A hSSB1 are hypersensitive to hydroxyurea and aphidicolin	88
Figure 4.3 hSSB1 serine residue 134 (S134) phosphorylation is enhanced in response to replication stress	95
Figure 4.4 Phosphorylation of hSSB1 S134 is mediated by DNA-PK	100
Figure 4.5 hSSB1 S134 may not be phosphorylated in response to double-strand DNA-break formation.....	105
Figure 4.6 hSSB1 is dephosphorylated by PPP-family protein phosphatases.....	110
Figure 4.7 Enzymatic regulation of hSSB1 phosphorylation is mediated similarly in HeLa and U-2 OS cells	115
Figure 4.8 hSSB1 may be phosphorylated independently of PAR- or DNA-binding.....	120
Figure 4.9 hSSB1-INTS3-binding promotes clonogenic survival of cells in response to replication stress, although may not be required for S134 phosphorylation	123
Figure 4.10 A pS134 peptide does not interact with pS/T reader proteins.....	129
Figure 4.11 Multiple SQ/TQ motifs are found in the SSB1 C-terminus of animal species	133
Figure 4.12 S134 phosphorylation may not affect hSSB1 protein half-life or poly- ubiquitination	139
Figure 4.13 S134 phosphorylation may alter the affinity of hSSB1 for replication fork junctions	143
Figure 4.14 hSSB1 may associate with proteins involved in chromatin remodelling, RNA metabolism, DNA repair and numerous other pathways	148

List of Tables

Table 2.1 Oligonucleotide primers used for site-directed mutagenesis	35
Table 2.2 siRNA oligonucleotides used for gene silencing	40
Table 6.1 Numerous hSSB1-associating proteins were identified by mass spectrometry	221

List of Abbreviations

µg	Microgram
µL	Microlitre
µM	Micromolar
53BP1	p53-binding protein 1
8-OHG	7,8-dihydro-8-hydroxyguanine
8-OxoG	8-oxo-7,8-dihydroguanine
9-1-1	Rad9-Rad1-Hus1
APE1	Apurinic/aprimidinic (AP) endonuclease 1
Aph	Aphidicolin
ATCC	American type culture collection
ATM	Ataxia telangiectasia mutated
ATP	Adenosine triphosphate
ATR	Ataxia telangiectasia and Rad3 related
ATRIP	ATR-interacting protein
BAZ1B	Bromodomain adjacent to zinc finger domain, 1B
BCA	Bicinchoninic acid
BER	Base excision repair
βTrCP	Beta-transducin repeat containing
BLM	Bloom syndrome RecQ like helicase
Bmax	Maximal binding
bp	Base pair
BRCA1	Breast cancer type 1 susceptibility protein
BRCT	Brca1 C-terminal
BSA	Bovine serum albumin
CA	Calyculin A
CDC4	Cell division control protein 4
CDS	Coding sequence
CHK1	Checkpoint kinase 1
CHK2	Checkpoint kinase 2
CHX	Cycloheximide

CI	Confidence interval
CPSF	Cleavage and polyadenylation specificity factor
CPT	Camptothecin
CtIP	CtBP-interacting protein
DMEM	Dublecco's modified eagle medium
DMSO	Dimethylsulfoxide
DNA	Deoxyribonucleic acid
DNA-PK	DNA-dependent protein kinase
DNA-PKcs	DNA-dependent protein kinase catalytic subunit
DSB	Double-strand DNA break
dsDNA	Double-strand DNA
DSS	4,4-dimethyl-4-silapentanesulfonic acid
DTT	Dithiothreitol
DUB	Deubiquitinating enzyme
<i>E. coli</i>	Escherichia coli
EDTA	Ethylenediaminetetraacetic acid
EMSA	Electrophoretic mobility shift assays
ESI	Electrospray ionisation
Exo1	Exonuclease 1
FAM	6-Carboxyfluorescein
FANC	Fanconi anemia group
FapyG	2,6-diamino-5-formamido-4-hydroxy-pyrimidine
FBS	Foetal bovine serum
FBW7	F-box/WD repeat-containing 7
FHA	Forkhead-associated domain
FITC	Flourescein isothiocyanate
FPLC	Fast protein liquid chromatography
g	Gram
GST	Glutathione S-transferase
Gy	Gray
h	Hour
HA	Haemagglutinin
HECT	Homologous to the E6AP carboxyl terminus

HEK	Human Embryonic Kidney
HEPES	4-(2-hydroxyethyl)-1-piperazineethanesulfonic acid
hexa-His	Hexa histidine
hOGG1	Human 8-oxoguanine glycosylase 1
HR	Homologous recombination
hSSB1	Human single-stranded DNA-binding protein 1
hSSB2	Human single-stranded DNA-binding protein 2
HU	Hydroxyurea
IGEPAL	Octylphenoxypolyethoxyethanol
IgG	Immunoglobulin G
INTS3	Integrator complex subunit 3
INTS6	Integrator complex subunit 6
IP	Immunoprecipitation
IR	Ionising radiation
K _d	Dissociation constant
kDa	Kilodalton
kg	Kilograms
KLH	Keyhole limpet hemocyanin
λ	Lambda
L	Litre
LB	Lysogeny broth
LIG1	DNA ligase 1
LIG3	DNA ligase 3
M	Molar
m/z	Mass-to-charge ratio
mAb	Monoclonal antibody
MCM	Minichromosome maintenance
MCPH1	Microcephalin 1
MDC1	Mediator of DNA damage checkpoint 1
min	Minute
mL	Millilitre
mm	Milimolar
MRN	Mre11-Rad50-Nbs1

MS	Mass spectrometry
NABP2	Nucleic acid binding protein 1
NBS1	Nibrin
ng	Nanogram
NHEJ	Nonhomologous end joining
Ni-NTA	Nickel – nitrilotriacetic acid
nM	Nanomolar
NMR	Nuclear magnetic resonance
nt	Nucleotide
OA	Okadaic acid
OB	Oligonucleotide/oligosaccharide binding
OBFC2B	OB-fold containing protein 2B
°C	Degrees Celsius
p53	Tumour suppressor protein 53
pAb	Polyclonal antibody
PAGE	Polyacrylamide gel electrophoresis
PAR	Poly(ADP-ribose)
PARP1	Poly(ADP-ribose) polymerase 1
PBS	Phosphatase buffered saline
PCNA	Proliferating cell nuclear antigen
PCR	Polymerase chain reaction
PDB	Protein database
phospho	Phosphorylated
PI3K	Phosphatidylinositol-4,5-bisphosphate 3-kinase
PIN1	Peptidyl-prolyl cis-trans isomerase NIMA-interacting 1
PLK1	Polo-like kinase 1
PMSF	Phenylmethylsulfonyl fluoride
Pol	Polymerase
poly-ubi	Poly ubiquitin
PP	Protein phosphatase
PTIP	PAX-interacting protein 1
RFC	Replication factor C
RING	Really interesting new gene

RIPA	Radioimmunoprecipitation
RPA	Replication protein A
RNF8	E3 ubiquitin-protein ligase RNF8
RPA32	RPA 32 kDa subunit
RPA70	RPA 70 kDa subunit
RPC	Replication pausing complex
RPM	Revolutions per minute
RPMI	Roswell Park Memorial Institute
SD	Standard deviation
SDM	Site-directed mutagenesis
SDS	Sodium dodecyl sulphate
SMARCA5	SWI/SNF Related, Matrix associated, Actin dependent regulator of chromatin, subfamily A, member 5
SOSS	Sensor of single-stranded
ssDNA	Single-stranded DNA
Std.	Standard
Tipin	Timeless interacting protein
TOF	Time-of-flight
TopBP1	Topoisomerase II β binding protein 1
U	Enzyme unit
V	Volt
WRN	Werner syndrome RecQ like helicase
WSTF	Williams syndrome transcription factor
WT	Wild type
XRCC1	X-ray cross-complementing protein 1

Statement of Original Authorship

The work contained in this thesis has not been previously submitted to meet requirements for an award at this or any other higher education institution. To the best of my knowledge and belief, the thesis contains no material previously published or written by another person except where due reference is made.

QUT Verified Signature

Signature:

Date: 1st of September 2016

Publications

Publications arising directly from, or including data contained within, this PhD study:

Paquet, N.¹, Adams, M.N.¹, **Ashton, N.W.**, Touma, C., Gamsjaeger, R., Cubeddu, L., Leong, V., Beard, S., Bolderson, E., O'Byrne, K.J., Richard, D.J. (2016) Oxidative hSSB1 (NABP2/OBFC2B) oligomerization regulates its activity in response to oxidative stress. *Scientific Reports* 6, 27446

Touma, C., Fernando, R., Gimenez, A., Bernardo, A., **Ashton, N.W.**, Adams, M., Paquet, N., Croll, T., O'Byrne, K., Richard, D., Cubeddu, L., Gamsjaeger, R. (2016) A structural analysis of DNA binding by hSSB1 (NABP2/OBFC2B) in solution. *Nucleic Acids Research [In Press]*

Ashton, N.W., Paquet, N., Shirran, S., Bolderson, E., Touma, C., Fallahbaghery, A., Gamsjaeger, R., Cubeddu, L., Botting, C., Pollock, P.M., O'Byrne, K.J., Richard, D.J. (2016) hSSB1 is regulated by DNA-PK-mediated phosphorylation during the repair of stalled replication forks. *Under review*

Ashton, N.W., Loo, D., Paquet, N., O'Byrne, K.J., Richard, D.J. (2016) Novel insight into the composition of hSSB1-containing protein complexes. *Under review*

Additional publications arising in the course of this PhD study

Ashton, N.W., Bolderson, E., Cubeddu, L., O'Byrne, K.J. & Richard, D.J. (2013) Human single-stranded DNA binding proteins are essential for maintaining genomic stability. *BMC molecular biology* 15 (1), 9

Paquet, N., Box, J.K., **Ashton, N.W.**, Suraweera, A., Croft, L.V., Urquhart, A.J., Bolderson, E., Zhang, S., O'Byrne, K.J., Richard, D.J. (2014) Néstor-Guillermo Progeria Syndrome: a biochemical insight into Barrier-to-Autointegration Factor 1, Alanine 12 Threonine mutation. *BMC molecular biology* 15 (1), 27

Adams, M.N., **Ashton, N.W.**, Paquet, N., O'Byrne, K.J. & Richard, D.J. (2014) Mechanisms of cisplatin resistance: DNA repair and cellular implications. *Advances in Drug Resistance Research*. 1st ed. 2014. pp. 1-38

Burgess, J.T., Croft, L.V., Wallace, N.C., Stephenson, S., Adams, M.N., **Ashton, N.W.**, Solomon, B., O'Byrne, K., Richard, DJ. (2014) DNA repair pathways and their therapeutic potential in lung cancer. *Lung Cancer Management* 3 (2), 159-173

Paquet, N.¹, Adams, M.N.¹, Leong, V.¹, **Ashton, N.W.**, Touma, C., Gamsjaeger, R., Cubeddu, L., Beard, S., Burgess, J.T., Bolderson, E., O'Byrne, K.J., Richard, D.J. (2015) hSSB1 (NABP2/OBFC2B) is required for the repair of 8-oxo-guanine by the hOOG1-mediated base excision repair pathway. *Nucleic Acids Research* 43 (18), 8817-8829

Acknowledgements

I wish to extend my sincere gratitude to my principal supervisor Associate Professor Derek Richard for the opportunity to work in his group for the last four years, as well as for his guidance and intellectual engagement during this time. In addition, I would like to thank my associate supervisors, Dr Nicolas Paquet, Dr Laura Croft and Associate Professor Pamela Pollock for their assistance and advice throughout my PhD.

I wish also to express gratitude to all members of the Cancer and Ageing Research Program, especially Mr (soon-to-be Dr) Joshua Burgess, Dr Emma Bolderson and Professor Kenneth O’Byrne for their helpful discussion. I also gratefully acknowledge the input of Associate Professor Brian Gabrielli of Mater Research for his input in the capacity as a panel member.

Thank you also to our collaborators Dr Roland Gamsjaeger and Dr Liza Cubeddu of the University of Western Sydney, as well as Dr Sally Shirran and Dr Catherine Botting of the University of St Andrews, for their assistance and intellectual input regarding this and other projects. I also thank Dr Dorothy Loo from the Translational Research Institute Proteomics Facility for her advice regarding mass spectrometry analysis.

I also acknowledge Cancer Council Queensland, especially Dr John Mayo, and the Queensland University of Technology, for their provision of my PhD scholarship.

Finally, I would like to sincerely thank my partner, Dr Lakmali Silva, as well as my parents and family for their encouragement and support.

Chapter 1: Introduction, Literature Review and Contextualisation of the Research Project

1.1 Genomic stability

DNA repair is essential for the prevention of chromosomal instability, a condition resulting from the incomplete maintenance of genetic material, which may lead to cell death, malignant transformation or other deregulation of cellular function (Polo and Jackson, 2011). This can manifest in a variety of disorders including neurological degeneration, premature ageing, developmental defects and cancer (Khanna and Jackson, 2001). The prevention and repair of DNA damage is a continuous process, with thousands of lesions occurring every day in each human cell (Jackson and Bartek, 2009). The vast majority of these lesions occur through endogenous cellular functions (De Bont and van Larebeke, 2004; Marnett and Plataras, 2001), however environmental conditions such as exposure to radiation and various chemicals (e.g. carcinogens, chemotherapeutics) may also cause further damage (Poirier, 2004; Willers et al., 2004).

The major aim of this PhD project is to further characterise the post-translational regulation of human single-stranded DNA binding protein 1 (hSSB1), a genome stability protein with roles in the repair of oxidative lesions (Paquet et al., 2015), the stabilisation of stalled replication forks (Bolderson et al., 2014) and the repair of double-strand DNA breaks by homologous recombination (Richard et al., 2008). The DNA repair pathways in which hSSB1 is known to function are therefore described below, with a special emphasis placed on post-translational signalling.

1.2 Oxidative base excision repair

Base excision repair (BER) is a major mechanism through which the cell is able to remove a variety of small base lesions, such as those caused by endogenous oxidation and alkylation events (Hsu et al., 2004). These base lesions are recognised by one of a number of DNA glycosylases, the identity of which is specific to the lesion type (David et al., 2007). Deamination of the damaged base by the glycosylase then leaves an abasic residue, which is recognized by endonuclease apurinic/apyrimidinic endonuclease 1 (APE1). APE1 nicks the phosphodiester backbone 5' to the abasic residue, creating a free 3'-hydroxyl site (Wilson and

Barsky, 2001). Removal of the 5'-terminal deoxyribose phosphate residue and closure of the strand break is then accomplished by either short- or long-patch repair. While short patch repair results in replacement of only the damaged base, up to 10 nucleotides downstream of the lesion are replaced by long-patch repair (Petermann et al., 2006).

Eleven DNA glycosylases are known to function in BER within mammalian cells, two major classes of which may be broadly defined: 1) mono-functional glycosylases and 2) bi-functional glycosylases (Brooks et al., 2013). While both classes possess a conserved helix-hairpin-helix motif and an invariant aspartate in their active site, their catalytic mechanisms differ greatly (Choi et al., 2004). In the instance of mono-functional glycosylases, the conserved aspartate residue acts to deprotonate and thereby activate a water molecule, which then nucleophilically attacks carbon 1 of the N-glycosidic bond; resolution of the reaction then yields the damaged base and a free abasic site (Mol et al., 1995). Unlike mono-functional glycosylases, which only possess glycosylase activity, the bifunctional glycosylases also possess lyase activity to cleave the phosphodiester backbone 3' of the abasic residue (Krokan et al., 1997). Here, the conserved aspartate residue seems to deprotonate a similarly conserved lysine residue in the catalytic domain, forming a nucleophilic amine (Dodson et al., 1994). Attack of the deoxyribose carbon 1 and the resulting rearrangements then leads to formation of a covalent Schiff-base, whereby the damaged base is released from the DNA, although it is held in position to assist in the lyase reaction (Sun et al., 1995). Here, proton transfer between the glycosylase and the abasic residue is apparently promoted by the excised base, leading to strand cleavage and regeneration of the enzyme (Fromme et al., 2003). Subsequent to cleavage of the damaged base, a number of glycosylases do however remain bound to the abasic site, and indeed, many glycosylases show higher affinity for the abasic site than they do to their substrate base (Parikh et al., 1998). As abasic sites are chemically unstable, it has been suggested their continued association with the glycosylase may help to protect the cell from their mutagenic effects (Banerjee et al., 2005). In keeping, several glycosylases appear to be removed only following association of the APE1 nuclease (Waters et al., 1999).

Cellular oxidative stress may result in the formation of either purine or pyrimidine adducts (Burrows and Muller, 1998). Guanine bases, however, seem to be particularly susceptible to damage, where attack of carbon 8 (C8) by a hydroxyl radical leads to formation of the intermediate compound 7,8-dihydro-8-hydroxyguanine (8-OHG). 8-OHG may then tautomerise to form two major products, 2,6-diamino-5-formamido-4-hydroxy-pyrimidine (FapyG) and 8-oxo-7,8-dihydroguanine (8-oxoG) (Kirpota et al., 2011). Of these, 8-oxoG is particularly mutagenic, as it is capable of base-pairing with both cytosine and adenine (Cheng et al., 1992). This occurs as 8-oxoG maintains the capacity to form correct Watson-Crick base-pairing with cytosine, however due to protonation of nitrogen 7 (N7), may also act as a hydrogen donor for interaction with adenine (Bjorås et al., 1997). Sustainment of these lesions into S-phase may therefore result in base transversion, where the replicative polymerases (Pols α , δ and ϵ) incorporate adenine into the new strand in place of guanine (Cheng et al., 1992; Hsu et al., 2004). Such conversions may however be suppressed by the X-family DNA polymerase Pol λ , which incorporates cytosine opposite 8-oxoG with a 1000-fold preference to adenine insertion (Maga et al., 2007). Furthermore, in cases where adenine:8-oxoG mismatches occur, the human adenine DNA glycosylase homologue MutY, is capable of excising the incorrectly paired adenine base (Williams and David, 1998). The abasic residue is then removed and replaced by the concerted efforts of APE1, DNA Pol λ , and DNA ligase 1 (van Loon and Hubscher, 2009).

Despite the existence of a mismatch repair pathway that can remove 8-oxoG post-replication, the cellular response to oxidative lesions is still largely reliant on their earlier removal (Arai et al., 2002; Kunisada, 2005). The human 8-oxoguanine DNA glycosylase (hOGG1) facilitates the direct removal of 8-oxoG lesions in human cells and is thus required for the efficient response to oxidative insult (German et al., 2013; Roldán-Arjona et al., 1997). As with most DNA glycosylases, hOGG1 is thought to detect its substrate base by migrating along the undamaged duplex DNA, forming a series of non-specific interactions through which it ‘senses’ 8-oxoG lesions (Blainey et al., 2009; Friedman and Stivers, 2010). This seems to form a ‘pre-selection’ process, whereby the enzyme is able to identify and discount non-substrate bases through superficial contacts. Once an 8-oxoG adduct is detected, the base is

flipped out of the double helix, into the hOGG1 active site (Banerjee et al., 2005). Here, the glycosylase binding energy itself seems sufficiently high to accomplish this task, including the breaking of the Watson-Crick base pairs, disruption of aromatic stacking bonds, and rotation of the phosphodiester backbone. Potentially, this energy cost may however be less than originally considered, based on a recent thermodynamic study that suggested nucleotides immediately 5' to the 8-oxoG are energetically less stable (Kirpota et al., 2011). Alternatively, these results may support a model of base-scanning, in which pre-selection is facilitated by 'breathing' of the area immediately surrounding the lesion (Friedman et al., 2009). Of further interest is the observation of high-specificity of hOGG1 for 8-oxoG base-paired with cytosine (Bjorås et al., 1997; Zharkov et al., 2000). Indeed, while a single hydrogen bond exists between hOGG1 G42 and the protonated N7 of the 8-oxoG, 5 hydrogen bonds are formed between R204, N149 and R154 of hOGG1 and the opposing cytosine (Bruner et al., 2000).

hOGG1 is generally considered as a bifunctional glycosylase, containing the catalytic residues, D268 and K249 (Brooks et al., 2013). As described for the general model above, D268 is here thought to deprotonate the K249 ϵ amino group, which forms a Schiff base with carbon 1 of the N-glycosidic bond, resulting in β -elimination (Nash et al., 1997). This view has however been challenged regarding the enzyme's activity in cells, based on the suggestion that APE1 may promote the glycosylase activity of hOGG1, then bind and excise the non-cleaved abasic site (Hill et al., 2001).

Through whichever means hOGG1 functions *in vivo*, further processing of the damaged site requires cleavage of the phosphodiester backbone 5' to the abasic residue, generating a free 3' hydroxyl site for polymerase mediated synthesis (Wilson and Barsky, 2001). While Pol β functions as the major BER DNA polymerase in mammalian cells, other polymerases may also have ancillary roles. For instance, Pol δ and Pol ϵ may act in long-patch BER, Pol ι , Pol λ and Pol θ may function in short-patch BER, and Pol γ may facilitate BER in the mitochondria (Dianov and Hübscher, 2013). During short-patch BER, the DNA polymerase catalyses the synthesis of a new base from the free 3' hydroxyl group generated by APE1 cleavage. Where lyase activity of the glycosylase has not nicked the phosphodiester backbone downstream of the adduct, end processing by the

polymerase must act to restore a 5' phosphate group, prior to XRCC1-DNA ligase III (LIG3)-mediated closure of the gap (Kubota et al., 1996; Wei et al., 1995). While this mechanism may be sufficient for the majority of BER events, in some instances, 5' end processing by the polymerase seems unable to restore a 5' phosphate group, potentially as a result of complex, incidental damage to these ends (Frosina et al., 1996). In addition, Pol δ and Pol ϵ do not possess apparent end-processing activity. In these instances, repair may be accomplished by long-patch BER (Matsumoto et al., 1994). Here, Pol δ or Pol ϵ acts to extend the first nucleotide added by Pol β in a reaction dependent on proliferating cell nuclear antigen (PCNA), displacing a 'flap' of 2-12 nucleotides (Dianov, 1999; Podlutzky et al., 2001). Flap structure-specific endonuclease 1 (FEN1) then degrades the displaced strand, leaving a single nick in the phosphodiester backbone, which is sealed by DNA ligase 1 (LIG1) (Kim et al., 1998; Liu et al., 2005; Ranalli et al., 2002).

In response to oxidative stress, the Ataxia telangiectasia mutated (ATM) kinase is activated as a disulphide cross-linked dimer, resulting from oxidation of cysteine 2991 (Guo et al., 2010a; Guo et al., 2010b). Interestingly, recent data suggests this may include dimerisation of cytoplasmic ATM (Kozlov et al., 2016). Activation is marked by its auto-phosphorylation of serine 1981 (S1981), an important modification that stimulates ATM kinase activity (Bakkenist and Kastan, 2003; Canman et al., 1998). Here, dimeric ATM is required to activate p53 through phosphorylation of serine 15 (S15) (Guo et al., 2010b). Activated p53 then seems to stimulate BER by directly binding DNA pol β , stabilising the interaction between the polymerase and the abasic residue (Zhou et al., 2001).

A role for hSSB1 in the response to hydrogen peroxide-induced oxidative stress has recently been suggested (Paquet et al., 2015). In these studies, hSSB1 was found to accumulate at chromatin following oxidative damage, likely by binding directly to 8-oxoG lesions. hSSB1 was also required for the efficient recruitment of the OGG1 glycosylase, as well as for the efficient removal of 8-oxoG post damage. In addition, the depletion of hSSB1 from cells suppressed the proper phosphorylation of ATM and p53. Further data from our group (Paquet et al., 2016) has also suggested that, in response to oxidative stress, hSSB1 may form a stable disulphide-linked dimer that is required for hSSB1-dependent cell survival.

1.3 DNA replication and replication stress

Although the base and nucleotide excision repair pathways are able to remove the majority of small adducts prior to initiation of replication, in some instances, lesions are able to persist into S-phase. This is especially true of lesions such as inter-strand cross-links, most likely due to their chemical complexity, as well as their inefficient recognition in highly condensed chromatin (Deans and West, 2011; Mu et al., 2000).

During eukaryotic replication, the mini-chromosome maintenance protein (MCM) helicase is responsible for unwinding the dsDNA helix, and the concurrent exposure of ssDNA (Bell and Dutta, 2002). These stretches are rapidly bound by replication protein A (RPA), a trimeric complex consisting of ~70 kDa (RPA70), ~32 kDa (RPA32) and ~14 kDa (RPA14) subunits (Waga and Stillman, 1998). At sites of replication, RPA both prevents formation of ssDNA secondary structures, as well as stabilises the DNA polymerase α -complex (Pol α) (Dornreiter et al., 1992; Yuzhakov et al., 1999). Pol α is required for the synthesis of short oligonucleotide primers from which the more processive polymerases δ and ϵ may synthesise new ssDNA strands complementary to those exposed by fork migration (Burgers, 2009). Here, removal of Pol α is facilitated by replication factor C (RFC), an essential clamp loader, which also recruits PCNA (McNally et al., 2010). PCNA here acts as a processivity factor for DNA polymerase δ (Burgers, 1988). In addition, PCNA interacts with various replication factors, tethering them to sites of replication (Schurtenberger et al., 1998).

While replication of undamaged DNA occurs both rapidly and continuously, endogenous and exogenous stresses can disrupt migration, causing the fork to stall. In these instances, the cell will firstly pause replication, before either repairing or bypassing the damage, processes which are facilitated by the concerted activities of the DNA replication and damage repair pathways (Petermann and Helleday, 2010). In general, the replication fork may stall for two major reasons: 1) a sustained bulky adduct may inhibit the processive DNA polymerases (Washington et al., 2010), or 2) covalent crosslinking of the opposing strands may prevent helicase-unwinding ahead of the fork (Nakano et al., 2013). In an artificial setting, the polymerase inhibitors hydroxyurea and aphidicolin may also disrupt the replication fork, where they cause

uncoupling of the replicative polymerases and the MCM helicase, leading to the generation of long ssDNA stretches (Byun et al., 2005).

Two major pathways are known to facilitate the re-initiation of replication following fork stalling, translesion repair, and homology-directed repair. While the former utilises a number of 'low-fidelity' polymerases to synthesise past the lesion, homology-directed repair makes use of a homologous region in the newly synthesised opposing strand (Burrows and Elledge, 2008; Friedberg, 2005). In addition, replication forks stalled following polymerase inhibition must be 're-wound' and replication restarted, either by fork remodelling, or by D-loop formation using the opposing nascent strand (Petermann and Helleday, 2010).

1.3.1 Stabilisation and restart of uncoupled replication forks

Following replication fork stalling, the accumulation of RPA is required to stabilise exposed ssDNA, as well as to promote the interaction of a number of other repair proteins (Robison et al., 2004; Zou, 2003). Of central importance is the interaction with the ataxia telangiectasia and Rad3 related (ATR)-interacting protein (ATRIP), which also promotes the recruitment, although not full activation, of the ataxia telangiectasia and Rad3 related (ATR) kinase (Ball et al., 2005; Namiki and Zou, 2006; Xu and Leffak, 2010). While the N-terminal 108 amino acids of ATRIP was initially suggested as the sole RPA70 interacting region (Ball et al., 2005), this has been contradicted by a latter study which indicated the regions flanking the ATRIP coiled-coil domain may also associate with RPA (Namiki and Zou, 2006). Recruitment of ATR/ATRIP to RPA-coated ssDNA here seems sufficient to induce early activation of ATR by auto-phosphorylation at threonine 1989 (Liu et al., 2011). ATR auto-phosphorylation is also dependent on the prior non-DNA damage induced phosphorylation of ATR and ATRIP by the Nek1 kinase (Liu et al., 2013). Full activation of ATR however also requires topoisomerase II β -binding protein 1 (TopBP1), a protein that directly binds RPA-coated ssDNA and interacts with both ATR and ATRIP (Acevedo et al., 2016; Burrows and Elledge, 2008; Kumagai et al., 2006; Mordes et al., 2008). Once activated, ATR is responsible for phosphorylation of CHK1 at S317 and S345, releasing it from chromatin and allowing it to phosphorylate cdc25, facilitating its degradation (Smits et al., 2006; Sørensen et al.,

2003). The importance of TopBP1 in the activation of ATR is supported by findings that *in vitro*, ATR, ATRIP and TopBP1 are the minimal components required for RPA-ssDNA induced Chk1 phosphorylation (Choi et al., 2010).

Independent of the RPA-ATRIP interaction, DNA polymerase α is required for recruitment of the Rad17-RFC clamp loader to sites of stalled replication (Byun et al., 2005; You et al., 2002). Analogous to its role in replication initiation, the Rad17-RFC clamp loader recruits the PCNA-like Rad9-Rad1-Hus1 (9-1-1) clamp (Bermudez et al., 2003; Ellison and Stillman, 2003; Yan and Michael, 2009a; Yan and Michael, 2009b), which may be stabilised through an interaction with the basic cleft of RPA70 (Xu et al., 2008). Rad9 may then directly interact with the N-terminus of TopBP1, facilitating its accumulation at the fork (Delacroix et al., 2007; Lee et al., 2007). TopBP1 may then act as a bridging protein between the ATR/ATRIP and 9-1-1 complexes (Kumagai et al., 2006). Additionally, the Mre11-Rad50-Nbs1 (MRN) complex has also recently been suggested to promote TopBP1 recruitment to stalled forks via a direct interaction between Nbs1 and the TopBP1 BRCT repeats 3-6 (Duursma et al., 2013). In addition, MRN may interact with the RPA70 N-terminal OB-fold (Robison et al., 2004). The significance of MRN at stalled replicative forks is further exemplified by the lack of ATR-mediated RPA32 threonine 21 phosphorylation in cells depleted of Nbs1 (Block et al., 2004; Manthey et al., 2007). Mediator of DNA damage checkpoint protein 1 (MDC1) has also been found to interact with both Nbs1 and TopBP1 at stalled forks and appears necessary for efficient ATR-signalling in response to replicative stress (Chapman and Jackson, 2008; Wang et al., 2011).

Once activated, the ATR kinase requires the Claspin mediator protein in order to efficiently phosphorylate Chk1 (Chini, 2003; Kumagai and Dunphy, 2000; Liu et al., 2006). This may involve coordination the ATR-Chk1 interaction and indeed ATR has a higher affinity for Chk1 when it is bound to Claspin, than when it is free (Lindsey-Boltz et al., 2009). Concurrently, Chk1-phosphorylation of Claspin T916 may promote accumulation of the protein through the suppression of proteasomal degradation (Chini et al., 2006). The interaction between Chk1 and Claspin may also be promoted by replication-stress-induced phosphorylation of Claspin residues S945 and S982 by casein kinase 1 (Meng et al., 2011). In addition, Chk1 phosphorylation

seems to be promoted by RPA-mediated interaction with Timeless-interacting partner (Tipin) (Kemp et al., 2010; Unsal-Kacmaz et al., 2007). Tipin is a component of the replication pausing complex (RPC), a protein complex required for the coordinated pausing of both the polymerase and helicase components of the replicative machinery (Errico and Costanzo, 2012). Here, Tipin and its binding partner Timeless (Tim1) form a central heterodimer, which appears essential for activation of the intra-S checkpoint (Chou and Elledge, 2006; Gotter et al., 2007; Yoshizawa-Sugata and Masai, 2007).

ATR is also responsible for phosphorylation of the DNA-dependent protein kinase catalytic subunit (DNA-PK_{CS}) at T2609, facilitating its activation (Yajima et al., 2006). DNA-PK_{CS} may then assist in the amplification of ATR checkpoint signalling (Shimura et al., 2007) where it interacts directly with Chk1 and promotes stabilisation of the Chk1-Claspin complex (Lin et al., 2014). In addition, DNA-PK_{CS} may act in concert with ATR to phosphorylate RPA32 (Liu et al., 2012). Here, in response to prior CDK-mediated phosphorylation of RPA32 S23 and S29 (Anantha et al., 2007; Zernik-Kobak et al., 1997), ATR catalyses phosphorylation of RPA32 S33 (Olson et al., 2006), which in turn promotes phosphorylation of S4, S8 and T21 by DNA-PK_{CS} (Block et al., 2004; Liu et al., 2012; Niu et al., 1997). Hyper-phosphorylation of the RPA32 N-terminus seems to be stimulatory for recruitment of the proteins Rad51 (Shi et al., 2010) and PALB2 (Murphy et al., 2014).

The restart of stalled replication forks theoretically may occur through two major mechanisms, the contributions of which in mammalian cells has remained subject to debate: 1) restart by remodelling and 2) D-loop-mediated fork restart (Petermann and Helleday, 2010). As replication fork disruption frequently involves the physical uncoupling of the replicative polymerases and the MCM helicase (Byun et al., 2005), the initial step of either method firstly requires regression of the replication fork and re-annealing of exposed ssDNA (Zellweger et al., 2015). This process is most likely facilitated through three major helicases, Werner's syndrome protein (WRN) (Constantinou et al., 2000; Sidorova et al., 2013), Bloom's syndrome protein (BLM) (Davies et al., 2007) and the annealing helicase, SWI/SNF-related, matrix-associated, actin-dependent regulator of chromatin, subfamily A-like 1 (SMARCA1) (Bansbach et al., 2009; Ciccina et al., 2009; Yusufzai and Kadonaga, 2008). Although

SMARCAL1-mediated re-annealing of exposed ssDNA could theoretically allow for fork re-start without the need for further processing, the WRN and BLM syndrome proteins may cause regression of the fork into a Holliday junction structure referred to as a 'chicken foot' (Machwe et al., 2006). Here, the fork may be regressed past the point of initial replication disruption, displacing the newly synthesised nascent strands. In a scenario where the fork is re-initiated by remodelling, the 'chicken foot' may then be reversed, presumably by the WRN and BLM helicases, separating the annealed nascent strands and allowing replication to re-start following the binding of these strands to the newly re-exposed parental DNA (Petermann and Helleday, 2010). Another possible means of fork re-start could involve the Rad51-mediated invasion of the nascent leading strand of the 'chicken foot' structure into the template dsDNA, downstream of the fork (McGlynn and Lloyd, 2002). This would lead to the formation of a double-Holliday junction, which could subsequently be resolved by Holliday junction dissolution (Li and Heyer, 2008).

Although the majority of hydroxyurea-stalled replication forks may restart after short treatments, this potential is gradually diminished over time. Indeed, whilst ~ 80% of stalled forks may restart after 2 hours of HU exposure, fewer than 20% may after 20 hours (Petermann et al., 2010). After sustained fork disruption, replication in the cell instead seems to continue predominantly through the initiation of new fork origins (Petermann et al., 2010). In addition, whilst the majority of replication forks remain structurally stable for greater than 12-18 hours post hydroxyurea treatment, after this time, stalled and de-activated replication forks may 'collapse' to form double-strand DNA breaks (Saintigny et al., 2001). This reaction seems to be catalysed by the MUS81-EME1 endonuclease (Hanada et al., 2007). The resulting one-sided double-strand DNA breaks can then be repaired by homologous recombination (Yeeles et al., 2013).

Recent data has also implicated a role for hSSB1 in the stabilisation and re-start of stalled replication forks, including the activation of ATR signalling (Bolderson et al., 2014). Here, hSSB1 was found to localise with sites of replication following fork disruption, where it was required for ATR-mediated phosphorylation of Chk1 at S317 and S345, as well as subsequent Chk1 auto-phosphorylation at S296. In addition, hSSB1-depletion prevented proper localisation of Mre11 and ATR at

chromatin following treatment of cells with the polymerase inhibitor, hydroxyurea. A requirement for hSSB1 in replication fork restart was found to manifest in hypersensitivity of hSSB1-depleted cells to hydroxyurea and camptothecin treatment.

Investigations into the role of mSSB1, the murine hSSB1 homologue, have also lead to similar conclusions regarding a function for these proteins in the suppression of replication-associated DNA damage (Feldhahn et al. 2012; Shi et al. 2013). These conclusions were inferred by the poor proliferation and loss of genomic integrity observed following mSSB1 knock-out. For these studies, conditional knockout mice were produced due to the embryonic lethality of mSSB1 germline deletions. Indeed, *Obfc2b*^{-/-} embryos developed severe skeletal defects, most likely associated with increased apoptosis (Feldhahn et al. 2012). Similarly to has been observed in human cell lines following hSSB1 siRNA-depletion (Li et al. 2009), the conditional knockout of hSSB1 was also found to enhance the protein levels of mSSB2 (murine homologue of hSSB2). In contrast to hSSB1 depletion studies, it is interesting to note that knockout of mSSB1 (or mSSB2) did not however result in deficient initiation of a DNA damage response when examined in irradiated murine fibroblasts. These data nevertheless support a role for these proteins in the restart of stalled replication forks.

1.4 Double-strand DNA break repair

Double-strand DNA breaks (DSBs) are often considered the most cytotoxic type of DNA lesion, as the failed repair of just one may lead to chromosomal fragmentation and rearrangement (Difilippantonio et al., 2000; Weinstock et al., 2006). Two major DNA repair pathways are employed for the repair of double-strand DNA breaks in cells, non-homologous end-joining (NHEJ) and homologous recombination (HR) (Khanna and Jackson, 2001). While non-homologous end-joining may be used at any stage during the cell cycle (Mao et al., 2008a), homologous recombination is only available during the S and G2 cell cycle phases where a sister chromatid is available (Saleh-Gohari and Helleday, 2004).

1.4.1 Repair of double-strand DNA breaks by homologous recombination

One of the earliest processes in homologous recombination is the recruitment of the MRE11-Rad50-NBS1 (MRN) complex to the site of DNA damage (de Jager et al., 2001; Hopfner et al., 2001). As well as binding single-stranded DNA overhangs,

MRN activates the ataxia telangiectasia mutated (ATM) serine/threonine kinase (Carson et al., 2003; Lee and Paull, 2005; Uziel et al., 2003). This, in turn, leads to the phosphorylation and activation of downstream targets involved in cell cycle checkpoint activation (e.g. Chk1, Chk2, p53) and directly in double-strand DNA break repair (e.g. NBS1, Exo1 and the histone variant H2AX) (Bolderson et al., 2010; Burma et al., 2001). One of the direct results of ATM signalling is the resection of double-strand DNA breaks to produce 3' single-stranded DNA tracts, the availability of which facilitates RAD51 nucleofilament formation and strand invasion into a sister chromatid (Garcia et al., 2011). As a result of this invasion, the sister chromatid can then be used as a homologous repair template (Bekker-Jensen and Mailand, 2010).

MRN is a large, highly conserved, multi-protein complex, consisting of an Mre11-Rad50 DNA-binding clamp, enfolded by an Nbs1 polypeptide (Schiller et al., 2012). Formation of the clamp is largely facilitated by an Mre11 dimer, as well as, in response to ATP binding, dimerisation of the Rad50 Walker A/B domains (de Jager et al., 2001; Hopfner et al., 2002; Lammens et al., 2011; Mockel et al., 2012). While not involved in binding DNA directly, crystallography of MRX, the *Saccharomyces pombe* MRN homologue, has suggested the NBS1 N-terminus is oriented such that it may interact with other proteins at the site of DSBs, adjacent to the Mre11-Rad50 clamp (Schiller et al., 2012).

The recruitment of ATM to sites of DSBs is largely reliant on ssDNA binding by the MRN complex (Carson et al., 2003). This is facilitated by a direct interaction between ATM and the C-terminus of NBS1, and is, at least initially, modulated by ATP-binding of the MRN Rad50 head domains (Lee et al., 2013; Nakada et al., 2003; You et al., 2005). ATP binding seems to cause a gross conformational change in MRN, moving the protein from an 'open' to 'closed' state. As well as pushing the Mre11 domains into a close dimer, an alteration which promotes ssDNA interaction, ATP-binding seems to promote association of Nbs1 to the complex; this, presumably, leads to an increase in ATM localisation (Lee et al., 2013). Interestingly, while Mre11 possesses both endo- and exo-nuclease activity, only the endonuclease activity appears necessary for DSB processing (Garcia et al., 2011).

A direct outcome of the MRN-ATM interaction is auto-phosphorylation of ATM at serine residues 267, 1893, 1981 and 2996 (Kozlov et al., 2011; Kozlov et al., 2006). In addition, full ATM activation requires acetylation of K3016 by the histone acetyltransferase, Tip60 (Sun et al., 2005; Sun et al., 2007). Here, the Tip60 chromodomain interacts with histone H3 trimethylated on lysine 9 (H3K9me3), which seems to activate the acetyltransferase activity of Tip60 (Sun et al., 2009). In addition, chromatin-binding of Tip60 also seems to be promoted by c-Abl kinase-mediated phosphorylation of Tip60 tyrosine residue 44 (Kaidi and Jackson, 2013). Together, auto-phosphorylation and Tip60-mediated acetylation cause a conformational change in ATM, transitioning the protein from a dimer to an active monomer (Bakkenist and Kastan, 2003; Sun et al., 2007).

Once activated, ATM seems to function in a positive feedback loop with MRN, whereby phosphorylation of Nbs1 S343 regulates MRN accumulation at DNA breaks (Wen et al., 2012). In addition, ATM is required for phosphorylation of H2AX serine 139 (γ H2AX), which allows recruitment of casein kinase 2 (CK2)-phosphorylated MDC1, a protein which appears to anchor MRN onto the chromatin (Spycher et al., 2008). ATM-mediated phosphorylation of MDC1 threonine 4 then leads to dimerisation of the protein, a requirements for proper foci formation (Jungmichel et al., 2012). The interaction of MDC1 with γ H2AX also seems to promote RNF168-mediated K63-linked ubiquitination of γ H2AX residues K13 and K15 (Gatti et al., 2012; Mattioli et al., 2012). Here, the function of RNF168 relies on the prior ATM-dependent recruitment of the RNF8 ligase to DSB sites (Mattioli et al., 2012), the reason for which remains unclear. The poly-ubiquitination of γ H2AX is important for localisation of the proteins 53BP1 and BRCA1, both of which seem to act as bridging proteins between ATM and MRN (Lee et al., 2010). In addition, the activities of both proteins may be promoted by ATM-mediated phosphorylation (53BP1 is phosphorylated at S25 and S1778 (Jowsey et al., 2007), and BRCA1 is phosphorylated at S1387, 1423, and 1457 (Gatei et al., 2000)), suggesting a possible further feedback loop. Interestingly, as well as binding ubiquitinated γ H2AX, the localisation of 53BP1 at DSB foci also seems to rely on dimethylation of histone H2 residue K20 (Fradet-Turcotte et al., 2013), as well as K63-linked poly-ubiquitination of K1268 by RNF168 (Bohgaki et al., 2013). JMJD1C-mediated demethylation of

MDCI may also allow its K63-linked ubiquitination by RNF8, promoting an association with the BRCA1 interacting protein RAP80 (Watanabe et al., 2013). Here, RAP80 appears to be phosphorylated at serine 205 by the ATM kinase (Yan et al., 2008), as well as at serine 677 by cyclin dependent kinase 1 (Cho et al., 2013). The interaction between RAP80 and BRCA1 may be further enhanced by the protein Abraxas, which, in concert with RAP80, may help to recruit BRCA1 to K63-linked ubiquitinated DSB foci (Wang and Elledge, 2007; Wang et al., 2007). Interestingly, BRCA1 also interacts with the K63-specific deubiquitinating enzyme, BRCC35, which may act to regulate the abundance of these chains at sites of DSBs (Feng et al., 2010).

The activated MRN complex is required for resection of the DSB 5' strand. For this, Mre11 nicks the target strand up to 300 bases from the break site, and resects the strand in the 3'-5' direction (Garcia et al., 2011). Concurrently, one of two DNA exonucleases, Dna2 helicase/nuclease or exonuclease 1 (Exo1), acts to digest the strand in the 5'-3' direction, away from the DSB site (Tomimatsu et al., 2012). Here, Mre11 endonuclease activity is stimulated by direct interaction with the CtBP-interacting protein (CtIP) (Ramírez-Lugo et al., 2011; Sartori et al., 2007). Additionally, CtIP interacts with BRCA1 to exclude the TopBP1-interacting protein, RIF1, a component of the non-homologous end-joining pathway which limits MRN resection (Chapman et al., 2013; Di Virgilio et al., 2013; Escribano-Díaz et al., 2013; Peterson et al., 2013; Xu et al., 2010a; Zimmermann et al., 2013). The PCNA clamp has also been shown to load at sites of double-strand DNA breaks, where it promotes resection processivity of Exo1 (Chen et al., 2013b). The DNA-dependent protein kinase catalytic subunit (DNA-PK_{CS}), an important P13K-like kinase involved in the coordination of DSB repair by non-homologous end joining, has also been suggested to promote Exo1 exonuclease activity in response to prior ATM-mediated phosphorylation of T2609 and T2647 (Zhou and Paull, 2013).

Unwinding of the DNA helix upstream of the DSB is another important requirement for end-resection. Here, the BLM RECQ helicase appears to have an essential role (Nimonkar et al., 2011). In response to DSB formation, BLM is recruited to DNA damage sites through a direct interaction with MRN, where it is phosphorylated by the ATM kinase (Ababou et al., 2000). BLM recruitment may be enhanced by the

human heterogeneous nuclear ribonucleoprotein U-like (hnRNPUL) proteins 1 and 2, both of which have been shown to bind the Nbs1 C-terminus and to promote efficient end-resection (Polo et al., 2012). Subsequent to its recruitment, BLM has been suggested to form two separate end resection complexes, where it interacts with and stimulates the exonuclease activity of Exo1 or Dna2 (Cejka et al., 2010; Gravel et al., 2008; Nimonkar et al., 2011). In addition, Mre11 and BLM are also known to interact directly with the Fanconi Anemia Group J Helicase (FANCD1) (Paliwal et al., 2013; Suhasini and Brosh, 2012; Suhasini et al., 2011; Suhasini et al., 2013). Here, FANCD1 is recruited to sites of DSBs in an MRN-dependent manner, where it seems to inhibit Mre11 exonuclease activity, and promote endonuclease mediated end-resection (Suhasini et al., 2013). Replication protein A (RPA) may also play a prominent role in end resection, where it appears to stimulate the exonuclease efficiency of Exo1 and Dna2 (Yan et al., 2011). Further, RPA binding of the exposed 3' DNA strand may prevent the formation of inappropriate hairpin fold-back structures, which may present as substrates for Mre11-mediated degradation (Chen et al., 2013a).

In addition to preventing the formation of inappropriate DNA secondary structures, ssDNA-binding of RPA is important for the recruitment of downstream repair proteins (Iftode et al., 1999). This includes, as with the stabilisation of stalled forks, the recruitment of ATR kinase via its interacting protein, ATRIP (Zou, 2003). In addition, ATM-phosphorylation of TopBP1 S1131 seems to promote a direct interaction between TopBP1 and the BRCT repeats of NBS1 (Yoo et al., 2009), as well as with the CtIP N-terminus (Ramírez-Lugo et al., 2011); both interactions also seem to further stimulate ATR activity. Interestingly, ATR seems to promote further accumulation of CtIP via phosphorylation of T859, leading to increased chromatin binding and the promotion of CtIP-dependent resection (Peterson et al., 2013). The Rad51 recombinase is another important RPA-interacting protein which, following displacement of RPA, rapidly coats the exposed ssDNA strand (Sung et al., 2003). Initially, Rad51 seems to be recruited to DSB sites via direct binding to Nbs1, which may be promoted by successive phosphorylation, firstly by Polo-like kinase 1 (Plk1) at serine 14 (S14), followed by phosphorylation of threonine 13 (T13) by casein kinase 2 (Ck2) (Yata et al., 2012). Phosphorylation of RAD51 S14 may also be

promoted by a direct interaction between TopBP1 and Plk1, which presumably scaffolds the kinase to sites of repair (Moudry et al., 2016).

The displacement of RPA and the coating of Rad51 may occur through a number of mechanisms. Of these, the direct interaction between the RPA70 N-terminal OB-fold and the N-terminus of Rad51 is likely to be of central importance (Stauffer and Chazin, 2004). By this method, exchange would likely occur as a result of Rad51 capture of transient RPA binding (Fanning et al., 2006). Rad52 has also been suggested to modulate the RPA-Rad51 exchange, whereby it binds both RPA34 and 70 in response to prior RPA phosphorylation, and seems to stimulate RPA displacement. RPA removal may also be promoted by BRCA2, a large ssDNA-binding protein, which may promote RPA displacement through competitive ssDNA interaction (Jensen et al., 2010; Liu et al., 2010; Yang et al., 2002). In addition, BRCA2 interacts directly with Rad51 through a series of eight 35 amino acid repeats, known as the BRC repeats (Bignell et al., 1997; Bork et al., 1996; Galkin et al., 2005). Interestingly, crystallography of BRCA2 BRC4 bound to Rad51 has indicated this interface may mimic that of the Rad51 homodimer, suggesting a possible mechanism through which BRCA2 is able to stabilise monomeric Rad51 for ssDNA loading (Carreira et al., 2009; Pellegrini et al., 2002). Further work has suggested the BRC repeats may form two distinct classes, BRC1-4, which binds free Rad51 with high affinity, and BRC5-8, which strongly interacts with Rad51 once it has bound ssDNA (Carreira and Kowalczykowski, 2011).

Once formed, the Rad51 presynaptic nucleofilament is responsible for capturing the sister chromatid, where it searches within it for a homologous sequence (San Filippo et al., 2008). This is achieved by the ability of Rad51 to hold two DNA molecules in close proximity, a feat attained by formation of a dsDNA binding groove on the exterior of the nucleofilament (Sung et al., 2003). Homology searching by Rad51 seems to be promoted by a direct interaction with Rad54, a protein which translocates along dsDNA and seems to endow the filament with a means of scanning the sister chromatid (Mazin et al., 2010). In addition, once a homologous region has been found, Rad54 promotes the DNA strand exchange activity of Rad51, in which the invading strand base pairs with the homologous template (Cejka et al., 2010). Here, RPA is required to bind and stabilise the displaced strand (Eggler et al.,

2002). Rad54 may then promote dissociation of Rad51 from the nucleofilament, leaving a free 3' end for polymerase-mediated extension (Kiianitsa et al., 2006; Li and Heyer, 2009; Solinger et al., 2002). Synthesis seems to be achieved by DNA pol δ (Lydeard et al., 2007; Maloisel et al., 2008), in association with the replicative PCNA clamp (Li et al., 2009a). In addition, the Pif1 helicase has been found to promote recombination-coupled DNA synthesis, where it allows migration of the replication bubble (Wilson et al., 2013). The RECQ5 helicase may also act to protect the invading strand, where it prevents the formation of new Rad51 filaments (Paliwal et al., 2013).

Second-end capture of the extended invading strand seems to be accomplished by Rad52, which facilitates annealing of this invading strand with the RPA-coated complementary sequence on the second end of the DSB (Nimonkar et al., 2009). The resulting structure, composed of two interlaced DNA strands, is known as a double Holliday junction (Bachrati and Hickson, 2009). The processing of these structures and the formation of two intact dsDNA strands may occur through two mechanisms 'dissolution' and 'resolution' (Matos and West, 2014). Dissolution of the junction results from the ATP-driven convergent migration of the double Holliday junction by the BML RecQ-like helicase, resulting in the formation of a hemicatenane structure. The entangled strands are then cleaved, unwound, and rejoined by Topoisomerase III α , generating two non-crossover dsDNA molecules (Swuec and Costa, 2014). Due to restoration of the two original DNA strands, 'dissolution' is generally the favoured pathway of Holliday junction processing in eukaryotic somatic cells. By contrast, processing by 'resolution', which involves Yen1 and Mus81/Mms4-mediated nucleolytic cleavage at each junction branch point (Blanco et al., 2010; Chan and West, 2015; Ho et al., 2010), may generate either crossover and non-crossover products, depending on the direction in which the junction is cleaved (Lee et al., 2015).

hSSB1 has also been reported to rapidly localise to double-strand DNA breaks (Richard et al., 2008), where it may interact directly with exposed ssDNA (Richard et al., 2011b) and poly(ADP) ribose chains (Zhang et al., 2014). Here, hSSB1 seems to promote the resection of double-strand DNA breaks, most likely by interacting with and stimulating activity of the MRN complex (Richard et al., 2011a) and/or the

EXO1 endonuclease (Yang et al., 2012). hSSB1 also promotes activation of the ATM kinase, as well as subsequent downstream signalling and checkpoint activation (Richard et al., 2008). In addition to these early roles, the persistence of hSSB1 at double-strand DNA breaks for several hours post damage have suggested hSSB1 may also be involved in subsequent steps of homologous recombination, however this remains to be tested (Zhang et al., 2009).

1.5 Human single-stranded DNA-binding protein 1 (hSSB1)

Human single-stranded DNA-binding protein 1 (hSSB1), also known as SOSS [sensor of single-stranded DNA] complex subunit B1 (SOSS-B1; recommended name given by the UniProt Consortium [uniprot.org]) or Oligonucleotide/oligosaccharide-binding fold-containing protein 2B (OBFC2B) is an ~ 22 kDa single-stranded DNA binding protein encoded by the gene *Nucleic acid binding protein 2* (NABP2, *H. sapiens* 12q13.3; approved name and symbol given by the HUGO Gene Nomenclature Committee [genenames.org]). hSSB1 is paralogous with hSSB2 (SOSS-B2/OBFC2A/NABP1; *H. sapiens* 2q32.2), a similarly sized protein with which it shares a common domain structure – a short N-terminus, an evolutionarily conserved oligonucleotide/oligosaccharide-binding (OB) fold and an unstructured, flexible C-terminus (Kang et al., 2006; Richard et al., 2008). The ssDNA-binding function of hSSB1 is facilitated by its OB-fold (Richard et al., 2008), a domain comprised of a cylindrical β -barrel (comprised of five antiparallel β -strands), which is capped at one end by an α -helix originating from between the third and fourth β -strands (Murzin, 1993). In other proteins, these domains interact with ssDNA substrates both through electrostatic interactions with the phosphodiester backbone, as well as by aromatic residue-mediated nucleotide base stacking (Bujalowski et al., 1988; Casas-Finet et al., 1987a; Casas-Finet et al., 1987b; Curth et al., 1993; Gamsjaeger et al., 2013; Khamis et al., 1987a; Khamis et al., 1987b; Lohman et al., 1988; Merrill et al., 1984; Overman and Lohman, 1994; Overman et al., 1988; Raghunathan et al., 2000; Savvides et al., 2004). Consistent with these observations, the recently solved crystal structure of hSSB1 (in complex with SOSSA) demonstrated an interaction with a poly(dT) oligonucleotide via numerous residues lining a groove on one side of the hSSB1-OB fold. This included the aromatic residues tryptophan 55 (W55), phenylalanine 78 (F78) and tyrosine 85

(Y85), each of which was involved in base stacking with various thymine bases (Ren et al., 2014). Furthermore, individual mutation of each of these residues to alanine reduced binding to a dT₆₈ oligonucleotide as assessed by electrophoretic mobility shift assays (EMSA). Interestingly, the crystal structure did not identify tyrosine 74 (Y74), another aromatic residue of the DNA-binding groove, as a likely contributor to DNA-binding. Mutation of this residue did however reduce interaction with the dT₆₈ substrate to a level comparable with the W55A mutant, perhaps indicating its erroneous assignment within the proposed structure, or indirect involvement in DNA binding via another residue (Ren et al., 2014). These results were largely consistent with mutational analysis of murine SSB1 (mSSB1), which demonstrated substantially reduced binding of W55A, Y74A (most prominently) and Y85A mutants to a dT₄₀ substrate (Gu et al., 2013). While these aromatic amino acids are likely to be the major residues involved in hSSB1 DNA-binding, other residues of the OB fold, as well of the N-terminal tail, likely have ancillary DNA-binding roles (Ren et al., 2014). DNA-binding may also be enhanced through an as yet unclear means by the hSSB1 C-terminal tail (Vidhyasagar et al., 2016).

In addition to binding ssDNA, the hSSB1 OB-fold is also important for mediating an interaction with integrator complex subunit 3 (INTS3; also known as SOSS complex subunit A [SOSS-A]), a protein which, together with SOSS complex subunit C (SOSS-C; also known as INTS3- and NABP-interacting protein (INIP) or SSB-interacting protein 1 (hSSBIP1)) constitutes the SOSS1 complex (Huang et al., 2009; Li et al., 2009b; Skaar et al., 2009; Zhang et al., 2009). By contrast, SOSS2 complexes containing hSSB2 may similarly form to the mutual exclusion of hSSB1 (Li et al., 2009b). In addition to mediating the interaction between hSSB1 and SOSS-C, INTS3 may also directly bind integrator complex subunit 6 (INTS6) or its paralogue DDX2b as potential fourth components of SOSS complexes (Zhang et al., 2013). Crystallography data (Ren et al., 2014), as well as earlier mutagenesis studies with mSSB1 (Gu et al., 2013), have demonstrated that hSSB1 may bind ssDNA and INTS3 simultaneously via separate OB-fold interfaces (Figure 1.1), suggesting hSSB1 may function as a scaffold through which the remainder of the complex may associate with DNA. As yet, however, the precise function of the SOSS1 (and SOSS2) complexes in DNA repair processes remains unclear. Indeed, whilst depletion or mutation of any component protein (Huang et al., 2009; Li et al., 2009b;

Ren et al., 2014) has been reported to sensitise cells to double-strand DNA break-inducing compounds, it is unclear whether the complex itself is directly involved in DNA repair. Such studies have further been hampered by the apparent requirement of INTS3 for hSSB1 gene expression, a technical issue that has limited the investigation of INTS3 function by standard siRNA-based approaches, as this would similarly cause depletion of hSSB1 (Skaar et al., 2009).

In addition to DNA repair, hSSB1 and hSSB2 have also recently been suggested to function with INTS3 and other components of the integrator complex to promote mRNA transcriptional termination at RNA polymerase II pause sites (Skaar, et al., 2015). Here, hSSB1 may interact with RNA polymerase II as well as the transcription termination factors NELFB and SPT5, most likely via the association with INTS3. In addition, hSSB1 and hSSB2 were reported to bind the 3' ends of replication-dependent histone genes, as well as the promoter proximal regions of genes with polyadenylated transcripts and to promote proper transcript processing. These data therefore demonstrate additional roles of hSSB1 and hSSB2, suggesting the function of these proteins is not restricted to DNA repair.

1.6 Post-translational regulation of hSSB1

Previous reports have suggested that, in response to ionising radiation-induced double-strand DNA break formation, hSSB1 function may require phosphorylation of threonine residue 117 (T117) (Richard et al., 2008). T117 is a component of an SQ/TQ motif (serine/threonine – glutamine), numerous of which are phosphorylated in other DNA repair proteins by the PI3K-like kinases, ATM, ATR and DNA-PK (Traven and Heierhorst, 2005). Although phosphorylation of T117 remains to be confirmed, and has only been assessed indirectly, the expression of a T117A hSSB1 mutant in cells has been shown to disrupt DNA repair signalling following ionising radiation exposure (Richard et al., 2008). Furthermore, while WT and T117A phosphomutant hSSB1 may associate with FBXL5, the E3 ubiquitin ligase responsible for hSSB1 poly-ubiquitination-mediated degradation, a T117E phosphomimetic hSSB1 reportedly does not (Chen et al., 2014). In addition, T117E hSSB1 may be less strongly ubiquitinated than the WT protein. Indeed, whilst WT hSSB1 protein levels have been suggested to accumulate in cells following double-strand DNA break formation, this may be reduced for T117A hSSB1. These results

suggest that while hSSB1 is relatively labile in cells, T117 phosphorylation may promote protein stabilisation by disrupting association with FBXL5 (Chen et al., 2014).

Although not unambiguously demonstrated, numerous reports have concluded that hSSB1 T117 is most likely phosphorylated by the ATM kinase (Chen et al., 2014; Skaar et al., 2009; Wu et al., 2015; Yang et al., 2012). These conclusions have been drawn from two major observations: 1) Accumulation of hSSB1 protein levels in cells following double-strand DNA break formation is suppressed by inhibition of ATM or by use of ATM deficient cell lines (Chen et al., 2014; Richard et al., 2008). (Chen et al., 2014). 2) hSSB1 may associate with ATM in cells and WT, although not T117A hSSB1, is phosphorylated by immunoprecipitated ATM *in vitro* (Richard et al., 2008). These findings do not however rule out the possibility that hSSB1 T117 may instead be phosphorylated by ATR or DNA-PK. Indeed, both of these kinases also function in response to double-strand DNA break formation and may associate with hSSB1 in cells ((Kar et al., 2015) and section 4.2.4 of this thesis).

Acetylation of hSSB1 lysine 94 (K94) has also recently been reported and was detected both by mass spectrometry and antibody immunodetection (Wu et al., 2015). Here, acetylation seems to be regulated by the opposing actions of the P300 acetyltransferase and the SIRT4 and HDAC10 deacetylases. Similarly to phosphorylation of T117, K94 acetylation was suggested to also stabilise hSSB1 by impairing its ubiquitination and subsequent proteasomal degradation. Furthermore, a hSSB1 K94R mutant was unable to rescue clonogenic survival of hSSB1-depleted cells in response to ionising radiation exposure or treatment with camptothecin.

Various mass spectrometry screens of immunoprecipitated cells have also detected a number of as yet un-validated instances of hSSB1 post-translational modifications and these have been curated on the online database, phosphositeplus (Hornbeck et al., 2015) (**Figure 1.1**).

Figure 1.1

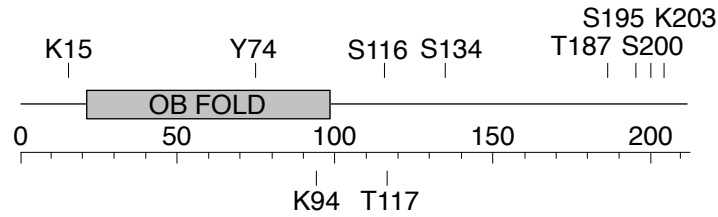


Figure 1.1 hSSB1 post-translational modifications may occur at numerous residues

A schematic of hSSB1 indicating potential sites of hSSB1 serine, threonine or tyrosine phosphorylation, as well as lysine acetylation. Modifications on the residues indicated above the schematic have been detected by mass spectrometry and are curated on the online database phosphositeplus (available at: www.phosphosite.org). Evidence of K94 and T117 acetylation and phosphorylation, respectively, have been published elsewhere and are listed below the hSSB1 schematic.

1.7 Study aims

The current study aims to further elucidate the mechanisms that regulate hSSB1 function in cells.

Specifically, this study aims to:

- 1) Characterise the proteasome-targeting poly-ubiquitination of hSSB1
- 2) Examine the regulation of hSSB1 in the response to replication stress

Chapter 2: Materials and Methods

2.1 *E. coli* strains and preparation of chemically competent cells

One Shot Stbl3 *E. coli* were purchased from Life Technologies (now part of ThermoFisher Scientific, Scoresby, Vic), α -Select Gold *E. coli* were purchased from Bioline (Alexandria, NSW) and Shuffle T7 Express BL21 competent *E. coli* were purchased from New England BioLabs (distributed by Genesearch, Arundel, QLD). Stbl3 or α -Select Gold *E. coli* were used for general plasmid propagation, generation of glycerol stocks and for the transformation of site-directed mutagenesis reactions. Shuffle T7 Express *E. coli* were employed for expression of recombinant protein. *E. coli* were typically grown either in lysogeny broth (Bertani, 1951; Sezonov et al., 2007) (10 g L⁻¹ tryptone, 5 g L⁻¹ yeast extract, 10 g L⁻¹ sodium chloride) or 2XYT liquid medium (Siedler et al., 2014) (16 g L⁻¹ tryptone, 10 g L⁻¹ yeast extract, 10 g L⁻¹ sodium chloride), or on solid LB medium containing 18 g L⁻¹ bacteriological agar. Where appropriate, media was supplemented with 100 μ g mL⁻¹ ampicillin or 50 μ g mL⁻¹ kanamycin. Cultures were typically incubated at 37 °C, or 30 °C for Shuffle T7 Express *E. coli*. Liquid cultures were grown in a shaking incubator set to 220 rpm. Chemically competent *E. coli* were prepared from commercial cells using an adaptation of a previously published protocol (Hanahan et al., 1991). Here, 10 mL of LB media was inoculated with a single colony of commercially prepared *E. coli* and grown overnight in a shaking incubator (220 rpm) at 37 °C. The following day this culture was used to inoculate 500 mL of 2XYT media, which was further grown to ~OD₆₀₀ 0.65. *E. coli* were then centrifuged at 5,000 x g for 10 minutes at 4 °C and re-suspended in 40 mL of cold RF1 solution (100 mM RbCl, 50 mM MnCl₂, 30 mM potassium acetate, 10 mM CaCl₂, 15% w/v glycerol, pH 5.8). Cells were incubated on wet-ice in a 4 °C cold-room for 1 hour, centrifuged as per previously and re-suspended in 7.5 mL cold RF2 (10 mM MOPS, 10 mM RbCl, 75 mM CaCl₂, 15% w/v glycerol, pH 6.8). After 15 minutes incubation at 4 °C, 100 μ L aliquots were snap-frozen in a dry-ice/ethanol bath. Competent cells were stored at -80 °C. Plasmid transformations were performed using a methodology based on standard ‘heat-shock’ protocols (Huff et al., 1990; Nakata et al., 1997). Briefly, an aliquot of chemically competent cells was thawed and 50 μ L incubated on ice with 100-200 ng of plasmid DNA for 30 minutes. Cells were heat-shocked at 42 °C for 45 seconds, and incubated

on ice for a further 10 minutes. 500 μL of LB was then added to each reaction and *E. coli* placed in a shaking incubator at 30 or 37 °C for 1 hour (for ampicillin resistance plasmids) or 2 hours (for kanamycin resistance plasmids) prior to spreading or streaking onto LB agar.

2.2 Plasmids and site-directed mutagenesis

The N-terminal hexa-His-ubiquitin plasmid (pMT107) (Treier et al., 1994), was kindly provided by Ronald T. Hay (University of Dundee). The hexa-His-hSSB1 bacterial expression plasmid has been described previously (Richard et al., 2008) and contains the coding sequence of hSSB1 cloned into the BamHI and Sall restriction sites of pet28A. Stocks of this construct were found to contain a G:C point mutation altering arginine 207 to a threonine residue (R207T). This mutation was restored to wild-type (WT) by site-directed mutagenesis. The 3x FLAG hSSB1 (pCMV6-AN-3DDK) mammalian expression vector (Paquet et al., 2015) was purchased from Origene with the hSSB1 coding sequence cloned into the MluI and AsiSI restriction sites. The coding sequence for the N-terminal 3x FLAG tag was exchanged for that of Myc or HA by inverse PCR with 5' hybridised primers (Figure 2.1). 3x FLAG hSSB1 with a C-terminal HA tag was prepared similarly. A principally similar PCR-based approach for such manipulations has been described previously (Liu and Naismith, 2008). PCR primers are listed in Table 2.1, as well as site-directed mutagenesis primers used to introduce point mutations in the 3x FLAG or hexa-His hSSB1 constructs. Primers were purchased from Sigma-Aldrich (Castle Hill, NSW) or Integrated DNA Technologies (Baulkham Hills, NSW). Site-directed mutagenesis was conducted as described previously (Paquet et al., 2014): AccuPrime Pfx polymerase (0.02 U μL^{-1} ; Life Technologies), 1x AccuPrime Pfx polymerase reaction mix (Life Technologies), primers (0.3 μM) and template (0.8 ng μL^{-1}), then PCR cycling 19x at: 94 °C (20 s), 57 °C (30 s), 68 °C (6 min 30 s). PCR was followed by *Dpn1* (New England Biolabs) digestion (0.8 U μL^{-1} , 2 h, 37 °C) and transformation into chemically competent Stb13 *E. coli*. DNA sequencing (AGRF, St. Lucia, QLD) of the forward strand using the primers VP1.5 (for pCMV6 vectors) or T7 Universal (for PET28 vectors) was used to confirm successful mutagenesis.

Table 2.1 Oligonucleotide primers used for site-directed mutagenesis.

Nucleotides in **Bold** represent mismatches with the target sequence.

Primer Set		Sequence (5'-3')
hSSB1 Phosphorylation Site Point Mutations	S134A	F: CAGCAACCCTTCAGCT GAG CAGCCTACCACTGGAC R: GTCCAGTGGTAGGCTG CTC AGCTGAAGGGTTGCTG
	S134E	F: CAGCAACCCTTCAGCT GAG CAGCCTACCACTGGAC R: GTCCAGTGGTAGGCTG CTC AGCTGAAGGGTTGCTG
	T117A	F: CCAGAGTACAGC G CCCAGCAGGCACC R: GGTGCCTGCTGGG C GCTGTACTCTGG
	T117E	F: CAAACCCAGAGTACAGC GAA CAGCAGGCACCCAACAAG R: CTTGTTGGGTGCCTGCTG TTTC GCTGTACTCTGGGTTTG
hSSB1 Lysine Point Mutations	K8R	F: GGAGACCTTTGTG A GGGATATCAAGCCTGG R: CCAGGCTTGATATCC C TCACAAAGGTCTCC
	K11R	F: CCTTTGTGAAGGATATC A GACCTGGGCTCAAGAATCTG R: CAGATTCTTGAGCCAGG TCT GATATCCTTCACAAAGG
	K15R	F: GATATCAAGCCTGGGCTC A GGAATCTGAACCTTATCTTC R: GAAGATAAGGTTTCAGATT C TGAGCCAGGCTTGATATC
	K31R	F: GCCGAGTGACC A GGACAAAGGACGGG R: CCCGTCCTTTGT C CTGGTCACTCGGC
	K33R	F: GAGTGACCAAGACA A GAGACGGGCATGAGGTTC R: GAACCTCATGCCCGT CTC TTGTCTTGGTCACTC
	K42R	F: GGTTCGGACCTGC A GAGTGGCGGACAAAAC R: GTTTTGTCCGCCACT C TGCAGGTCCGAACC
	K46R	F: CAAAGTGGCGGAC A GAAACAGGCAGCATC R: GATGCTGCCTGTT C TGTCCGCCACTTTG
	K72R	F: GACATTATCCGGCTCACC CGT GGGTACGCTTCAGTTTTTC R: GAAAACCTGAAGCGTACCC ACG GGTGAGCCGGATAATGTC

hSSB1 Lysine Point Mutations	K79R	F: GGGTACGCTTCAGTTTTTCAG GGGG TTGTCTGACACTATAT AC R: GTATATAGTGTCAGACAACCC CCT GAAAACCTGAAGCGTAC CC
	K94R	F: GGGGTGATCTGCAGAG GGATT GGAGAATTCTG R: CAGAATTCTCCAATC CTCT GCAGATCACCCC
	K123R	F: CAGGCACCCAACAG GGGCGGT GCAGAAC R: GTTCTGCACCGCC CTGTT GGGTGCCTG
	K203R	F: CTGTTAGTAACGGCAG GAGAA ACCCGGAGGAG R: CTCCTCCGGGTTTCT CTG CCGTTACTAACAG
	K210R	F: CGGAGGAGCAGCAG GAGAA CGCGTTAAG R: CTTAACCGGTTCTC CTG CTGCTCCTCCG
	K11R (K8R)	F: CTTTGTGAG GGATATC CGGC CTGGGCTCAAGAATC R: GATTCTTGAGCCCAGGC CGGATATC CTC CACAAAG
	K15R (K11R)	F: GATATCAG ACCTGGG CTCAG AAATCT GAACTTATCTTC R: GAAGATAAGGTTTCAGATTT CTG AGCCCAGG TCT GATATC
	K33R (K31R)	F: GAGTGACCAG GACAAG AGACGGGCATGAGGTTTC R: GAACCTCATGCCCGTCT CTTGTCT GGTCACTC
	K46R (K42R)	F: CAGAGTGGCGGACAG GAACAG GCAGCATC R: GATGCTGCCTGTT CTGT CCGCCACT CTG
INTS3-Binding Point Mutations	E97A	F: GATCTGCAGAAGATTGGAG CATTCT GTATGGTTTATTCTG R: CAGAATAAACCATACAGAAT GCTCCA ATCTTCTGCAGATC
	F98A	F: CTGCAGAAGATTGGAGAA GCCT GTATGGTTTATTCTGAG R: CTCAGAATAAACCATACAG GCTTCT CCAATCTTCTGCAG
	E104A	F: CTGTATGGTTTATTCTG CGGTT CCTAACTTCAGTG R: CACTGAAGTTAGGAACCG GAGAATAA ACCATACAG

hSSB1 PAR-Binding Point Mutations	VL23AA	F: CTGAACCTTATCTTCATTG CTGCGG GAGACAGGCCGAGTGA CC R: GGTCACTCGGCCTGTCTCC GCAG CAATGAAGATAAGGTTTC AG
	TG47AA	F: CCTGCAAAGTGGCGGACAAAG GCCGCC CAGCATCAATATCTC TGTC R: GACAGAGATATTGATGCTG GCGGCT TTTGTCCGCCACTTTG CAGG
	WD55AA	F: GCAGCATCAATATCTCTGT CGCCGC CGATGTTGGCAATCT GATCC R: GGATCAGATTGCCAACATCG GCGGC GACAGAGATATTGAT GCTGC
hSSB1 DNA-Binding Aromatic Point Mutations	W55A	F: CAGCATCAATATCTCTGT CGCC GACGATGTTGGCAATCTG R: CAGATTGCCAACATCGT CGGC GACAGAGATATTGATGCTG
	Y74A	F: CCGGCTCACCAAAGGG GCT GCTTCAGTTTTCAAAGG R: CCTTTGAAAACCTGAAGC AGC CCCTTTGGTGAGCCGG
	F78A	F: GGGTACGCTTCAGTT GC CAAAGGTTGTCTGAC R: GTCAGACAACCTTT GGC AACTGAAGCGTACCC
	Y85A	F: CAGTTTTCAAAGGTTGTCTGACACT AGCT ACTGGCCGTGG GG R: CCCACGGCCAGT AGCT AGTGTCAGACAACCTTTGAAAAC TG
	Y74A_F78A	F: TCCGGCTCACCAAAGGG GCC GCTTCAGTT GC CAAAGGTTG TCTGACAC R: GTGTCAGACAACCTTT GGC AACTGAAGCG GCC CCCTTTGGT GAGCCGGA
hSSB1 siRNA-Resistance	hSSB1 siRNA Resistance	F: CAGGCCCGCCTGGCCCTTCT TTCCAATCCCG TTAGTAACGG CAAAGAAAC R: GTTTCTTTGCCGTTACTAAC GGGATTGGA AGAAGGGCCAG GCGGGCCTG

hSSB1 Tag Manipulations	N-term Myc	F: GAACAAAACTTATTTCTGAAGAAGATCTGGCGATCGCCA TGACGACGGAGACC R: CAGATCTTCTTCAGAAATAAGTTTTTGTCCATGGTGGCA GATCTCCTCGGTACCGG
	N-term HA	F: TACCCATACGATGTTCCAGATTACGCTGCGATCGCCATGA CGACGGAGACC R: AGCGTAATCTGGAACATCGTATGGGTACATGGTGGCAGAT CTCCTCGGTACCGG
	C-term HA	F: GCATACCCATACGATGTTCCAGATTACGCATAAGCGGCCG CACTCGAGGTTTAAACGGC R: TGCGTAATCTGGAACATCGTATGGGTATGCCGTTCTCTTG CTGCTCCTCCGGGTTTCTTTGC
Other	M1A	F: GATAAGGCGATCGCC GCC ACGACGGAGACCTTTG R: CAAAGGTCTCCGTCGT GCG GGCGATCGCCTTATC
	pET28A repair	F: GCAAAGAAACCCGGAG GG AGCAGCAAGAGATAG R: CTATCTCTTGCTGCTC CT CCGGGTTTCTTTGC
Sequencing	VP1.5	F: GGACTTTC AAAATGTCTG
	T7 Universal	F: TAATACGACTCACTATAGGG

Figure 2.1

(A) Generation of Point Mutations e.g. hSSB1 siRNA resistance

```

5` - CAGGCCCGCCTGGCCCTTCTTCCAATCCCGTTAGTAACGGCAAAGAAAC - 3`
5` - ...CAGGCCCGCCTGGCCCTTCCAGCAACCCTGTTAGTAACGGCAAAGAAAC ... - 3`
3` - ...GTCGGGCGGACCGGGAAGGTCGTTGGGACAATCATTGCCGTTTCTTTG ... - 5`
3` - GTCGGGCGGACCGGGAAGAAGGTTAGGGCAATCATTGCCGTTTCTTTG - 5`

```

(B) Exchange of Epitope Tags e.g. 3x FLAG hSSB1 to HA hSSB1

```

27 bp (HA Tag)
5` - TACCCATACGATGTTCCAGATTACGCTGCGATCGCCATGACGACGGAGACC - 3`
5` - ...CCGGTACCGAGGAGATCTGCCACCATG ... 78 bp (3x FLAG Tag) ... GCGATCGCCATGACGACGGAGACC ... - 3`
3` - ...GGCCATGGCTCCTCTAGACGGTGGTAC ... CGCTAGCGGTACTGCTGCCTCTGG ... - 5`
5` - GGCCATGGCTCCTCTAGACGGTGGTACATGGGTATGCTACAAGGTTAATGCCA - 5`

```

Figure 2.1 Site directed mutagenesis (SDM) approaches described in section 2.2

(A) Example of SDM primers used for the introduction of point mutations.

Primer pairs were designed with 100% complementarity and containing central mismatches with the template sequence. Primers typically contained 25-45 nucleotides, a G:C content of 30-70% and a melting temperature of ~78 °C. Primers were designed using primerX software (www.bioinformatics.org/primerx/).

(B) Example of SDM primers used for protein epitope tag manipulation.

Primer pairs contained 100% complementary 5' ends encoding the exogenous DNA sequence. Primer 3' ends were 100% complementary to the target sequence, contained 25-30 nt and had a calculated melting temperature of ~76 °C. Primers were visualised using SnapGene Viewer software (from GSL Biotech; available at snapgene.com).

2.3 Cell culture reagents, cell lines and transfections

HeLa, Human Embryonic Kidney (HEK) 293T and U-2 OS osteosarcoma cells were obtained from the American Type Culture Collection (ATCC) and maintained in Roswell Park Memorial Institute (RPMI) 1640 medium + L-glutamine (Sigma-Aldrich) supplemented with 10% foetal bovine serum (FBS; Sigma-Aldrich). All cell cultures were grown at 37 °C, 5% CO₂, in a humidified 2% or 21% O₂ incubator. For clonogenic assays, cell media was further supplemented with 100 U mL⁻¹ penicillin – streptomycin (Life Technologies). Cell cultures were tested for mycoplasma contamination every 2-3 months at the TRI mycoplasma testing facility. Lipofectamine 2000 and Lipofectamine RNAiMAX (Life Technologies) were used for transfection of plasmids and RNAi, respectively, as per the manufacturer's instructions. Typically 1 µg of plasmid and 2 µL of lipofectamine 2000 were used to transfect ~70% confluent cells grown in one well of a 6-well plate. The quantity of DNA and lipofectamine 2000 used was scaled proportionately for larger tissue culture vessels. Stealth or Silencer Select siRNA was purchased from Life Technologies. Lyophilised Stealth siRNA were resuspended to a concentration of 20 µM in DEPC-treated H₂O and transfected at a concentration of 50 nM. A stealth siRNA:lipofectamine RNAiMAX ratio of 0.75 µL:1 µL was typically used. Stealth siRNA negative control med GC (20 µM; Life Technologies) was used as a negative control siRNA. Silencer Select siRNA were resuspended to a concentration of 50 µM

and used at a concentration of 10 nM. A silencer select siRNA:lipofectamine RNAiMAX ratio of 0.9 μL :3 μL was typically used. Silencer select negative control no.1 was used as negative control siRNAs. All transfection solutions were prepared in Opti-MEM reduced serum media (Life Technologies).

Table 2.2 siRNA oligonucleotides used for gene silencing.

Gene target	Chemistry	Sense Sequence (5'-3')	Usage concentration
hSSB1	Stealth	GCCCUUCCAGCAACCCUGU UAGUAA	30 – 50 nM
ATM	Stealth	AGUCUAGUACUUAUGAUC UGCUUA	30 – 50 nM
ATR	Stealth	CAACCUCCGUGAUGUUGCU UGAUUU	30 – 50 nM
DNA-PKcs	Silencer Select	CAAGCGACUUUAUAGCCUU TT	10 nM

2.4 Induction of genotoxic stress and other cell treatments

The genotoxic compounds hydroxyurea, aphidicolin and camptothecin, inhibitors of ribonucleotide reductase (Koç et al., 2004), DNA polymerase α (Krokan et al., 1981) and topoisomerase I (Staker et al., 2002), respectively, were purchased from Sigma-Aldrich. Hydroxyurea was dissolved to 300 mM in RPMI and cells typically treated with a concentration of 3 mM unless otherwise indicated. Aphidicolin was purchased as a 1 mg mL⁻¹ solution in DMSO and cells typically treated with 6 $\mu\text{g mL}^{-1}$. Cells were treated with 2 μM Camptothecin, diluted from a 2 mM stock prepared in DMSO. Cycloheximide, an inhibitor of the 60S ribosomal subunit (Schneider-Poetsch et al., 2010), was also purchased from Sigma-Aldrich. Cycloheximide was dissolved in DMSO to 10 mg mL⁻¹ and cells treated by dissolving 1:200 in media to a final concentration of 50 $\mu\text{g mL}^{-1}$. The 26S proteasome inhibitor MG-132 (Goldberg, 2012) was purchased from Selleck Chemicals (distributed by Jomar Life

Research, Scoresby, Victoria) and used in poly-ubiquitination assays as described in section 2.10. KU-60019, VE-821 and NU7441, inhibitors of ATM, ATR and DNA-PK, respectively, were also purchased from Selleck Chemicals. Each drug was dissolved in DMSO at 5 mM for KU-60019 and NU7441 and 10 mM for VE-821. Cells were treated with each compound diluted 1:1000 in cell culture media. The PPP-family phosphatase inhibitors okadaic acid and calyculin A (Swingle et al., 2007) were purchased from Cell Signaling Technology (distributed by Genesearch) and dissolved in DMSO to concentrations of 1 mM and 100 μ M, respectively. Okadaic acid was added to cells at concentrations of 25 nM or 1 μ M. Calyculin A was added to cells at a final concentration of 50 nM. Double-strand DNA breaks were induced in cells by exposure to ionising radiation using a Gammacell 40 Exactor caesium-source irradiator.

2.5 Clonogenic survival assays and statistical analysis

Clonogenic assays were performed essentially as described previously (Paquet et al., 2015). For these assays, hSSB1 was depleted from HeLa cells by transfection of siRNA targeting the hSSB1 CDS twice, separated by a 24-hour interval. WT or mutant siRNA-resistant 3x FLAG hSSB1 plasmids were then transiently expressed 24 hours later, and after 6 hours, cells seeded at a density of 400 cells per well into wells of a 6-well plate. Wells for three technical repeats were prepared. For clonogenic assays where cells were to be exposed to ionising radiation, cells were seeded in media containing penicillin-streptomycin. Alternatively, cells were seeded in normal media, treated with hydroxurea or ampicillin as indicated, washed with PBS and then penicillin-streptomycin-containing media added. Cells were grown for 10-days post-treatment and then fixed and stained with 4% methylene blue (Sigma-Aldrich) dissolved in methanol. Colonies were manually counted and the surviving fraction at each dose calculated (average number of colonies counted/number of cell seeded) and expressed relative to un-treated cells for each data set. Each assay was performed 3 or 4 times as indicated and results presented as the mean \pm 1 standard deviation (SD). Student's *t* tests were performed to assess statistical significance between data sets using GraphPad Prism version 6 software (GraphPad Software, La Jolla California USA, available: www.graphpad.com). $P < 0.05$ was considered statistically significant.

2.6 Preparation of whole cell lysates, polyacrylamide gel electrophoresis (PAGE) and immunoblotting

Whole cell lysates were prepared by incubation of cells on ice for 30 minutes in Radioimmunoprecipitation buffer (RIPA buffer; 50 mM Tris pH 8.0, 150 mM NaCl, 0.1% SDS, 0.5% sodium deoxycholate, 1% Triton X100) supplemented with 1x phosphatase inhibitor cocktail (Cell Signaling Technology) and 1x protease inhibitor cocktail (Roche, distributed by Sigma-Aldrich; cOmplete, EDTA free). Samples were sonicated (Vibra-Cell, 3 mm probe; Sonics and Materials incBalcstone, QLD), with 3x 3 s bursts (10% output) and clarified by successive centrifugation at 5,000 x g and 21,000 x g, at 4 °C. Protein concentrations were estimated by bicinchoninic acid assay (BCA assay) (Sigma-Aldrich) and comparison to known concentrations of bovine serum albumin (BSA; Sigma-Aldrich). Samples were reduced and denatured by heating at 90 °C for 5 minutes in 1x SDS loading buffer (prepared by addition of 6x SDS loading buffer: 375 mM Tris pH 6.8, 0.12 g mL⁻¹ SDS, 0.03 g mL⁻¹ bromophenol blue, 60% (v/v) glycerol with 20 % (v/v) β-mercaptoethanol added immediately prior to use).

Whole cell lysate (typically 15 µg) was separated by electrophoresis using a 4-12% Bis-Tris Plus Bolt precast gel (Life Technologies), 1x MOPS running buffer (Life Technologies) and run at 165 V for 75 minutes. For immunoblotting, proteins were transferred to nitrocellulose (BioTrace NT, 0.2 µM pore size; Pall corporation) using the XCell II Blot Module (Life Technologies) system, typically in transfer buffer (3 g L⁻¹ glycine, 6 g L⁻¹ Tris, 20% methanol, 0.05% SDS) run at 35 V for 60 minutes. For immunoblotting of ATM, ATR and DNA-PKcs, the above buffer was modified to contain 10 % methanol and 0.01 % SDS and transfer run at 15 V for 16 hours. Membranes were blocked in 2 % v/v fish gelatin (Sigma-Aldrich) prepared in PBS-T and incubated for 2 hours at room temperature with gentle agitation. Membranes were incubated with antibody solutions prepared as indicated in Table 2.3. Incubations were typically performed overnight at 4 °C with agitation, with the exception of the FLAG and actin antibody solutions, which were incubated for 1 hour at room temperature. Membranes were then washed with PBS-T and incubated with IRDye 680RD or 800CW-conjugated donkey anti- mouse, rabbit, goat or rat fluorescent secondary antibodies (Li-Cor, distributed by Millennium Science, Mulgrave, Vic) for 1 hour at room temperature. Membranes were then washed a

second time, and visualised using the Odyssey Imaging System (Li-Cor). Protein molecular weights were determined by comparison to the relative electrophoretic mobility of molecular weight standards (Precision Plus Protein Dual Colour; Bio-Rad). When necessary, immunoblots were quantified using ImageJ software. Phosphorylation of hSSB1 S134 was expressed relative to total immunoprecipitated endogenous hSSB1, or to total 3x FLAG hSSB1, as appropriate. RPA32 phosphorylation was calculated as the relative ratio of the 34 kDa to 32 kDa RPA32 bands.

Sheep-anti-hSSB1 was purified from anti-serum described previously (Richard et al., 2008) using cyanogen bromide beads (Sigma-Aldrich) bound to recombinant His-tagged hSSB1. Recombinant hSSB1 was expressed from T7 BL21 *E. coli* and purified as per below. Cyanogen bromide activated sepharose beads were prepared by swelling in 1 mM HCl for 30 minutes, prior to incubation with recombinant hSSB1 in coupling buffer (0.1 M NaHCO₃, 0.5 M NaCl, pH 8.5). Unreacted cyanogen bromide groups were then blocked by 5 wash cycles of coupling buffer followed by 0.1 M acetate buffer. Beads were subsequently incubated with hSSB1-anti-serum overnight at 4 °C, washed 5x with PBS and antibody eluted with pH 2.8 200 mM glycine. 0.5 mL fractions were collected into tubes containing 13.5 µL 3M Tris-HCl pH 8 and 50 µL 3 M KCl. Antibody-containing fractions were identified by spectrometry at 280 nM, pooled, snap-frozen and stored at -80 °C. To detect pS134 hSSB1, a rabbit polyclonal antibody was raised against the hSSB1 peptide PSA{pS}QPTTGPKC conjugated to the carrier protein keyhole limpet hemocyanin (KLH) by GenScript. 12 weeks after immunization, the antibody was affinity purified using the phosphorylated immunisation peptide. To prevent any non-specific binding of the antibody to non-phosphorylated hSSB1 on an immunoblot, a 200 x molar excess of a control peptide (PSAQPTTGPKC) was included in the antibody working solution. A 200 x molar excess of the phosphorylated immunisation peptides was used for antibody blocking in Figure 4.3. For validation of the antibody, whole cell lysates were dephosphorylated by addition of 200 U of lambda (λ) phosphatase (New England Biolabs) and incubation at 30 °C for 45 minutes.

Table 2.3 Primary antibody usage conditions

	Antigen	Species / Clone/ Cat #	Usage Concentration	Diluent
Cell Signaling Technology (CST)	p-S317 Chk1	Rabbit mAb D12H3 Cat # 12302	WB = 1:500	TBS-T
	p-S345 Chk1	Rabbit mAb 133D3 Cat # 2348	WB = 1:500	TBS-T
	Chk1	Mouse mAb 2G1D5 Cat # 2360	WB = 1:500	Fish Gelatin
	p-T68 Chk2	Rabbit mAb C13C1 Cat # 2197	WB = 1:500	TBS-T
	Chk2	Mouse mAb 1C12 Cat # 3440	WB = 1:500	Fish Gelatin
	RPA32	Rat mAb 4E4 Cat # 2208	WB = 1:500	Fish Gelatin
	DNA-PK_{cs}	Mouse mAb 3H6 Cat # 12311	WB = 1:500	Fish Gelatin
	ATR	Rabbit mAb E1S3S Cat # 13934	WB = 1:500	Fish Gelatin
	p-S1981 ATM	Rabbit mAb D6H9 Cat # 5883	WB = 1:500	TBS-T
	ATM	Rabbit mAb D2E2 Cat # 2873	WB = 1:500	Fish Gelatin

Cell Signaling Technology (CST)	HA	Rabbit mAb C29F4 Cat # 2348	WB = 1:1000	Fish Gelatin
	Myc	Mouse mAb 9B11 Cat # 2276	WB = 1:1000 IP = 1:500	Fish Gelatin IP Buffer
	Nucleolin	Rabbit mAb D4C7O Cat # 14574	WB = 1:1000	Fish Gelatin
	PARP1	Rabbit mAb 46D11 Cat # 9532	WB = 1:1000	Fish Gelatin
	PP2AC	Rabbit pAb Cat # 2038	WB = 1:500	Fish Gelatin
	β-actin	Rabbit mAb 13E5 Cat # 4970	WB = 1:2,500	Fish Gelatin
Abcam	SMARCA5/ SNF2H	Rabbit pAb Cat # ab3749	WB = 1:500	Fish Gelatin
	BAZ1B/ WSTF	Rabbit mAb EP1704Y Cat # ab51256	WB = 1:5000	Fish Gelatin
	MTA2	Rabbit pAb Cat # ab8106	WB = 1:500	Fish Gelatin
	RbAp48/ RBBP4	Rabbit pAb Cat # ab1765	WB = 1:1000	Fish Gelatin

Bethyl	INTS3	Rabbit pAb Cat # A302-050	WB = 1:2000	Fish Gelatin
	FANCI	Rabbit pAb Cat # A300-212	WB = 1:1000	Fish Gelatin
	p-S33 RPA32	Rabbit pAb Cat # A300-246A	WB = 1:1000	TBS-T
Sigma	FLAG epitope	Mouse mAb (M2) Cat # F1804	WB = 1:2000 (1 hour)	Fish Gelatin
BD	Actin	Mouse mAb C4 Cat # 612656	WB = 1:10,000 (1 hour)	Fish Gelatin
Non-commercial	hSSB1	Sheep pAb	WB/IP = 1:500	Fish Gelatin
	pS134 hSSB1	Rabbit pAb	WB = 1:444	TBS-T

2.7 Immunoprecipitation

Cells were resuspended in immunoprecipitation buffer (20 mM HEPES pH 7.5, 150 mM KCl, 5% glycerol, 10 mM MgCl₂, 0.5% Triton X-100) supplemented with 1x phosphatase inhibitor cocktail (Cell Signaling Technology) and 1x protease inhibitor cocktail (Roche, distributed by Sigma-Aldrich; cOmplete, EDTA free), sonicated and quantified as per section 2.6. Protein A or G magnetic dynabeads (Life Technologies) were prepared by incubation with antigen-specific antibodies as indicated in Table 2.3 or with equivalent quantities of mouse, rabbit, or sheep isotype control IgGs for 1 hour at 4 °C. Alternatively, for the precipitation of FLAG-tagged proteins, magnetic anti-FLAG M2 beads (Sigma-Aldrich) were resuspended and

prepared by washing in immunoprecipitation buffer. In either instance, whole cell lysates were incubated with antibody-bound beads from 2 hours to overnight at 4 °C, beads washed 5x with immunoprecipitation buffer and proteins eluted by heating to 90 °C in 3x SDS loading buffer. Whole cell lysates (input) and eluted proteins were immunoblotted as described in section 2.6.

2.8 Subcellular fractionation

Subcellular fractionation was performed using an adaptation of a previously described methodology (Xia et al., 2006). Here, cells were resuspended in Buffer A (20 mM HEPES pH 7.9, 10 mM MgCl₂, 10 nM KCl, 0.05 mM Dithiothreitol (DTT), 0.05% Triton X-100, 1x protease inhibitors 1x phosphatase inhibitors) vortexed at maximum speed for 5 s, then incubated at 4 °C with agitation for 10 minutes before passing through a 26 gauge needle 6 times. Solutions were then centrifuged at 500 x g for 10 minutes at 4 °C and the supernatant (cytoplasmic fraction) discarded. Nuclei were washed once in Buffer A before resuspension in Buffer C (20 mM HEPES pH 7.9, 10 mM MgCl₂, 0.05 mM EDTA, 420 mM NaCl, 25% glycerol, 0.05% Triton X-100, 1x protease inhibitors 1x phosphatase inhibitors). Solutions were vortexed at maximum speed for 15 s, then incubated at 4 °C with agitation for 30 minutes, before centrifugation at 2,000 x g for 10 minutes at 4 °C. Supernatant (soluble nuclear fraction) was collected, and the pellet washed once with Buffer C. The pellet was resuspended in Buffer C containing 4,000 units of micrococcal nuclease, vortexed for 15 s and incubated for 30 minutes at room temperature with agitation. Solutions were centrifuged at 21,000 x g for 10 minutes and the supernatant (chromatin-bound fraction) collected. Fractions were quantified as per section 2.6. For immunoprecipitation from the chromatin-bound fraction, samples were diluted by addition of an equal volume of Buffer A and this sample incubated with antibody-bound beads as per section 2.7.

2.9 Mass spectrometry and data analysis

For the detection of putative hSSB1 phosphorylation sites, 3x FLAG hSSB1 was transiently over-expressed in HEK293T cells for 24 hours and FLAG-tagged proteins immunoprecipitated from 12 mg of whole cell lysate by incubation with magnetic anti-FLAG M2 beads overnight at 4 °C as described in section 2.7. Protein eluent was separated by electrophoresis as described in section 2.6 and the gel stained overnight by gentle agitation in colloidal coomassie brilliant blue G-250 (fixative

solution prepared by dissolving 85 g $(\text{NH}_4)_2\text{SO}_4$ and 15 mL H_3PO_4 in 330 mL H_2O and then adding 165 mL methanol and shaking for 1 hour. 330 mg of coomassie brilliant blue G-250 was separately dissolved in 5 mL methanol to prepare the staining solution. Immediately prior to use, 500 μl of staining solution was added to 24.5 mL of fixative solution). The gel was destained with multiple washes in H_2O and gel bands excised and posted to the BRSC mass spectrometry facility at the University of St. Andrews. Here, gel bands were cut into 1 mm³ slices and subjected to in-gel digestion using a ProGest Investigator in-gel digestion robot (Digilab, Hannover, Germany). Briefly, the gel cubes were destained and washed with acetonitrile then reduced and alkylated before digestion with trypsin at 37 °C. The peptides were extracted with 5% formic acid and concentrated to a volume of 20 μL , using a Savant SpeedVac (Thermo Scientific, part of ThermoFisher Scientific, Paisley PA4 9RF, UK). Peptides were then separated on an Acclaim PepMap 100 C18 trap and an Acclaim PepMap RSLC C18 column (ThermoFisher Scientific), using a nanoLC Ultra 2D plus loading pump and nanoLC AS-2 autosampler (Eksigent, Dublin, CA, USA). A quarter (5 μL) of the sample was loaded. Peptides were eluted with a gradient of increasing acetonitrile, containing 0.1 % formic acid (5-40% acetonitrile in 5 min, 40-95% in a further 1 min, followed by 95% acetonitrile to clean the column, before re-equilibration to 5% acetonitrile). The eluate was sprayed into a TripleTOF 5600 electrospray tandem mass spectrometer (ABSciex, Cheshire WA1 1RX, UK) and analysed in Information Dependent Acquisition (IDA) mode, performing 250 msec of MS followed by 150 msec MS/MS analyses on the 15 most intense peaks seen by MS. The MS/MS data file generated was analysed using the Mascot algorithm (Matrix Science) against the NCBI non-redundant database July 2014 with no species restriction, trypsin as the cleavage enzyme, carbamidomethyl as a fixed modification of cysteines and methionine oxidation, deamidation of glutamines and asparagines and phosphorylation of serine, threonine and tyrosine as variable modifications. The raw mass spectrometry data and Mascot search files have been deposited to the ProteomeXchange Consortium via the PRIDE partner repository (Vizcaíno et al., 2016) with the dataset identifier PXD003964

For the identification of proteins that associate with hSSB1, chromatin-bound proteins were isolated from HeLa cells as described in section 2.8 and hSSB1

immunoprecipitated by incubation with antibody-bound Dynabeads overnight at 4 °C as described in section 2.7. Eluent was then submitted to the TRI proteomics facility and was separated on a 10% acrylamide Mini-PROTEAN TGX precast SDS-PAGE Gel (Bio-Rad, Gladesville, NSW) to a depth of 8 mm. The gel was stained with colloidal coomassie brilliant blue G-250 as per above and the sample divided in eight 1 mM gel bands. Here in-gel digestion was performed using an Agilent Bravo automated liquid handling platform (Agilent Technologies, Mulgrave, Victoria) to achieve the following: 90 minutes incubation in de-stain buffer (50% v/v acetonitrile, 25 mM NH₄HCO₃), dehydration for 10 minutes using a SpeedVac, 20 minutes incubation in alkylation buffer (50 mM iodoacetamide), overnight trypsin digestion (0.4 µg trypsin, 10% acetonitrile, 25mM NH₄HCO₃), trypsin inactivation with 5% formic acid and peptide elution in extraction buffer (1% formic acid, 60% acetonitrile). Peptides were dried using a SpeedVac, resuspended in 5% formic acid and analysed using an Agilent HPLC CHIP QTOF 6530 system (Agilent Technologies). Peptides were loaded onto an Agilent (Agilent Technologies) G4240-62010 large capacity chip in a solution containing 0.1% formic acid and 90% acetonitrile with a flow rate of 2.5 µl min⁻¹. Peptides were separated with a gradient of 0.1% formic acid and 90% acetonitrile to 0.1% formic acid excluding acetonitrile. The MS1 analyzer acquired ions from 100m/z to 1700m/z at a rate of 10 spectra/s. The MS2 analyzer acquired ions from 50m/z to 1700m/z at a rate of 3spectra/s. A maximum of 10 precursors were selected per cycle and ions were excluded after 1 spectra and released after 15 s. Data obtained in this way was processed using Spectrum Mill (Agilent technologies, B.04.00.127) and extracted data searched against the Swiss-Prot Human (version 11/2014) database. Search parameters included trypsin digestion, carbamidomethyl as a fixed modification of cysteine residues and methionine oxidation.

2.10 Poly-ubiquitination assay using hexa-His-tagged ubiquitin

HEK293T cells were grown to ~70% confluence in 75 cm² flasks before co-transfection with equal quantities of a 3x FLAG hSSB1 expression vector and a plasmid encoding hexa-His tagged ubiquitin. Cells were grown for a further 24 hours and treated with 25 µM of the proteasome inhibitor MG132 for 4 hours. Cells were then harvested and lysed in 500 µL urea buffer (8 M urea, 20 mM sodium phosphate pH 7.8, 500 mM NaCl, 20 mM imidazole). Whole cell lysates were then sonicated

and quantified as per section 2.6. 20 μL of HIS-select HF nickel agarose beads (40 μL slurry; Sigma-Aldrich) were prepared by washing 2x in denaturing binding buffer and added to 1000 μg of total cell lysates and incubated at room temperature with gentle agitation for 1-2 h. Beads were then washed 5x with urea buffer and protein eluted by heating to 90 $^{\circ}\text{C}$ in 3x SDS loading buffer. Whole cell lysates (input) and eluted proteins were immunoblotted as described in section 2.6.

2.11 Protein purification

Shuffle T7 *E. coli* were transformed with plasmids encoding hexa-His tagged hSSB1 and grown in 1 L of LB media at 30 $^{\circ}\text{C}$. Cultures were grown to OD_{600} 0.6-0.8 and protein expression induced overnight at 16 $^{\circ}\text{C}$ by addition of 0.3 mM IPTG. *E. coli* were harvested by centrifugation at 5,000 x g for 10 minutes and cell pellets resuspended in 1x breaking buffer (50 mM Tris pH 7.5, 10 % sucrose, 10 mM EDTA, 600 mM KCl, 1 mM DTT, 1mM phenylmethylsulfonyl fluoride (PMSF) + 1x protease inhibitor cocktail) and lysed by sonication (10 x 20 s). IGEPAL was then added to a final concentration of 0.01% and the lysate clarified by centrifugation at 17,000 x g for 25 minutes at 4 $^{\circ}\text{C}$, following by 100,000 x g for 1 h at 4 $^{\circ}\text{C}$. During this time, 500 μL of HIS-Select Nickel Affinity Gel (Sigma-Aldrich) was prepared by washing 3x in PBS. Beads were then incubated with the lysate at 4 $^{\circ}\text{C}$ for 2 h. Slurry was poured onto a gravity chromatography column (Bio-Rad), and washed 2x with 10 packed bead volumes of buffer K (1 M KCl, 0.01% IGEPAL, 20 mM Imidazole). Protein was then eluted with 5x 1000 μL additions of buffer K + 250 mM Imidazole) and concentrated to a volume of 250 μL using a 10 kDa cut-off Vivaspin column (GE Healthcare; Silverwaterm NSW). This volume was loaded onto a Superdex 200 size exclusion chromatography column (GE healthcare) and run in buffer K containing 300 mM KCl, using an AKTA FPLC (GE healthcare). 0.5 mL fractions were collected and those containing the target protein identified by separating 10 μL of sample on a PAGE gel as described in section 2.6 and staining with coomassie blue (1 g L^{-1} coomassie brilliant blue G-250, 50% v/v methanol, 10% v/v glacial acetic acid, 40% H_2O ; the solution was stirred for 3-4 hours and then filtered through Whatman filter paper) for 2 hours with agitation at room temperature. Gel was then de-stained overnight in de-stain buffer (50% v/v methanol, 10% v/v glacial acetic acid, 40% H_2O). Fractions containing hSSB1 with little contamination were pooled, concentrated as per above, aliquoted, snap frozen in dry-

ice/ethanol and stored at -80 °C. The concentration of fully reduced hSSB1 was initially determined by spectrometry at 280 nM and then relative to other samples by electrophoresis and staining with coomassie blue.

2.12 *In vitro* DNA-PK kinase assays

10 U of DNA-PK (DNA-PKcs/Ku70/Ku80) purified from HeLa cells (Promega, Alexandria, NSW) was incubated with 500 ng of hexa-His hSSB1 in 50 µl of kinase buffer (20 mM HEPES, 50 mM NaCl, 10 mM MgCl₂, 10 mM MnCl, 1 mM DTT) containing 100 µM ATP (Sigma-Aldrich) and 10 µg mL⁻¹ sonicated salmon sperm DNA (Life Technologies). Reactions were incubated for 30 minutes at 30 °C and then stopped by addition of 1x SDS loading buffer containing 20% β-mercaptoethanol. Reactions were heated to 90 °C for 10 minutes and eluent analysed by immunoblotting as per section 2.6.

2.13 One dimensional nuclear magnetic resonance spectroscopy (1D-NMR)

Approximately 100-200 µM of WT, S134A or S134E hexa-His hSSB1 was resuspended in NMR buffer (20 mM Tris pH 6.9, 100 mM NaCl, 1 mM EDTA, 1 mM TCEP) with 10% ²H₂O and analysed at 298 K on a Bruker 600 Mhz spectrometer (Bruker Avance III; Bruker, Preston, VIC) equipped with a 5-mm TCI cryoprobe. Proton chemical shifts are references to 4,4-dimethyl-4-silapentanesulfonic acid (DSS) at 0 ppm. Data were processed using Topspin software (Bruker). These experiments were performed by Dr Roland Gamsjaeger at the University of Western Sydney

2.14 Electrophoretic mobility shift assays (EMSA)

FAM (6-Carboxyfluorescein)-labelled oligonucleotides were purchased from Integrated DNA Technologies (IDT). The fork substrate has been described previously (Marini and Krejci, 2012). The FAM-labelled ssDNA strand of this substrate was used as the ssDNA oligonucleotide in the EMSA assays. Substrates were annealed and purified as previously described (Prakash et al., 2009). Briefly, oligonucleotides were firstly purified on 12 % polyacrylamide, 8 M urea gels. Following electroelution, equimolar quantities of oligonucleotides were mixed in hybridization buffer (50 mM Tris pH 7.5, 100 mM NaCl, 10 mM MgCl₂), heated at 99 °C for 10 minutes and slowly cooled down to room temperature. Annealed structures were purified on a 10% polyacrylamide gel, electroeluted and concentrated

using EMD Millipore *Amicon Ultra-4* centrifugal filter units with a 3 kDa cut-off. Concentrations were determined using absorbance at 260 nm and the oligonucleotide molar extinction coefficients ($\epsilon_{\text{fluorescein},260} = 13,700 \text{ L mol}^{-1} \text{ cm}^{-1}$). For EMSA assays, increasing concentrations of hSSB1 (0, 0.05, 0.1, 0.25, 0.5, 0.75, 1.0, 2.0 μM) were incubated with 10 μmol of FAM-labelled synthetic substrates, in 10 μL of binding buffer (50 mM Tris-HCl pH 7.5, 100 mM KCl, 100 $\mu\text{g mL}^{-1}$ BSA, 1 mM DTT) for 15 minutes at 37 °C. Samples were electrophoresed on 10% polyacrylamide gels and visualized using a Starion FLA-9000 image scanner (GE Healthcare). Non-linear regression analysis was performed using the GraphPad Prism version 6 software and the equation ‘one site: specific binding with Hill slope’.

2.15 pS/T-Reader protein domain array

Proteins microarrays were prepared and utilised as previously described (Espejo et al., 2002) by the “protein array and analysis core” at the University of Texas MD Anderson Cancer Center. Briefly, glutathione S-transferase (GST)-tagged proteins were arrayed onto a glass slide pre-coated with nitrocellulose (FAST Slide; Schleicher and Schuell Bioscience; NH, USA) using an Aushon 2470 Arrayer (Aushon BioSystems, MA, USA) with a 24 pinhead. GST-tagged proteins are given in Figure 4.10. The protein chips contained 20 grids allowing up to 9 GST-tagged proteins to be spotted onto each chip in duplicate, as well as GST alone that was spotted in the middle of each chip. N-terminal biotinylated peptides were synthesised by Sigma-Aldrich of sequence Biotin-KAVQNDSNPSASQPTTGPS and Biotin-KAVQNDSNPSA{pSer}QPTTGPS, representing hSSB1 amino acids K123 to S141. 10 μg of each peptide was pre-bound with 5 μL of Cy3-streptavidin (Amersham, GE Life Sciences, PA, USA) in PBS containing 0.1% Tween 20. The solution was then incubated with 20 μL of biotin agarose beads (Sigma-Aldrich) to capture any free Cy3-streptavidin label. Arrayed slides were blocked in PBS-T containing 3% powdered milk (w/v) then incubated with the Cy3-labeled peptide for 1 hour at room temperature. Alternatively, the array was probed with an anti-GST primary antibody, which was then detected with a Fluorescein isothiocyanate (FITC)-conjugated secondary antibody. Slides were washed three times with PBS-T, air dried and scanned with a GenePix 4400A microarray scanner using a 550 nm long pass filter (Molecular Devices; CA, USA).

Chapter 3: Identification of hSSB1 Post-Translational Modifications

3.1 Introduction

Ubiquitination is a post-translational modification whereby a ubiquitin peptide protein is covalently conjugated to (predominantly) lysine residues of a target substrate protein (Li and Ye, 2008). This process occurs through the concerted function of three types of enzymes, generically referred to as E1, E2 and E3 (Komander, 2009). Here, the E1 ubiquitin-activating enzyme initially binds the ubiquitin peptide via an ATP-dependent reaction, forming a thioester bond with the ubiquitin c-terminal carboxyl group. Ubiquitin is then transferred from the E1 to an E2 conjugating enzyme via a trans-thiolation reaction. In the final step, the ubiquitin peptide c-terminal carboxyl group is covalently attached to the ϵ -amino group of a substrate lysine residue, in a reaction mediated by an E3 ubiquitin ligase (Metzger et al., 2012). The E3 enzyme is responsible for substrate specificity, which it ensures by binding and aligning both the E2-ubiquitin thioester and the correct protein substrate (Berndsen and Wolberger, 2014). To enable this high specificity, human cells encode ~600 E3 enzymes (1-2% of all human genes), which work in concert with fewer than 40 E2 and only 2 E1 enzymes (Li et al., 2008). Of the ~600 E3 ligases, 95% belong to the really interesting new gene (RING) domain family, which function to direct the transfer of ubiquitin from the E2 to the substrate protein. By contrast, the remaining ~30 E3 ligases predominantly belong to the homologous to the E6AP carboxyl terminus (HECT) domain family, which mediate ubiquitin transfer through a two-step mechanism. Here, ubiquitin is covalently bound to a ligase active site cysteine, prior to subsequent transfer to the substrate protein (Metzger et al., 2012).

Proteins may be modified by mono-ubiquitination, the attachment of a single ubiquitin peptide on one or more residues, however many are also poly-ubiquitinated (Sadowski and Sarcevic, 2010). In this process, the ubiquitin molecule covalently attached to a substrate is further ubiquitinated at one of seven lysine residues, forming a di-ubiquitin chain. Longer, linear polymers can also form by successive ubiquitination of the terminal ubiquitin molecule, as can branched chains, formed at multiple ubiquitin lysine residues (Sadowski and Sarcevic, 2010). A poly-ubiquitin

chain topology that has been thoroughly studied results from the successive linkage of ubiquitin lysine residue 48 (K48). Here, the generation of K48-linked chains of 4 or more ubiquitin molecules in length appears to be the primary signal for proteasomal degradation (Thrower et al., 2000). The eukaryotic 26S proteasome is a large protein structure composed of a cylindrical 20S core particle, which is capped at either end by 19S regulatory particles (Husnjak et al., 2008). Detection of K48-linked ubiquitin chains is mediated by the 19S components, which contains the receptor proteins RPN10 and RPN13 (Husnjak et al., 2008; Schreiner et al., 2008). Binding to the 19S cap stimulates ATP-dependent conformational changes in the 20S particle, allowing accessibility of the substrate protein to the inner catalytic cavity (Bech-Otschir et al., 2009). Entry however first requires removal of the poly-ubiquitin chain, catalysed by the 19S de-ubiquitinating enzymes (DUBs), Usp14, Uch37 and Rpn11 (Finley, 2009). This thereby allows recycling of the ubiquitin peptides, whilst exposing the target protein to the proteolytic enzymes of the 20S inner chamber. Proteolysis is here provided by the 20S β 1, β 2 and β 5 subunits, which possess chymotrypsin-like, trypsin-like and caspase-like activities, respectively (Xie, 2010).

Unlike K48 chains linkages, other poly-ubiquitination topologies, as well as mono-ubiquitination, do not seem to similarly mark proteins for proteasomal degradation. Instead, these modifications facilitate a wide range of other processes, including intracellular signalling, the mediation of protein-protein interactions and endosomal trafficking to the lysosome (Nathan et al., 2013). Indeed, whilst the RPN10 and RPN13 proteasome ubiquitin receptors can also detect K63-linked ubiquitin chains *in vitro* (Peth et al., 2010), these chains may be more rapidly bound by proteins of the endosomal sorting complex required for transport (ESCRT) pathway (Nathan et al., 2013; Williams and Urbé, 2007). In addition, whilst K48-linked ubiquitinated protein are ‘shuttled’ to the proteasome by Rad23, this protein seems to have little affinity for other chain types (Nathan et al., 2013).

A potential role for K48-linked poly-ubiquitination in the regulation of hSSB1 was initially suggested based on the observation that hSSB1 protein levels are elevated following treatment of cells with the proteasome inhibitor, MG132 (Richard et al., 2008). This compound, a small hydrophobic peptide (carbobenzyl-Leu-Leu-Leu-

aldehyde), is able to penetrate cell membranes and by virtue of its aldehyde group, inhibit the chymotrypsin-like active sites of the 20S proteasome (Goldberg, 2012). hSSB1 protein levels were also seen to increase in cells following exposure to ionising radiation, which was not further enhanced by proteasomal inhibition. It was therefore interpreted that hSSB1 is most likely maintained at low-levels in undamaged cells by proteasomal degradation, presumably as a consequence of K48-linked poly-ubiquitination (Richard et al., 2008). Poly-ubiquitination of hSSB1 was later directly demonstrated through nickel agarose pull-down assays, performed from cells transiently expressing hexa-histidine tagged ubiquitin (Chen et al., 2014). Here, ubiquitination of hSSB1 seems to be mediated by Skp1-Cul1-F-box (SCF) complexes containing the F-box protein, FBXL5 (Chen et al., 2014).

Despite progress in the characterisation of hSSB1 ubiquitination, the residues of hSSB1 modified in this way have remained elusive. In this chapter, site-directed mutagenesis was employed to prepare single and combination hSSB1 lysine-to-arginine mutant proteins and ubiquitination of these assessed using hexa-His-ubiquitin pull-down assays. In the final section of the chapter, mass spectrometry was employed and while not providing further information regarding sites of hSSB1 ubiquitination, identified numerous potentially phosphorylated serine and threonine residues that are of relevance to the following chapter.

3.2 Results

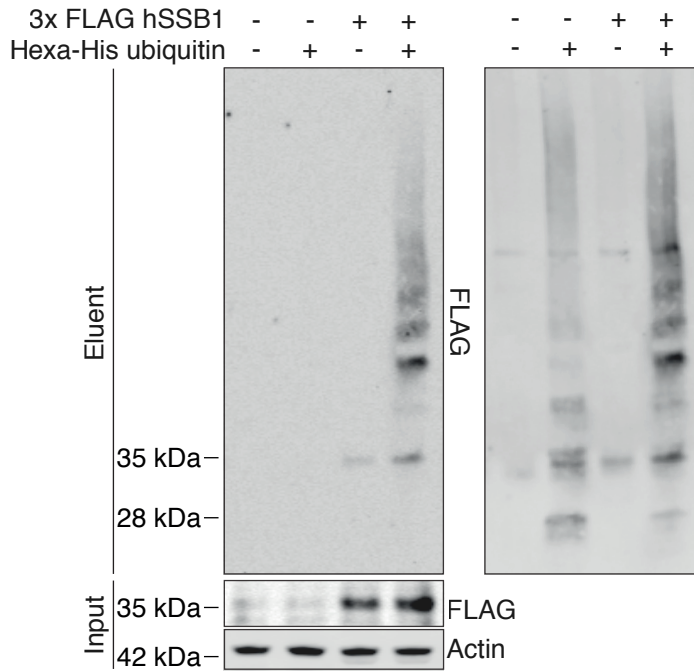
3.2.1 Poly-ubiquitinated hSSB1 may be detected following nickel agarose pull-down of hexa-histidine tagged ubiquitin

Regulation of hSSB1 by poly-ubiquitination-mediated targeting to the proteasome was initially suggested based on the protein accumulation observed in cells treated with the proteasome inhibitor MG132 (Richard et al., 2008). It was therefore of initial interest to directly demonstrate the ubiquitination of hSSB1 in cells. His-ubiquitin pull-down assays are one of the most commonly employed techniques for such purposes and involve the capture of ubiquitinated proteins on nickel agarose beads (Ehrlund et al., 2009). To employ this technique, HEK293T cells were co-transfected with plasmids encoding 3x FLAG hSSB1 and N-terminal hexa-His-tagged ubiquitin. These constructs were expressed for 24 hours prior to the treatment of cells with 25 μ M MG132 for 4 hours. Cells were then harvested and resuspended in a buffer containing 8 M urea, which functioned both to lyse cells, as well as to denature cellular de-ubiquitinating enzymes (DUBs). Whole cell lysates were then incubated with Ni-NTA agarose beads for 2 hours to capture hexa-His-tagged ubiquitinated proteins, prior to elution in SDS loading buffer. Proteins were then immunoblotted and probed with antibodies against hSSB1 and the FLAG epitope (**Figure 3.1A**). Using either antibody, a number of distinct hSSB1 bands were detected that were specific to those lanes in which cells had been transfected with hexa-His tagged ubiquitin. It should be noted that, consistent with prior findings (Chen et al. 2014), non-ubiquitinated hSSB1 was also found to bind Ni-NTA agarose, most likely due to non-specific electrostatic interaction.

As the assay above suggested that hSSB1 was most likely poly-ubiquitinated, it was of interest to consider on which lysine residue this may occur. As a preliminary assessment of the likelihood of each residue being modified, the amino acid sequence of a number of hSSB1 homologues from a variety of animal species were retrieved and aligned (**Figure 3.1B**). A high level of conservation was however observed for each lysine residue (at least 8 of 9 sequences) and indeed only in the *Danio rerio* (Zebrafish) SSB1 protein was any variation in terms of number and position of lysine residues observed in relation to the *Homo sapiens* sequence.

Figure 3.1

A



B

```
Homo.sapiens      -----MTTETFWKDIKKPKGLKKNLNLIFIVLETGRVTKKDKGHEVRTCKVADKIKGSGINISVW  55
Papio.anubis     -----MTTETFWKDIKKPKGLKKNLNLIFIVLETGRVTKKDKGHEVRTCKVADKIKGSGINISVW  55
Mus.musculus     -----MTTETFWKDIKKPKGLKKNLNLIFIVLETGRVTKKDKGHEVRTCKVADKIKGSGINISVW  55
Sus.scrofa       -----MTTETFWKDIKKPKGLKKNLNLIFIVLETGRVTKKDKGHEVRTCKVADKIKGSGINISVW  55
Canis.lupus      -----MTTETFWKDIKKPKGLKKNLNLIFIVLETGRVTKKDKGHEVRTCKVADKIKGSGINISVW  55
Python.bivittatus -----MTTETLVKDKIKKPGMKLNLNLIFIVLETGRVTKKDKGHEVRTCKVADKIKGSGINISVW  55
Chrysemys.picta  -----MTTETFWKDIKKPKGLKKNLNLIFIVLETGRVTKKDKGHEVRTCKVADKIKGSGINISVW  55
Xenopus.laepis   -----MTTETFWKDVKPKGLKKNLSVLFIVLETGRVTKKDKGHEVRTCKVADKIKGTINISVW  55
Danio.erio       MSNISNEAVILIKDVKPGSKNLNIVFVLEIGRVTKKDKGHEVRSRVAIKKSGSIAISVW  60
                  :  :::** ** ** **:::***** *****:*****::** **
                  :  :::** ** ** **:::***** *****:*****::** **

                  72 79 94
Homo.sapiens     DDVGNLIQPGDI IRLTKGYASVFKK ECLTLYTGRGGDLCKI GEFMCMVYSEVPNFSEPNPEY  115
Papio.anubis     DDVGNLIQPGDI IRLTKGYASVFKK ECLTLYTGRGGDLCKI GEFMCMVYSEVPNFSEPNPEY  115
Mus.musculus     DDVGNLIQPGDI IRLTKGYASVFKK ECLTLYTGRGGDLCKI GEFMCMVYSEVPNFSEPNPEY  115
Sus.scrofa       DDVGNLIQPGDI IRLTKGYASVFKK ECLTLYTGRGGDLCKI GEFMCMVYSEVPNFSEPNPEY  115
Canis.lupus      DDVGNLIQPGDI IRLTKGYASVFKK ECLTLYTGRGGDLCKI GEFMCMVYSEVPNFSEPNPEY  115
Python.bivittatus DDVGNLIQPGDI IRLTKGYSSIFK ECLTLYTGRGGDLCKI GEFMCMVYSEVPNFSEPNPEY  115
Chrysemys.picta  DDVGNLIQPGDI IRLTKGYASIFK ECLTLYTGRGGDLCKI GEFMCMVYSEVPNFSEPNPEY  115
Xenopus.laepis   DEVGNFIQPGDI IRLTKGYASLIFK ECLTLYTGRGGDLCKI GEFMCMVYSEVPNFSEPNPEY  115
Danio.erio       DELGSLIQPGDI IRLTRGYASIKK ECLTLYTGRGGDLCKI GEFMCMVYSEVPNFSEPNPEL  120
                  : : * . : *****: * . : *****: *****: *****: *****
                  : : * . : *****: * . : *****: *****: *****: *****

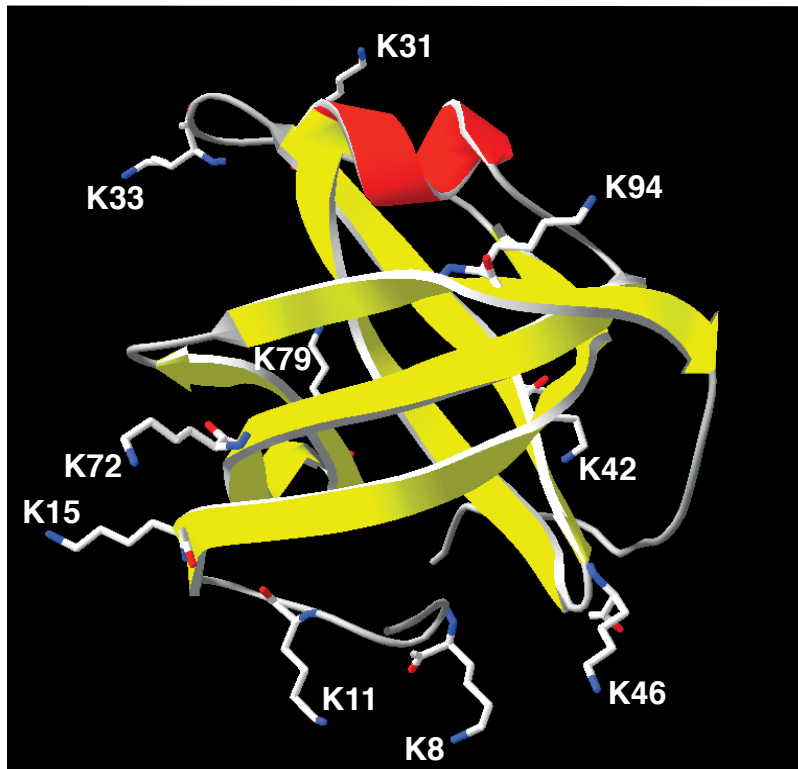
                  123
Homo.sapiens     STQQAPNRAVQN-DSNPSASQPTTGPSAASPASENQNGNGLSAPPGPGGGHPHPTPSHP  174
Papio.anubis     STQQTPNRAVQN-DSNPSASQPTTGPSAASPASESQNGNGLSAPTGPGGGHPHPTPSHP  174
Mus.musculus     NTQQAPNRAVQN-DSNPNNSPTAPQATTGPPAASPASENQNGNGLSTQLGPGVGGHPHPTPSHP  175
Sus.scrofa       SAQQAPNRAVQN-DSSPTAPQPATGPPAASPASESQNGNGLSAPPGPGGGHPHPTPSHP  174
Canis.lupus      SAQQAPNRAVQN-DSSPTAPQPATGPPAVSPAENQNGNGLSAPPGPGGGHPHPTPSHP  174
Python.bivittatus VAQQSQNRAVQN-DSSPTAPQPATGPPAASPASESQNGNGLSAPPGPGGGHPHPTPSHP  173
Chrysemys.picta  VTQQSQNRAVQN-DSSPTAPQPATGPPAASPASESQNGNGLSA-PGPGAPPHPHPTPSHP  174
Xenopus.laepis   TAQQSQNRAVQN-DSSPTAPQPATGPPAASPASESQNGNGLSAPPGPGGGHPHPTPSHP  170
Danio.erio       LAQANQNKTSKEQRGNSPP-----NQNAGNGTVVPSNNNAAPVPRDPNPF  167
                  : * . : . : : : : : : : : : : : : : : : : : : : : : * .

                  203 210
Homo.sapiens     PSTRI TRS----QPNTHPAGPPG--PSSNPVSNCKE TRRS SKR  211
Papio.anubis     PSTRI TRS----QPNTHPAGPPG--PSSNPVSNCKE TRRS SKR  211
Mus.musculus     PSTRI TRS----QPNTHPAGPPG--PSSNPVSNCKE TRRS SKR  212
Sus.scrofa       PSTRI TRS----QPNTHPAGPPG--PSSNPVSNCKE TRRS SKR  211
Canis.lupus      PSTRI TRS----QPNTHPAGPPG--PSSNPVSNCKE TRRS SKR  211
Python.bivittatus TSGRI TRS----QPNTHQGSSSSGIGSSSNPVSNCKE TRRS SKR  212
Chrysemys.picta  TSGRI TRS----QPNTHQAGSAGSSSSSSPISNCKE TRRS SKR  213
Xenopus.laepis   TSGRI TRS----QPNTSLPGAP-----NSVSNCKE PRRT CKR  203
Danio.erio       ASGRPNGRAPGNPPTVAGGTPAPPKPTVSI SNRDP RRAS CKR  211
                  * * . * . : : : : : * : : : : *
```

continued over page

Figure 3.1

C



D

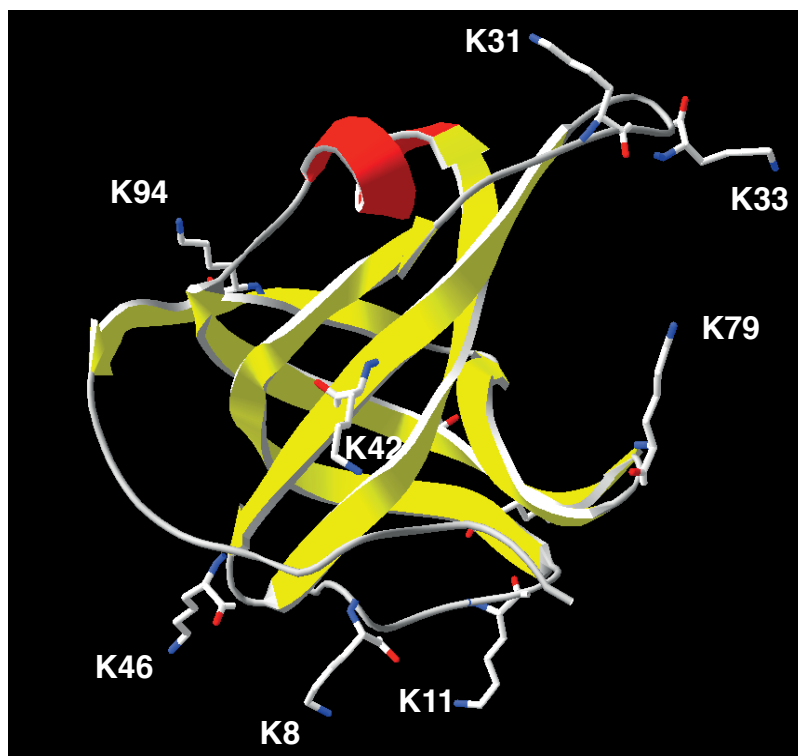


Figure legend over page

Figure 3.1 hSSB1 is poly-ubiquitinated at an unidentified residue

(A) Detection of poly-ubiquitinated hSSB1. HEK293T cells were co-transfected with plasmids encoding 3x FLAG hSSB1 and hexa-His tagged ubiquitin and expressed for 24 h. Cells were treated with 25 μ M MG132 for 4 hours, harvested, and lysed in a buffer containing 8 M urea. 1000 μ g of whole cell lysate was incubated with 20 μ L of Ni-NTA agarose beads for 2 hours at room temperature, washed 3x with 8 M urea and eluted by heating to 90 $^{\circ}$ C for 10 minutes in SDS loading buffer. Eluent was immunoblotted and probed with antibodies against the FLAG tag and hSSB1. 15 μ g of whole cell lysate (input) was immunoblotted and probed with antibodies against the FLAG tag and actin. These results are representative of three independent experiments.

(B) hSSB1 lysine residues are conserved amongst animal species. Amino acid sequences of proteins homologous to hSSB1 from the indicated species were retrieved and aligned using Clustal Omega software ([ebi.ac.uk /Tools/msa/clustalo/](http://ebi.ac.uk/Tools/msa/clustalo/)). Lysine residues are outlined by rectangles with numbers corresponding to the hSSB1 protein sequence. Amino acids of the OB-fold are underlined. Consensus symbols given below each row should be interpreted as: * = a fully conserved residue, : = conservation between groups of strongly similar properties, . = conservation between groups of weakly similar properties.

(C and D) hSSB1 lysine residues are surface-exposed. hSSB1 X-ray diffraction crystal structure PDB file 4OOW (Ren et al., 2014) (downloaded from RCSB PDB; rcsb.org) was modelled and visualised using Swiss-PdbViewer software (spdv.vital-it.ch). This file comprises hSSB1 residues T5 to P111 (primarily the N-terminus and OB-fold shown), as well as INTS3 residues R35 to C497, SOSS-C residues G62 to R100 and 6 nucleotides of ssDNA (not shown). The hSSB1 protein structure is shown as a ribbon diagram and is coloured by secondary structure (red = helices, yellow = beta-sheet, grey = unstructured). Lysine residues are shown as three-dimensional wireframe models including the backbone oxygen and are labelled and CPK coloured (white = hydrogen, blue = nitrogen, red = oxygen). Two views are given (C vs D) where the model was rotated 180 $^{\circ}$ around the Y-axis.

As the essentially complete conservation of SSB1 lysine residue prevented the exclusion of poorly conserved and therefore unlikely sites of ubiquitination, the hSSB1 crystal (containing amino acids 5-111) was instead visualised with the prospect that certain amino acids could instead be excluded based on their lack of apparent accessibility (**Figure 3.1C and D**). This modelling however indicated that each hSSB1 lysine side-chain is likely to be surface exposed and therefore may be available for modification.

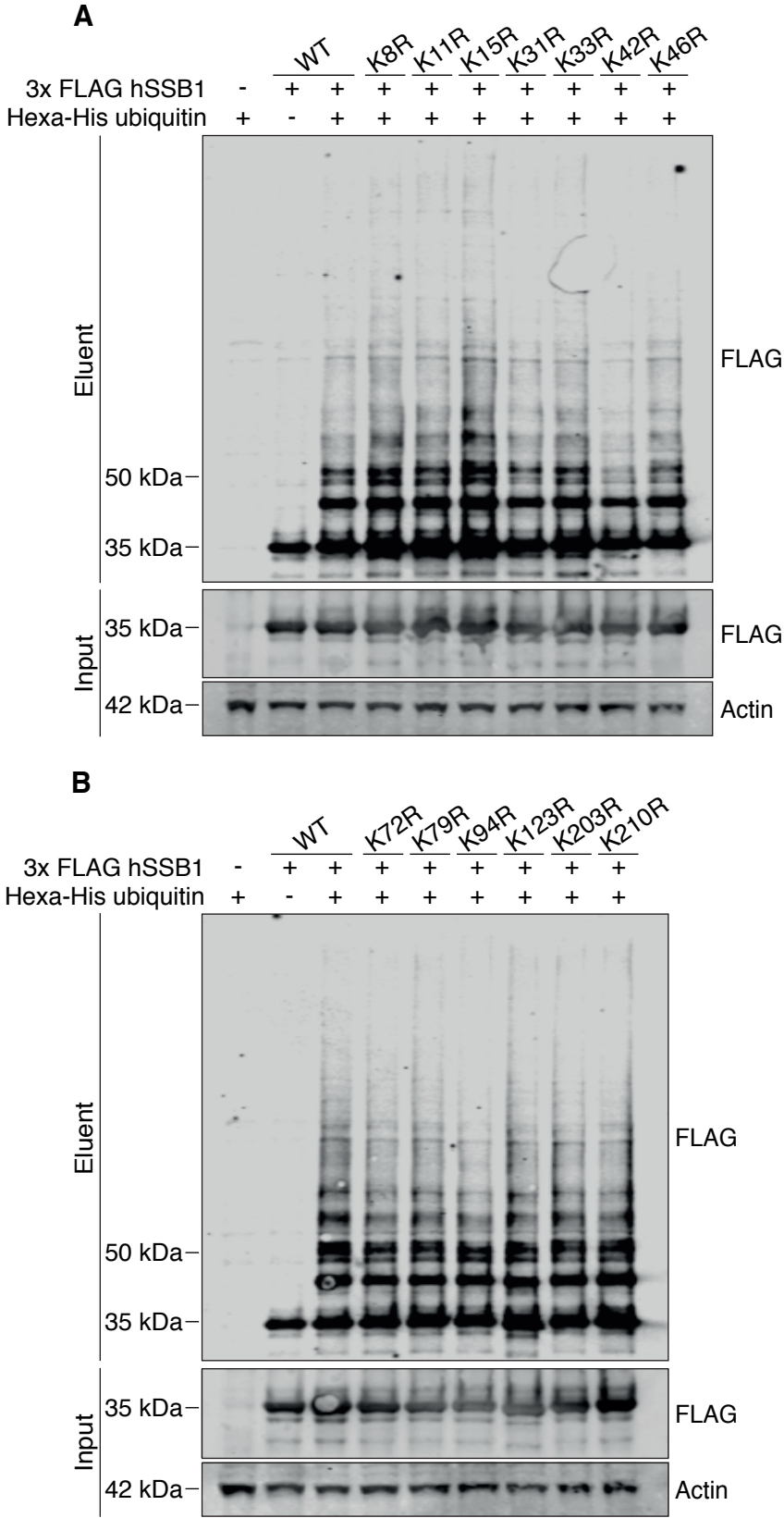
3.2.2 The disruption of hSSB1 poly-ubiquitination requires the complete removal of lysine residues

As the ubiquitination of exogenously expressed 3x FLAG hSSB1 could be readily detected from cells, a mutagenesis approach was therefore employed to disrupt each putative ubiquitination site. Here, lysine residues were individually mutated to arginine and co-expressed with hexa-His-ubiquitin in HEK293T cells. Hexa-His-ubiquitin pull-down assays were then performed as previously, and eluent immunoblotted with antibodies against the 3x FLAG tag (**Figure 3.2A and B**). The mutation of single lysine residues was however unable to disrupt or reduce the detection of ubiquitinated hSSB1.

The ubiquitination of multiple lysine residues has been detected in numerous other proteins and is often localised to a group of residues within a particular region. Indeed, poly-ubiquitination of the tumour suppressor p53 most likely involves six lysine residues located within a sixteen amino acid region of its C-terminus (Rodriguez et al., 2000b). hSSB1 contains three distinct regions, the N-terminus, the OB-fold and the C-terminus and so it was interesting to consider that ubiquitination may be restricted to one of these regions.

To assess this, hSSB1 combination mutants were prepared where lysine residues on the N-terminus, OB-fold and C-terminus were mutated to arginine (K-N-R, K-OB-R and K-C-R, respectively) (**Figure 3.2C**). Hexa-His-ubiquitin pull-down assays were then performed and eluent immunoblotted for 3x FLAG hSSB1 as above (**Figure 3.2D**). Ubiquitination of each combination mutant was however observed to a similar degree as of the WT protein.

Figure 3.2



continued over page

Figure 3.2

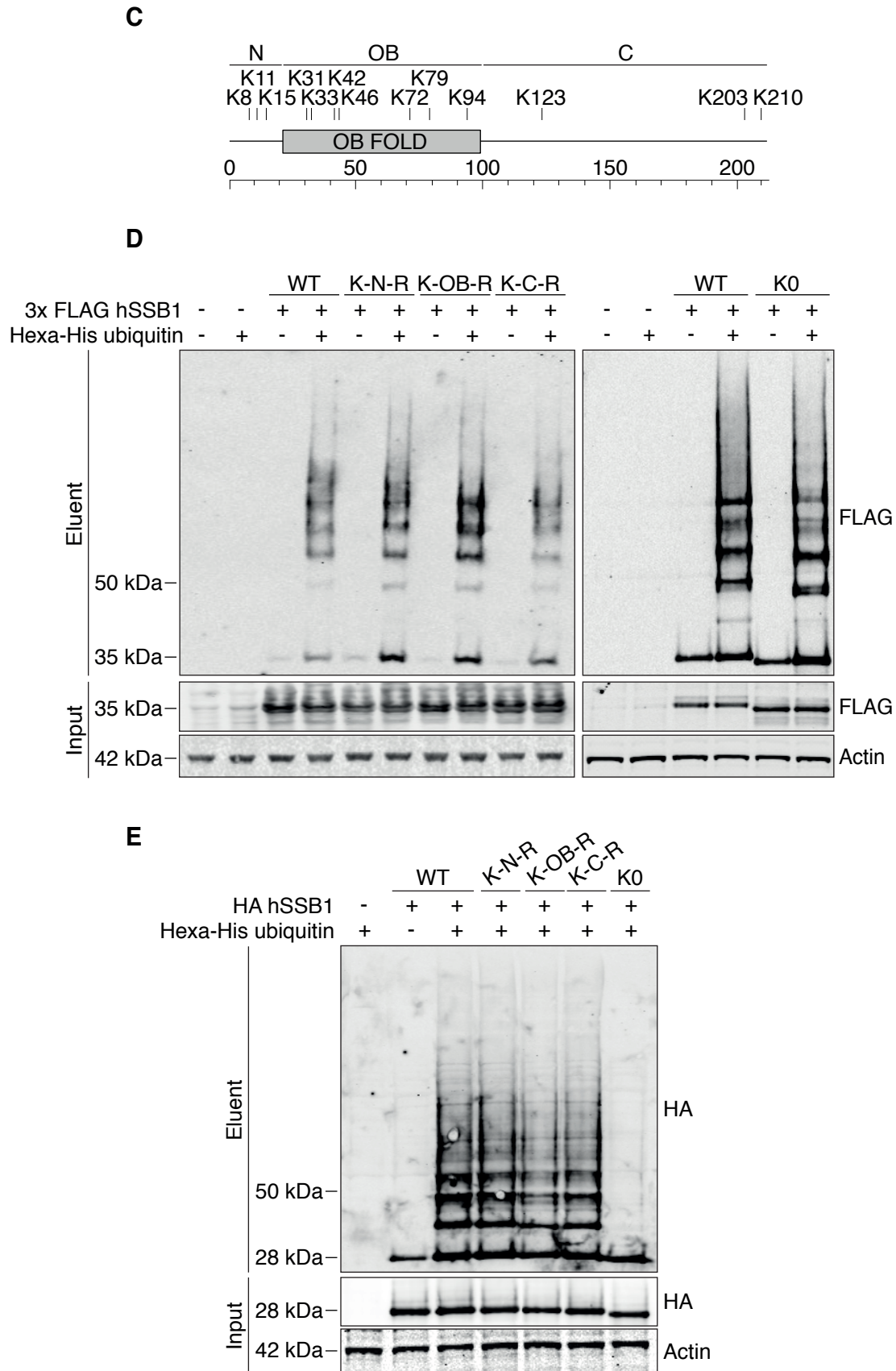


Figure legend over page

Figure 3.2 The disruption of hSSB1 poly-ubiquitination requires the complete removal of lysine residues

(A and B) Individual mutation of lysine residues to arginine does not prevent poly-ubiquitination of 3x FLAG hSSB1. hSSB1 lysine residues were individually mutated to arginine by site-directed mutagenesis of the WT 3x FLAG hSSB1 construct. Each construct was co-transfected into HEK293T cells with a plasmid encoding hexa-His tagged ubiquitin and expressed for 24 hours. Cells were treated with 25 μ M MG132 for 4 hours, harvested, and lysed in a buffer containing 8 M urea. 1000 μ g of whole cell lysate was incubated with 20 μ l of Ni-NTA agarose beads for 2 hours at room temperature, washed 3x with 8 M urea and eluted by heating to 90 $^{\circ}$ C for 10 minutes in SDS loading buffer. Eluent was immunoblotted and probed with antibodies against the FLAG tag. 15 μ g of whole cell lysate (input) was immunoblotted and probed with antibodies against the 3x FLAG tag, hSSB1 and actin. These results are representative of three independent experiments.

(C) hSSB1 lysine residues are found on the N-terminus, OB-fold and C-terminal tail. A schematic of hSSB1 indicating the location of each lysine residue.

(D) The mutation of every lysine residue in the hSSB1 protein sequence of the 3x FLAG construct is insufficient to disrupt poly-ubiquitination. 3x FLAG hSSB1 constructs were prepared where lysine residues of the N-terminus (K-N-R), OB-fold (K-OB-R) or C-terminus (K-C-R) were mutated in combination. A 3x FLAG hSSB1 construct where all thirteen endogenous lysine residues were mutated to arginine (K0) was prepared from the OB fold lysine hSSB1 mutant. Constructs were co-expressed with hexa-His-tagged ubiquitin in HEK293T cells and poly-ubiquitination experiments performed as per (A and B). These results are representative of three independent experiments.

(E) The disruption of hSSB1 poly-ubiquitination requires the complete removal of lysine residues. HA-tagged WT, K-N-R, K-OB-R, K-C-R and K0 constructs were prepared by inverse PCR with 5' hybridised primers (see section 2.2) using the 3x FLAG-tagged hSSB1 constructs. Constructs were co-expressed with hexa-His-

tagged ubiquitin in HEK293T cells and poly-ubiquitination experiments performed as per (A and B). These results are representative of three independent experiments.

The data above indicates that in addition to no single residue of hSSB1 functioning as the sole available site of modification, potentially ubiquitinated residues may be located in multiple regions of the protein. Indeed, it is tempting to consider that the mutation of an endogenously ubiquitinated lysine residue may promote the ubiquitination of other sites. As misfolded proteins may also be non-specifically poly-ubiquitinated for degradation (Eisele and Wolf, 2008; Heck et al., 2010), this may represent an explanation for the poly-ubiquitination of the lysine combination hSSB1 mutants. At this stage it was interesting to note that the 3x FLAG epitope tag of hSSB1 also contained six lysine residues (two on each repeat). As these residues could also represent sites of ubiquitination that are not found on endogenous hSSB1, it was reasoned that the ubiquitination of these may be informative as to the specificity of 3x FLAG hSSB1 ubiquitination in this assay. To test whether the 3x FLAG tag may be ubiquitinated, the remainder of the lysine residues from the K-OB-R hSSB1 amino acid sequence were mutated to arginine (K0 hSSB1), such that only those lysine residues of the 3x FLAG tag were still present. This construct was then used in a poly-ubiquitination assay as per above and the eluted protein immunoblotted for the 3x FLAG tag (**Figure 3.2D**). As similar levels of ubiquitination were detected for both WT and K0 3x FLAG hSSB1, this suggests that the 3x FLAG tag may indeed also be ubiquitinated in cells. These data indicate that ubiquitination of endogenous hSSB1 lysine residues and of those within the 3x FLAG tag cannot be distinguished in this assay.

Although the above conclusions seem likely, one other possible explanation could be that hSSB1 is ubiquitinated on non-lysine residues. Indeed, whilst only observed in a limited number of instances, ubiquitination of cysteine, serine and threonine residues (Ishikura et al., 2010; Okumoto et al., 2011; Tokarev et al., 2011; Williams et al., 2007), as well as the N-terminal NH₂ group of the polypeptide backbone (Breitschopf et al., 1998; Fajerman et al., 2004) has been described previously. To determine whether hSSB1 may be modified at non-lysine amino acids, an inverse PCR strategy (Figure 2.1) was used to exchange the coding sequence for the 3x FLAG epitope tag of the WT, K-N-R, K-OB-R, K-C-R and K0 3x FLAG hSSB1

constructs with that of HA, an epitope tag which lacks lysine residues. This construct was then used in a poly-ubiquitination assay and eluent immunoblotted with an anti-HA antibody (**Figure 3.2E**). Whilst ubiquitination of WT, K-N-R, K-OB-R, and K-C-R HA-hSSB1 was readily detected at equal levels, ubiquitination of K0 HA-hSSB1 was not. These results indicate that poly-ubiquitination of transiently expressed hSSB1 occurs at lysine residues, although is not restricted to a single site.

3.2.3 The N-terminal 3x FLAG tag of hSSB1 may be modified

An interesting observation from the above section was that while 3x FLAG hSSB1 migrated with an observed molecular weight of ~ 35 kDa (theoretical molecular weight = 26.1 kDa), HA hSSB1 migrated at ~ 28 kDa (theoretical molecular weight = 24.1 kDa). Although a small difference in observed molecular weight may be expected due to the difference in size the 3x FLAG and HA epitope tags, as well in the isoelectric point of the resulting hSSB1 proteins (3x FLAG hSSB1 = 5.97, HA hSSB1 = 8.94), this may not be a sufficient explanation for the differences observed. As plasmids encoding Myc hSSB1 or 3x FLAG hSSB1 with an additional C-terminal HA tag had also recently been prepared, each of these four constructs was expressed in cells and proteins immunoblotted with antibodies against each epitope tag (**Figure 3.3A**). Whilst an observed molecular weight of ~28-30 kDa was observed for both Myc and HA tagged hSSB1, 3x FLAG hSSB1 was consistently detected at ~35 kDa with an anti-FLAG antibody. Unexpectedly, however, a lower molecular weight 3x FLAG hSSB1 band of similar size to Myc hSSB1 (~30 kDa) was also detected using the hSSB1 antibody. One explanation that was considered for the differences in bands detected for 3x FLAG hSSB1 with the FLAG or hSSB1 antibodies was the presence of the endogenous methionine codon downstream of the N-terminal 3x FLAG tag. Here it was envisaged that this might act as an internal start codon that would allow for expression of an hSSB1 transcript lacking the 3x FLAG tag. As this might explain the difference in detected bands, the endogenous methionine codon (M1) was mutated to alanine and this mutant expressed in cells. Whole cell lysates were then prepared and immunoblotted with antibodies against hSSB1 and the 3x FLAG tag (**Figure 3.3B**).

Figure 3.3

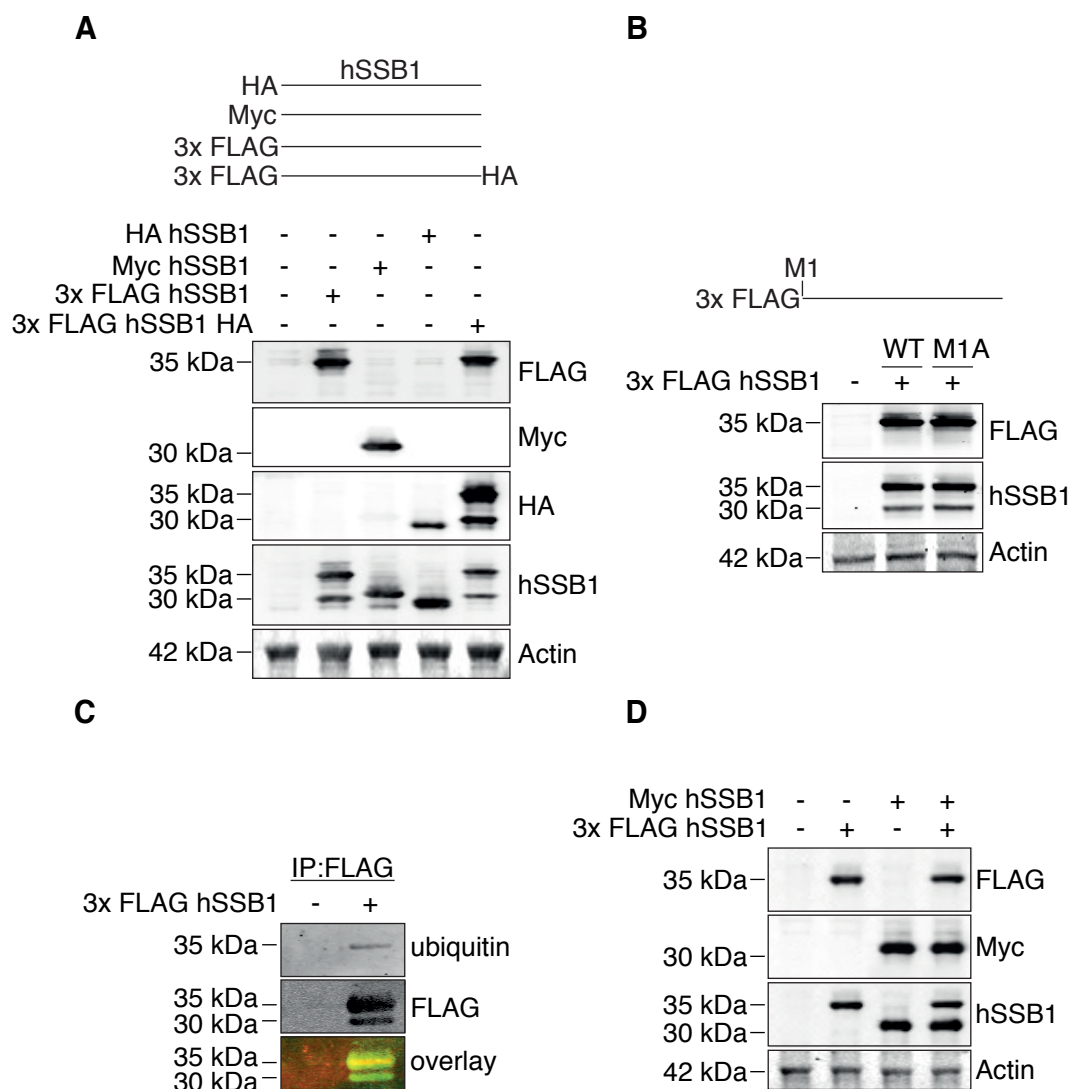


Figure 3.3 The N-terminal FLAG tag may be modified

(A) The ~35 kDa hSSB1 band may be specific to 3x FLAG hSSB1. The coding sequence for the N-terminal tag of the 3x FLAG hSSB1 construct was exchanged with the CDS sequence of the HA or Myc epitopes using inverse PCR with 5' hybridised primers. The coding sequence of the HA epitope was separately added to the C-terminus of the 3x FLAG hSSB1 construct by the same method. Each construct, or a control vector, were expressed in HEK293T cells for 24 hours before cells were lysed and 15 μ g of whole cell lysate immunoblotted with antibodies against FLAG, HA, Myc, hSSB1 and actin (loading control). These results are representative of two independent experiments.

(B) The ~30 kDa 3x FLAG hSSB1 band is not caused by the endogenous hSSB1 ATG functioning as an internal initiator codon. Site-directed mutagenesis was employed to mutate hSSB1 residue M1 of the N-terminal 3x FLAG hSSB1 construct. This construct, or a control vector, was expressed in HEK293T cells for 24 hours before cells were lysed and 15 µg of whole cell lysate immunoblotted with antibodies against FLAG, hSSB1 and actin (loading control). These results are representative of two independent experiments.

(C) The ~35 kDa 3x FLAG hSSB1 band may be ubiquitinated. 3x FLAG hSSB1 was transiently expressed in HEK293T cells for 24 hours. Cells were then harvested and lysed before incubation of 500 µg whole cell lysate with M2 FLAG magnetic beads overnight at 4 °C. Beads were washed the following day and protein eluted by heating to 90 °C for 10 min in SDS loading buffer. Eluent was immunoblotted and probed with antibodies against FLAG (green) and ubiquitin (red). These results are representative of two independent experiments.

(D) A single predominant 3x FLAG hSSB1 band is observed in cells grown at 2 % O₂. HeLa cells grown at 2 % O₂ were transfected with the 3x FLAG and MYC hSSB1 constructs, separately or together, and then harvested after 24 hours. Whole cell lysates were prepared and 15 µg immunoblotted with antibodies against FLAG, Myc, hSSB1 and actin (loading control). These results are representative of three independent experiments.

Two hSSB1 bands were however similarly detected for WT and M1A hSSB1, suggesting the observed banding pattern was not due to translational initiation at the endogenous ATG codon. These observations also indirectly suggest both bands may contain the FLAG tag. Indeed, this is consistent with the ~ 2 kDa difference in the observed molecular weight of endogenous hSSB1 (~ 28 kDa) and the lower 3x FLAG hSSB1 band (~ 30 kDa), corresponding to the approximate molecular mass of the 3x FLAG tag (2.7 kDa).

From the above data it can be observed that while 3x FLAG hSSB1 migrates at two predominant molecular weights, the lower band does so most similarly to

endogenous hSSB1. In addition, in Figure 3.3A, both bands of the 3x FLAG hSSB1 HA construct were detected with the HA antibody, suggesting the lower band is not formed due to a C-terminal cleavage event. Although formation of ~30 kDa hSSB1 due to an N-terminal cleavage event could not be excluded based on this data, it seemed more likely that the upper 3x FLAG hSSB1 band may instead be modified.

As previous observations suggested 3x FLAG hSSB1 may be non-specifically poly-ubiquitinated, it was tempting to consider that the ~35 kDa 3x FLAG hSSB1 band observed may also reflect this event. To test this, 3x FLAG hSSB1 was transiently expressed in cells prior to immunoprecipitation of FLAG tagged proteins. These were then immunoblotted and probed with antibodies against the FLAG tag and ubiquitin (**Figure 3.3C**). In doing so, an ubiquitin band corresponding to ~35 kDa 3x FLAG hSSB1 was detected, supporting that the ~35 kDa 3x FLAG hSSB1 band may be ubiquitinated. Unexpectedly, in this assay, both ~30 and 35 kDa bands were also detected using the FLAG antibody (the ~30 kDa band was not detected by immunoblotting of whole cell lysates with the FLAG antibody previously). An explanation for this may involve the greater antigenicity ~30 kDa 3x FLAG hSSB1 in its native state, allowing for its enrichment by immunoprecipitation. These observations nevertheless support that both 3x FLAG hSSB1 bands are FLAG tagged and full-length, as well as that ~35 kDa hSSB1 may be ubiquitinated.

One explanation for the ubiquitination of ~35 kDa hSSB1 may be that this modification is the first step of poly-ubiquitin chain formation. It was therefore interesting to notice that while both 3x FLAG hSSB1 bands are present when cells are grown at 21 % O₂, only ~35 kDa hSSB1 was observed in cells grown at 2% O₂ (**Figure 3.3D**). In this experiment, cells were grown at 2% O₂ for 2 weeks and then transfected with plasmids encoding 3x FLAG hSSB1, Myc hSSB1 or co-transfected with both. Whole cell lysates were then immunoblotted and probed with antibodies against the Myc and 3x FLAG epitope tags. While initially performed as part of a separate study, the absence of the lower 3x FLAG hSSB1 band was particularly striking. Although yet to be demonstrated, it is tempting to speculate that this may represent a greater turnover of hSSB1 protein at low oxygen conditions in the absence of oxidative DNA damage. It should be noted that while this experiment was performed in HeLa cells, unlike other experiments here which were performed in

HEK293T cells, this observation is unlikely to represent a cell line difference, as ~30 and ~35 kDa hSSB1 bands are observed from HeLa cells grown at 21% O₂ in chapter 4 (e.g. Figure 4.2A).

3.2.4 Mass spectrometric analysis of immunoprecipitated 3x FLAG hSSB1

The data reported above suggests that site-directed mutagenesis studies may not be an effective approach to detect residues of hSSB1 that may be ubiquitinated. Indeed, it seems likely that transiently expressed hSSB1 is highly ubiquitinated and that mutation of those lysine residues that are ubiquitinated in the endogenous protein may go undetected in the over-expressed protein. This may be due to non-residue-specific ubiquitination of the protein in general, or due to ubiquitination of additional residues on mutant hSSB1. These observations nevertheless indicate that an alternate approach to assess hSSB1 ubiquitination may be required.

The use of mass spectrometry to identify ubiquitinated lysine residues has been frequently reported, most often subsequent to trypsin digestion of the target protein (Udeshi et al., 2012). Here, trypsin cleaves the ubiquitin peptide, leaving only the two C-terminal ubiquitin glycine residues attached to the ϵ -amino group of the ubiquitinated substrate lysine residue. Although trypsin characteristically cleaves proteins C-terminal to acidic residues (lysine and arginine) (Olsen et al., 2004), the di-glycyl moiety remaining on the modified lysine residues prevents this activity (Udeshi et al., 2013a), resulting in an internal modified lysine residue that may be detected with an additional mass of 114.04 Da (Fiedler and Cotter, 2013; Xu and Peng, 2006). Enrichment of the target protein, or of ubiquitinated proteins in general, is however essential for this approach due to the low stoichiometric presence of ubiquitinated proteins, as well as their rapid degradation in cells. For this purpose, isolation of ubiquitinated proteins has been reported by the capture of hexa-histidine tagged ubiquitin on Ni-NTA beads (Peng et al., 2003), or by immunoprecipitation of the di-glycyl group from trypsin digested proteins (Kim et al., 2011; Udeshi et al., 2013b; Xu et al., 2010b). As yet, however, the detection of ubiquitinated hSSB1 by mass spectrometry has not been reported using these approaches.

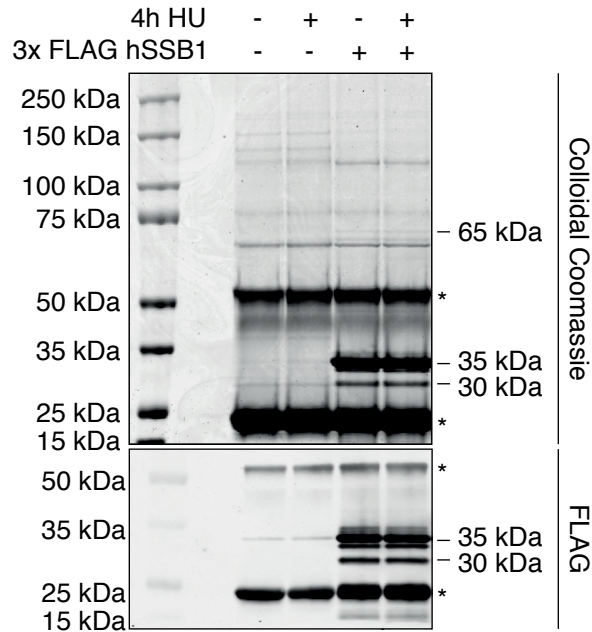
It was therefore envisaged that hSSB1 ubiquitination might be assessed more successfully following immunoprecipitation of hSSB1 directly. To assess this, HEK293T cells were firstly treated with 25 μ M MG132 for 4 hours. Cells were then lysed and 6000 μ g of whole cell lysate incubated with protein G magnetic beads bound either to an IgG isotype control, or the hSSB1 antibody, overnight at 4 °C. The following day, beads were washed and protein eluted by heating in SDS-loading buffer at 80 °C for 10 minutes. Proteins were then separated by electrophoresis and stained with colloidal coomassie brilliant blue G-250. Although bands were specifically detected in the hSSB1:IP lane, these were however considered too faint to justify their extraction and subsequent mass spectral analysis.

As it is seemed unlikely that enough endogenous hSSB1 could be isolated to assess hSSB1 ubiquitination by mass spectrometry, it was therefore conceded that over-expressed protein would need to be employed. Indeed, while such protein is likely highly-ubiquitinated, regardless of the epitope tag used, it was reasoned that a certain level of specificity may still exist when using the WT protein. For these studies, it was therefore concluded that 3x FLAG hSSB1 would be used, both as the plasmid has previously been published by our group (Paquet et al., 2015), as well as due to the higher running molecular weight of the protein, which would allow greatest separation from the FLAG antibody IgG light chain. As our group (Bolderson et al., 2014) and others (Kar et al., 2015) recently identified a novel role for hSSB1 in the response to replication stress, a response during which the regulation of hSSB1 is unclear, it was further considered that this experiment would be conducted in the presence or absence of treatment with the replication inhibitor hydroxyurea.

For this experiment, WT 3x FLAG hSSB1 was transiently expressed in HEK293T cells for 24 hours. Cells were then treated with 3 mM hydroxyurea for 4 hours, or mock treated, prior to collection of cells and preparation of whole cell lysates. Exogenously expressed hSSB1 was then immunoprecipitated from 12 mg of whole cell lysate overnight at 4 °C using anti-FLAG M2 magnetic beads and separated on a BOLT precast PAGE gel. This gel was stained overnight with colloidal coomassie blue as per above and the following day de-stained in H₂O (**Figure 3.4A**). Here, 3x FLAG hSSB1 bands were detected at ~30 and 35 kDa.

Figure 3.4

A



B

- HU 35 kDa

MTTETFVKDIK**PGLKNLNLI**FIVLETGRVTKTKDGHEVRTCKVADKTGSINISVWDDVGN
LIQPGDIIRLTKGYASVFKGCLTLYTGRGGDLQKIGEFM~~VYSEVPNFSEPNPEYSTQQA~~
PNKAVQND**SNPSASQPTTGPSAASPA**ENQNGNLSAPPGPGGGPHPPHTPSHPPSTRIT
RSQPNHT**PAGPPGPSSNPV**SNGKETRRSSKR

- HU 30 kDa

MTTETFVKDIK**PGLKNLNLI**FIVLETGRVTKTKDGHEVRTCKVADKTGSINISVWDDVGN
LIQPGDIIRLTKGYASVFKGCLTLYTGRGGDLQKIGEFM~~VYSEVPNFSEPNPEYSTQQA~~
PNKAVQND**SNPSASQPTTGPSAASPA**ENQNGNLSAPPGPGGGPHPPHTPSHPPSTRIT
RSQPNHT**PAGPPGPSSNPV**SNGKETRRSSKR

+ HU 35 kDa

MTTETFVKDIK**PGLKNLNLI**FIVLETGRVTKTKDGHEVRTCKVADKTGSINISVWDDVGN
LIQPGDIIRLTKGYASVFKGCLTLYTGRGGDLQKIGEFM~~VYSEVPNFSEPNPEYSTQQA~~
PNKAVQND**SNPSASQPTTGPSAASPA**ENQNGNLSAPPGPGGGPHPPHTPSHPPSTRIT
RSQPNHT**PAGPPGPSSNPV**SNGKETRRSSKR

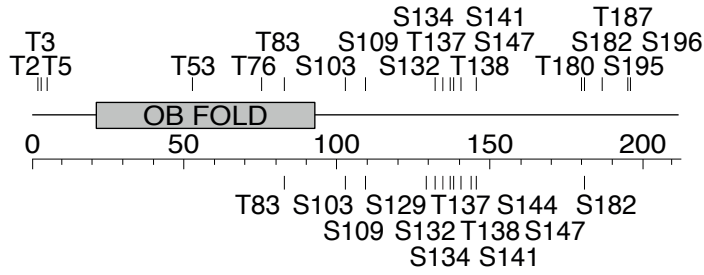
+ HU 30 kDa

MTTETFVKDIK**PGLKNLNLI**FIVLETGRVTKTKDGHEVRTCKVADKTGSINISVWDDVGN
LIQPGDIIRLTKGYASVFKGCLTLYTGRGGDLQKIGEFM~~VYSEVPNFSEPNPEYSTQQA~~
PNKAVQND**SNPSASQPTTGPSAASPA**ENQNGNLSAPPGPGGGPHPPHTPSHPPSTRIT
RSQPNHT**PAGPPGPSSNPV**SNGKETRRSSKR

continued over page

Figure 3.4

C



D

Bands	Potentially phosphorylated residues
- HU 35 kDa	S53, S76, T83, S103, S109, S132, S134, T137, T138, S141, S144, S147, T180, S182, T187, S195, S196
- HU 30 kDa	T2, T3, T5, T83, S103, S109, T187
4h HU 35 kDa	T83, S103, S109, S129, S132, S134, T137, T138, S141, S144, S147, S182
4h HU 30 kDa	T83

E

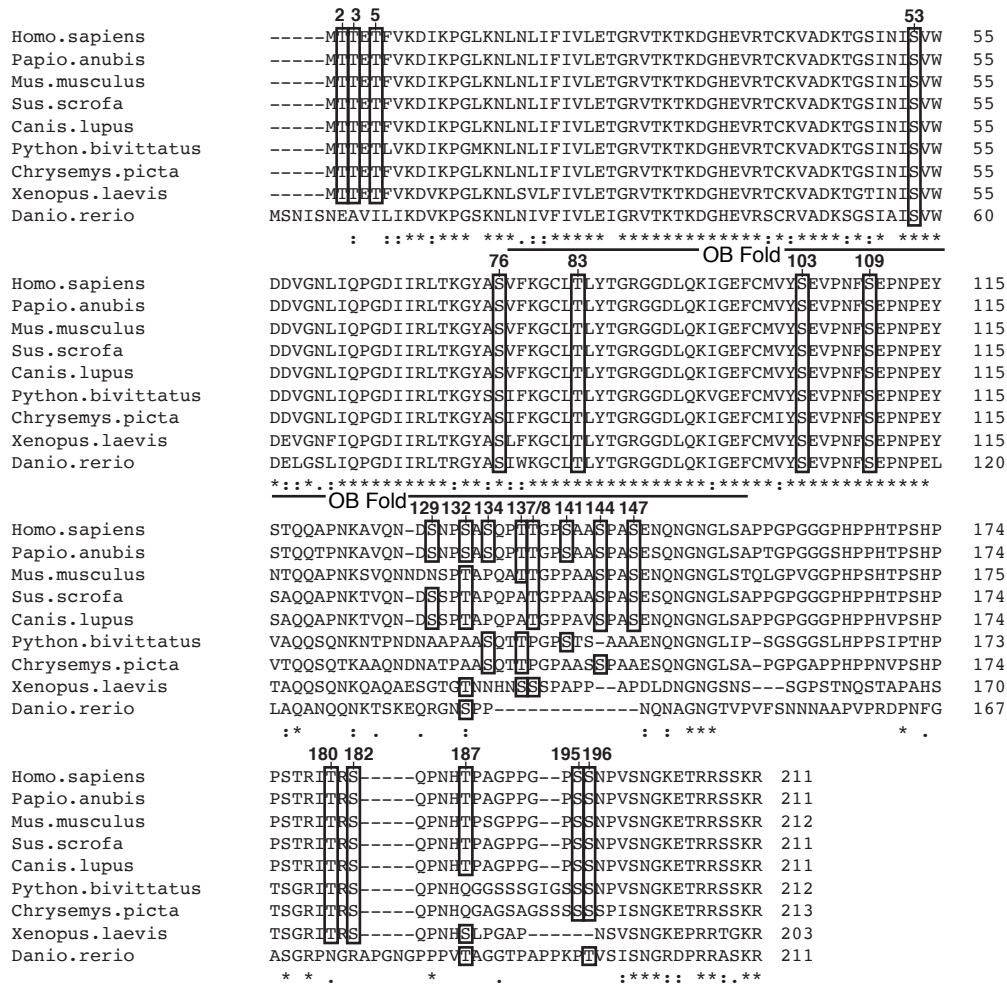


Figure legend over page

Figure 3.4 Mass spectrometric analysis of immunoprecipitated 3x FLAG hSSB1

(A) Immunoprecipitation of 3x FLAG hSSB1 from cells treated with hydroxyurea. 3x FLAG hSSB1 was transiently expressed in HEK293T cells for 24 hours, prior to treatment with 3 mM hydroxyurea (HU) for 4 hours. Whole cell lysates were then prepared from these cells and 12 mg incubated with 40 μ l of magnetic M2 FLAG beads overnight at 4 °C. Beads were then washed and protein eluted by heating to 90 °C in SDS loading buffer for 10 min. Two-thirds of the eluent was separated by PAGE and stained with colloidal coomassie brilliant blue G-250. The remaining eluent was immunoblotted with antibodies against the FLAG tag. The upper ~30 and ~35 kDa hSSB1 bands are indicated, as well as bands of ~65 kDa. * = IgG proteins

(B) Peptides spanning the N- and C- terminus of hSSB1 were identified for the ~30 and ~35 kDa bands in (A). The ~30 and 35 kDa bands indicated for both 3x FLAG hSSB1 lanes were excised from the colloidal coomassie blue-stained gel and transported to the BSRC mass spectrometry facility at the University of St Andrews. Gel slices were excised and digested with trypsin. Peptides were detected by ESI-MS/MS and data analysed using the Mascot algorithm against the NCBI non redundant database with carbamidomethyl as a fixed modification of cysteines and methionine oxidation, deamidation of glutamines and asparagines and phosphorylation of serine, threonine and tyrosine as variable modifications. Red bold font indicates hSSB1 residues that were detected from each band.

(C and D) Numerous phosphorylated hSSB1 residues were detected for each band excised in (B). The mascot algorithm detected numerous potentially phosphorylated serine and threonine residues. (C) A schematic of hSSB1 indicating putative phosphorylation sites detected prior to (above) and following (below) HU treatment. (D) A table of detected putative phosphorylation sites, indicating the band from which they were detected.

(E) Putative phosphorylation residues on the hSSB1 N-terminus, OB-fold and far C-terminus are strongly conserved. Amino acid sequences of proteins homologous to hSSB1 from the indicated species were compiled and aligned using

Clustal Omega software (ebi.ac.uk). Putative residues of phosphorylation are outlined by rectangles with numbers corresponding to the hSSB1 protein sequence. Amino acids of the OB-fold are underlined. Consensus symbols given below each row should be interpreted: * = a fully conserved residue, : = conservation between groups of strongly similar properties, . = conservation between groups of weakly similar properties

These bands were also detected by immunoblotting the same eluent with an antibody against the FLAG epitope (**Figure 3.4A**), further confirming that these were transiently expressed hSSB1. Interestingly, when separated in this way, the ‘~35 kDa hSSB1’ was actually found to be composed of multiple similar molecular weight species, potentially signifying different forms of modified hSSB1. Whilst mono-ubiquitination may represent the difference between ~30 and 35 kDa hSSB1 (ubiquitin is a 8.5 kDa protein which migrates with an apparent molecular weight on 5.5 kDa (Beers and Callis, 1993)), it is unclear whether the differences between the bands at ~35 kDa hSSB1 represent an additional ubiquitination event, or one or more other modifications. With the exception of faint bands at ~65 kDa, few other specific high-molecular weight bands were identified, suggesting that poly-ubiquitinated hSSB1 had not been efficiently isolated. Despite this, it was considered that identification of ~30 and ~35 kDa hSSB1 bands may still be useful, especially considering cells were treated +/- hydroxyurea. These bands were therefore excised for analysis at the BRSC mass spectrometry and proteomics facility at the University of St Andrews. Here, bands were cut into 1 mm slices and subjected to in-gel trypsin digestion. Peptides were then extracted with formic acid and separated on a reverse phase chromatography column prior to detection by electrospray ionisation quadrupole time-of-flight mass spectrometry (ESI-Q-TOF-MS).

Error tolerant searches using the Mascot algorithm were then performed against the St. Andrews Mascot database with carbamidomethyl as a fixed modification of cysteines and methionine oxidation, deamidation of glutamines and asparagines and phosphorylation of serine, threonine and tyrosine as variable modifications. In doing so, peptides from each sample were detected that corresponded to the hSSB1 protein sequence (Figure 3.4B). Consistent with Figures 3.3 A and B, peptides representing the N - and C-terminus of hSSB1 were detected in all samples, suggesting that both

the ~30 and 35 kDa bands contain full-length hSSB1. Furthermore, in bands where a peptide containing the N-terminal methionine was detected, this was with an additional 271.1487 Da at the N-terminus. This is consistent with the additional mass expected from the cleaved 3x FLAG tag (K.AIA-MTTETFVK) and further demonstrates that the lower full-length hSSB1 band is not caused by translation initiation at the internal methionine codon C-terminal to the 3x FLAG protein tag

Interestingly, while none of the hSSB1 lysine residues were detected with an additional mass of 114.04 Da, as would be expected of an ubiquitinated lysine residue, numerous putative phosphorylated serine and threonine residues were identified from each hSSB1 band (**Figure 3.4 C and D**). Of the phosphorylation sites detected, two (S134 and T187) have previously been reported by other mass spectrometry screens and have been curated on the PhosphoSitePlus database (Hornbeck et al., 2015), potentially supporting them as likely phosphorylation sites. By contrast, phosphorylation of S116, T117 and S200, phosphorylation events reported by PhosphoSitePlus, were not detected in this data set.

It should be noted that certain ambiguities do exist in the assignment of phosphorylation to specific residues, especially in peptides that contain multiple serine or threonine residues (Déphoure et al., 2013). This is an issue further discussed in chapter 4. To indirectly assess the likelihood of each phosphorylation site, the protein alignment in Figure 3.1 was further examined (**Figure 3.4 E**). Interestingly, each of the putative phosphorylated residues residing on the N-terminus, as well as the OB fold, were highly conserved amongst the examined species, whilst these were less so on the C-terminus tail. These findings may however represent the high conservation of the DNA-binding region of hSSB1, rather than of particular phosphorylation sites. Further validation of these residues will therefore be required.

3.4 Discussion

In this chapter, site-directed mutagenesis was employed to determine hSSB1 lysine residues that may be ubiquitinated in cells (Figure 3.2). The mutation of single lysine residues, or each lysine residue in a particular region, was however unable to prevent or suppress hSSB1 ubiquitination, suggesting this modification may occur at multiple sites. Indeed, examination of the hSSB1 crystal structure revealed that each hSSB1 lysine residue is surface exposed and likely accessible for modification (Figure 3.1).

Although the data obtained here indicate that transiently expressed hSSB1 may be ubiquitinated at multiple lysine residues, it is unclear whether endogenous hSSB1 is also modified in this way. One interpretation may be that while hSSB1 could be normally ubiquitinated only at specific sites, the ubiquitination of other lysine residues may be promoted by high-level hSSB1 transient over-expression. This could be explained by a detrimental effect of hSSB1 over-expression, such that a certain pressure exists to remove excess hSSB1 in the cell. Another possibility is that while FBXL5, the endogenous hSSB1 E3 ligase (Chen et al., 2014), may specifically ubiquitinate certain residues, non-specific ubiquitination of hSSB1 by other enzymes may be increasingly favourable at higher hSSB1 concentrations.

One method that could be useful for the identification of specific hSSB1 ubiquitination events is similar to that which has been employed for the characterisation of MDM2-mediated p53 ubiquitination (Kubbutat et al., 1998; Rodriguez et al., 2000b). In these studies, co-expressed MDM2 caused the rapid degradation of WT p53, although not of a p53 mutant truncated of its c-terminal 30 amino acids (Kubbutat et al., 1998), or where the six c-terminal residues within this region were mutated to arginine (Rodriguez et al., 2000a). While these data suggest that MDM2 catalyses the poly-ubiquitination of these six p53 lysine residues, eventuating in p53 degradation, similar poly-ubiquitination of WT and lysine mutant p53 was observed in an *in vitro* MDM2 ubiquitination assay. These data thereby suggest multiple other p53 lysine residues may also be modified in an artificial setting (Rodriguez et al., 2000a), reminiscent of the observations for hSSB1 ubiquitination observed in this chapter. It is therefore interesting to consider that, similarly to MDM2 and p53, the co-over-expression of FBXL5 with hSSB1 lysine

mutants may be one method of identifying specific residues of FBXL5-catalysed hSSB1 ubiquitination.

Another potentially confounding issue is that while it seems likely that hSSB1 is modified by K48-linked poly-ubiquitination, as hSSB1 does seem to be proteasomally degraded (Richard et al., 2008), it is possible that hSSB1 may also be modified (specifically or non-specifically) by other ubiquitin chain types. One method through which different poly-ubiquitin topologies have been discriminated previously has included the mutation of certain ubiquitin peptide lysine residues, to prevent the formation of certain chain types (such as by mutating K48), or limit chain formation to a certain lysine residue (for instance if every lysine except K48 is mutated). Such methods would allow further investigation into the nature of the hSSB1 poly-ubiquitination chains reported here.

In addition to the non-specific ubiquitination of transiently expressed hSSB1 described above, the data provided here suggests that the 3x FLAG epitope tag may also be poly-ubiquitinated, further supporting the non-specific nature of transiently expressed hSSB1 poly-ubiquitination in cells (Figure 3.2). Interestingly, 3x FLAG hSSB1 was found to form two prominent bands on an immunoblot at ~30 and 35 kDa when probed with an hSSB1 antibody (Figure 3.3). Whilst the FLAG antibody poorly detected the lower band, both bands nevertheless do seem to contain this epitope tag and to represent full-length hSSB1. Immunoblotting of immunoprecipitated 3x FLAG hSSB1 then suggested that the ~35 kDa band might be ubiquitinated. Although it remains possible that hSSB1 may be modified by mono-ubiquitination at an endogenous lysine residue, based on the non-specific ubiquitination of the 3x FLAG epitope tag suggested above, it is tempting to consider the difference between ~30 and ~35 kDa 3x FLAG hSSB1 may result from similar mono-ubiquitination of the 3x FLAG tag. Indeed, a higher molecular weight species was not detected for HA or Myc tagged hSSB1 (which contain 0 and 1 lysine residue, respectively, compared to 6 on the 3x FLAG tag). It is curious however that although potentially ubiquitination, the epitope tag of ~35 kDa 3x FLAG hSSB1 appears to be more antigenic when using the FLAG antibody than the band at ~30 kDa, which is presumably unmodified. It is also important to note that while the 3x FLAG tag may be modified, this does not appear to affect hSSB1 function, as

transiently expressed 3x FLAG hSSB1 is able to recapitulate siRNA-depleted endogenous hSSB1 in cells (Paquet et al., 2015) (and Chapter 4 of this thesis).

Given that non-specific hSSB1 poly-ubiquitination is likely to be stimulated by transient over-expression, it is interesting to consider that the ubiquitination observed for ~35 kDa 3x FLAG hSSB1 may occur as an intermediate in this process. This may be supported by the observation that 3x FLAG hSSB1 expressed in cells grown at 2% O₂, unlike those grown at 21 % O₂, migrates solely at ~35 kDa on a PAGE gel, rather than also at ~30 kDa. Here, it may be interpreted that while hSSB1 is rapidly poly-ubiquitinated in cells grown at 2% O₂, leading to the predominant formation of the ~35 kDa band, ubiquitination may be partially suppressed at 21 % O₂. This potentially may occur due to increased oxidative stress resulting in the stabilisation of hSSB1, causing a relative increase in hSSB1 of ~30 kDa. Conversely, non-specific ubiquitination of ~35 kDa hSSB1 may occur not as an intermediate, although rather as a separate mono-ubiquitination event. This indeed may be more consistent with prior conceptions of poly-ubiquitin chain formation, where initial ubiquitination of the substrate is rate limiting, while subsequent chain extension occurs more rapidly (Petroski and Deshaies, 2005). Under this circumstance, the formation of a stable mono-ubiquitinated intermediate may be unexpected to form. Alternatively, although initial ubiquitination and subsequent poly-ubiquitin chain extension is often mediated by the same E3 ligase, in some instances, chain extension is catalysed by a distinct class of specific ligases, referred to as E4 (Kuhlbrodt et al., 2005). A discrepancy in the enzymatic constituents of each stage of hSSB1 poly-ubiquitination, which may be differentially affected by hSSB1 over-expression, such as by free components of one or the other becoming 'saturated', may therefore explain the stable formation of the mono-ubiquitinated form of hSSB1.

In view of the likely ubiquitination of the ~35 kDa hSSB1 band, it may be unexpected that lysine residues containing an additional di-glycyl group, remnants from ubiquitin trypsinisation, were not detected by mass spectrometry. If ubiquitination does predominantly occur on FLAG tag lysine residues, these however would not be detected in the analysis, which was performed using the NCB1 non-redundant database of endogenous proteins (and therefore does not contain epitope-tagged proteins). Indeed, whilst a fragment of the FLAG tag (K.AIA) can be detected

as an additional mass fused to the hSSB1 N-terminus, other tryptic peptides of the tag have not been analysed.

The mass spectrometric-detection of numerous putative phosphorylation sites on immunoprecipitated hSSB1 does however provide valuable new insight into the regulation of hSSB1. It should be noted however that while specific residues of phosphorylation were represented in Figure 3.4, these represent only the ‘most-likely’ sites of modification for each phosphorylated tryptic peptide detected. Indeed, whilst these were identified based on ‘confidence scores’ generated by the Mascot algorithm, a complete array of high confidence fragment ions was not obtained for each tryptic fragment. Definitive site assignment of phosphorylation within each tryptic peptide is therefore unachievable. Such issues are further elaborated in Section 4.2.1. Nevertheless, these data may provide a useful guide for the further investigation of hSSB1 regulation by phosphorylation.

Chapter 4: Regulation of hSSB1 in the Response to Replication Stress

4.1 Introduction

DNA replication constitutes one of the most important processes within the cell and allows for the accurate duplication of genomic information prior to cell division. While this process occurs rapidly in unperturbed cells, numerous endogenous and exogenous sources may either slow or stall replication fork progression (Branzei and Foiani, 2005). Such disruption results in the exposure of single-stranded DNA (ssDNA) that must be protected and stabilised to prevent replication fork collapse and double-strand DNA break formation (Toledo et al., 2013). This process includes the coating of exposed ssDNA by replication protein A (RPA), as well as the subsequent accumulation and activation of the ataxia telangiectasia and Rad3-related (ATR) kinase (Ball et al., 2005). ATR may then phosphorylate Chk1, which promotes intra-S cell cycle checkpoint activation (Zhao and Piwnicka-Worms, 2001), as well as other proteins involved in stabilising and remodelling the replication fork (Couch et al., 2013). In addition to ATR, numerous additional regulatory enzymes are also activated by replication stress, including the related P13K-like kinases, ataxia telangiectasia mutated (ATM) and DNA-dependent protein kinase (DNA-PK) (Lin et al., 2014; Liu et al., 2012; Ying et al., 2015). Activation of these enzymes results in the coordinated regulation of numerous DNA repair proteins. Such regulation is exemplified by phosphorylation of the RPA 32 kDa subunit (RPA32) and is mediated by ATM, ATR and DNA-PK, as well as by cyclin-CDK (Anantha et al., 2007; Liu et al., 2012; Shao et al., 1999). Here, RPA32 phosphorylation is required for efficient restart of stalled replication forks following their disruption (Ashley et al., 2014), potentially due to an association with the BRCA2-interacting protein, PALB2 (Murphy et al., 2014).

Recently our group and others provided evidence that the restart of stalled replication forks is also promoted by human single-stranded DNA-binding protein 1 (hSSB1) (Bolderson et al., 2014; Kar et al., 2015). Following the disruption of replication, hSSB1 was found to localise to stalled replication forks, where it promotes the

activation of the ATR kinase and the subsequent phosphorylation of Chk1. The importance of hSSB1 in these processes is highlighted by the inefficiency of hSSB1-depleted cells to activate checkpoint signalling following replication stress, as well as to restart stalled replication forks. These deficiencies are manifested by hypersensitivity to multiple replication inhibitors (Bolderson et al., 2014).

While the precise function of hSSB1 following fork disruption remains unclear, one explanation may be that hSSB1 functions in a similar way to RPA. Following replication disruption, RPA is known to sequester exposed ssDNA and recruit the ATR kinase through a direct interaction with the ATR-interacting protein, ATRIP (Ball et al., 2005). Indeed, hSSB1 also associates with the ATR-ATRIP heterodimer in cells and is required for the recruitment of these proteins to chromatin (Bolderson et al., 2014; Kar et al., 2015). In addition, hSSB1 is able to promote the interaction of ATR-ATRIP with a ssDNA substrate *in vitro* (Kar et al., 2015). The coordination of hSSB1 and RPA in cells, however, remains unclear. The considerably lower affinity of hSSB1 than RPA for ssDNA (Yang et al., 2012) indeed does suggest these proteins are more likely to function by separate means, rather than by competing for the same substrate. An alternative explanation for the involvement of hSSB1 in ATR activation may therefore reflect a functional interplay with other proteins known to promote ATR activity following fork stalling. This may include components of the MRN complex, with which hSSB1 has been suggested to interact previously (Richard et al., 2011a) and which also inefficiently localise to replication forks following hSSB1 depletion (Bolderson et al., 2014). Although the function of this complex at sites of replication disruption remains a subject of debate, a role in the activation of ATR has been suggested (Duursma et al., 2013). Here, MRN was suggested to promote the association of TopBP1 with the 9-1-1 complex at replication fork junctions, where it may interact with and subsequently activate the ATR kinase (Delacroix et al., 2007). An involvement of hSSB1 in these processes may therefore offer some explanation for its role in stimulating ATR-mediated Chk1 phosphorylation.

Whilst the precise mechanism through which hSSB1 functions at sites of stalled forks remains unclear, it is tempting to draw and infer parallels with its described roles in the repair of double-strand DNA breaks by homologous recombination

(Richard et al., 2008). In this process, hSSB1 is thought to bind exposed ssDNA (Richard et al., 2011b), as well as poly-(ADP) ribose (PAR) (Zhang et al., 2014) and to promote resection of the break by either the MRN (Richard et al., 2011a) or Exo1 nucleases (Yang et al., 2012). In addition, hSSB1 is required for efficient activation of the ATM kinase (Richard et al., 2008). ATM has then been inferred to phosphorylate hSSB1 at threonine residue 117 (T117), initiating a positive feedback loop to further promote ATM signalling (Richard et al., 2008). It is therefore interesting to hypothesise that hSSB1 may be regulated through a similar means in the stabilisation of stalled replication forks, especially given the role of hSSB1 in the stimulation of ATR (a kinase related to ATM).

In Chapter 3, numerous putative phosphorylation events were detected by mass spectrometric analysis of hSSB1 that had been immunoprecipitated from HEK293T cells. In this chapter, the phosphorylation of one of these, serine residue 134 (S134) is further characterised and found to be required for hSSB1-dependent cell survival following replication fork inhibition. Evidence is also provided for the necessity of an interaction between hSSB1 and the INTS3 complex in the response to replicative stress, although this is likely to modulate hSSB1 through a means that is independent of S134 phosphorylation. Chromatin-bound hSSB1 is also found to associate with numerous complexes that have been implicated in nucleosome remodelling following fork disruption, potentially suggesting a novel process in which hSSB1 may be involved.

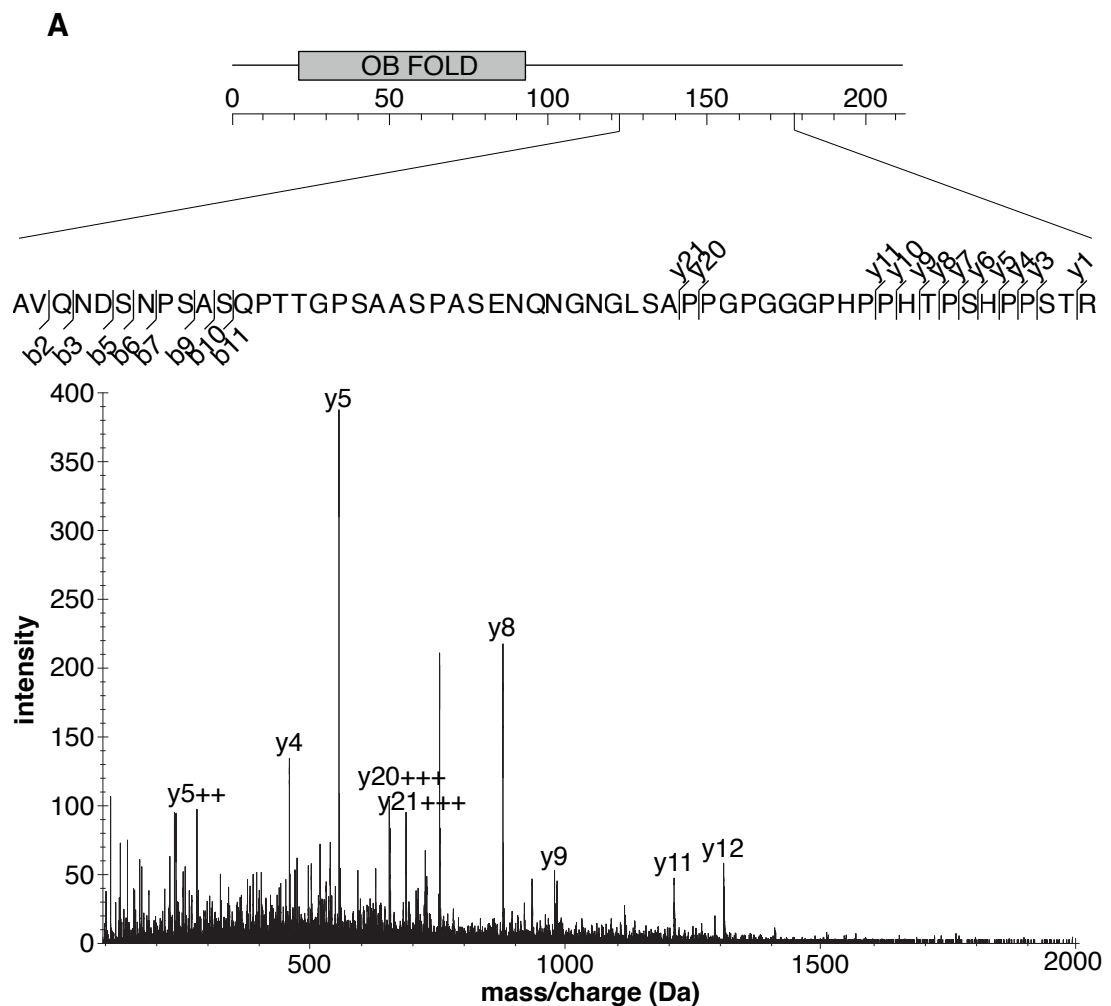
4.2 Results

4.2.1 Detection of phosphorylated hSSB1 by mass spectrometry

In response to ionising radiation-induced double-strand DNA break formation, hSSB1 function may require phosphorylation of threonine residue 117 (T117) (Richard et al., 2008). T117 is a component of a SQ/TQ motif (serine/threonine – glutamine), numerous of which are phosphorylated in other DNA repair proteins by the PI3K-like kinases, ATM, ATR and DNA-PK (Traven and Heierhorst, 2005). Although phosphorylation of T117 remains to be confirmed and has only been assessed indirectly, the expression of a T117A hSSB1 mutant in cells has been shown to disrupt DNA repair signalling following ionising radiation exposure (Richard et al., 2008). The mass spectrometry data reported in Figure 3.4 indicated the potential presence of two other phosphorylated hSSB1 SQ/TQ residues at S134 and S182, both of which may represent PI3K-like kinase-mediated regulatory sites. Of these, the putative phosphorylation of S134 was of particular interest due to its proximity to T117, suggesting that this region might represent a DNA damage-responsive “regulatory region”.

In addition to S134, the putative phosphorylation of S132 was also reported in section 3.4. Although these may represent separate phosphorylation events and indeed both were listed on the Mascot database user interface, the unambiguous site-assignment of phosphorylation to either of these residues could not be achieved. Indeed, whilst the tryptic peptide (amino acids 124-178; **Figure 4.1A**) containing S132 and S134 was detected twice from HU-treated cells with a neutral loss of ~98 Da (5351.389 da vs 5271.4227 da), most likely resulting from gas-phase β -elimination of phosphoserine to dehydroaminobutyric acid (Palumbo et al., 2011), this may be due to phosphorylation of one of several serine residues (S129, S132, S134, S141, S144, S147, S156, S172, S176). The detection of numerous high-confidence non-phosphorylated y-fragment ions generated at the c-terminus of these peptides however does suggest that phosphorylation is unlikely to occur C-terminal to A157, at S172 or S176 (**Figure 4.1B**).

Figure 4.1



B

b Ion	pS129	pS132	pS134	p C-term to S134	y Ion	p N-term to A157
b1	72.0444	72.0444	72.0444	72.0444	y1	175.1190
b2	171.1128	171.1128	171.1128	171.1128	y2	276.1666
b3	299.1714	299.1714	299.1714	299.1714	y3	363.1987
b4	413.2143	413.2143	413.2143	413.2143	y4	460.2514
b5	528.2413	528.2413	528.2413	528.2413	y5	557.3042
b6	597.2627	615.2733	615.2733	615.2733	y6	694.3631
b7	711.3056	729.3162	729.3162	729.3162	y7	781.3951
b8	808.3584	826.3690	826.3690	826.3690	y8	878.4479
b9	895.3904	895.3904	913.4010	913.4010	y9	979.4956
b10	966.4275	966.4275	984.4381	984.4381	y10	1213.072
b11	1053.4596	1053.4596	1053.4596	1071.4701	y11	1310.6000
b12	1181.5182	1181.5182	1181.5182	1199.5287	y12	1447.7189
b13	1278.5710	1278.5710	1278.5710	1296.5815	y13	1544.7717
b14	1379.6182	1379.6182	1379.6186	1397.6292	y14	1658.8146

Figure legend over page

Figure 4.1 Detection of phosphorylated hSSB1 by mass spectrometry

(A) Detection of a singularly phosphorylated peptide corresponding to hSSB1 amino acids 124-178. The fragment ion spectrum of a tryptic peptide corresponding to hSSB1 amino acids 124-178 with neutral loss of ~98 Da (5351.389 da vs 5271.4227 da) was interrogated and major peaks correlated with various y- ions. The intensity of each peak is given in arbitrary units of intensity. The hSSB1 schematic and amino acid sequence at the top of the spectrum indicate the region and sequence of hSSB1 represented by the peptide, as well as the detected b- and y- ions.

(B) The residue of hSSB1 phosphorylation is ambiguous. The expected b- and y- ions for hSSB1 phosphorylated at S129, S132, S134 or a c-terminal residue are given in the indicated columns. b- or y- ions are listed in mass/charge units. Values in green are confident matches to peaks in the spectra, whilst peaks in amber are observed but of low signal to noise ratio and are thus less confident.

In addition, the presence of numerous (albeit low confidence) b- fragment ions N-terminal to Q135, including b11-98, suggests that phosphorylation might occur at S129, S132 or S134. Although these data do indicate that b ions C-terminal to S134 should also contain neutral losses of ~ 98 Da, b- fragment ions containing Q135 or any subsequence residues of these peptides were not detected. Furthermore, although a signal corresponding to a b6-98 ion was detected (with low confidence), suggesting phosphorylation may occur at S129, the presence of contradictory high confidence b6 and b7 ions instead indicate that phosphorylation of S132 or S134 is more probable. Indeed, the Mascot algorithm designated phosphorylation of S132 or S134 an identical probability score for either peptide that was greater than that of phosphorylation at other serine residues. Moreover, whilst peaks were detected corresponding to b9 and b10, which support that phosphorylation occurs C-terminal to S132 at S134, a contradictory signal was also observed of similar m/z to b9-98, consistent with phosphorylation of S132.

It is worth noting that hSSB1 S134 phosphorylation has also recently been detected in another study and was listed on the curation website, phosphositeplus (Hornbeck

et al., 2012). Here, a phospho-serine 14-3-3 binding motif antibody was used to immunoprecipitate phosphorylated proteins from the chronic myelogenous leukemia cell line K562 and these analysed by tandem mass spectrometry. Although hSSB1 does not actually contain a 14-3-3 binding motif, this most likely reflects cross-reactivity of the antibody (Cell Signaling Technology cat # 9606) with other serine-phosphorylated motifs.

4.2.2 S134A hSSB1 is unable to rescue cells from the hydroxyurea and aphidicolin-sensitivity caused by hSSB1 depletion

The data above suggests that hSSB1 may be phosphorylated at S132 or S134, although that these events cannot be distinguished based on the mass spectrometry data. As the putative phosphorylation of S134 was of particular interest due to its presence within an SQ motif, which may suggest a role in the regulation of hSSB1 during DNA repair, it was of interest to test this directly. hSSB1 has previously been demonstrated to promote clonogenic survival following hydroxyurea treatment (Bolderson et al., 2014) and so it was reasoned that S134 phosphorylation may be required for this response. In order to assess this, a rescue experiment was planned in which endogenous hSSB1 would be firstly depleted and cells transiently reconstituted with siRNA-resistant WT hSSB1, or with a mutant where the putative S134 phosphorylation site was disrupted.

To achieve this, the preparation of siRNA-resistant hSSB1 constructs was firstly required. To this end, 5 silent point mutations were introduced into the hSSB1 CDS to disrupt the binding region of a previously optimised hSSB1 siRNA. Resistance of transiently expressed hSSB1 was then assessed by successive transfection of HeLa cells with hSSB1 siRNA over 48 hours, followed by transient over-expression of WT or siRNA-resistant 3x FLAG hSSB1 (5 Δ). Cells were then harvested and immunoblotted using an M2 FLAG antibody (**Fig 4.2A**). While WT 3x FLAG hSSB1 was almost entirely depleted in hSSB1 siRNA transfected cells, siRNA-resistant hSSB1 protein levels were only partially reduced and were indeed maintained at a level greater than that of endogenous hSSB1 in non-siRNA transfected cells. This level of resistance was reasoned as sufficient for the purpose of restoring hSSB1 levels in previously depleted cells.

Figure 4.2

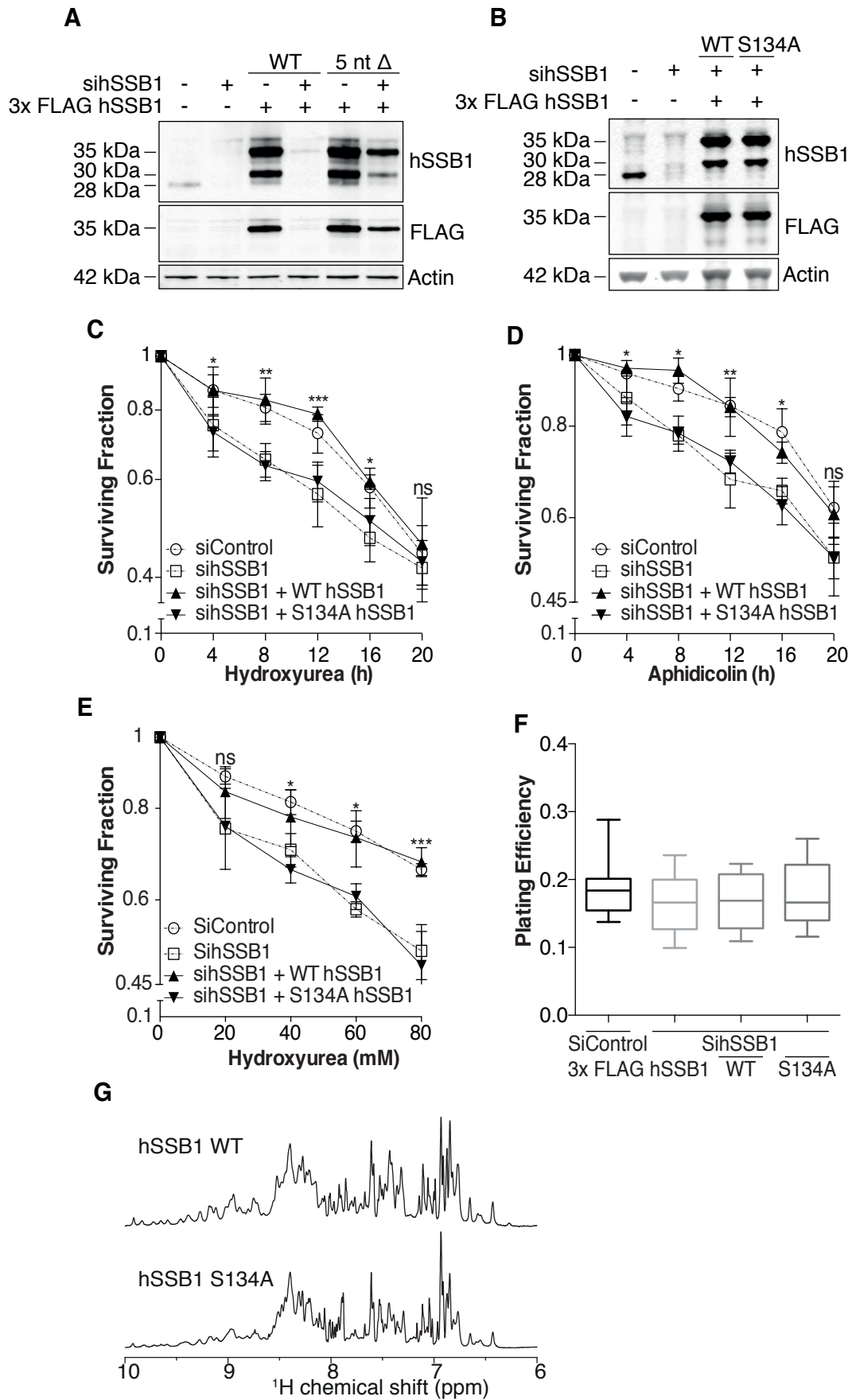


Figure legend over page

Figure 4.2 Cells expressing S134A hSSB1 are hypersensitive to hydroxyurea and aphidicolin

(A) Preparation of siRNA-resistant 3x FLAG hSSB1. Five silent point mutations were introduced into the coding sequence of the WT and S134A 3x FLAG hSSB1 pCMV6 vectors by site-directed mutagenesis in the region targeted by the hSSB1 siRNA. HeLa cells were then transfected with 50 nM stealth siRNA targeting the hSSB1 coding sequence, or with a negative control siRNA, twice, separated by 24 hours. The original plasmid, or the siRNA-resistant WT 3x FLAG hSSB1 construct, was then transiently expressed 24 hours later. Cells were harvested after 24 hours and lysed in RIPA buffer. 15 µg of whole cell lysate was immunoblotted and probed with antibodies against hSSB1, FLAG and actin.

(B) Expression of WT and S134A siRNA-resistant 3x FLAG hSSB1 in HeLa cells depleted of endogenous hSSB1. HeLa cells were depleted of endogenous hSSB1 as per (A). Cells were then transfected with WT or S134A siRNA-resistant 3x FLAG hSSB1, or an empty plasmid, 6 hours prior to seeding into wells of a 6-well plate at a density of 400 cells per well. Remaining cells were grown for an additional 24 hours and lysed in RIPA buffer. 15 µg of whole cell lysate was immunoblotted and probed with antibodies against hSSB1, FLAG and actin.

(C, D E) Cells expressing S134A hSSB1 are hypersensitive to hydroxyurea and aphidicolin. The cells plated in (B) were incubated for 24 hours and treated with 3 mM hydroxyurea (HU) (C) or 6 µg µL⁻¹ aphidicolin (Aph) (D) for 4, 8, 12, 16 or 20 hours, or left untreated, prior to exchange with fresh media. Alternatively, cells were treated with 20, 40, 60 or 80 mM hydroxyurea (HU), or mock-treated, for 4 hours (E). Three technical repeats were performed per dose. Cells were then grown for 10 days prior to staining of colonies with methylene blue. Colonies were manually counted and normalised to untreated cells. Data is graphed as the mean ± 1 standard deviation from 4 independent experiments. *t* tests were used to compare the ‘sihSSB1 + WT hSSB1’ and ‘sihSSB1 + S134A hSSB1’ datasets at each dose. ns = *P* > 0.05, * = *P* < 0.05, ** = *P* < 0.01, *** = *P* < 0.001

(F) A similar plating efficiency was observed regardless of hSSB1 depletion/expression in clonogenic assays. The plating efficiency for the untreated cells of each data set in (C) was calculated as the average colony count between technical replicates divided by the number of cells seeded (400). Data is graphed as the mean \pm 1 standard deviation from 12 independent experiments. No statistically significant difference was observed between data sets.

(G) WT and S134A hexa-His-tagged hSSB1 is similarly folded *in vitro*. WT and S134A hexa-His-tagged hSSB1 was expressed in SHuffle T7 *E. coli* and purified by Ni-NTA affinity capture, followed by size exclusion chromatography. 100-200 μ M of WT or S134A hSSB1 was analysed by one-dimensional NMR and proton chemical shifts measured relative to 4,4-dimethyl-4-silapentanesulfonic acid (DSS) at 0 ppm. The 1D NMR spectra of amide protons for WT and S134A hSSB1 are depicted.

To determine the requirement of S134 for hSSB1 function following hydroxyurea treatment, HeLa cells were depleted of endogenous hSSB1 over 48 hours using siRNA and WT or S134A siRNA-resistant 3x FLAG hSSB1 transiently re-introduced (**Fig 4.2B**). Cells were then seeded into wells of a 6-well plate and after 24 hours treated with 3 mM HU for 4, 8, 12, 16 or 20 hours. Cells were then released into fresh media and grown for 10 days before the surviving fraction of cells at each dose calculated relative to untreated cells (**Fig 4.2C**). Consistent with previously published data (Bolderson et al., 2014), hSSB1-depleted cells were hypersensitive to hydroxyurea treatment and a statistically significant numerical difference in the relative surviving fraction of cells transfected with control siRNA (siControl) or hSSB1 siRNA (sihSSB1) was observed between those treated with 3 mM HU for 4, 8, 12 and 16 hours. Interestingly however, a similar surviving fraction was observed for cells treated with 3 mM hydroxyurea for 20 hours regardless of hSSB1 status. Transient expression of WT siRNA resistant 3x FLAG hSSB1 was found to rescue cells from the hydroxyurea-sensitivity observed for hSSB1 depleted cells and no statistically significant difference in surviving fraction was observed at any time-point when compared with control siRNA transfected cells. By contrast, a statistically significant difference in surviving fraction was observed between cells depleted of endogenous hSSB1 and those reconstituted with WT siRNA resistant 3x

FLAG hSSB1. The transient expression of siRNA resistant S134A 3x FLAG hSSB1 was however unable to rescue cells from depletion of endogenous hSSB1 and no statistically significant difference in cell survival was observed between cells depleted of hSSB1 and those re-constituted with 3x FLAG S134A hSSB1. In addition, when compared to control siRNA transfected cells, or those cells expressing WT 3x FLAG hSSB1, HeLa cells reconstituted with S134A hSSB1 showed a statically significant difference in cell survival following hydroxyurea treatment for 4, 8, 12, and 16 hours. These data suggest that phosphorylation of residue S134 may be required for the function of hSSB1 following hydroxyurea treatment.

Hydroxyurea stalls replication forks through the depletion of dNTPs within the cells, which thereby disrupts new DNA synthesis (Koç et al., 2004). To confirm that our findings were due to fork disruption and not other effects of hydroxurea treatment, cells were also treated with $6 \mu\text{g } \mu\text{L}^{-1}$ of the DNA polymerase α inhibitor aphidicolin (Aph) as per above. Similarly to hydroxyurea treatment, hSSB1-depleted cells were hypersensitive to treatment with Aph, which could be rescued by re-introduction with WT, although not S134A, siRNA resistant 3x FLAG hSSB1 (**Fig 4.2D**). Interestingly, while these trends are similar to those observed following HU treatment, the reduction in surviving fraction observed at any time-point was markedly milder.

In the above two experiments, cells were treated with either 3 mM hydroxyurea or $6 \mu\text{g } \mu\text{L}^{-1}$ aphidicolin for 4, 8, 12, 16, or 20 hours. Under either of these treatments, a significant decrease in cell survival was observed for cells depleted of hSSB1 relative to control siRNA transfected cells, which could be rescued by over-expression of WT although not S134A siRNA resistant 3x FLAG hSSB1. These findings suggest that hSSB1 S134 is functionally important in the response to replicative stress. To confirm this further, an alternative treatment regime was employed where HeLa cells were treated with 20, 40, 60 or 80 mM hydroxyurea for a constant time of 4 hours prior to release into fresh media (**Fig 4.2E**). Similarly to above, hSSB1-depleted cells were hypersensitive to this treatment, which could be rescued by transient expression of siRNA resistant WT, although not S134A, 3x FLAG hSSB1. It should be noted that while hSSB1 depleted cells, as well as those

expressing S134A hSSB1, were hypersensitive to replication stress, a statistically significant difference in the colony count of untreated cells between datasets was not observed (**Fig 4.2F**). These data suggest that hSSB1 S134, or indeed hSSB1 in general, may not affect cell survival in the absence of exogenous DNA damage.

The data presented here indicate that phosphorylation of hSSB1 S134 may promote clonogenic survival following replication stress. A similar inability to rescue hSSB1 depletion may however also result from incorrect folding of the S134A hSSB1 phosphomutant. To assess whether S134A hSSB1 is folded similarly to the WT protein, site-directed mutagenesis was used to prepare a S134A hexa-His hSSB1 bacterial expression plasmid. This construct was then transported to Dr Roland Gamsjaeger at the University of Western Sydney who performed 1D NMR analysis using recombinant protein. Here, WT and S134A hexa-His hSSB1 were expressed and purified from BL21 *E. coli* using Ni-NTA beads and size exclusion chromatography. WT or S134A hexa-His-hSSB1 were then analysed by one-dimensional NMR and proton chemical shifts measured relative to 4,4-dimethyl-4-silapentanesulfonic acid (DSS) at 0 ppm (**Fig 4.2G**) As a similar spectrum was observed for WT and S134 hSSB1, these data demonstrate that S134A does not affect the folding of hSSB1. This indicates that the lack of complementation in HU/Aph survival assays is not merely due to general protein destabilisation but to a specific biological function normally carried out by S134

4.2.3 hSSB1 is phosphorylated at serine residue 134 (S134)

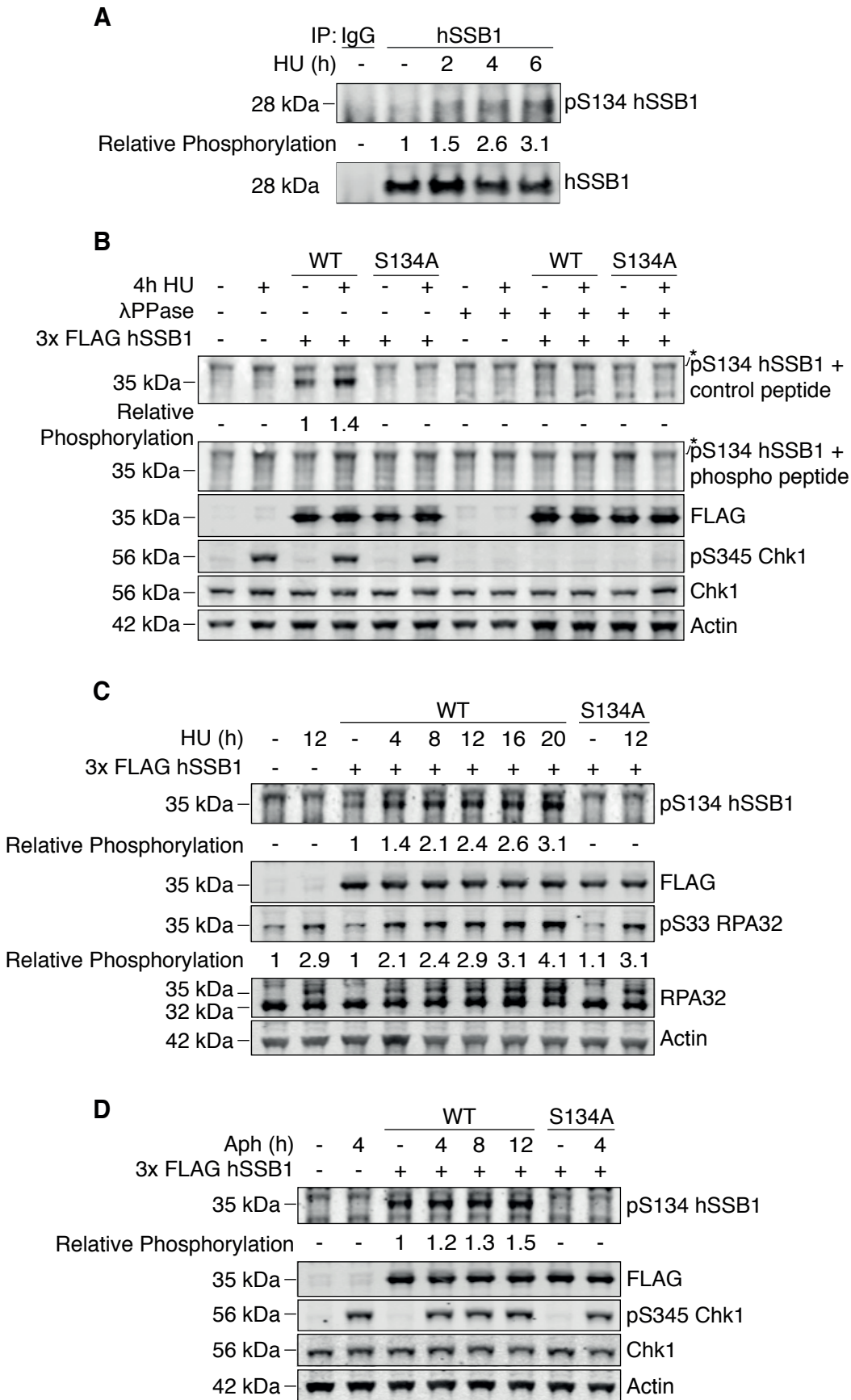
The data obtained in sections 4.2.1 and 4.2.2 suggests that hSSB1 may be phosphorylated at residue S134 following hydroxyurea treatment of cells and that this modification may promote clonogenic survival of cells following such treatment. These findings thereby warranted further investigation into the potential phosphorylation of this residue. To do so, a rabbit polyclonal antibody was raised against a peptide representing residues 131-140 of hSSB1 and containing phosphoserine at residue 134 (PSA{pS}QPTTGPKC). The peptide also contained a lysine – cysteine (KC) motif at the 3' termini. While, the lysine residue afforded the peptide a net positive charge, the cysteine was added to facilitate conjugation to keyhole limpet hemocyanin (KLH), the carrier protein used during immunisation. Approximately 12 weeks later, the antibody was then affinity purified from serum

using the phosphorylated immunisation peptide. This work was conducted by the contract research organisation, GenScript.

Upon receipt of the S134 phospho-antibody, whole cell lysates were prepared from HeLa cells treated with 3 mM hydroxyurea for a range of time periods. Under all conditions tested, a band corresponding to the approximate size of hSSB1 could however not be detected by immunoblotting. As this may be due to the low abundance of endogenous phosphorylated hSSB1 in these samples, hSSB1 was instead immunoprecipitated from similar samples using a sheep polyclonal hSSB1 antibody bound to protein G magnetic dynabeads. Immunoprecipitated protein was then immunoblotted and probed with the pS134 hSSB1 antibody. In doing so, a hSSB1-specific band was detected, which was enhanced following hydroxyurea treatment (**Fig 4.3A**). These results suggest that hSSB1 may be phosphorylated at S134 following hydroxyurea treatment.

Although hSSB1 S134 phosphorylation could be detected as above, only a relatively indistinct band could ever be observed from immunoprecipitated endogenous protein. In an attempt to amplify this signal, WT 3x FLAG hSSB1 was instead transiently over-expressed in cells. In this way, immunoblotting of whole cell lysates revealed a distinct band that was specific to the over-expressed protein and which was enhanced following hydroxyurea treatment. The antibody did however also detect a non-phosphorylatable hSSB1 mutant where serine 134 was converted to alanine (S134A); this suggested that the antibody might also detect non-phosphorylated hSSB1. To overcome the non-specificity of the hSSB1 phospho-antibody, a non-phosphorylated peptide was included in the antibody working solution (**Fig 4.3B**; + control peptide). This peptide was of the same sequence as the immunisation peptide, although contained a serine residue in place of phosphoserine. The peptide was included at a 200 x molar excess to the antibody to prevent non-specific binding by competing with non-phosphorylated hSSB1 in the whole cell lysate. Specificity of the pS134 antibody was further demonstrated by incubation of whole cell lysates from HeLa cells expressing WT or S134A 3x FLAG hSSB1 and treated with or without 3 mM hydroxyurea for 4 hours with lambda phosphatase (λ PPase) for 45 minutes at 30 °C.

Figure 4.3



continued over page

Figure 4.3

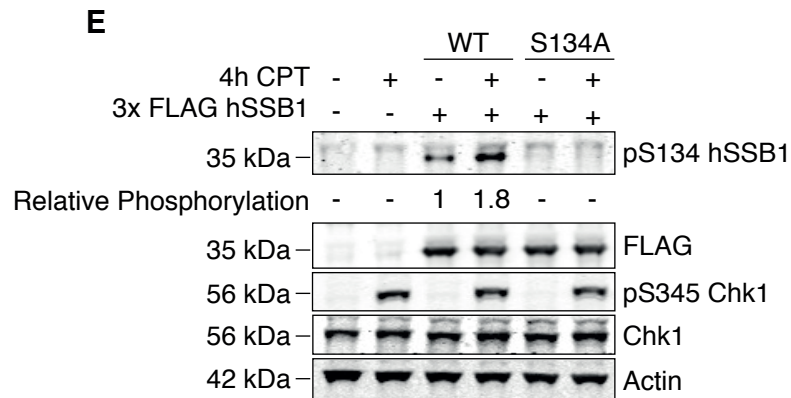


Figure 4.3 hSSB1 serine residue 134 (S134) phosphorylation is enhanced in response to replication stress

(A) Phosphorylation of immunoprecipitated hSSB1. HeLa cells were treated with 3 mM hydroxyurea for 2, 4, or 6 hours, or mock treated, prior to harvesting. Cells were lysed in IP buffer and 1 mg of whole cell lysate incubated with protein G dynabeads bound to a hSSB1 antibody, or an isotype control IgG. Beads were incubated with sample overnight at 4 °C with rotation, washed 5x with IP buffer and protein eluted by heating to 80 °C for 10 minutes. Eluent was then immunoblotted and probed with antibodies against total and S134 phosphorylated hSSB1. Densitometry of pS134 hSSB1 bands was performed using ImageJ, normalised to total hSSB1, and expressed relative to the untreated sample. These results are representative of three independent experiments.

(B) The S134 phospho-antibody is specific for transiently expressed S134 phosphorylated hSSB1 when incubated with a non-phosphorylated S134 hSSB1 peptide. HeLa cells were transiently transfected with WT or S134A 3x FLAG hSSB1, or a pCMV6 empty vector, 24 hours prior to treatment with or without 3 mM hydroxyurea (HU). Cells were then harvested, lysed in RIPA buffer and incubated either with or without addition of lambda (λ) phosphatase at 30 °C for 45 minutes. Each sample (15 μ g) was then immunoblotted and probed with a novel polyclonal antibody raised against the hSSB1 peptide PSA{pS}QPTTGPKC, representing hSSB1 phosphorylated at S134. The antibody was pre-incubated either for 30 minutes with a control non-phosphorylated peptide (+ control peptide), which functioned to prevent binding of the antibody to non-phosphorylated hSSB1, or with

the phosphorylated immunisation peptide (+ phosphopeptide), which functioned to block the binding to phosphorylated hSSB1. The immunoblot was also probed for S345 phosphorylated and total Chk1, which functioned as a positive control for HU treatment, as well as for lambda phosphatase activity. Actin served as a loading control. Densitometry of pS134 hSSB1 bands was performed using ImageJ, normalised to FLAG, and expressed relative to untreated WT 3x FLAG hSSB1-expressing cells. * = non-specific band. These results are representative of three independent experiments.

(C) hSSB1 phosphorylation increases with up to 20 hours HU treatment. HeLa cells were transfected as per (A) and treated with 3 mM hydroxyurea (HU) for 4, 8, 12, 16 or 20 hours, or left untreated and harvested. Whole cell lysates were prepared in RIPA buffer and 15 µg immunoblotted with antibodies against S134 phosphorylated hSSB1, FLAG and actin. Blots were also probed for total and serine 33 phosphorylated RPA32, which was used as a positive control. Densitometry of pS134 hSSB1 bands was performed as per (B). Phosphorylation of RPA32 is expressed as the relative ratio of the 34 kDa to 32 kDa RPA32 bands. These results are representative of three independent experiments

(D and E) hSSB1 S134 phosphorylation is enhanced following treatment with aphidicolin or camptothecin. HeLa cells were transfected with WT or S134A 3x FLAG hSSB1, or a vector control, 24 hours prior to treatment of cells with 6 µg µl⁻¹ Aph for 4, 8, or 12 hours (E), or with 2 µM CPT for 4 hours (F). Whole cell lysates prepared from these cells were immunoblotted for S134 phosphorylated hSSB1, FLAG, S345 phosphorylated and total Chk1 (positive control) and actin (loading control). Densitometry of pS134 hSSB1 bands was performed as per (B). These results are representative of three independent experiments

λPPase is a serine/threonine/tyrosine protein phosphatase and under such incubation conditions may remove phosphate groups from other proteins. These samples were then immunoblotted and probed with the pS134 hSSB1 antibody (**Fig 4.3B**). As depicted in Figure 4.3B, phosphorylated hSSB1 could not be detected in λPPase-treated whole cell lysates from WT 3x FLAG hSSB1-expressing cells. As a third

specificity control, a pS134 antibody working solution was also prepared containing the phosphorylated immunisation peptide (**Fig 4.3B**; + phospho peptide). Inclusion of this peptide entirely blocked detection of WT 3x FLAG hSSB1 and further confirms specificity of this antibody for S134 phosphorylated hSSB1. By confirming specificity of the pS134 antibody for S134 phosphorylated hSSB1, these data also confirm the phosphorylation of this residue in cells.

To further characterise the phosphorylation of hSSB1 S134 following replicative fork disruption, HeLa cells transiently expressing WT or S134A 3x FLAG hSSB1 were treated with 3 mM hydroxyurea for increasing time periods over 20 hours (treatments were staggered and cells harvested at the same time). Immunoblotting of whole cell lysates demonstrated a gradual increase in hSSB1 S134 phosphorylation over this time, increasing in intensity by over 3-fold (**Fig 4.3C**). Phosphorylation of serine 33 of the RPA 32 kDa subunit (pS33 RPA32) was also seen to increase over this time and functioned as a positive control for this assay. Interestingly, densitometry of hSSB1 S134 and RPA32 S33 demonstrated a comparable relative increase in phosphorylation over this time, indicating that these residues may be phosphorylated with similar kinetics.

To further confirm that hSSB1 is phosphorylated at S134 in response to replication fork disruption, HeLa cells expressing 3x FLAG hSSB1 were treated with 6 $\mu\text{g } \mu\text{L}^{-1}$ of the polymerase α inhibitor aphidicolin (Aph) for 4, 8, and 12 hours. This treatment also resulted in a significant increase in hSSB1 S134 phosphorylation that continued for at least 12 hours (**Fig 4.3D**).

Hydroxyurea and aphidicolin cause disruption to replication by inhibiting polymerase progression. In both instances, affected replication forks are rapidly stabilised by numerous DNA repair proteins whilst the cell attempts to re-initiate replication. Stalled replication forks are typically stable for at least 12-18 hours, before collapsing to form double-strand DNA breaks (Saintigny et al., 2001). In contrast to the fork disruption caused by hydroxyurea and aphidicolin, compounds that directly inhibit separation of the DNA strands ahead of the replisome cause the essentially immediate formation of double-strand DNA breaks (Saleh-Gohari et al., 2005). To determine if hSSB1 is also phosphorylated following such stress, HeLa

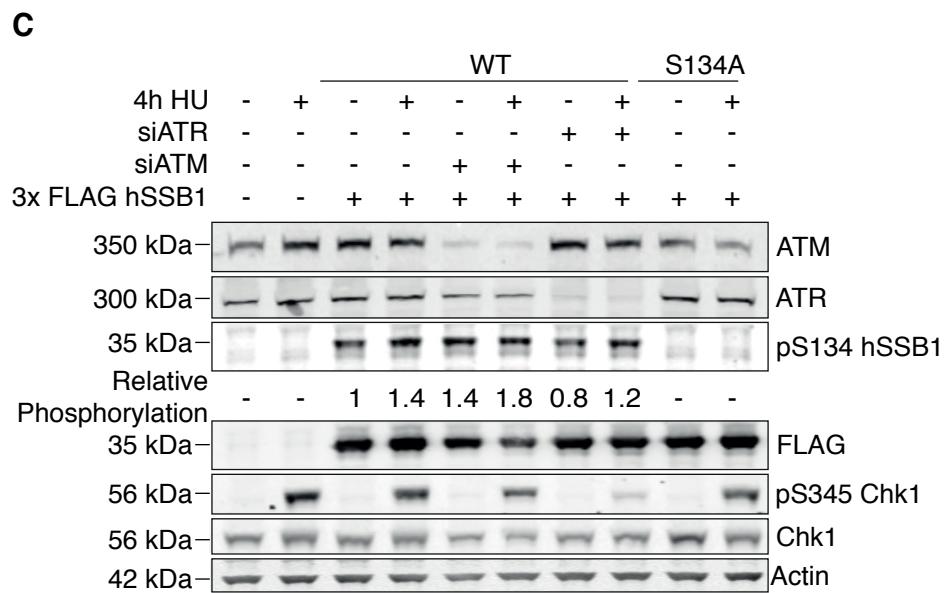
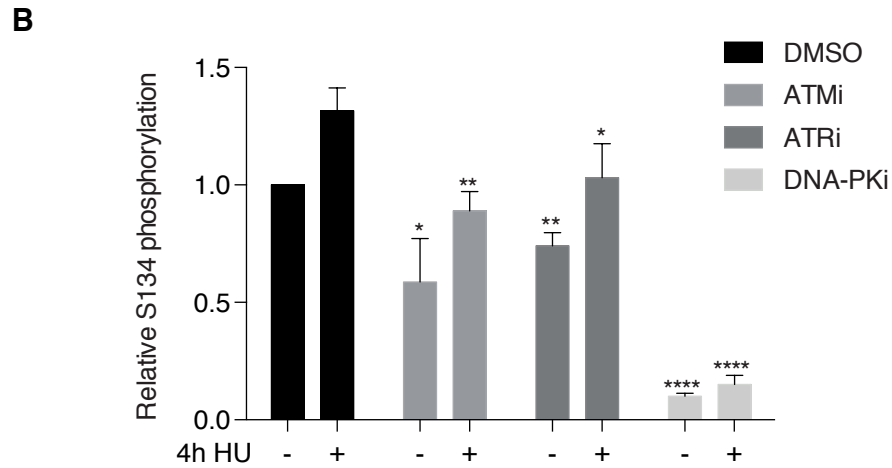
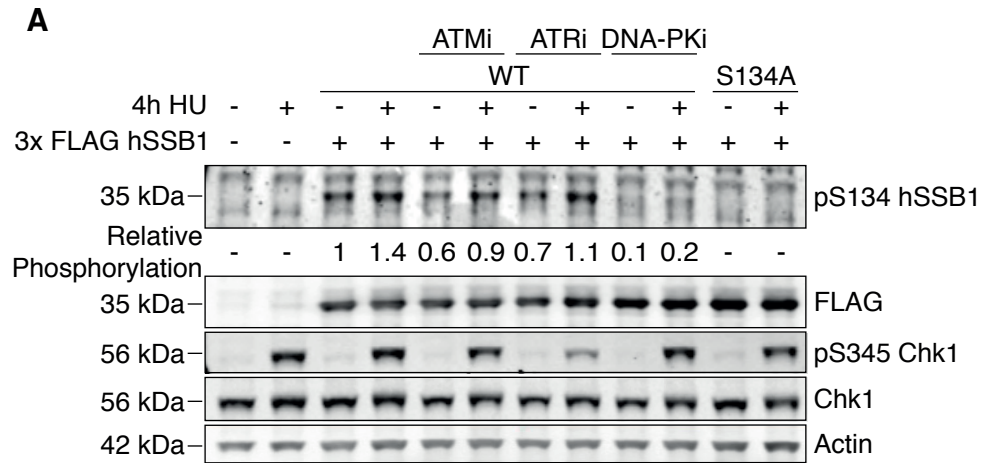
cells transiently expressing 3x FLAG hSSB1 were treated with 2 μ M of the DNA topoisomerase II inhibitor camptothecin for 4 hours. Whole cell lysates were then prepared and immunoblotted. In doing so, a marked increase in hSSB1 S134 phosphorylation was observed that was comparable to 8 hours treatment with 3 mM hydroxyurea (**Fig 4.3E**). Together, these data support that hSSB1 is phosphorylated in response to genotoxic stress during replication.

4.2.4 hSSB1 S134 phosphorylation is mediated by the DNA-dependent protein kinase

As mentioned in previous sections, residue S134 of hSSB1 is a component of an SQ (serine-glutamine) motif. As these motifs frequently function as phosphorylation substrates of the PI3K-like kinases, ATM, ATR and DNA-PK (Liu et al., 2012), it was interesting to consider that one of these enzymes may be responsible for hSSB1 S134 phosphorylation. Indeed, each of these kinases is known to function in the response to replication disruption (Liu et al., 2012). To determine if one of these kinases is responsible for hSSB1 S134 phosphorylation, HeLa cells transiently expressing 3x FLAG hSSB1 were pre-treated with chemical inhibitors against each of these kinases 30 min prior to addition of 3 mM hydroxyurea for 4 hours. Inhibitors were used at concentrations described in previous publications (Couch et al., 2013; Farber-Katz et al., 2014; Fujisawa et al., 2015; Gautam and Bridge, 2013). While a small decrease in hSSB1 phosphorylation was consistently observed following addition of KU-60019 and VE-821, inhibitors of ATM and ATR, respectively, an ~90% reduction in both basal and HU-induced hSSB1 phosphorylation was observed by treatment of cells with the DNA-PK inhibitor NU7441 (**Fig 4.4A and B**).

To further explore the role of ATM, ATR and DNA-PK in the phosphorylation of hSSB1 S134, each kinase was depleted from HeLa cells by double transfection with single-sequence siRNA. 3x FLAG hSSB1 was then transiently over-expressed in these cells for 24 hours prior to 4 h treatment with 3 mM HU. While Stealth siRNA was used for ATM and ATR depletion, Silencer Select siRNA was employed for depletion of the DNA-PK catalytic subunit (DNA-PKcs).

Figure 4.4



continued over page

Figure 4.4

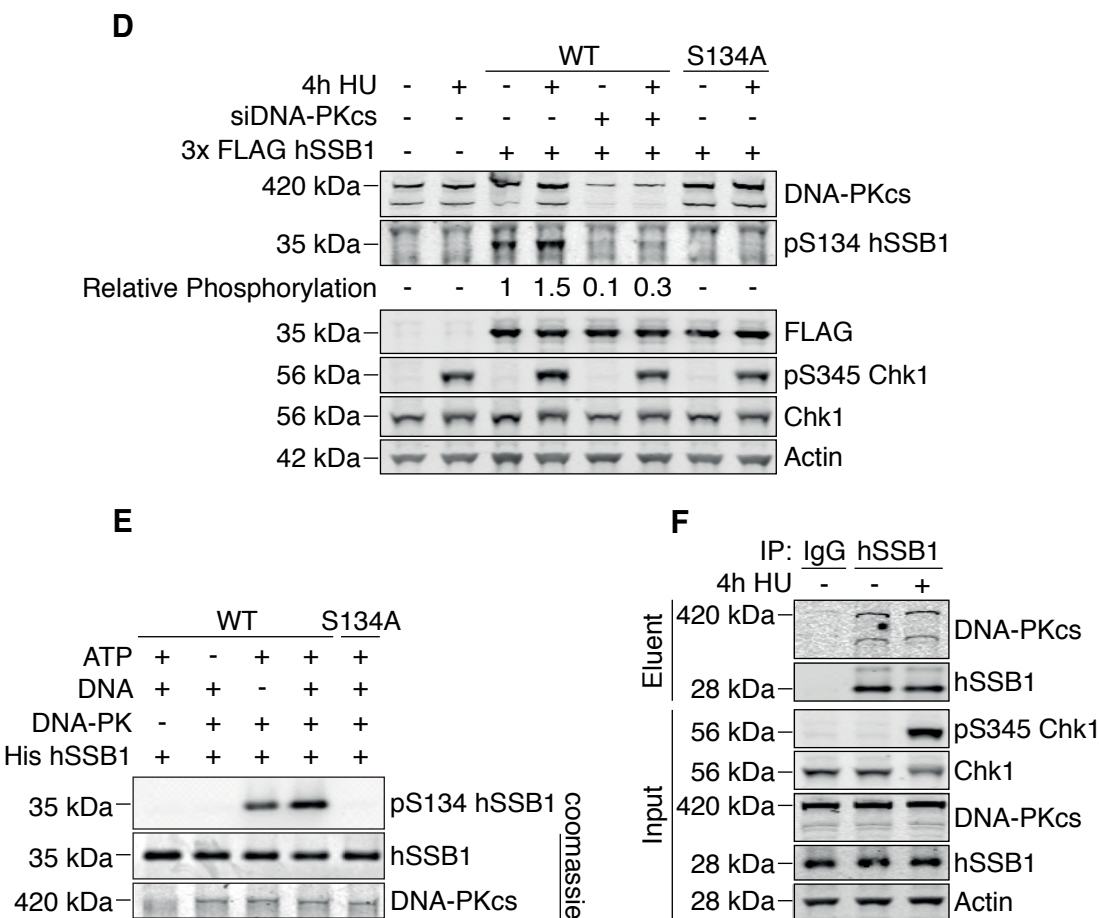


Figure 4.4 Phosphorylation of hSSB1 S134 is mediated by DNA-PK

(A and B) hSSB1 S134 phosphorylation is suppressed by inhibition of ATM, ATR and DNA-PKcs. HeLa cells transiently expressing WT or S134A 3x FLAG hSSB1, or an empty vector, for 24 hours were pre-treated with 5 μ M KU-60019 (ATMi), 10 μ M VE-821 (ATRi) or 5 μ M NU7441 (DNA-PKi) for 30 min, or with DMSO, prior to treatment with 3 mM HU for 4 hours. (A) Whole cell lysates were then prepared and immunoblotted for phosphorylation of hSSB1 S134, FLAG, pS345 and total Chk1, and actin (loading control). Densitometry of pS134 hSSB1 bands was performed using ImageJ, normalised to FLAG, and expressed relative to untreated WT 3x FLAG hSSB1-expressing cells. (B) Bar graph illustrating relative hSSB1 S134 phosphorylation from 3 independent repeats of (A). Data is graphed as the mean \pm 1 standard deviation. *t* tests were used to compare phosphorylation of hSSB1 S134 for each inhibitor data set relative to DMSO lanes for each dose. ns = $P > 0.05$, * = $P < 0.05$, ** = $P < 0.01$, *** = $P < 0.001$, **** = $P < 0.0001$.

(C) hSSB1 S134 phosphorylation is not suppressed by siRNA-depletion of ATM or ATR. HeLa cells were depleted of ATM or ATR by transfection of 50 nM siRNA twice, separated by 24 hours. The following day, cells were transiently transfected with plasmids encoding WT or S134A 3x FLAG hSSB1 for 24 hours. Cells were then treated with 3 mM HU for 4 hours, lysed and immunoblotted with antibodies against ATM, ATR, pS134 hSSB1, FLAG, pS345 and total Chk1, and actin (loading control). Densitometry of pS134 hSSB1 bands was performed using ImageJ, normalised to FLAG, and expressed relative to untreated control siRNA WT 3x FLAG hSSB1-expressing cells. These results are representative of three independent experiments.

(D) hSSB1 S134 phosphorylation is strongly suppressed by siRNA-depletion of DNA-PKcs. DNA-PKcs was depleted from HeLa cells by double transfection with 10 nM silencer select siRNA, prior to transient expression of WT or S134A 3x FLAG hSSB1, or an empty control, for 24 hours. Cells were then treated with 3 mM HU for 4 hours and whole cell lysates immunoblotted for phosphorylation of S134 hSSB1, FLAG, pS345 and total Chk1, and actin (loading control). Densitometry of pS134 hSSB1 bands was performed as per (C). These results are representative of three independent experiments.

(E) hSSB1 S134 is phosphorylated by DNA-PK *in vitro*. 500 ng of recombinant WT or S134A hexa-His-hSSB1 was incubated with 10 U of DNA-PKcs/Ku for 30 mins at 30 °C with or without 100 μ M ATP and 10 μ g mL⁻¹ sonicated salmon sperm DNA. Reactions were separated on a SDS-PAGE gel and either immunoblotted for hSSB1 S134 phosphorylation or stained with colloidal coomassie blue (shown in greyscale). These results are representative of three independent experiments.

(F) hSSB1 associates with DNA-PKcs in cells before and after HU treatment. HeLa cells were treated with 3 mM HU, or mock treated, for 4 h. Whole cell lysates were then prepared and 500 μ g incubated with protein G magnetic dynabeads bound to antibodies against hSSB1, or a sheep isotype control IgG, for 2 hours at 4 °C. Beads were washed and protein eluted by heating to 90 °C in SDS loading buffer for 10 min. Eluent was immunoblotted for hSSB1 and DNA-PKcs. Whole cell lysates

were immunoblotted with antibodies against hSSB1, DNA-PKcs, pS345 and total Chk1 and actin (loading control). These results are representative of three independent experiments.

Immunoblotting of whole cell lysates from these experiments demonstrated that while ATM and ATR depletion did not suppress phosphorylation of hSSB1 S134 (**Fig 4.4C**), basal and HU-induced phosphorylation was largely reduced in cell depleted of DNA-PKcs (**Fig 4.4D**). These data support that while ATM and ATR may have a role in the regulation of hSSB1 S134 phosphorylation, DNA-PK is most likely the major kinase involved in cells and may function both prior to and following replication fork disruption.

To further determine whether DNA-PK may directly phosphorylate hSSB1 S134, an *in vitro* kinase assay using purified DNA-PK and recombinant hexa-His-hSSB1 was employed. For this assay, WT and S134A hexa-His hSSB1 was expressed and purified from Shuffle T7 Express *E. coli*. Recombinant hSSB1 was purified similarly to in Figure 4.2G and concentrations estimated on coomassie blue-stained SDS-PAGE gels. Kinase assays were performed by incubating 500 ng of recombinant WT or S134A hexa-His hSSB1 with 10 U of DNA-PK for 30 mins at 30 °C +/- 100 μ M ATP and 10 μ g mL⁻¹ sheared salmon sperm DNA. Immunoblotting of the reaction with the pS134 hSSB1 antibody demonstrated robust phosphorylation of WT, although not of S134A hexa-His hSSB1, which was substantially increased following stimulation of DNA-PK activity by the addition of ssDNA (**Figure 4.4E**).

Although the data above suggests that DNA-PK may phosphorylate hSSB1 S134 *in vitro*, it remained important to ensure that DNA-PK may be spatially available to act on hSSB1 in cells. To test this, hSSB1 was immunoprecipitated from whole cell lysates of HeLa cells treated with +/- 3 mM hydroxyurea for 4 hours and immunoblotted for DNA-PKcs. In doing so, hSSB1 was found to associate with DNA-PKcs both before and following hydroxyurea treatment, suggesting that hSSB1 and DNA-PK may form a complex independently of exogenous DNA damage. Indeed, these observations are consistent with the finding that DNA-PKcs depletion or inhibition reduces both hydroxyurea-induced and basal hSSB1 S134

phosphorylation. These findings provide evidence that hSSB1 is regulated by direct DNA-PK phosphorylation of S134, which is enhanced following replication fork disruption.

4.2.5 hSSB1 S134 may not be phosphorylated in response to double-strand DNA break formation

Previous work on hSSB1 has largely focussed on its potential role in the repair of double-strand DNA breaks by homologous recombination. Here, hSSB1 may be involved in the detection of ssDNA exposed as a result of break formation (Richard et al., 2008), as well as the subsequent recruitment and stimulation of the MRN nuclease complex (Richard et al., 2011b; Richard et al., 2011a). In addition, hSSB1 may promote Exo1-mediated end-resection of the break (Yang et al., 2012), as well as the activation of cell cycle checkpoints (Richard et al., 2008). It was therefore of interest to determine whether hSSB1 S134 may also be phosphorylated in response to the formation of double-strand DNA breaks. To assess this, HeLa cells transiently expressing 3x FLAG hSSB1 were exposed to 6 Gy of ionising radiation to cause such breaks and then harvested 0.5, 1, 2, or 4 hours later. 4 h treatment with 3 mM hydroxyurea was used as an antibody control. Whole cell lysates were then prepared and immunoblotted for hSSB1 phosphorylation, as well as auto-phosphorylation of ATM 1981, a marker of double-strand DNA break formation (**Figure 4.5A**). While phosphorylation of ATM was observed following DNA damage, an increase in the phosphorylation of hSSB1 S134 comparable to that observed following 4h HU treatment was not detected at any time-point post-irradiation. These data indicate that hSSB1 S134 may not be phosphorylated during the homology-directed repair of double-strand DNA breaks.

In addition to homologous recombination, a relatively rare pathway that occurs exclusively during S and G2 of the cell cycle, double-strand DNA breaks may also be repaired via the more frequently employed and cell cycle-wide process of non-homologous end-joining (NHEJ) (Shrivastav et al., 2008).

Figure 4.5

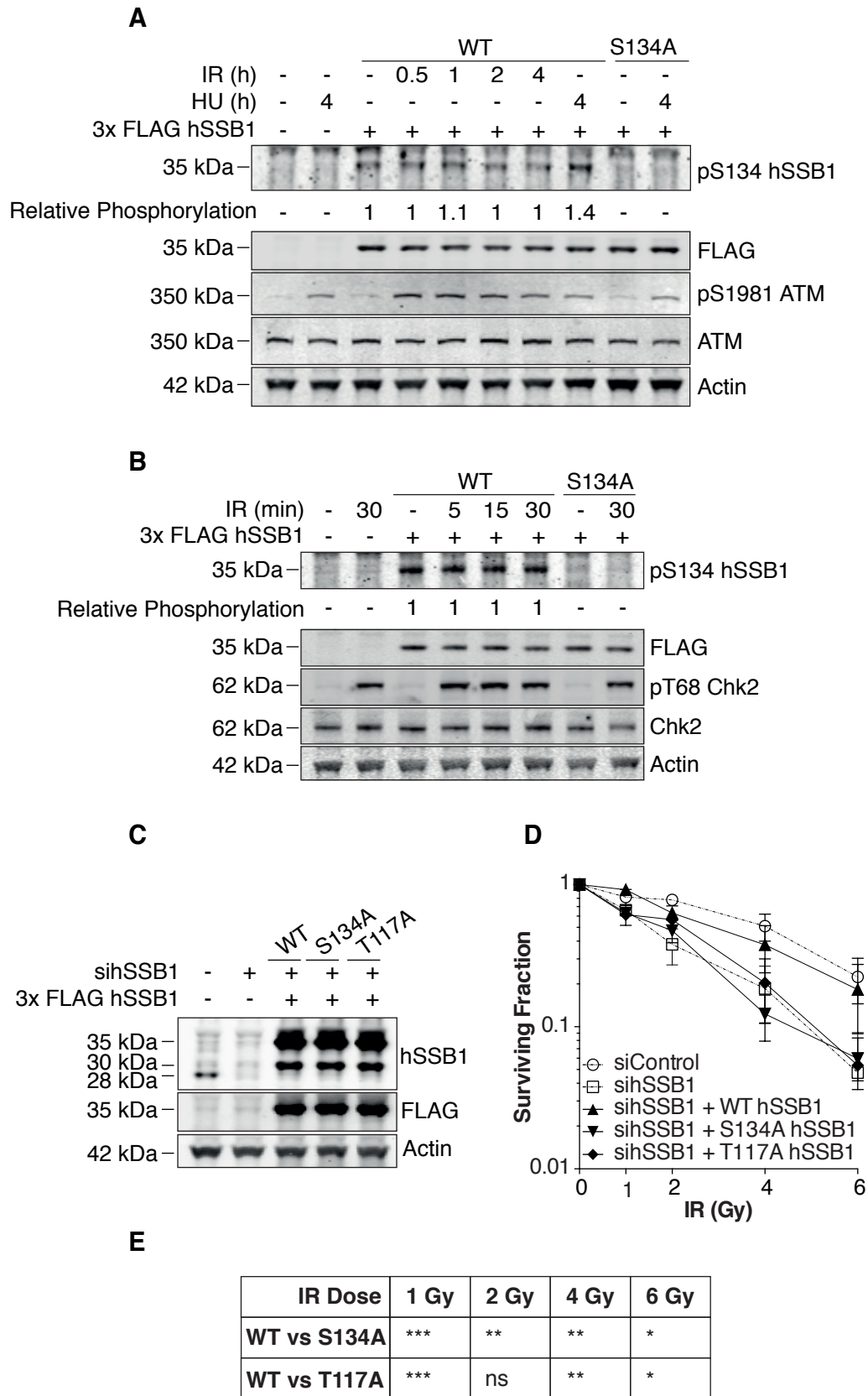


Figure legend over page

Figure 4.5 hSSB1 S134 may not be phosphorylated in response to double-strand DNA-break formation

(A) hSSB1 S134 may not be phosphorylated in response to double-strand DNA-break formation. HeLa cells transiently expressing WT or S134A 3x FLAG hSSB1 for 24 hours were exposed to 6 Gy ionising radiation (IR) and harvested after 0.5, 1, 2, or 4 hours. Alternatively, cells were treated with hydroxyurea (HU) for 4 hours and then harvested. Whole cell lysates were then prepared and 15 µg immunoblotted with antibodies against pS134 hSSB1 and FLAG, as well as pS1981 and total ATM (IR and HU positive control) and actin (loading control). Densitometry of pS134 hSSB1 bands was performed using ImageJ, normalised to FLAG, and expressed relative to untreated WT 3x FLAG hSSB1-expressing cells. These results are representative of three independent experiments

(B) hSSB1 S134 phosphorylation is not enhanced at short time-points after ionising radiation exposure. HeLa cells were transfected with WT or S134A 3x FLAG hSSB1 as per (A) and exposed to 6 Gy ionising radiation for 5, 15 or 30 minutes. Cells were then harvested, lysed, and 15 µg of whole cell lysate immunoblotted with antibodies against pS134 hSSB1 and FLAG, as well as pT68 and total Chk2 (positive control) and actin (loading control). Densitometry of pS134 hSSB1 bands was performed as per (A). These results are representative of two independent experiments.

(C) Expression of WT, S134A and T117A siRNA-resistant 3x FLAG hSSB1 in HeLa cells depleted of endogenous hSSB1. HeLa cells were depleted of endogenous hSSB1 by double transfection with siRNA. Cells were then transfected with WT or S134A siRNA-resistant 3x FLAG hSSB1, or an empty plasmid, 6 hours prior to seeding into wells of a 6-well plate at a density of 400 cells per well. Remaining cells were grown for an additional 24 hours and lysed in RIPA buffer. 15 µg of whole cell lysate was immunoblotted and probed with antibodies against hSSB1, FLAG and actin. This figure is representative of each repeat shown in (D).

(D and E) Cells expressing S134A or T117A hSSB1 are hypersensitive to ionising radiation (IR). The cells plated in (C) were incubated for 24 hours and treated with 1, 2, 4 or 6 Gy ionising radiation (IR). Three technical repeats were performed for each. Cells were grown for 10 days prior to staining of colonies with methylene blue. Colonies were manually counted and counts normalised to untreated cells. Data is graphed as the mean \pm 1 standard deviation from 3 independent experiments (D). *t* tests were used to compare the ‘sihSSB1 + WT hSSB1’ and ‘sihSSB1 + mutant hSSB1’ datasets at each dose. ns = $P > 0.05$, * = $P < 0.05$, ** = $P < 0.01$, *** = $P < 0.001$ (E).

Furthermore, whilst DNA-PK may have roles in the negative regulation of homologous recombination (Zhou & Paull, 2013), it is mostly associated with repair by NHEJ (Bekker-Jensen and Mailand, 2010; Zhou and Paull, 2013). Although a role for hSSB1 in this process has not been directly assessed, numerous data have indirectly implied its involvement. These include: 1) hSSB1 forms distinct nuclear foci in 95% of cells within 30 minutes of exposure to ionising radiation, presumably at sites of double-strand DNA breaks (Richard et al., 2008). This percentage is considerably higher than would be expected if foci formation were restricted to S and G2 phase cells. 2) hSSB1 is required for the fast repair of double-strand DNA breaks in cells synchronised in G1 by a double thymidine block (Zhang et al., 2014). It is therefore interesting to consider that while hSSB1 S134 may not be phosphorylated during homologous recombination, it may be during non-homologous end joining.

Whilst the time-points assessed in Figure 4.5A are appropriate for homologous recombination repair, which requires \sim 7 hours, non-homologous end joining will typically conclude within 10-30 minutes of double-strand DNA break formation (Mao et al., 2008b). It is therefore possible that hSSB1 is phosphorylated and dephosphorylated within the time-points assessed. To determine whether S134 may be phosphorylated at earlier time-points post ionising radiation exposure, HeLa cells transiently expressing 3x FLAG hSSB1 were irradiated and harvested after 5, 15 or 30 minutes. Whole cell lysates prepared from these cells were then immunoblotted for S134 phosphorylation (**Figure 4.5B**). In this instance, phosphorylation of Chk2 T68 was used as a DNA damage positive control (Ward et al., 2001). While Chk2 phosphorylation was detected within 5 minutes of ionising radiation exposure, a

change in hSSB1 S134 phosphorylation was not observed. These data suggest that phosphorylation of hSSB1 S134 may not be enhanced following double-strand DNA break exposure.

Based on these observations it seemed reasonable that while phosphorylation of hSSB1 S134 may be required for the response to replication inhibition, it may be dispensable following double-strand DNA break formation. Furthermore, it is tempting to speculate that S134 and T117 phosphorylation may be differentially required - S134 phosphorylation during S phase disruption and T117 phosphorylation in the response to double-strand DNA breaks. To confirm that S134 is not required following ionising radiation exposure, cells were depleted of endogenous hSSB1 as described previously (Section 4.2.2) and then transiently expressed with WT, S134A or T117A siRNA-resistant 3x FLAG hSSB1 (**Figure 4.5C**). Cells were then seeded into wells of a 6-well plate and after 24 hours exposed to 1, 2, 4 or 6 Gy of ionising radiation. After 10 days, cells were stained with methylene blue and the surviving fraction of cells at each dose calculated relative to the survival of untreated cells (**Figure 4.5D and E**). Consistent with previous data, a statistically significant decrease in cell survival was observed at all doses for hSSB1-depleted cells relative to control cells (Ren et al., 2014; Richard et al., 2008). Surprisingly, while WT 3x FLAG hSSB1 was able to rescue the sensitivity associated with hSSB1 depletion, cells expressing S134A or T117A 3x FLAG hSSB1 phenocopied the hSSB1 knock down cells. Indeed, a statistically significant reduction in the relative surviving fraction of cells was observed at multiple doses when compared to WT. These data may suggest that hSSB1 S134 phosphorylation is required for the response to double-strand DNA breaks, despite the lack of additional S134 phosphorylation observed under such conditions.

4.2.6 S134 hSSB1 is suppressed by PPP-family protein phosphatases

In undamaged cells, several DNA repair proteins, including Chk1 and ATM are maintained in a hypo-phosphorylated state through the function of PPP-family serine/threonine phosphatases (protein phosphatases (PP) 1, 2A, 4, 5, 6) (Goodarzi et al., 2004; Leung-Pineda et al., 2006). As data presented in earlier sections suggests that hSSB1 S134 may be partially phosphorylated in undamaged cells and then

enhanced following replication stress, we reasoned that steady-state hSSB1 phosphorylation might also be subject to enzymatic suppression. To determine whether hSSB1 S134 may be de-phosphorylated by one of these phosphatases, HeLa cells were transiently transfected with WT or S134A 3x FLAG hSSB1 24 hours prior to treatment with 3 mM hydroxyurea for 4 hours. Thirty minutes before harvesting, cells were additionally treated with the PPP-family phosphatase inhibitors okadaic acid and calycurin A (**Figure 4.6A**). Whole cells lysates were then prepared and immunoblotted for hSSB1 S134 phosphorylation (**Figure 4.6B**).

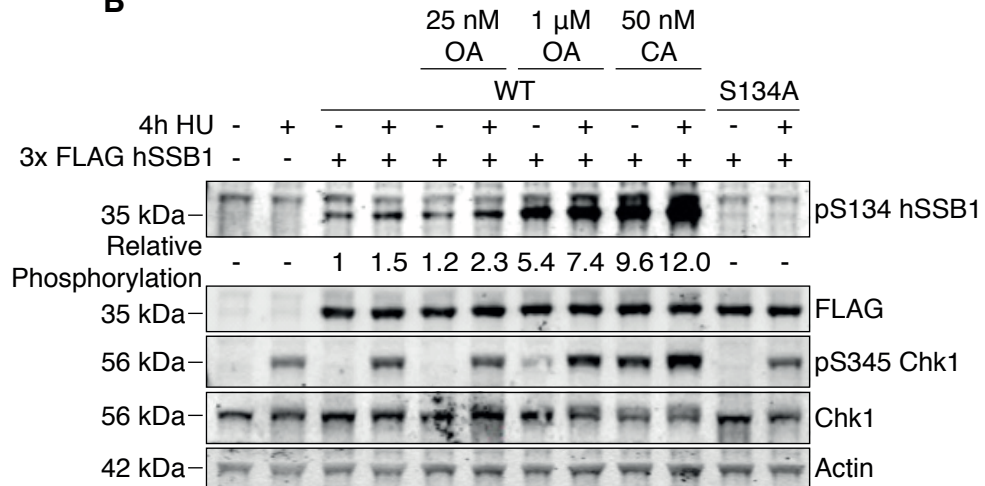
Okadaic acid (OA) was used either at 25 nM or 1 μ M. 25 nM was chosen to cause ‘low-level’ of inhibition of PP2A (~10%) (Goodarzi et al., 2004), as well as, by similarity, of PP4 and PP6 (Prickett and Brautigan, 2006; Swingle et al., 2007). 1 μ M of okadaic acid was then chosen as a dose that has been reported to inhibit PP2A, as well as presumably PP4 and PP6, by close to 100% (Goodarzi et al., 2004; Swingle et al., 2007). Such assumptions are based on the high sequence similarity of PP2A, PP4 and PP6 which together constitute the type 2 family of PPP-family phosphatases (Andreeva and Kutuzov, 2001). Indeed, whilst okadaic acid inhibition of PP6 has not been reported to date, almost identical IC_{50} values have been reported for inhibition of PP2A and PP4 by okadaic acid *in vitro* (Honkanen and Golden, 2002). As PP1 is much less sensitive to okadaic acid inhibition than PP2A (PP1 IC_{50} = ~ 10 nM, PP2A IC_{50} = ~ 0.1 nM (Obara and Yabu, 1993)), a concentration of 25 nM is unlikely to cause any substantial inhibition in cells, while 1 μ M is expected to inhibit PP1 by ~ 15% (Resjö et al., 2002). Although relatively uncharacterised, the intermediate sensitivity of PP5 to okadaic acid (IC_{50} = 3.5 nM) (Swingle et al., 2007) indicates this enzyme is likely to be less efficiently inhibited by okadaic acid in cells than PP2A, PP4 or PP6, although more so than PP1. By contrast, 50 nM of calyculin A (CA) was chosen as a concentration that should inhibit PP1, PP2A, PP4, PP5 and PP6 by at least 70% (Favre et al., 1997; Swingle et al., 2007). At the concentrations used, neither okadaic acid nor calyculin A are known to inhibit PP2B, PP2C, PP7 or any other protein phosphatases to a detectable degree (Swingle et al., 2007).

Figure 4.6

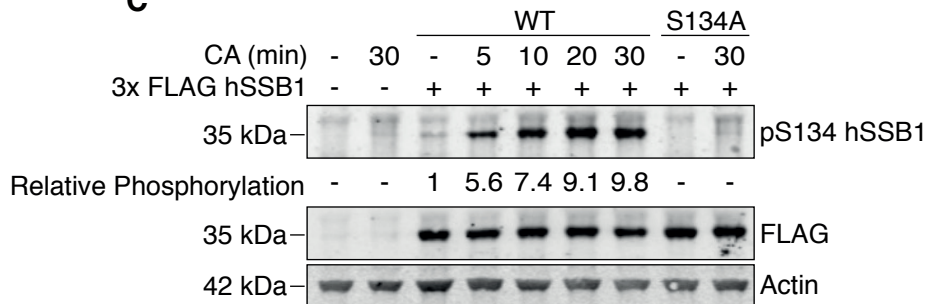
A

	PP1	PP2A	PP4	PP5	PP6
25 nM OA	-	10 %	10 %	-	10 %
1 μ M OA	15 %	> 95 %	> 95 %	10 - 95 %	> 95 %
50 nM CA	> 70 %	> 70 %	> 70 %	> 70 %	> 70 %

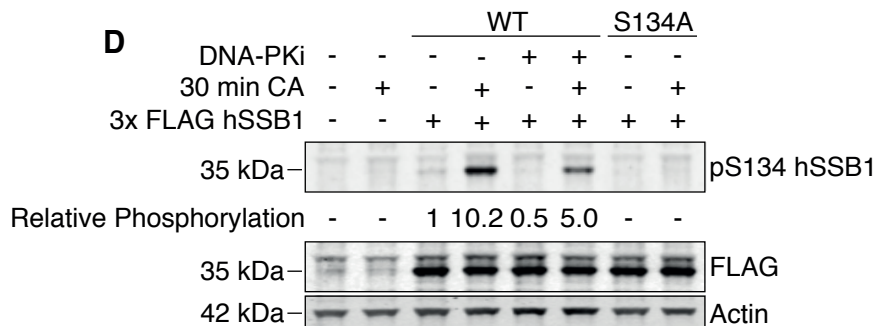
B



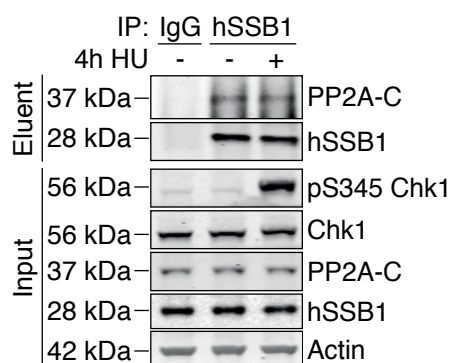
C



D



continued over page

Figure 4.6**E****Figure 4.6 hSSB1 is dephosphorylated by PPP-family protein phosphatases**

(A) Okadaic acid and calyculin A are inhibitors of PPP-family protein phosphatases. A table illustrating the previously reported inhibition of PP1, PP2A, PP4, PP5 and PP6 by the doses of okadaic acid and calyculin A used in Figure 4.6B (Goodarzi et al., 2004; Honkanen and Golden, 2002; Prickett and Brautigam, 2006; Swingle et al., 2007).

(B) hSSB1 S134 phosphorylation is enhanced by inhibition of PPP-family protein phosphatases. HeLa cells transiently expressing WT or S134A 3x FLAG hSSB1, or an empty vector, for 24 hours, were treated with 3 mM HU for 3.5 hours prior to addition of 25 nM okadaic acid (OA), 1 μ M OA, or 50 nM calyculin A (CA) for 30 minutes. Whole cell lysates were prepared and 15 μ g immunoblotted for phosphorylation of S134 hSSB1, FLAG, pS345 and total Chk1 (HU positive control) and actin (loading control). Densitometry of pS134 hSSB1 bands was performed using ImageJ, normalised to FLAG, and expressed relative to untreated WT 3x FLAG hSSB1-expressing cells. These results are representative of three independent experiments.

(C) hSSB1 S134 is phosphorylated within 5 minutes of phosphatase inhibition. HeLa cells transiently expressing WT or S134A 3x FLAG hSSB1, or an empty vector, for 24 hours were treated with 50 nM calyculin A (CA) for 5, 10, 20 or 30 minutes. Cells were then harvested and 15 μ g of whole cell lysate immunoblotted with antibodies against pS134 hSSB1, FLAG and actin (loading control).

Densitometry of pS134 hSSB1 bands was performed as per (B). These results are representative of three independent experiments.

(D) DNA-PKi suppresses CA-enhanced hSSB1 S134 phosphorylation. HeLa cells transiently expressing WT or S134A 3x FLAG hSSB1, or an empty vector, for 24 hours, were treated 5 μ M of NU7441 (DNA-PKi) for 10 minutes and then with 50 nM calyculin A (CA) for an additional 30 minutes. Cells were then harvested and 15 μ g of whole cell lysate immunoblotted with antibodies against pS134 hSSB1, FLAG and actin (loading control). Densitometry of pS134 hSSB1 bands was performed as per (B). These results are representative of three independent experiments.

(E) hSSB1 associates with the catalytic subunit of PP2A in cells. HeLa cells were treated with 3 mM HU, or mock treated, for 4 h. Whole cell lysates were then prepared and 500 μ g incubated with protein G magnetic dynabeads bound to antibodies against hSSB1, or a sheep isotype control IgG, for 2 hours at 4 $^{\circ}$ C. Beads were washed and protein eluted by heating to 90 $^{\circ}$ C in SDS loading buffer for 10 min. Eluent was immunoblotted for hSSB1 and PP2A-C. 15 μ g whole cell lysate (input) was immunoblotted with antibodies against hSSB1, PP2A-C, pS345 and total Chk1 and actin (loading control). These results are representative of three independent experiments.

Strikingly, the treatment of undamaged cells with 1 μ M OA or 50 nM CA led to an increase in hSSB1 S134 phosphorylation of greater than 5- and 8-fold, respectively, which was further increased in cells treated with hydroxyurea (**Figure 4.6B**). Indeed, a comparably small although consistent increase in S134 phosphorylation was observed even following 10% inhibition of PP2A, PP4 and PP6 with 25 nM of okadaic acid. Consistent with previous data, the treatment of cells with 1 μ M okadaic acid or 50 nM calyculin A, compounds that inhibit PP1, caused a substantial increase in Chk1 S345 phosphorylation even in non-hydroxyurea treated cells (Leung-Pineda et al., 2006). To further investigate the rapidity by which the phosphatase inhibitors increase hSSB1 S134 phosphorylation, cells transiently expressing WT or S134A 3x FLAG hSSB1 were treated with 50 nM calyculin A for 5, 10, 20 or 30 minutes prior to preparation of whole cell lysates and immunoblotting for hSSB1 S134

phosphorylation. In doing so, an increase in hSSB1 S134 phosphorylation of ~ 5 fold was observed within 5 minutes of 50 nM calyculin treatment (**Figure 4.6C**). These findings are particularly striking when it is considered that an increase of only 3.3 fold was observed even after 20 hours of hydroxyurea treatment (Figure 4.3D). Together, these data suggest that hSSB1 S134 phosphorylation may be dynamically phosphorylated although largely suppressed in undamaged cells, most likely by PPP-family protein phosphatases.

The inhibition of DNA-PK for 4.5 hours (Figure 4.4 A and B) or the depletion of the DNA-PK catalytic subunit (Figure 4.4 D), was found in section 4.2.4 to reduce hSSB1 S134 phosphorylation by 80-90%, suggesting that this kinase may phosphorylate hSSB1 even in undamaged cells. Indeed, hSSB1 was found to immunoprecipitate DNA-PKcs even prior to hydroxyurea treatment (Figure 4.4F). It is therefore tempting to speculate that DNA-PK may mediate the increase in S134 phosphorylation observed following PPP-family phosphatase inhibition. By means of assessing this, cells transiently expressing WT or S134A 3x FLAG hSSB1 were treated with 5 μ M of the DNA-PK inhibitor NU7441 for 15 minutes prior to addition of 50 nM calyculin A for 30 minutes. Whole cell lysates were then immunoblotted for hSSB1 S134 phosphorylation (**Figure 4.6D**). Consistent with the observations of section 4.2.4, the co-inhibition of DNA-PK and PPP-family phosphatases markedly reduced calyculin A-induced S134 phosphorylation by ~ 50% (10.2-fold increase vs. 3-fold). These results do however suggest that while DNA-PK is likely the major hSSB1 S134 kinase in cells, other kinases may have additional ancillary roles.

Although the increase in hSSB1 S134 phosphorylation observed following treatment with okadaic acid or calyculin A suggests the involvement of PPP-family protein phosphatases in the dephosphorylation of hSSB1, it remains unclear which member is directly involved. The availability of an antibody against the catalytic subunit of PP2A (PP2A-C) however enabled the enquiry of whether hSSB1 may associate with this enzyme in cells. Indeed, PP2A has also been suggested to dephosphorylate the DNA repair proteins RPA32 (Feng et al., 2009) and H2A.X (Chowdhury et al., 2005), suggesting this enzyme is a reasonable candidate. To assess this, hSSB1 was immunoprecipitated from HeLa whole cell lysates treated +/- 3 mM HU for 4 hours and immunoblotted for PP2A-C and hSSB1 (**Figure 4.6E**). In doing so, PP2A-C was

found to co-immunoprecipitate with hSSB1, although not with a control isotype IgG. These findings provide evidence that hSSB1 may associate with PP2A in cells, potentially suggesting the involvement of this enzyme in hSSB1 S134 dephosphorylation.

4.2.7 Enzymatic regulation of hSSB1 phosphorylation is mediated similarly in HeLa and U-2 OS cells

In the preceding chapter, 3x FLAG hSSB1 was transiently expressed in HEK293T cells for 24 hours, immunoprecipitated using anti-FLAG beads, and analysed by LC-MS/MS. By doing so, numerous peptides were detected which may correspond to hSSB1 phosphorylated at various residues. This included the detection of peptides that may be phosphorylated at hSSB1 S134 and prompted the preparation of the S134 phospho-specific antibody that has been used in this chapter. Although HEK293T cells had been utilised for the isolation of hSSB1 for mass spectrometry, largely due to the high protein yield obtainable from these cells, HeLa cells were used for immunodetection experiments. These cells were employed due to their status as a major model cell line for DNA repair research. HeLa cells do however exhibit substantial genomic and transcriptomic differences when compared to normal human tissues, including high levels of aneuploidy and genomic rearrangements, as well as gene expression profiles differences in pathways including DNA repair and cell cycle maintenance (Landry et al., 2013). It was therefore possible that hSSB1 may be uniquely regulated in this cell line. Due to these concerns, it was deemed appropriate that a second cell line should be used to reassess the enzymatic regulation of hSSB1 S134 phosphorylation.

U-2 OS are an additional cell line model that has been extensively employed for the characterisation of DNA repair mechanisms. Indeed, whilst these cells are also aneuploid and contain numerous chromosomal rearrangements, deletions and duplications, they are not known to contain mutations in the core DNA repair pathways (Akan et al., 2012; Conery and Harlow, 2010). These cells were therefore chosen for the further assessment of hSSB1 S134 phosphorylation.

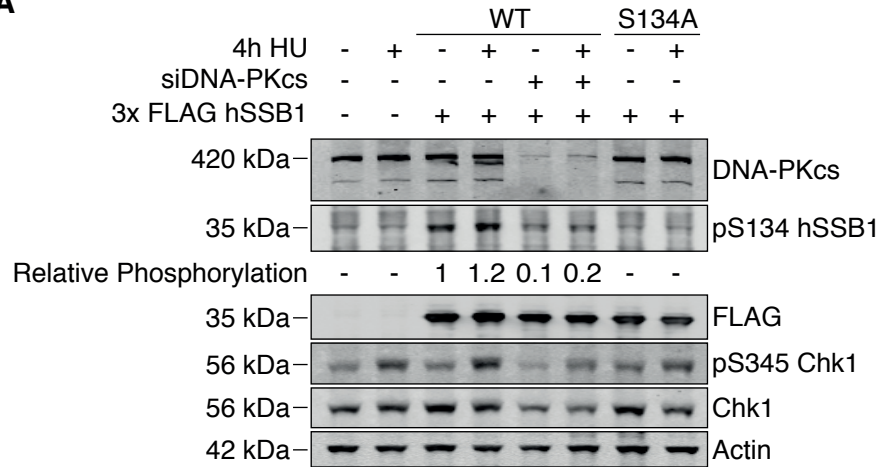
To test the occurrence and HU-stimulation of hSSB1 S134 phosphorylation in U-2 OS cells, as well as the involvement of DNA-PK, U-2 OS cells were initially depleted of DNA-PKcs using siRNA. WT or S134A 3x FLAG hSSB1 was then over-expressed and cells treated with 3 mM HU for 4 hours. Whole cell lysates were then prepared and immunoblotted (**Figure 4.7A**). Here, an increase in hSSB1 S134 phosphorylation was observed following HU treatment, albeit to a milder degree than observed in HeLa cells (~ 20 – 30 % in U-2 OS cells vs. 40 – 50% in HeLa cells after 4h treatment). The depletion of DNA-PKcs was also found to reduce hSSB1 phosphorylation by ~ 80 - 90% prior to and following HU treatment. These data support a major role for DNA-PK in the phosphorylation of hSSB1 S134 phosphorylation and suggest this modification is not limited to the HeLa cell line. It was interesting to note that, similarly to phosphorylation of hSSB1, a less striking increase in Chk1 S345 phosphorylation was also observed in U-2 OS cells, in comparison to in HeLa cells (e.g. Figure 4.3), following HU treatment. Although an explanation for these discrepancies is not immediately apparent, U-2 OS cells were observed to proliferate at a lower rate than HeLa cells in culture. It therefore seems reasonable to consider that a less robust response to replication inhibition may occur in U-2 OS cells, simply due to a lower proliferative rate.

Another interesting observation from Figure 4.7A was the reduction in Chk1 protein levels, as well as HU-induced Chk1 S345 phosphorylation, observed in U-2 OS cells depleted of DNA-PKcs. Indeed, whilst DNA-PK has previously been reported to promote Chk1 stability and HU-induced phosphorylation (Lin et al., 2014), a comparably striking effect on Chk1 was not observed following depletion of DNA-PKcs from HeLa cells in Figure 4.4D. These findings may represent variations in the regulation of Chk1 in U-2 OS cells compared to HeLa cells.

An increase in S134 phosphorylation was also observed in HeLa cells treated with the PPP-family phosphatase inhibitor, calyculin A, which was suppressed by co-treatment with the DNA-PK inhibitor NU7441. It was therefore of interest to determine whether these inhibitors would also affect hSSB1 S134 phosphorylation in U-2 OS cells.

Figure 4.7

A



B

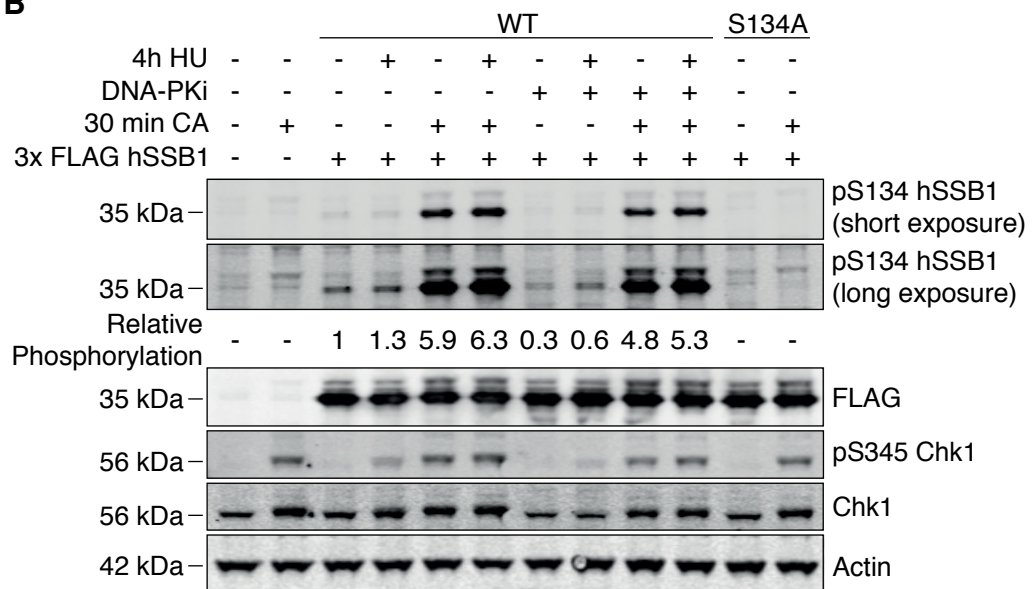


Figure 4.7 Enzymatic regulation of hSSB1 phosphorylation is mediated similarly in HeLa and U-2 OS cells

(A) DNA-PK depletion suppresses phosphorylation of hSSB1 S134 in U-2 OS cells. U-2 OS cells were transfected with 10 nM of siRNA targeting the DNA-PKcs transcript, or with a control siRNA sequence, twice, separated by 24 hours. WT or S134A 3x FLAG hSSB1 was then expressed for 24 hours, prior to treatment of cells with 3 mM HU for 4 hours. Whole cell lysates prepared from these cells were then immunoblotted with antibodies against DNA-PKcs pS134 hSSB1, FLAG, pS345 or total CHK1, or actin (loading control). Densitometry of pS134 hSSB1 bands was performed using ImageJ, normalised to FLAG, and expressed relative to untreated

WT 3x FLAG hSSB1-expressing cells. Data is representative of two independent repeats.

(B) hSSB1 S134 phosphorylation is enhanced by HU treatment or inhibition of PPP-family protein phosphatases, and suppressed by DNA-PK inhibition, in U-2 OS cells. WT or S134A 3x FLAG hSSB1, or an empty vector control, was transiently expressed in U-2 OS cells for 24 hours. Cells then treated either with 5 μ M NU7441, or DMSO, for 30 minutes, prior to addition of 3 mM HU, or mock-treatment, for 3.5 hours. Cells were then treated with 50 nM calyculin A, or DMSO, for 30 minutes. Whole cell lysates were then prepared and immunoblotted with antibodies against pS134 hSSB1, FLAG, pS345 or total CHK1, or actin (loading control). Densitometry of pS134 hSSB1 bands was performed as per (A). Data is representative of three independent repeats.

To test this, plasmids encoding WT or S134A 3x FLAG hSSB1 were transfected into U-2 OS cells, and then 24 hours later, cells treated either with 5 μ M of the DNA-PK inhibitor NU7441 or with DMSO, 30 minutes prior to treatment with 3 mM hydroxyurea or mock-treatment. In the final 30 minutes of the HU treatment, cells were also treated with 50 nM calyculin A, or DMSO. Whole cell lysates were then prepared from these cells and immunoblotted for hSSB1 S134 phosphorylation, as well as for phosphorylation of CHK1 S345 (**Figure 4.7B**). As per HeLa cells, the inhibition of DNA-PK substantially reduced phosphorylation of hSSB1 S134 in both damaged and undamaged cells. This was, however, to a smaller degree than observed in HeLa cells. The treatment of U-2 OS cells with calyculin A (CA) also caused an increase in S134 phosphorylation of \sim 6-fold, (compared to \sim 10-fold in HeLa cells), which was enhanced following HU treatment. CA-induced hSSB1 S134 phosphorylation was also detectably suppressed by addition of the DNA-PK inhibitor by \sim 20% (compared to \sim 50% in HeLa cells). These data support that hSSB1 S134 phosphorylation is suppressed in U2-OS cells by PPP-family phosphatases. Although the DNA-PK inhibitor was not as efficacious in preventing hSSB1 phosphorylation in U-2 OS, compared to in HeLa cells, these discrepancies most likely represent pharmacogenetic differences between these cell lines. For instance, while 5 μ M of NU7441 may be sufficient to inhibit DNA-PK in HeLa cells, higher doses may be

required in the U-2 OS cell line. This explanation is supported by the almost complete suppression of S134 phosphorylation in U-2 OS cells depleted of DNA-PKcs (and which therefore largely lacked active DNA-PK) (Figure 4.7A).

The data above therefore support that in U-2 OS cells, as in HeLa cells, hSSB1 is phosphorylated at S134, predominantly by DNA-PK and that this modification is enhanced following replication inhibition. Phosphorylation of hSSB1 in U-2 OS is also stimulated by the inhibition of PPP-family protein phosphatases. Together, these data suggest that this mechanism of hSSB1 regulation is likely broadly employed amongst cell lines.

4.2.8 hSSB1 may be phosphorylated at S134 independently of PAR- or DNA-binding

The observation that hSSB1 S134 is phosphorylated in response to replication inhibition by DNA-PK may indicate that phosphorylation occurs directly at sites of fork disruption. Indeed, as hSSB1 has been suggested to associate with such lesions in cells (Bolderson et al., 2014), it is interesting to consider that phosphorylation may occur subsequently to hSSB1-fork binding. Recently, hSSB1 was found to bind poly(ADP-ribose) (PAR) *in vitro*, an action which may be required for the efficient recruitment of hSSB1 to sites of double-strand DNA breaks (Zhang et al., 2014). Although it remains unclear whether hSSB1 also binds to PAR substrates at sites of stalled replication forks, PAR binding is known to stimulate the recruitment of other proteins that facilitate DNA repair, including Chk1 (Min et al., 2013). As numerous hSSB1 PAR-binding mutants have recently been described (WD55AA that does not bind PAR, as well as VL23AA and TG47AA which do not bind PAR and INTS3) (Zhang et al., 2014) it was therefore envisaged that these mutants could be used to assess the requirement of PAR-binding for hSSB1 phosphorylation. VL23AA, TG47AA and WD55AA 3x FLAG hSSB1 were therefore prepared by site-directed mutagenesis and transiently expressed in HeLa cells alongside WT or S134A hSSB1. Cells were then treated with 3 mM hydroxyurea for 4 hours and whole cell lysates immunoblotted for hSSB1 S134 phosphorylation (**Figure 4.8A**). Only minimal differences in hSSB1 S134 phosphorylation were however observed for any of the PAR-binding mutants when compared to phosphorylation of the WT protein. These

data suggest that PAR-binding may not be essential for hSSB1 S134 phosphorylation in response to replication inhibition.

Despite the above observations, it is likely that hSSB1 may also bind to single-stranded DNA exposed by replication inhibition and that this binding may instead be required for hSSB1 S134 phosphorylation. The recently solved crystal structure of hSSB1 in complex with INTS3 illustrates that numerous aromatic residues in the OB-fold (W55, Y74, F78, Y85) may be predominantly responsible for hSSB1-DNA binding (Ren et al., 2014). Indeed, individual mutation of each of these residues was demonstrated to largely reduce binding to a dT48 oligonucleotide *in vitro*. The requirement of these residues for DNA-binding has also been supported by similar assays performed using murine SSB1 (mSSB1) (Gu et al., 2013). Here, mSSB1 aromatic mutants were additionally unable to recapitulate ionising radiation-induced DNA repair signalling following mSSB1 depletion. Given that a similar requirement for these residues could be demonstrated with hSSB1, it therefore seemed reasonable that such constructs could be used to assess the importance of DNA-binding for hSSB1 S134 phosphorylation.

Firstly, to determine the requirement of the hSSB1 OB-fold aromatic residues for hSSB1 function, siRNA resistant 3x FLAG hSSB1 constructs were prepared where W55, Y74, F78 or Y85 were individually mutated to alanine. Clonogenic assays were then performed by depletion of endogenous hSSB1 as in Section 4.2.2, followed by transient expression of each mutant construct (**Figure 4.8B**). Cells were then seeded into wells of a 6-well plate and after 24 hours exposed to 1, 2, 4 or 6 Gy of ionising radiation. After 10 days, cells were stained with methylene blue and the surviving fraction of cells at each dose calculated relative to the survival of untreated cells (**Figure 4.8C and D**). Ionising radiation was used as the DNA damaging agent as this is most relevant to existing hSSB1 literature and is most comparable to previous work with mSSB1. As per figure 4.5D, cells depleted of hSSB1 were hypersensitive to ionising radiation, which could be rescued by transient expression of the WT protein. Cells expressing any of the OB-fold aromatic residue mutants were however comparably sensitive to hSSB1-depleted cells. Indeed, a statistically significant difference in surviving fraction was calculated between each mutant and the WT protein at multiple doses.

Figure 4.8

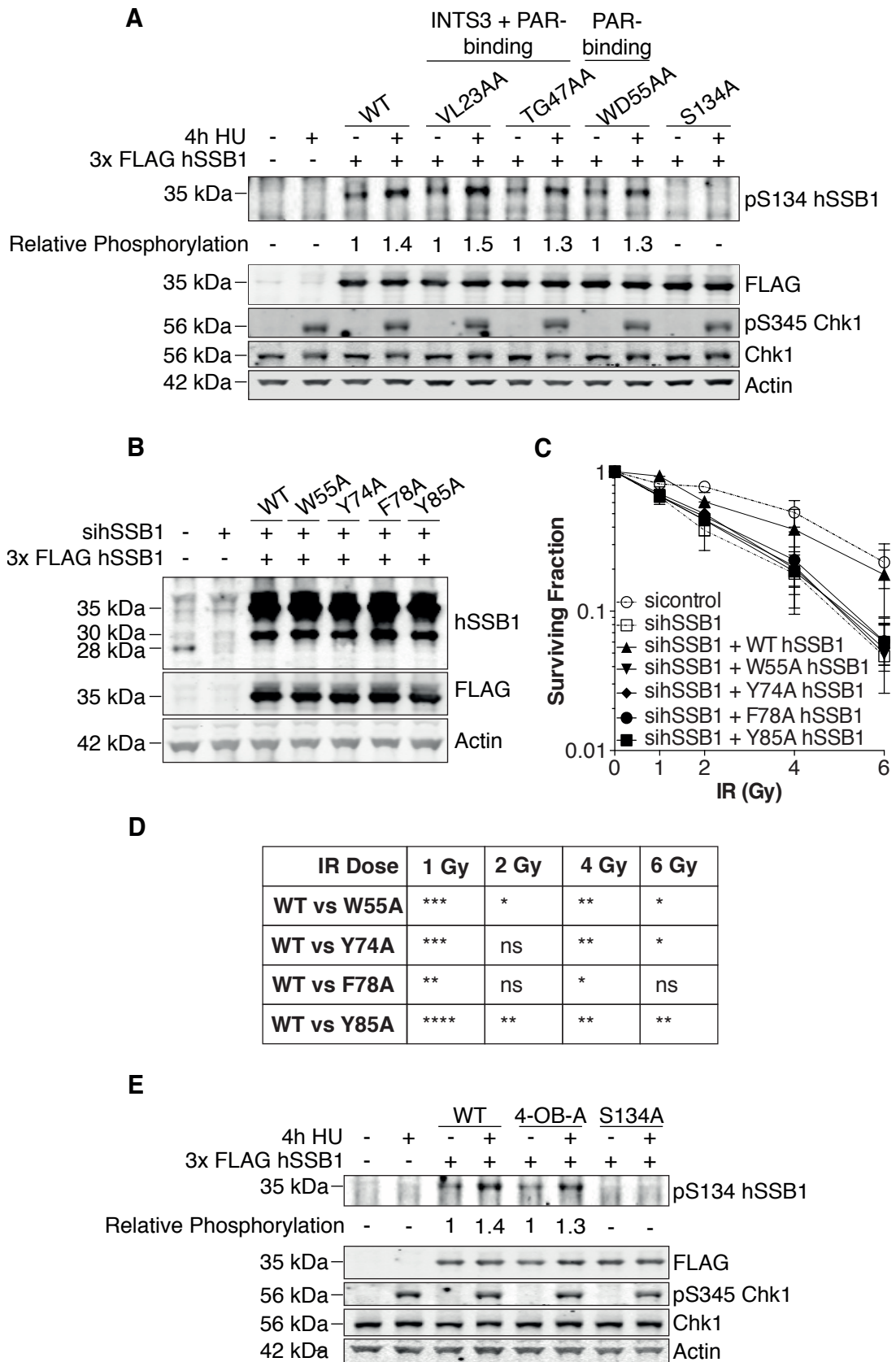


Figure legend over page

Figure 4.8 hSSB1 may be phosphorylated independently of PAR- or DNA-binding

(A) hSSB1 S134 phosphorylation may not require PAR- binding. VL23AA, TG47AA and WD55AA hSSB1 mutations were introduced into the 3x FLAG hSSB1 construct by site-directed mutagenesis. Each mutant has previously been described to diminish PAR-binding, while VL23AA and TG47AA have also been demonstrated not to bind INTS3 (Zhang et al., 2014). HeLa cells expressing each mutant, WT hSSB1 or an empty control vector for 24 hours were treated with 3 mM HU for 4 hours. Whole cell lysates were then prepared and immunoblotted for pS134 hSSB1, FLAG, pS345 and total Chk1 and actin (loading control). Densitometry of pS134 hSSB1 bands was performed using ImageJ, normalised to FLAG, and expressed relative to untreated WT 3x FLAG hSSB1-expressing cells. These results are representative of two independent experiments.

(B) Expression of hSSB1 DNA-binding mutants in HeLa cells depleted of endogenous hSSB1. HeLa cells were depleted of endogenous hSSB1 by double transfection with siRNA. Cells were then transfected with WT, W55A, Y74A, F78A or Y85A siRNA-resistant 3x FLAG hSSB1, or an empty plasmid, 6 hours prior to seeding into wells of a 6-well plate at a density of 400 cells per well. Remaining cells were grown for an additional 24 hours and lysed in RIPA buffer. Whole cell lysate (15 µg) was immunoblotted and probed with antibodies against hSSB1, FLAG and actin. This figure is representative of each repeat in (C).

(C and D) Cells expressing hSSB1 DNA-binding mutants are hypersensitive to ionising radiation (IR). The cells plated in (C) were incubated for 24 hours and treated with 1, 2, 4 or 6 Gy ionising radiation (IR). Three technical repeats were performed per dose. Cells were grown for 10 days prior to staining of colonies with methylene blue. Colonies were manually counted and normalised to untreated cells. Data is graphed as the mean \pm 1 standard deviation from 3 independent experiments (D) *t* tests were used to compare the ‘sihSSB1 + WT hSSB1’ and ‘sihSSB1 + mutant hSSB1’ datasets at each dose. ns = $P > 0.05$, * = $P < 0.05$, ** = $P < 0.01$, *** = $P < 0.001$.

(E) hSSB1 S134 phosphorylation may not require DNA-binding. Site-directed mutagenesis was used to create a 3x FLAG hSSB1 construct lacking each DNA-binding aromatic residue (4-OB-A). HeLa cells expressing this mutant, WT hSSB1 or an empty control vector for 24 hours were treated with 3 mM HU for 4 hours. Whole cell lysates were then prepared and immunoblotted for pS134 hSSB1, FLAG, pS345 and total Chk1 and actin (loading control). Densitometry of pS134 hSSB1 bands was performed as per (A). These results are representative of two independent experiments

These findings suggest that W55, Y74, F78 and Y85 may be required for hSSB1 function in cells, presumably by facilitating DNA binding.

Although the data above suggests that each OB aromatic residue is important for hSSB1 function, it should be noted that *in vitro*, some residual DNA binding of each mutant to DNA is still observed (which may or may not be physiologically relevant) (Ren et al., 2014). To ensure the full disruption of hSSB1 DNA-binding, a quadruple mutant was therefore prepared where each of the established DNA-binding aromatic residues was mutated to alanine and this construct used to assess S134 phosphorylation in response to hydroxyurea treatment. For this, HeLa cells expressing WT or 4-OB-A hSSB1 were treated with 3 mM hydroxyurea for 4 hours and then whole cell lysates immunoblotted for hSSB1 S134 phosphorylation (**Figure 4.8E**). Similarly to the PAR-binding mutants, only a minimal decrease in hSSB1 S134 phosphorylation was however observed for the OB-fold quadruple mutant, suggesting that DNA-binding also may not be required for phosphorylation of hSSB1 S134.

4.2.9 hSSB1-INTS3 binding promotes clonogenic survival of cells in response to replication stress

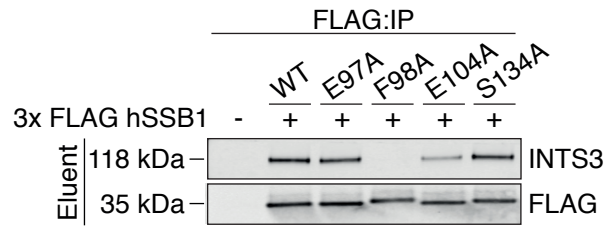
Numerous reports have suggested that hSSB1 may associate with INTS3 and SOSS-C in cells to form a complex referred to as SOSS1 (Li et al., 2009b; Skaar et al., 2009; Zhang et al., 2009; Zhang et al., 2013). Here, INTS3 directly interacts with the hSSB1 OB-fold on the opposing surface to the DNA-binding groove such that hSSB1 may bind ssDNA and INTS3 simultaneously. In addition to binding hSSB1,

INTS3 also directly interacts with SOSS-C (Ren et al., 2014). Although the precise function of the INTS3 complex remains unclear, it is likely that INTS3 is required for the full activity of hSSB1 in the repair of double-strand DNA breaks. Indeed, hSSB1 INTS3-binding mutants seem unable to rescue the hypersensitivity to ionising radiation caused by hSSB1 depletion (Ren et al., 2014). As INTS3 has been found to co-localise with hSSB1 following hydroxyurea treatment (Bolderson et al., 2014), it is therefore interesting to consider whether INTS3-binding may also be required for hSSB1 function following replication inhibition.

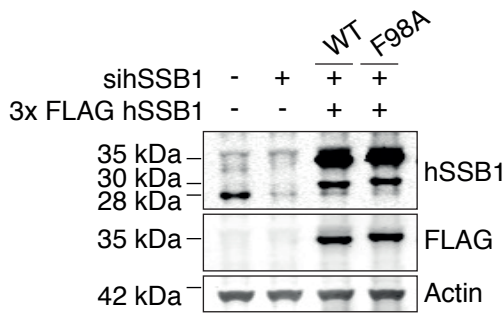
Although the VL23AA and TG47AA hSSB1 mutants used in section 4.2.7 have been described not to bind INTS3, PAR-binding for these proteins was also diminished (Zhang et al., 2014). Helpfully, the recently solved crystal structure of hSSB1 demonstrated that the OB-fold residues E97, F98 and E104 are predominantly responsible for INTS3 binding. Furthermore, mutation of these residues was demonstrated to disrupt this interaction (Ren et al., 2014). To validate this directly, E97, F98 and E104 of the WT 3x FLAG hSSB1 construct were individually mutated to alanine and these constructs, as well as WT and S134A hSSB1, expressed in HeLa cells. After 24 hours, cells were lysed and FLAG-tagged proteins immunoprecipitated with magnetic M2 anti-FLAG beads. Immunoprecipitated proteins were then separated by gel electrophoresis and immunoblotted for FLAG and INTS3 (**Figure 4.9A**). By doing so, INTS3 was immunoprecipitated in cells expressing WT hSSB1, although not in those transfected with an empty control plasmid. Of the hSSB1 mutants expressed, INTS3-association was undetectable for the F98A mutant and markedly reduced for E104A 3x FLAG hSSB1. By contrast, however, only a barely detectable decrease in INTS3 association was observed for E97A hSSB1. These results are largely consistent with previous findings, where hSSB1-INTS3 binding was predominantly disrupted by F98A and E104A mutation and partially by mutation of E97 (Ren et al., 2014). As the greatest reduction in INTS3-binding was however observed with the F98A hSSB1 mutant, this construct was used in subsequent experiments. It is also worth noting that in this assay, INTS3 was immunoprecipitated with S134A 3x FLAG hSSB1 similarly to that seen with WT, suggesting that S134 phosphorylation is not required for INTS3 binding.

Figure 4.9

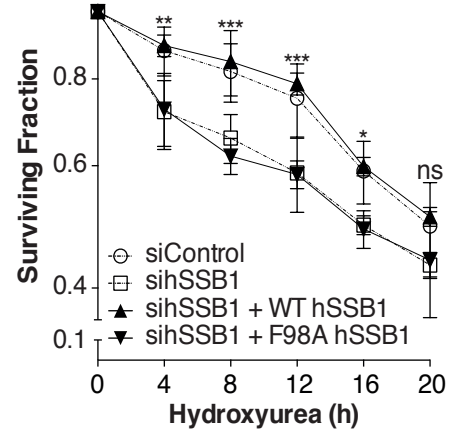
A



B



C



D

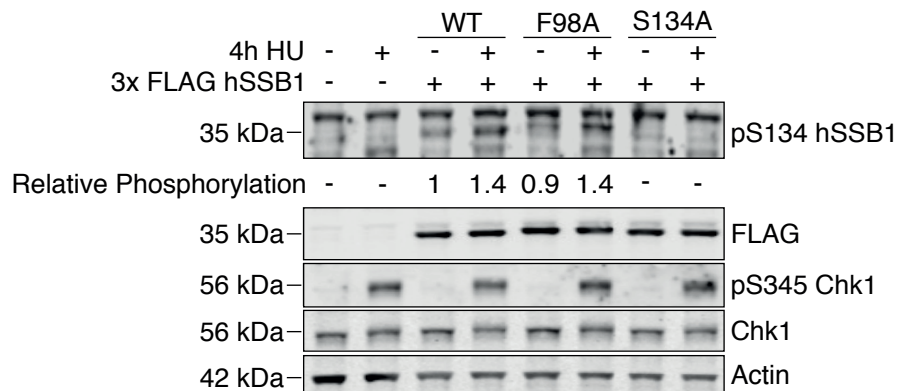


Figure 4.9 hSSB1-INTS3-binding promotes clonogenic survival of cells in response to replication stress, although may not be required for S134 phosphorylation

(A) F98 is required for hSSB1-INTS3 association in cells. Site-directed mutagenesis was used to individually mutate hSSB1 E97, F98A and E104A of the 3x FLAG hSSB1 construct to alanine residues. HeLa cells were transiently transfected with WT, E97A, F98A, E104A or S134A 3x FLAG hSSB1, or an empty control plasmid, and incubated for a further 24 hours. Cells were then harvested and 500 μ g

of whole cell lysate incubated with M2 FLAG magnetic beads for 2 hours at 4 °C. Beads were then washed and protein eluted by heating to 90 °C for 10 minutes in SDS loading buffer. Eluent was immunoblotted with antibodies against FLAG and INTS3. These results are representative of three independent experiments.

(B) Expression of F98A hSSB1 in HeLa cells depleted of endogenous hSSB1.

HeLa cells were depleted of endogenous hSSB1 by double transfection with siRNA. Cells were then transfected with WT or F98A siRNA-resistant 3x FLAG hSSB1, or an empty plasmid, 6 hours prior to seeding into wells of a 6-well plate at a density of 400 cells per well. Remaining cells were grown for an additional 24 hours and lysed in RIPA buffer. 15 µg of whole cell lysate was immunoblotted and probed with antibodies against hSSB1, FLAG and actin. This figure is representative of each repeat in (C).

(C) HeLa cells expressing F98A hSSB1 are hypersensitive to hydroxyurea (HU).

The cells plated in (B) were incubated for 24 hours and treated with 3 mM HU for 4, 8, 12, 16 or 20 hours. Three technical repeats were performed per dose. Cells were grown for 10 days prior to staining of colonies with methylene blue. Colonies were manually counted and counts normalised to untreated cells. Data is graphed as the mean ± 1 standard deviation from 3 independent experiments. *t* tests were used to compare the ‘sihSSB1 + WT hSSB1’ and ‘sihSSB1 + F98A hSSB1’ datasets at each dose. ns = $P > 0.05$, * = $P < 0.05$, ** = $P < 0.01$, *** = $P < 0.001$.

(D) hSSB1 S134 phosphorylation may not require INTS3-binding.

HeLa cells expressing WT, F98A or S134A 3x FLAG hSSB1, or an empty control vector, for 24 hours were treated with 3 mM HU for 4 hours. Whole cell lysates were then prepared and immunoblotted for pS134 hSSB1, FLAG, pS345 Chk1, total Chk1 and actin (loading control). Densitometry of pS134 hSSB1 bands was performed using ImageJ, normalised to FLAG, and expressed relative to untreated WT 3x FLAG hSSB1-expressing cells. These results are representative of three independent experiments.

It was also noted that F98A 3x FLAG hSSB1 was detected at a slightly higher molecular weight than the WT, consistent with prior observations (Ren et al., 2014). Although it remains unclear why this may be, it is noted that hSSB1 K94, a recently

described residue of acetylation (Wu et al., 2015), is seemingly localised to this same hSSB1-INTS3 interface. The increased occurrence of this or other post-translational modifications on the F98A mutant may therefore offer some explanation for the difference in observed migration when compared to the WT protein.

To determine whether INTS3 binding is required for hSSB1 function following replication inhibition, HeLa cells were depleted of endogenous hSSB1 over 48 hours using siRNA and WT or F98A siRNA-resistant 3x FLAG hSSB1 transiently re-introduced (**Fig 4.9B**). Cells were then seeded into wells of a 6-well plate and after 24 hours treated with 3 mM HU for 4, 8, 12, 16 or 20 hours. Cells were then released into fresh media and grown for 10 days before the surviving fraction of cells at each dose calculated relative to the survival of untreated cells (**Fig 4.9C**). Consistent with Figure 4.2C, cells depleted of hSSB1 were hypersensitive to hydroxyurea treatment, which could be rescued by expression of WT 3x FLAG hSSB1. By contrast, F98A hSSB1 was unable to rescue cells from hSSB1-depletion and a statistically significant difference in surviving fraction was calculated when compared to WT at multiple HU time-points. These data suggest that INTS3-binding is required for hSSB1 function following replication stress.

As the data presented here has suggested that both hSSB1 S134 phosphorylation and INTS3-binding promote clonogenic survival in response to hydroxyurea treatment, it is tempting to speculate that these requirements are related. As Figure 4.8A indicated that S134 phosphorylation is not required for INTS3 binding, it was therefore of interest to determine whether INTS3-binding may be required for S134 phosphorylation. To assess this, HeLa cells transiently expressing WT, F98A or S134A hSSB1 were treated with 3 mM hydroxyurea for 4 hours and then whole cell lysates prepared and immunoblotted for hSSB1 S134 phosphorylation. (**Figure 4.9D**). As WT and F98A 3x FLAG hSSB1 were however similarly phosphorylated at S134 in response to hydroxyurea treatment, these data suggest that S134 phosphorylation and INTS3 binding are regulated independently.

4.2.10 A phosphorylated S134 peptide does not interact with pS/T reader proteins

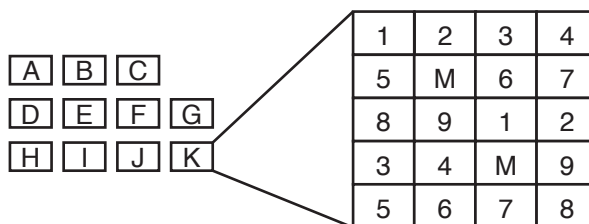
The data presented in previous sections suggests that DNA-PK-mediated phosphorylation of hSSB1 S134 is enhanced in response to replication disruption and that this modification promotes clonogenic survival under such conditions. Furthermore, hSSB1 S134 phosphorylation may be dynamically regulated in undamaged cells. As yet, however, the mechanism through which S134 may function remains unclear.

The phosphorylation of specific amino acids in some proteins facilitates a direct interaction with one of many phospho-serine/threonine binding domain-containing proteins, numerous of which function in DNA repair. This includes members of the 14-3-3 family, the FHA domain proteins MDC1, RNF8, NBS1 and Chk2, the BRCT (BRCA1 c-terminus) repeat proteins, MDC1, NBS1, BRCA1, MCPH1, 53BP1, PTIP and TopBP-1, the WW domain protein PIN1, the polo-box protein polo-like kinase 1 (PLK1) and the WD repeat proteins β TrCP, CDC4 and FBW7 (Mohammad and Yaffe, 2009; Reinhardt and Yaffe, 2013). It was therefore interesting to consider whether hSSB1 S134 phosphorylation may promote binding to one of these proteins. Indeed, whilst S134 does not recognisably constitute a specific consensus-binding motif, ‘non-consensus’ substrate binding is not uncommon for many phospho-serine/threonine binding proteins (Madeira et al., 2015).

To assess whether S134 phosphorylation may promote such an interaction, control and phosphorylated hSSB1 biotinylated peptides representing amino acids K123 to S141 (Biotin-KAVQNDSNPSASQPTTGPS and Biotin-KAVQNDSNPSA {pSer}QP TTGPS) were designed and purchased. These peptides were then sent to the “protein array and analysis core” at the University of Texas MD Anderson Cancer Centre. Here, peptides were labelled with a Cy3-streptavidin label and used to probe a micro array of GST-fusion phospho-serine/threonine binding domain-containing proteins. Arrays were then washed and the fluorescent signal measured using a slide scanner equipped with a 550 nm long pass filter (**Figure 4.10A**). As each microarray contained proteins arrayed in duplicate, two fluorescent signals (dots) are expected for a positive interaction. Additionally, for an S134-specific interaction, a signal would be expected for the phosphorylated and not for the control peptide.

Figure 4.10

A

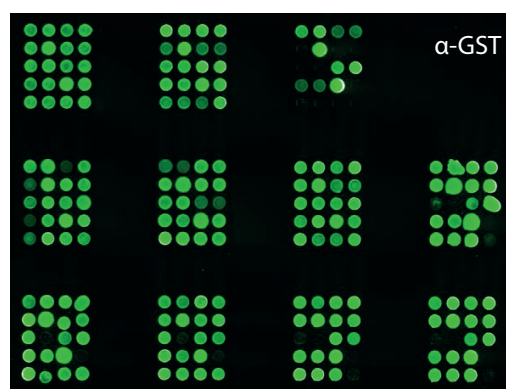
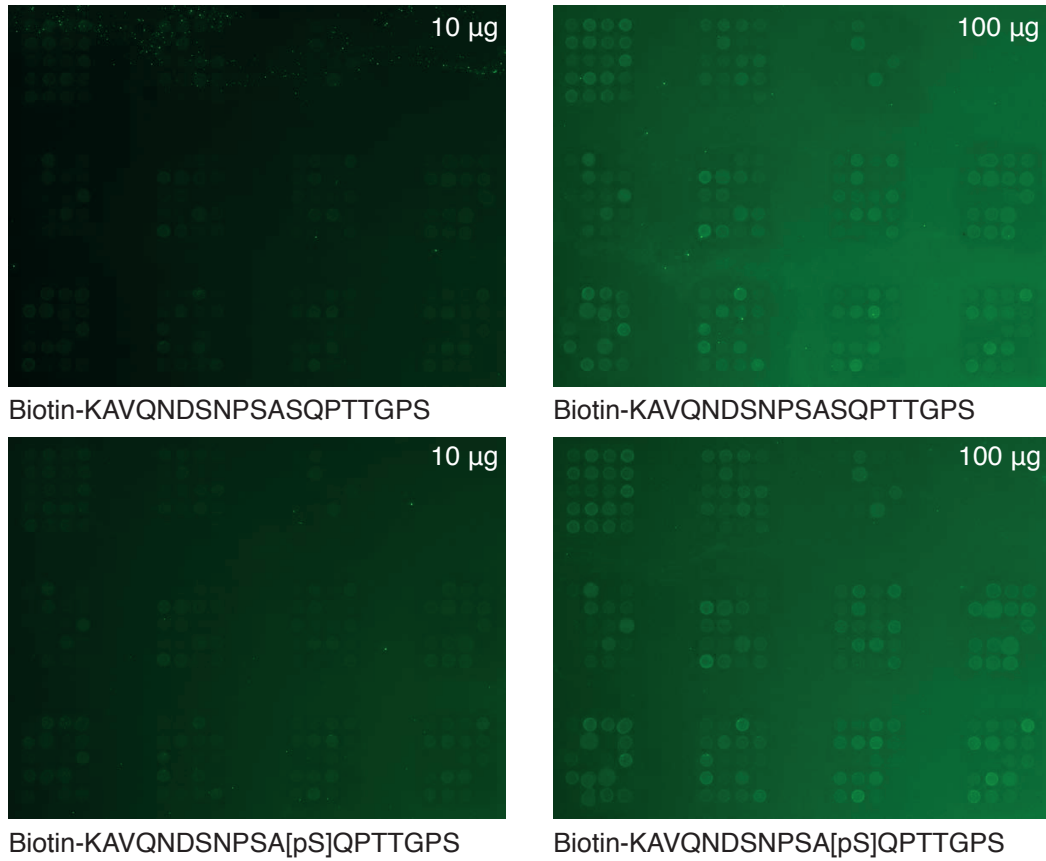


<u>14-3-3</u> A1) Sigma A2) Beta/Alpha A3) Epsilon A4) Gamma A5) Eta A6) Theta A7) Zeta/Delta <u>14-3-3-like</u> A8) SMG5 A9) SMG7	<u>WW</u> B1) Sigma <u>WW/SRI</u> B2) Sigma <u>FF</u> B3) TCERG1 <u>BIR</u> B4) Survivin <u>POLO Box</u> B5) PLK1 B6) PLK2 B7) PLK3 B8) PLK4 B9) PLK5	<u>MH2</u> C1) SMAD2 C2) SMAD4 <u>WD40</u> C3) Cdc4/Fbw7 C4) β TrCP	
<u>FHA</u> D1) AF6/Afadin D2) AGGF1 D3) APTX D4) CEP170 D5) CEP170B D6) CHFR D7) CHK2 D8) FHAD1 D9) KLP6	<u>FHA</u> E1) FOXK1 E2) FOXK2 E3) Kanadaplin E4) KI-67 E5) MCRS1 E6) MDC1 E7) TCF19 E8) TIFA E9) TIFAB	<u>FHA</u> F1) NBS1 F2) NIPP1 F3) PHF12 F4) PHLDB1 F5) RADIL F6) RNF8 F7) SLMAP F8) SNIP1 F9) STARD9	<u>FHA</u> G1) KIF13A G2) KIF13B G3) KIF14 G4) KIF16B G5) KIF1A G6) KIF1B G7) KIF1C
<u>BRCT</u> H1) 53BP1 (1-2) H2) ANKRD32 H3) BARD1 (1-2) H4) BRCA1 (1-2) H5) DBF4 (1-2) H6) DNTT H7) ECT2 (1-2) H8) FCP1	<u>BRCT</u> I1) LIG3 I2) LIG4 (1-2) I3) MCPH1 (1) I4) MCPH1 (2-3) I5) MDC1 (1-2) I6) NBS1 I7) PARP1 I8) PARP4	<u>BRCT</u> J1) PAXIP1 (1-2) J2) PAXIP1 (3-4) J3) PAXIP1 (5-6) J4) PES1 J5) POLL J6) REV1 J7) RFC1	<u>BRCT</u> K1) TOPBP1 (1-2) K2) TOPBP1 (3) K3) TOPBP1 (4-5) K4) TOPBP1 (6) K5) TOPBP1 (7-8) K6) XRCC1 (1) K7) XRCC1 (2)

continued over page

Figure 4.10

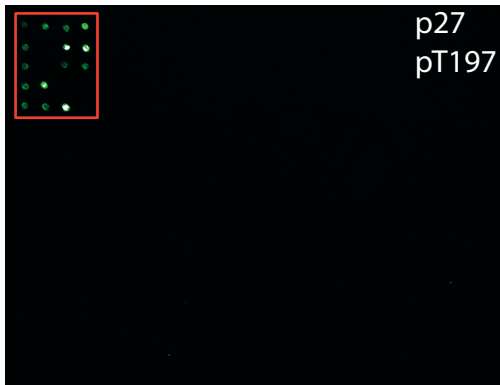
B



continued over page

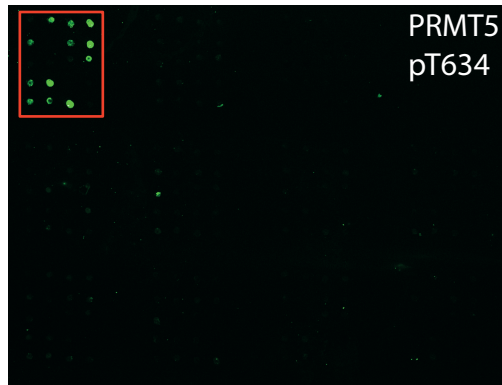
Figure 4.10

C



p27
pT197

14-3-3: Sigma, Beta/Alpha, Epsilon,
Gamma, Eta, Theta, Zeta/Delta



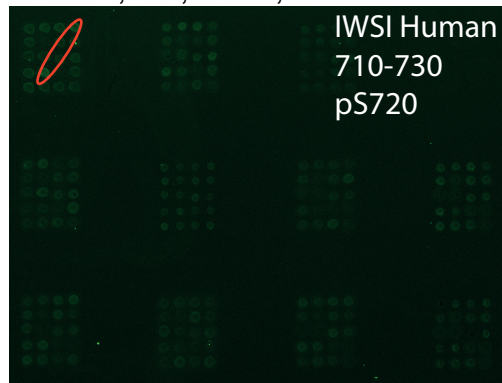
PRMT5
pT634

14-3-3: Sigma, Beta/Alpha, Epsilon,
Gamma, Eta, Theta, Zeta/Delta



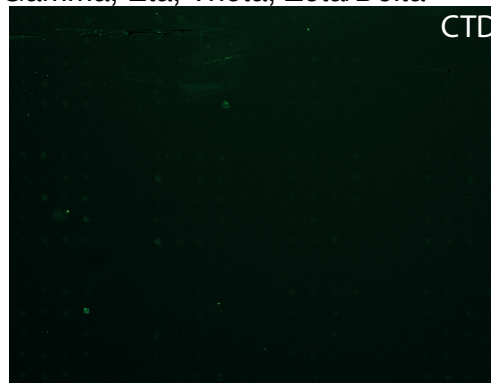
RICTR Human
1125-1145
pT1135

14-3-3: Sigma, Beta/Alpha, Epsilon,
Gamma, Eta, Theta, Zeta/Delta

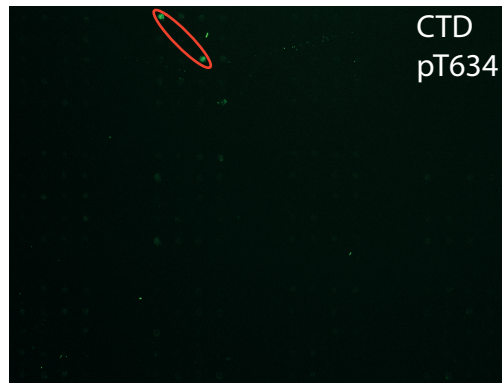


IWSI Human
710-730
pS720

14-3-3: Gamma

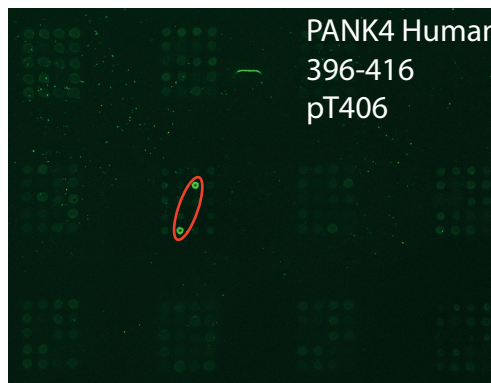


CTD



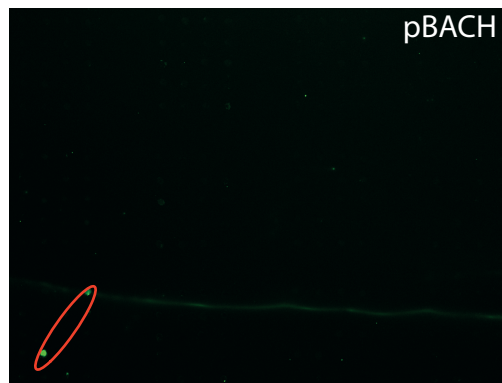
CTD
pT634

WW: Pin1



PANK4 Human
396-416
pT406

FHA: MDC1



pBACH

BRCT: BRCA1 (1-2)

Figure legend over page

Figure 4.10 A pS134 peptide does not interact with pS/T reader proteins

(A) Schematic of the pS/T reader protein micro array. The numbered squares at the top represent how each GST-fusion peptide listed was arrayed in duplicate. M = GST alone. The rectangles labelled with letters at the top of the page correspond with those listed below it. Each rectangle represents a different protein array.

(B) A pS134 peptide does not detect pS/T reader proteins. 10 or 100 μg of control (Biotin KAVQNDSNPSASQPTTGPS) and phosphorylated (Biotin-KAVQNDSNPSA{pSer}QPTTGPS) hSSB1 biotinylated peptides were pre-bound with a Cy3-streptavidin label and incubated with each chip of the pS/T reader micro array. A duplicate microarray was also probed with a GST antibody and detected using a FITC-conjugated secondary antibody. Fluorescent signals were detected using a slide scanner equipped with a 550 nm long pass filter. As each microarray contained proteins arrayed in duplicate, two fluorescent signals (dots) were expected for positive interactions. Although faint fluorescent signals were detected, these were not specific to the phosphorylated peptide.

(C) Positive interactions were detected for a set of control peptides. 10 μg of the indicated peptides (white text) were incubated with each microarray as per (B). Positive signals are indicated with red lines and the corresponding GST-proteins listed below each image.

In doing so, however, a signal specific to the S134 phosphorylated peptide was not observed (**Figure 4.10B**). This is unlikely to be due to an issue with the arraying of pS/T reader proteins, as demonstrated by the detection of these proteins using a GST antibody. In addition, a panel of positive control peptides screened inline with the S134 peptides were able to interact with their respective binding partner and produced the expected fluorescent signals (**Figure 4.10C**).

Although these data most likely suggest that S134 may not mediate a direct interaction with one of these phospho-serine/threonine binding domain-containing proteins, it should be noted that due to the recent establishment of this microarray,

few positive interactions have as yet been identified with many of the proteins outside of the 14-3-3 family. It is therefore possible (or probable) that not all of the proteins on the array are folded correctly (M. Bedford, personal communication, November 11 2014). In addition, even if S134 phosphorylated hSSB1 does mediate a direct protein interaction, this may not necessarily be supported by a phosphorylated peptide.

4.2.11 Multiple SQ/TQ motifs are found in the SSB1 C-terminus of animal species

In the previous chapter (Figure 3.4E) it was observed that S134 and T117, despite being of importance for hSSB1, were only partially conserved amongst the species examined. The relatively close proximity of these motifs is however of some interest and it was proposed that these amino acids may form part of a DNA damage responsive regulatory region. As the previous alignment was relatively limited in the number of species examined, a larger alignment of SSB1 sequences was undertaken. For this, the hSSB1 amino acid sequence was entered as a query sequence in the blastn program and searched against the NCBI ‘nucleotide collection nr/nt’ database for ‘highly similar sequences’. The 69 unique sequences returned were then collected and the region of each corresponding to hSSB1 residues 110 to 160 aligned using Clustal Omega. Sequences were manually ordered and grouped to reflect their common phylogenetic clades (**Figure 4.11A**).

In the mammalian species examined, an SQ motif homologous to hSSB1 S134 was predominantly identified in the simian primates (infraorder Simiiformes; higher primates) as well as in the Lagomorpha species (suborder of Gliriform; rabbits, pikas) *O. princeps* (American pika).

Figure 4.11

A

		Order	Species	110	117	134	149	160			
Magna-Super-	Placentalia - mammalia	Boreoeutheria	Euarchonta	Hominiini	EPNPEYSTQ	QAPNKAVQ	NDNSNPSA	SCPTTGPSA	ASPASENQN	GNGLSAPP	
				Simiiformes	P.paniscus	EPNPEYSTQ	QAPNKAVQ	NDNSNPSA	SCPTTGPSA	ASPASENQN	GNGLSAPP
				C.atys	EPNPEYSTQ	QOTPNKAVQ	NDNSNPSA	SCPTTGPSA	ASPASENQN	GNGLSAPP	
				M.fascicularis	EPNPEYSTQ	QOTPNKAVQ	NDNSNPSA	SCPTTGPSA	ASPASENQN	GNGLSAPP	
				C.sabaeus	EPNPEYSTQ	QOTPNKAVQ	NDNSNPSA	SCPTTGPSA	ASPASENQN	GNGLSAPP	
				C.angolensis	EPNPEYSTQ	QAPNKAVQ	NDNSNPSA	SCPTTGPSA	ASPASENQN	GNGLSAPP	
				M.leucophaeus	EPNPEYSTQ	QOTPNKAVQ	NDNSNPSA	SCPTTGPSA	ASPASENQN	GNGLSAPP	
				P.anubis	EPNPEYSTQ	QOTPNKAVQ	NDNSNPSA	SCPTTGPSA	ASPASENQN	GNGLSAPP	
				C.jacchus	EPNPEYSTQ	QAPNKAVQ	NDNSNPSA	SCPTTGPSA	ASPASENQN	GNGLSAPP	
				A.nancymae	EPNPEYSTQ	QAPNKAVQ	NDNSNPSA	SCPTTGPSA	ASPASENQN	GNGLSAPP	
Euarchothylres	Euarchonta	Primates	S.boliviensis	EPNPEYSTQ	QAPNKAVQ	NDNSNPSA	SCPTTGPSA	ASPASENQN	GNGLSAPP		
			T.syrichta	EPNPEYSTQ	QAPNKAVQ	NDSSPTAPQ	TTIGPPAAS	PASENQN	GNGLSATP		
			O.garnettii	EPNPEYSTQ	QAPNKAVQ	NDSSPTT	TPQTTGPPA	TSPASENQN	GNGLSAPP		
			T.chinensis	EPNPEYSTQ	QAPNKAVQ	NDSTPTAP	QPTGPPAAS	PASENQN	GNGLNAPP		
			Dermoptera	G.variegatus	EPNPEYSTQ	QAPNKAVQ	NDNSPTAP	QPTTIGPPA	APPASENQN	GNGLSTSP	
			Lagomorpha	O.princeps	EPNPEYSTQ	QAPNKAVQ	NDSCPPA	SCPTTGPPA	ASPASENQN	GNGLSTSP	
				O.cuniculus	EPNPEYSTQ	QAPNKAVQ	NDSSPTAP	QAGPPASS	PASENQN	GNGLSAPP	
			Glliriformes	Rodentia	I.tridecemlineatus	EPNPEYSTQ	QAPNKAVQ	NDSSPTAP	QATTGPPA	ASPASENQN	GNGLSTPP
					H.glaber	EPNPEYSTQ	QAPNKAVQ	NDSSPTA	TQATGSPV	SVSPASENQN	GNGLSAPP
					F.damarensis	EPNPEYSTQ	QAPNKAVQ	NDSSLPAT	QATGPPV	SVSPASENQN	GNGLSVPP
C.porcellus	EPNPEYSTQ	QAPNKAVQ			NDSSPTA	TQATGSSA	VSPASENQN	GNGLSTPP			
O.degus	EPNPEYSTQ	QAPNKAVQ			NDSSPTA	TQATGPPV	SVSPASENQN	GNGLSPAPP			
M.musculus	EPNPEYSTQ	QAPNKAVQ			NDNSPTAP	QATTGPPA	ASPASENQN	GNGLSTOL			
R.norvegicus	EPNPEYSTQ	QASNKVQ			NDSSPTAP	QATTGPPA	ASPASENQN	GNGLSTOL			
C.griseus	EPNPEYSTQ	QAPNKAVQ			NDSSPTA	TQATGPPA	ASPASENQN	GNGLSTOL			
M.auratus	EPNPEYSTQ	QAPNKAVQ			NDSSPAAP	QATTGAPAG	SPASENQN	GNGLSTOL			
P.maniculatus	EPNPEYSTQ	QAPNKAVQ			NDSSPTA	QATGPPA	ASPASENQN	GNGLSTOL			
Muridae Arvicolinae	Rodentia	M.ochrogaster	EPNPEYSTQ	QAPNKAVQ	NDSSPTA	QATGPPA	ASPASENQN	GNGLSTPP			
		N.galili	EPNPEYSTQ	QAPNKAVQ	NDSSPTA	QATGPPA	ASPASENQN	GNGLSTPP			
		J.jaculus	EPNPEYSTQ	QAPNKAVQ	NDSSPTA	QPTTGP	PATSPASENQN	GNGLSTSS			
		S.scrofa	EPNPEYSTQ	QAPNKAVQ	NDSSPTA	QPTATG	PPAASPASENQN	GNGLSAPP			
		B.bison	EPNPEYSTQ	QAPNKAVQ	NDSSPAAP	QPTTGP	PATSPASENQN	GNGLSAPP			
		B.taurus	EPNPEYSTQ	QAPNKAVQ	NDSSPAAP	QPTTGP	PATSPASENQN	GNGLSAPP			
		B.mutus	EPNPEYSTQ	QAPNKAVQ	NDSSPAAP	QPTTGP	PATSPASENQN	GNGLSAPP			
		C.hircus	EPNPEYSTQ	QAPNKAVQ	NDSSPAAP	QATTGP	PATSPASENQN	GNGLSAPP			
		P.hodgsonii	EPNPEYSTQ	QAPNKAVQ	NDGGVAP	QPTTGP	PATSPASENQN	GNGLSAPP			
		V.pacos	EPNPEYSTQ	QAPNKAVQ	NDSSPTA	QPTTGP	PATSPASENQN	GNGLSAPP			
Camelidae	Artiodactyla	C.bactrianus	EPNPEYSTQ	QAPNKAVQ	NDSSPTA	QPTTGP	PATSPASENQN	GNGLSAPP			
		C.ferus	EPNPEYSTQ	QAPNKAVQ	NDSSPTA	QPTTGP	PATSPASENQN	GNGLSAPP			
		O.orca	EPNPEYSTQ	QAPNKAVQ	NDSSPTA	QPTTGP	PATSPASENQN	GNGLSTPP			
		T.truncatus	EPNPEYSTQ	QAPNKAVQ	NDSSPTA	QPTTGP	PATSPASENQN	GNGLSTPP			
		P.catodon	EPNPEYSTQ	QAPNKAVQ	NDSSPTA	QPTTAG	PATSPASENQN	GNGLSTPP			
		B.acutorostrata	EPNPEYSTQ	QAPNKAVQ	NDSSPTA	QPTTGP	PATSPASENQN	GNGLSTPP			
		C.simum	EPNPEYSTQ	QAPNKAVQ	NDSSPTA	QPTTGP	PATSPASENQN	GNGLSAPP			
		E.caballus	EPNPEYSTQ	QAPNKAVQ	NDSSPTA	QPTTGP	PATSPASENQN	GNGLSTPP			
		F.catus	EPNPEYSTQ	QAPNKAVQ	NDSSPTA	QPTTGP	PAVSPASENQN	GNGLSAPP			
		C.lupus	EPNPEYSTQ	QAPNKAVQ	NDSSPTA	QPTTGP	PAVSPASENQN	GNGLSAPP			
Caniformia	Carnivora	A.melanoleuca	EPNPEYSTQ	QAPNKAVQ	NDSSPTA	QPTTGP	PAVSPASENQN	GNGLSAPP			
		M.putorius	EPNPEYSTQ	QAPNKAVQ	NDSSPTA	QPTTGP	PAVSPASENQN	GNGLSAPP			
		E.fuscus	EPNPEYSTQ	QAPNKAVQ	NDSSPTA	QPTTGP	PAVSPASENQN	GNGLSAPP			
		M.lucifugus	EPNPEYSTQ	QAPNKAVQ	NDSSPAAP	QPTTGP	PAVSPASENQN	GNGLSAPP			
		P.alecto	EPNPEYSTQ	QAPNKAVQ	NDSSPTA	QPTTGP	PAASPAASENQN	GNGLSTPP			
		C.cristata	EPNPEYSTQ	QAPNKAVQ	NDSSPAAP	TPATG	PSAASPAASENQN	GNGLNAPP			
		E.europaeus	EPNPEYSTQ	QAPNKAVQ	NDSSPTA	QPPAGS	PATPPVSE	NQNGLSVPP			
		S.araneus	EPNPEYSTQ	QAPNKAVQ	NDSSPTA	SPPTG	APTASE	NQNGLNAPA			
		L.africana	EPNPEYSTQ	QAPNKAVQ	NDSSPSAL	QPTTGP	PAASPAASENQN	GNGLSAPP			
		T.manatus	EPNPEYSTQ	QAPNKAVQ	NDSSSAPP	PTTGP	PAASPAASENQN	GNGLSTPP			
Afroinsectiphilia	Tubulidentata	O.afer	EPNPEYSTQ	QOTPNKAVQ	NDSSPAAP	QPTTGP	PAASPAASENQN	GNGLSTLP			
		C.asiatica	EPNPEYSTQ	QAPNKAVQ	NDNSPAT	QPTTGP	PATSPASENQN	GNGLSPLP			
		E.telfairi	EPNPEYSTQ	QAPNKAVQ	NDSSPAAP	QPTTGP	PAASPAASENQN	GNGLSALP			
		E.edwardii	EPNPEYSTQ	QAPNKAVQ	NDSSSAPP	QPPAG	PAASPAASENQN	GNGLSALP			
		D.novemcinctus	EPNPEYSTQ	QAPNKAVQ	LDSSPGAP	PPSGPPA	APPASENQN	GNGLSTPP			
		Toxloofera	Squamata	A.carolinensis	EPNPEYSTQ	QAPNKAVQ	NDSSSAPP	QPPAG	PAASPAASENQN	GNGLSALP	
			P.bivittatus	EPNPEYSTQ	QAPNKAVQ	NDSSSAPP	QPPAG	PAASPAASENQN	GNGLSALP		
			O.hannah	EPNPEYSTQ	QAPNKAVQ	NDSSSAPP	QPPAG	PAASPAASENQN	GNGLSALP		
		P.sinensis	EPNPEYSTQ	QAPNKAVQ	NDSSSAPP	QPPAG	PAASPAASENQN	GNGLSALP			
		Testudines	C.mydas	EPNPEYSTQ	QAPNKAVQ	NDSSSAPP	QPPAG	PAASPAASENQN	GNGLSALP		
C.picta	EPNPEYSTQ		QAPNKAVQ	NDSSSAPP	QPPAG	PAASPAASENQN	GNGLSALP				
Crocidilia	A.sinensis	EPNPEYSTQ	QAPNKAVQ	NDSSSAPP	QPPAG	PAASPAASENQN	GNGLSALP				
	A.sinensis	EPNPEYSTQ	QAPNKAVQ	NDSSSAPP	QPPAG	PAASPAASENQN	GNGLSALP				

continued over page

Figure 4.11

B

		Order	Species	170	182	209 211
Magna-Super-	Euarchontoglires	Euarchonta	H.sapiens	TP--SHPPSTRITRSCPNHTPAGPP--GPSSNPVSNKGTTRRSSKR		
			P.paniscus	TP--SHPPSTRITRSCPNHTPAGPP--GPSSNPVSNKGTTRRSSKR		
			C.atys	TP--SHPPSTRITRSCPNHTPAGPP--GPSSNPVSNKGTTRRSSKR		
			M.fascicularis	TP--SHPPSTRITRSCPNHTPAGPP--GPSSNPVSNKGTTRRSSKR		
			C.sabaeus	TP--SHPPSTRITRSCPNHTPAGPP--GPSSNPVSNKGTTRRSSKR		
			C.angolensis	TP--SHPPSTRITRSCPNHTPAGPP--GPSSNPVSNKGTTRRSSKR		
			M.leucophaeus	TP--SHPPSTRITRSCPNHTPAGPP--GPSSNPVSNKGTTRRSSKR		
			P.anubis	TP--SHPPSTRITRSCPNHTPAGPP--GPSSNPVSNKGTTRRSSKR		
			C.jacchus	TP--SHPPSTRITRSCPNHTPAGPP--GPSSNPVSNKGTTRRSSKR		
			A.nancymae	TP--SHPPSTRITRSCPNHTPAGPP--GPSSNPVSNKGTTRRSSKR		
Boreoeutheria	Euungulata	Artiodactyla	S.boliviensis	TP--SHPPSTRITRSCPNHTPAGPP--GPSSNPVSNKGTTRRSSKR		
			T.syrichtha	TP--SHPPSTRITRSCPNHTPAGPP--GPSSNPVSNKGTTRRSSKR		
			O.garnettii	AP--SHTPSTRITRSCPNHTPAGPP--GPSNPNVSNKGTTRRSSKR		
			T.chinensis	AP--SHPPSTRITRSCPNHTPAGPP--GPSSNPVSNKGTTRRSSKR		
			G.variegatus	TP--SHPPSTRITRSCPNHTPAGPP--GPSSNPVSNKGTTRRSSKR		
			O.princeps	TP--SHPPSTRITRSCPNHTPAGPP--GPSSNPVSNKGTTRRSSKR		
			O.cuniculus	TP--SHPPSTRITRSCPNHTPAGPP--GPSSNPVSNKGTTRRSSKR		
			I.tridecemlineatus	TP--SHPPSTRITRSCPNHTPAGPP--GPSSNPVSNKGTTRRSSKR		
			H.glaber	AP--THPPSTRITRSCPNHTPAGPP--GPSSNPVSNKGTTRRSSKR		
			F.damarensis	TP--AHPPSTRITRSCPNHTPAGPP--GPSSNPVSNKGTTRRSSKR		
Placentalia - mammalia	Laurasiatheria	Euungulata	C.porcillus	TP--SHPPSTRITRSCPNHTPAGPP--GPSSNPVSNKGTTRRSSKR		
			O.degus	TP--SHPPSTRITRSCPNHTPAGPP--GPSSNPVSNKGTTRRSSKR		
			M.musculus	TP--SHPPSTRITRSCPNHTPAGPP--GPSSNPVSNKGTTRRSSKR		
			R.norvegicus	AP--SHPPSTRITRSCPNHTPAGPP--GPSSNPVSNKGTTRRSSKR		
			C.griseus	TA--SHAPSTRITRSCPNHTPAGPP--GPSSNPVSNKGTTRRSSKR		
			M.auratus	TA--SHAPSTRITRSCPNHTPAGPP--GPSSNPVSNKGTTRRSSKR		
			P.paniculatus	TP--SHPPSTRITRSCPNHTPAGPP--GPSSNPVSNKGTTRRSSKR		
			M.ochrogaster	TP--SHPPSTRITRSCPNHTPAGPP--GPSSNPVSNKGTTRRSSKR		
			N.galili	TP--SHPPSTRITRSCPNHTPAGPP--GPSSNPVSNKGTTRRSSKR		
			J.jaculus	TP--SHPPSTRITRSCPNHTPAGPP--GPSSNPVSNKGTTRRSSKR		
Boreoeutheria	Euungulata	Artiodactyla	S.scrofa	TP--SHPPSTRITRSCPNHTPAGPP--GPSSNPVSNKGTTRRSSKR		
			B.bison	TP--SHPPSTRITRSCPNHTPAGPP--GPSSNPVSNKGTTRRSSKR		
			B.taurus	TP--SHPPSTRITRSCPNHTPAGPP--GPSSNPVSNKGTTRRSSKR		
			B.mutus	TPSPHPPSTRITRSCPNHTPAGPP--GPSSNPVSNKGTTRRSSKR		
			C.hircus	TSPASEQNGLSAPPNHTPAGPP--GPSSNPVSNKGTTRRSSKR		
			P.hodgsonii	TP--SHPPSTRITRSCPNHTPAGPP--GPSSNPVSNKGTTRRSSKR		
			V.pacos	TP--SHPPSTRITRSCPNHTPAGPP--GPSSNPVSNKGTTRRSSKR		
			C.bactrianus	TP--SHPPSTRITRSCPNHTPAGPP--GPSSNPVSNKGTTRRSSKR		
			C.ferus	TP--SHPPSTRITRSCPNHTPAGPP--GPSSNPVSNKGTTRRSSKR		
			O.orca	TP--PHPPTPRITRSCPNHTPAGPP--GPSSNPVSNKGTTRRSSKR		
Laurasiatheria	Perissodactyla	Carnivora	T.truncatus	TP--PHPPTPRITRSCPNHTPAGPP--GPSSNPVSNKGTTRRSSKR		
			P.catodon	TP--XHPPTPRITRSCPNHTPAGPP--GPSSNPVSNKGTTRRSSKR		
			B.acutorostrata	TP--SHPPTPRITRSCPNHTPAGPP--GPSSNPVSNKGTTRRSSKR		
			C.simum	TP--SHPPSTRITRSCPNHTPAGPP--GPSSNPVSNKGTTRRSSKR		
			E.caballus	TP--SHPPSTRITRSCPNHTPAGPP--GPSSNPVSNKGTTRRSSKR		
			F.catus	AP--SHPPSTRITRSCPNHTPAGPP--GPSSNPVSNKGTTRRSSKR		
			C.lupus	HP--SHPPSTRITRSCPNHTPAGPP--GPSSNPVSNKGTTRRSSKR		
			A.melanoleuca	AP--SHPPSTRITRSCPNHTPAGPP--GPSSNPVSNKGTTRRSSKR		
			M.putorius	TP--SHPPSTRITRSCPNHTPAGPP--GPSSNPVSNKGTTRRSSKR		
			E.fuscus	TP--SHPPSTRITRSCPNHTPAGPP--GPSSNPVSNKGTTRRSSKR		
Laurasiatheria	Chiroptera	Eulipotyphla	M.lucifugus	AP--SHPPSTRITRSCPNHTPAGPP--GPSSNPVSNKGTTRRSSKR		
			P.alecto	TP--SHAPSTRITRSCPNHTPAGPP--GPSNPNVSNKGTTRRSSKR		
			C.cristata	TP--PHPPSTRITRSCPNHTPAGPP--GPSSNPVSNKGTTRRSSKR		
			E.europaeus	TP--SHPPSTRITRSCPNHTPAGPP--GPSSNPVSNKGTTRRSSKR		
			S.araneus	AP--PHPPSTRITRSCPNHTPAGPP--GPSSNPVSNKGTTRRSSKR		
			I.africana	TP--SHPPSTRITRSCPNHTPAGPP--GPSSNPVSNKGTTRRSSKR		
			T.manatus	TP--SHPPSTRITRSCPNHTPAGPP--GPSSNPVSNKGTTRRSSKR		
			O.afer	AP--SHPPSTRITRSCPNHTPAGPP--GPSSNPVSNKGTTRRSSKR		
			C.asiatica	AP--SHPPSTRITRSCPNHTPAGPP--GPSSNPVSNKGTTRRSSKR		
			E.telfairi	AP--SHPPSTRITRSCPNHTPAGPP--GPSSNPVSNKGTTRRSSKR		
Laurasiatheria	Macroscelidea	Cingulata	E.edwardii	AP--SHPPSTRITRSCPNHTPAGPP--GPSSNPVSNKGTTRRSSKR		
			D.novemcinctus	AT--PHPPSTRITRSCPNHTPAGPP--GAPNNSVSNKGTTRRSSKR		
			A.carolinensis	VP--THPTSGRITRSCPNHQSGSSTGTGSSSNVSNKGTTRRSSKR		
			P.bivittatus	IP--THPTSGRITRSCPNHQGGSSSGIGSSSNVSNKGTTRRSSKR		
			O.hannah	IS--THPTTGRITRSCPNHQGGSSSSIGSSSNVSNKGTTRRSSKR		
			P.sinensis	GP--AHPSTGRITRSCPNHQGAGSAGSSSNVSNKGTTRRSSKR		
			C.mydas	VP--SHPTSGRITRSCPNHQGVGAGSAGSSSNVSNKGTTRRSSKR		
			C.picata	VP--SHPTSGRITRSCPNHQGAGSAGSSSSPISNKGKTRRSSKR		
			A.sinensis	PPAAPHASGRITRSCPNHAST-----AGAVSNKGTTRRSSKR		

C

hSSB1	----MTTETFKVDIKPGLKLNLIIVLETGRVTKTKDGHEVRTCKVADKTGSINISVWDDVGNLIQPGDIIRLTKGYASVF	78
hSSB2	MNRVNDPLIFIRDIKPLKLNLVVIVLEIGRVTKTKDGHEVRSCKVADKTGSITISVWDEIGGLIQPGDIIRLTRGYASMW	82
hSSB1	KGCLTLTYTGRGGDLQKIGFCMVYSEVPNFSEPNPEYS[TO]QAPNKAVQNDNSPSA[SO]PTTGPSAASPASENQNGLSAPP	160
hSSB2	KGCLTLTYTGRGGELQKIGFCMVYSEVPNFSEPNPEYRGGQNKGAQSEKNNMNSNM-----GTGTFGPVG	149
hSSB1	PGGGPHPP---HTPSHPST-RITRSCPNHTPAGPPGPSSNPVSNKGTTRRSSKR	211
hSSB2	NGVHTGPESREHQFESHAGRSNGRLINPQLQCTASNOVTMTTISNGDRPRAFKR	204

Figure legend over page

Figure 4.11 Multiple SQ/TQ motifs are found in the SSB1 C-terminus of animal species

(A) A SQ/TQ motif homologous to hSSB1 S134 is conserved in simiiform primates, some gliriformes, and numerous reptiles. The amino acid sequence of hSSB1 was entered as a query sequence in the blastn program (<https://blast.ncbi.nlm.nih.gov>) and searched against the NCBI ‘nucleotide collection nr/nt’ database for ‘highly similar sequences’ (megablast). Unique sequence matches were collected and labelled by species name. The region of each sequence corresponding to hSSB1 residues 110 to 160 was isolated and aligned using Clustal Omega (ebi.ac.uk) with default parameters. Sequences were manually ordered and grouped based on currently accepted phylogenetic clades. SQ/TQ motifs are outlined by rectangles with numbers corresponding to the hSSB1 protein sequence.

(B) An SQ/TQ motif homologous to hSSB1 S182, as well as an RXXS motif homologous with hSSB1 S209, is highly conserved in animal species. Amino acid sequences corresponding to hSSB1 residues 170-211 from each sequence in (A) were similarly isolated, ordered and aligned. SQ and RXXS motifs are outlined by rectangles with numbers corresponding to the hSSB1 protein sequence.

(C) SQ/TQ and RXXS motifs are not conserved in hSSB2. The amino acid sequences of hSSB1 and hSSB2 were isolated and aligned using EMBOSS Needle (ebi.ac.uk) with default parameters. SQ/TQ and RXXS motifs are outlined by rectangles with numbers corresponding to the hSSB1 protein sequence

In addition, a TQ motif was observed at this site in a small number of other Gliriform species within the Rodentia (Rodents) suborder Hystricomorpha (guinea pigs, porcupines etc.). Strikingly, whilst a S134 homologous motif was not observed in the remainder of mammalian species examined, this motif was identified in all of the aligned reptilia species (reptiles; including snakes, lizards, turtles and crocodiles). It is also interesting to note that in the majority of species that did not contain an SQ motif at S134, a proline residue was almost invariably observed.

Similarly to S134, a TQ motif homologous to hSSB1 T117 was only observed in a subset of mammals, as well as in two species of turtle (Reptilia, Testudines). Interestingly, neither SQ nor TQ motifs homologous to S134 or T117 were observed in the mammalian Laurasiatheria superorder (shrews, bats, carnivorans and odd and even-toed ungulates), with the single exception of *S. araneus* (the common shrew), which contained a motif homologous to T117. In addition, an S134 SQ motif was not observed in the Afrotheria superorder (elephants, sea cows, Aardvaks), while an SQ/TQ motif homologous to T117 was only observed in the order Afrosoricida (golden moles and tenrecs). An unexpected observation was the detection of a SQ motif corresponding to hSSB1 residue 149, which was more highly conserved than T117 or S134, although was not identified in humans. Indeed, this motif was identified in all other primate sequences aligned other than of the Hominini subgroup (humans and chimpanzees). Additional other SQ/TQ motifs were identified in a small number of non-human species at positions corresponding to hSSB1 residues 120, 125 and 158.

Outside of this ~ 50 amino acid region, it is interesting to note that only a single other SQ motif was observed in any of the aligned sequences. Furthermore, this motif, which in humans is found at S182, was conserved in 68 of the 69 species examined (**Figure 4.11B**). This may however reflect the overall high sequence conservation of the SSB1 far C-terminus. Indeed, an RXXS motif (the consensus phosphorylation sequence of Chk1 and Chk2) was also observed in all species examined at residues corresponding to hSSB1 R206 to S209.

It is also noteworthy that while hSSB1 contains three SQ motifs (T117, S134, S182) and one RXXS motif (R206-S209) no such sequences were observed in hSSB2 (**Figure 4.11C**).

4.2.12 S134 phosphorylation may not affect hSSB1 protein half-life or poly-ubiquitination

In the previous section it was noted that while an SQ motif homologous to S134 was observed in simian primates, few other animals contained this specific motif at this position. Indeed, specific SSB1 SQ/TQ motifs within an ~ 50 amino acid section of

the C-terminus in general were only intermediately conserved. Despite this, the majority of animal species examined did contain one or more SQ/TQ motifs somewhere within this region. It was therefore interesting to consider that while phosphorylation of a specific residue may not be essential, selective pressure may exist for the conservation of a phosphorylation site within this region of the protein. If this possibility is considered, it may therefore seem reasonable to conclude that phosphorylation of any of these residue may have a similar effect. Such a conclusion does however require the assumption that SSB1 proteins function similarly in various animal species.

The phosphorylation of hSSB1 T117 has previously been postulated to affect protein activity by interfering with proteasome-targeting poly-ubiquitination and thereby limiting protein turnover (Chen et al., 2014; Richard et al., 2008). Here, hSSB1 T117 was suggested to be phosphorylated by the ATM kinase in response to double-strand DNA break formation to thereby increase the concentration of hSSB1, thus facilitating DNA repair. Indeed, even in undamaged cells, a T117A hSSB1 phosphomutant was found to be hyper-poly-ubiquitinated, whilst ubiquitination was barely detected for a T117E phosphomimetic (that mimics phosphorylated hSSB1) (Chen et al., 2014). Although an increase in hSSB1 protein levels following hydroxyurea treatment has not been observed in previous sections, or in other reports (Bolderson et al., 2014), it seemed possible that the proportional increase in phosphorylated hSSB1 following damage may be too low for such changes to be observed simply by immunoblotting.

A time course assay using the inhibitor of protein biosynthesis, cycloheximide, has previously been employed to demonstrate the reduced half-life of K94R (acetylation mutant) FLAG-tagged hSSB1 (Wu et al., 2015). It was therefore reasoned that a similar experiment could also be performed with S134A phosphomutant and S134E phosphomimetic 3x FLAG hSSB1. For comparison with phosphorylation of T117, T117A and T117E hSSB1 were also included. Here, WT or mutant 3x FLAG hSSB1 was transiently expressed in HeLa cells for 24 hours, prior to addition of 50 $\mu\text{g mL}^{-1}$ cycloheximide or DMSO. Cells were then harvested 4, 8, 12, 16 or 20 hours post treatment. Whole cell lysates prepared from these cells were then immunoblotted for the FLAG epitope, as well for PARP1, the cleavage of which was used a positive

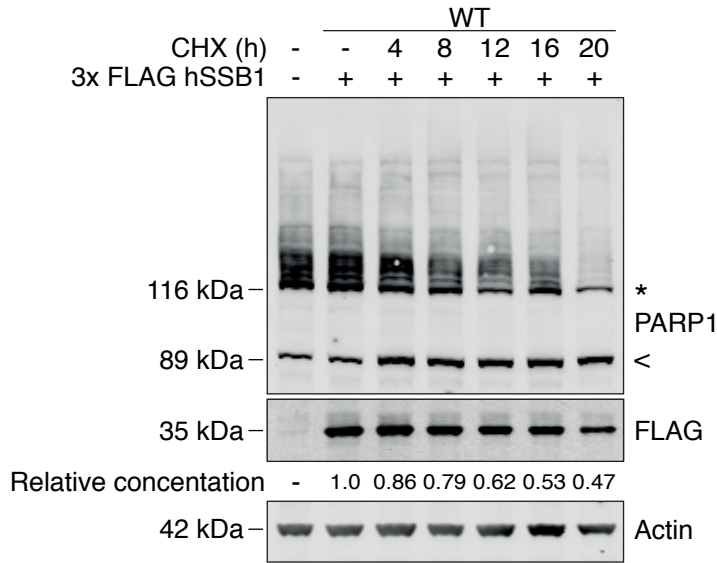
control (Chen et al., 2013c) (**Figure 4.12A, B and C**). A similar half-life was however consistently observed between the WT protein and the S134 mutants. In contrast to previous studies (Chen et al., 2014), a substantial difference in the half-life of T117A or E hSSB1 was also not observed.

Although the data above suggests that S134 phosphorylation may not affect protein half-life, the observation that T117A and E hSSB1 are also similarly stable may suggest that cycloheximide time courses are not the optimal assessment means. As hexa-His-ubiquitin pull-down assays have previously been employed to assess poly-ubiquitination of T117A and E hSSB1 (Chen et al., 2014), these assays were also performed with S134A and E hSSB1. Based on the findings in section 3.2.2 that the 3x FLAG tag of hSSB1 may be poly-ubiquitinated, these assays instead used HA-tagged hSSB1 phosphorylation mutants.

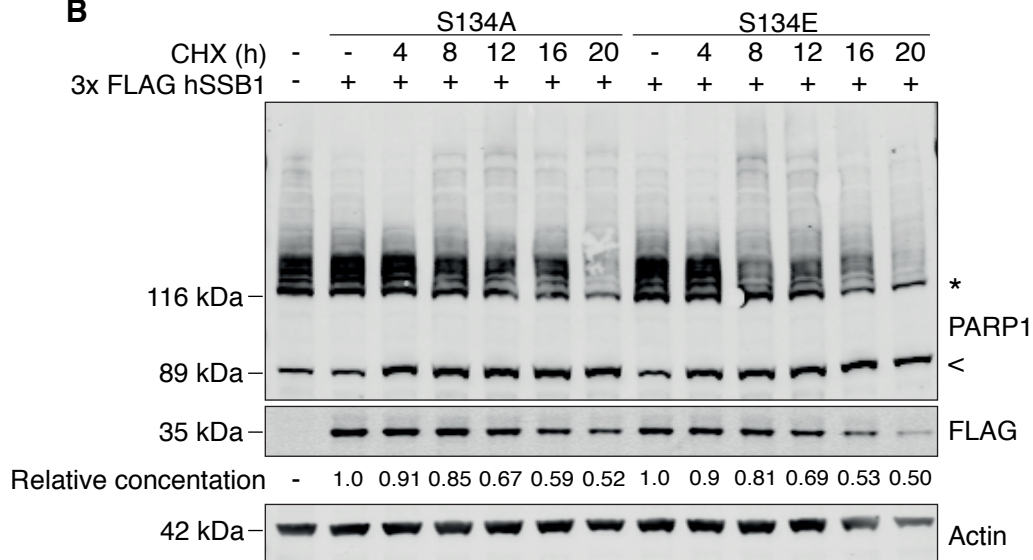
His-ubiquitin pull-down assays were performed in the same manner as in chapter 3 by co-transfecting HEK293T cells with plasmids expressing hexa-His ubiquitin and HA-tagged hSSB1. After 24 hours, cells were then treated with 50 μ M MG-132 and harvested after 4 hours. Cells were then lysed in 8 M urea and hexa-His-tagged ubiquitinated proteins captured on Ni-NTA agarose beads. Proteins were then eluted and immunoblotted with a HA antibody (**Figure 4.12D**). In doing so, no consistent, sizeable differences in the ubiquitination of WT, S134 or T117 phosphomutant hSSB1 was observed. These data further support that S134 phosphorylation does not regulate hSSB1 protein turnover. In addition, the observations of this section are in disagreement with the attributed role of hSSB1 T117 phosphorylation to the regulation of protein half-life. It cannot however be excluded that these discrepancies represent variations in experimental conditions. Indeed, whilst the experiments conducted here employed HeLa cells for CHX experiments and HEK293T cells for hexa-His-ubiquitin pull down assay, earlier works have used a combination of A549, NCI-H23 and NCI-H460 cell lines (Chen et al., 2014). Nevertheless, these data may suggest that T117 and S134 phosphorylation regulate hSSB1 through a means independent of, or in addition to, protein stabilisation in DNA repair processes.

Figure 4.12

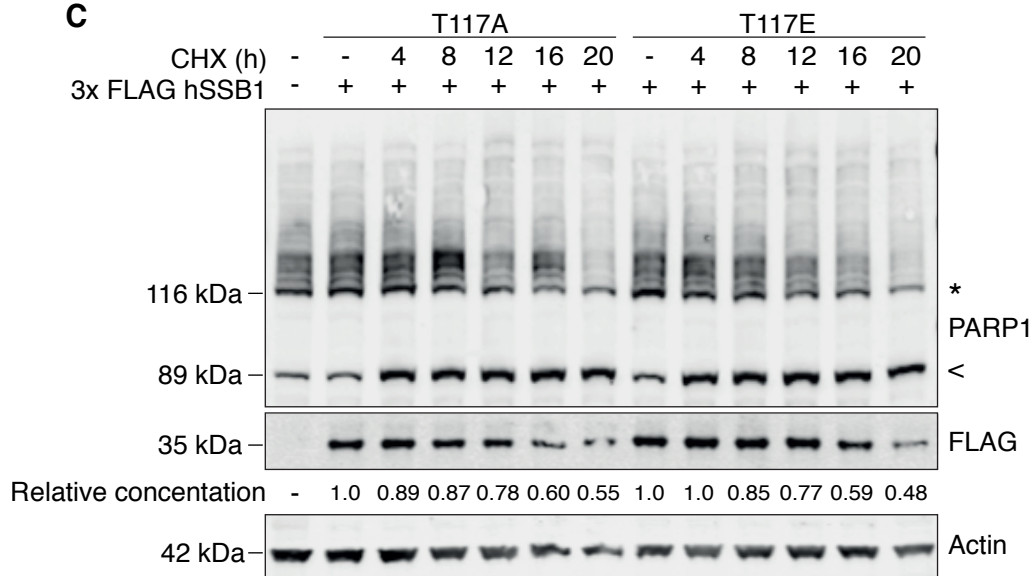
A



B



C



Continued over page

Figure 4.12

D

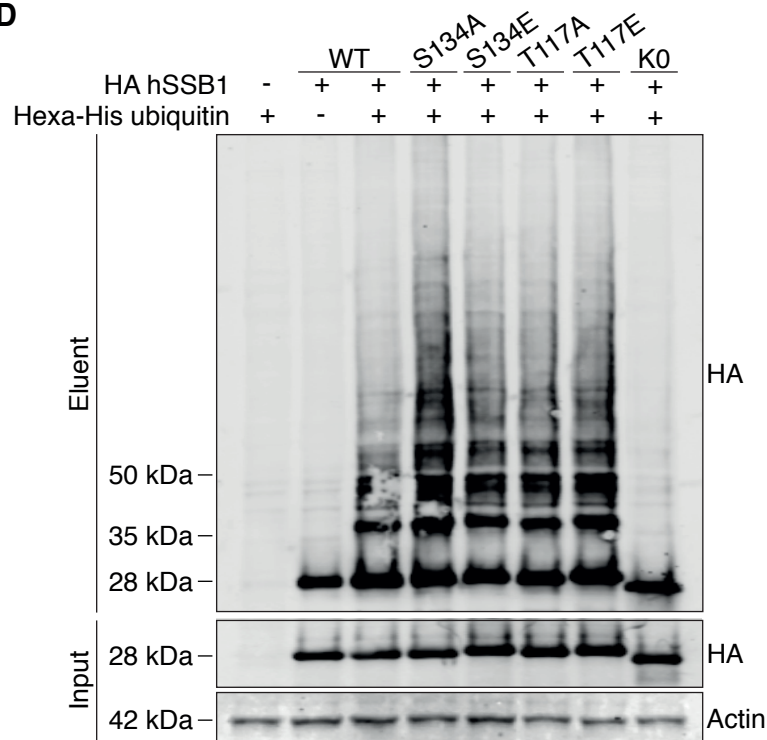


Figure 4.12 S134 phosphorylation may not affect hSSB1 protein half-life or poly-ubiquitination

(A, B and C) S134 and T117 phosphorylation mutants have a similar half-life to WT hSSB1. WT (A), S134A, S134E (B), T117A and T117E (C) 3x FLAG hSSB1 constructs were transiently expressed in HeLa cells for 24 hours, prior to addition of $50 \mu\text{g mL}^{-1}$ cycloheximide or DMSO. Cells were harvested 4, 8, 12, 16 or 20 hours post treatment. Cells pellets were resuspended and lysed in RIPA buffer and $15 \mu\text{g}$ of whole cell lysate immunoblotted with antibodies against FLAG, PARP1 (CHX positive control), or actin (loading control). * = Full-length PARP1, < = cleaved PARP1. Densitometry of FLAG bands was performed using ImageJ and expressed relative to untreated 3x FLAG hSSB1-expressing cells. These results are representative of three independent experiments.

(D) S134 and T117 hSSB1 phosphorylation mutants are poly-ubiquitinated similarly to WT. HA-tagged S134 and T117 phosphorylation mutant (S134A and T117A) and mimetic (S134E and T117E) constructs were prepared by site-directed mutagenesis of the corresponding 3x FLAG hSSB1 plasmids. Each construct was co-

transfected into HEK293T cells with a plasmid encoding hexa-His tagged ubiquitin and expressed for 24 hours. Cells were treated with 25 μ M MG132 for 4 hours, harvested, and lysed in a buffer containing 8 M urea. 1000 μ g of whole cell lysate was incubated with 20 μ l of Ni-NTA agarose beads for 2 hours at room temperature, washed 3x with 8 M urea and eluted by heating to 90 $^{\circ}$ C for 10 minutes in SDS loading buffer. Eluent was immunoblotted and probed with antibodies against the HA tag. 15 μ g of whole cell lysate (input) was immunoblotted and probed with antibodies against HA and actin. These results are representative of three independent experiments.

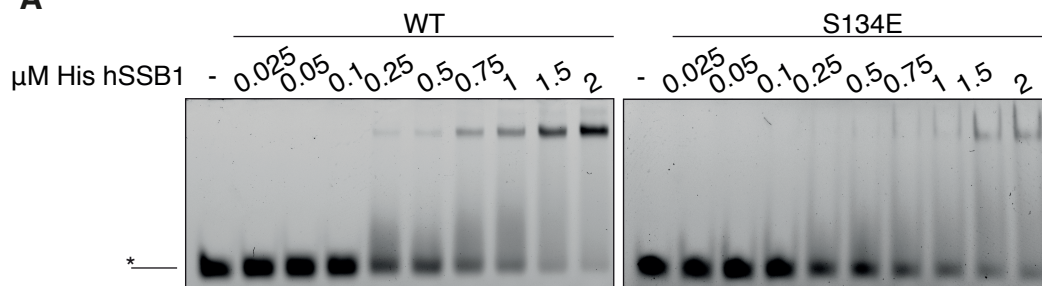
4.2.13 Phosphorylation of hSSB1 S134 may alter the affinity of hSSB1 for replication fork junctions

In a recent publication, the C-terminus of hSSB1 (and hSSB2) was found to be important for efficient binding to DNA substrates (Vidhyasagar et al., 2016). Indeed, truncation of this region of the protein (residues 138 - 211) reduced hSSB1 DNA binding by \sim 4-fold. As S134 is situated at the start of this region, it was therefore interesting to consider that phosphorylation of this residue may affect the C-terminus of the protein in such a way as to alter DNA substrate binding.

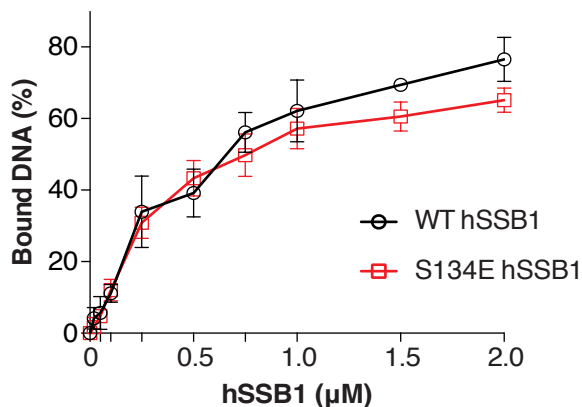
The disruption of replication forks results in the accumulation of leading and lagging strand ssDNA (Sogo et al., 2002). To test whether S134 phosphorylation may alter hSSB1 binding to such substrates, electrophoretic mobility shift assays (EMSAs) were performed using recombinant WT or S134E phosphomimetic hexa-His hSSB1. Dr Nicolas Paquet performed this work. Here, WT and S134E hexa-His-hSSB1 were purified as per section 2.2 and increasing concentrations of these proteins incubated for 20 minutes at 37 $^{\circ}$ C with 10 nM of FAM-labelled ssDNA oligonucleotides. Reactions were then separated by electrophoresis on 10% polyacrylamide/TBE gels and the FAM label visualised using a Typhoon FLA 7000 laser scanner (GE healthcare) (**Figure 4.13A and B**). Protein-DNA binding was quantified as a function of the disappearance of free DNA, using ImageQuant TL software (GE Healthcare).

Figure 4.13

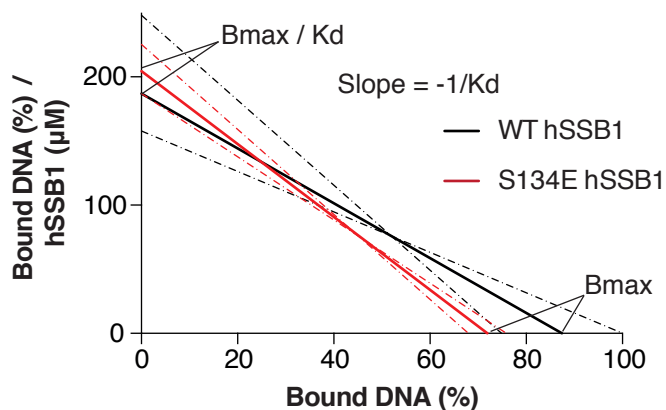
A



B



C



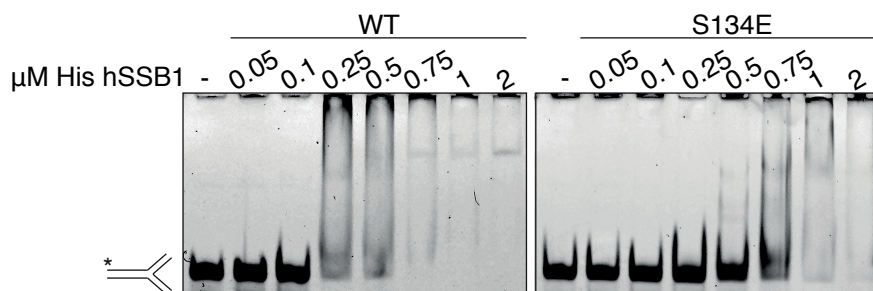
D

		Best-Fit	Std. Error	95 % Confidence Interval
WT hSSB1	Bmax	87.44	5.433	74.87 to 100.00
	h	1.14	0.1365	0.8248 to 1.455
	Kd (μM)	0.4677	0.07195	0.3018 to 0.6336
S134E hSSB1	Bmax	71.93	1.712	67.98 to 75.88
	h	1.232	0.06872	1.074 to 1.391
	Kd (μM)	0.3517	0.02165	0.3017 to 0.4016

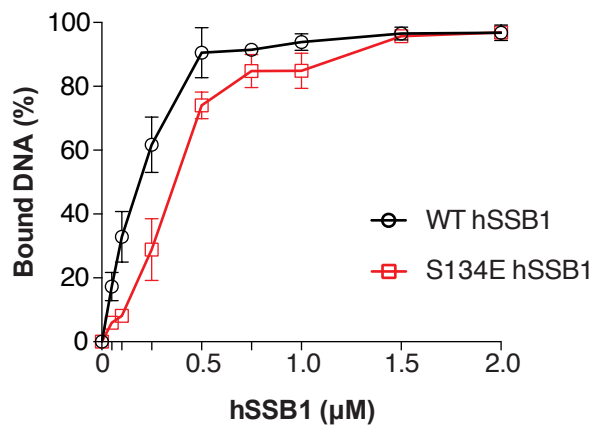
continued over page

Figure 4.13

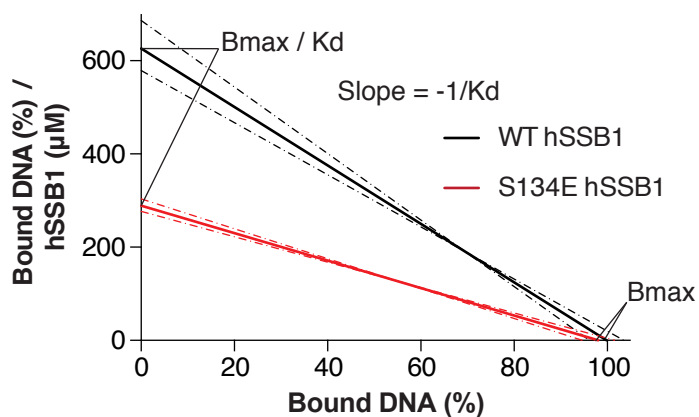
E



F



G



H

		Best-Fit	Std. Error	95 % Confidence Interval
WT hSSB1	Bmax	99.86	1.814	96.19 to 103.5
	h	1.508	0.1158	1.274 to 1.743
	Kd (μM)	0.1594	0.009559	0.1401 to 0.1788
S134E hSSB1	Bmax	98.05	1.712	94.58 to 101.5
	h	2.292	0.1814	1.924 to 2.660
	Kd (μM)	0.3391	0.01371	0.3113 to 0.3669

continued over page

Figure 4.13

I

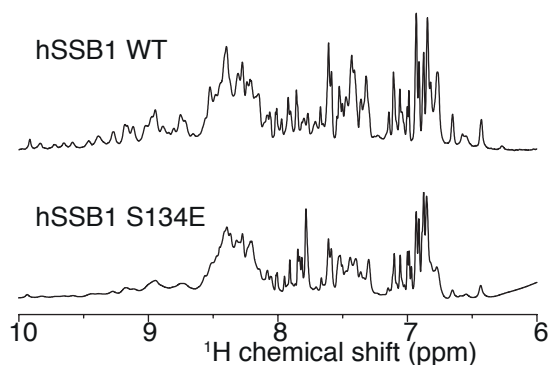


Figure 4.13 S134 phosphorylation may alter the affinity of hSSB1 for replication fork junctions

(A and B) WT and S134E hexa-His-hSSB1 binding to a ssDNA substrate. WT and S134E hexa-His-tagged hSSB1 were expressed in SHuffle T7 *E. coli* and purified by anion exchange chromatography, followed by Ni-NTA affinity capture, and size exclusion chromatography. Increasing concentrations of hSSB1 (0, 0.025, 0.05, 0.1, 0.25, 0.5, 0.75, 1, 1.5 and 2 μM) were incubated with 10 nM of synthetic substrates, in 10 μL of binding buffer (50 mM Tris-HCl pH 7.5, 100 mM KCl, 100 $\mu\text{g ml}^{-1}$ BSA) for 20 min at 37 $^{\circ}\text{C}$. Samples were separated on 10% polyacrylamide gels for 90 min at 90 V and visualized using a Typhoon FLA 7000 laser scanner (GE healthcare). Densitometry was performed on the free FAM labelled substrate using ImageQuant TL and calculated as a percentage of the 0 μM hSSB1 lane. Data is graphed as the mean \pm 1 standard deviation from a minimum of 4 independent experiments.

(C and D) WT and S134E hexa-His-hSSB1 bind to ssDNA similarly. Non-linear regression analysis was performed on the data generated in A using GraphPad Prism version 6 software and the equation ‘one site: specific binding with Hill slope’. BMax, Kd and h values were in this way calculated, as well as the corresponding standard error and 95% confidence intervals. Bmax and Kd values for WT and S134E hexa-His hSSB1 are graphically represented by Scatchard plots (C). The solid line represents best-fit Bmax and Kd values, whilst the dotted lines represent 95% confidence intervals. The calculated values are also tabulated (D).

(E and F) WT and S134E hexa-His-hSSB1 binding to a fork substrate.

Electrophoretic mobility shift assays were performed and visualised as per (A) using WT and S134E hexa-His-tagged hSSB1 and increasing concentrations (0, 0.05, 0.1, 0.25, 0.5, 0.75, 1, and 2 μM) of synthetic fork substrate. Data is graphed as the mean \pm 1 standard deviation from a minimum of 4 independent experiments.

(G and H) S134E hexa-His-hSSB1 binds to fork substrates with less affinity than WT. Non-linear regression analysis was performed on the data generated in (E) and presented as per (C and D).

(I) WT and S134E Hexa-His-tagged hSSB1 is similarly folded *in vitro*. WT and S134A hexa-His-tagged hSSB1 was expressed in SHuffle T7 *E. coli* and purified by Ni^{2+} -NTA affinity capture, followed by size exclusion chromatography. 100-200 μM of WT or S134A hSSB1 was analysed by one-dimensional NMR and proton chemical shifts measured relative to 4,4-dimethyl-4-silapentanesulfonic acid (DSS) at 0 ppm. The 1D NMR spectra of amide protons for WT and S134A hSSB1 are depicted. This experiment was performed in parallel with Figure 4.2G

Whilst a small difference in the mean K_d (dissociation constant) and B_{max} (maximal binding) values were calculated, these were however not statistically significant over multiple experiments (**Figure 4.13C and D**). These data therefore suggest that S134 phosphorylation may not alter the interaction of hSSB1 with ssDNA.

In addition to ssDNA-binding, a number of replication fork proteins have also been found to bind to replication fork junctions. To assess whether hSSB1 may bind such substrates, EMSA assays were also performed using DNA substrates composed of partial DNA duplex fork substrates where the ssDNA of each arm was annealed to a separate ssDNA oligo. Unexpectedly, while hSSB1 has previously been shown not to bind dsDNA duplexes (Paquet et al., 2015), fork junction binding was readily observed for WT hexa-His-hSSB1 (**Figure 4.13 E and F**). Whilst this substrate was also bound by S134E hexa-His hSSB1, this was however with a significantly reduced affinity (WT $K_d = 0.16 \mu\text{M}$, 95% confidence interval (CI) = 0.140 – 0.179 vs S134E $K_d = 0.34 \mu\text{M}$, 95% CI = 0.311 – 0.367) (**Figure 4.13 G and H**). In addition, a

significant difference in the Hill coefficient (h) for WT and S134E hexa-His-hSSB1 was calculated (WT $h = 1.508$, 95% CI = 1.274 – 1.743 vs S134E $h = 2.292$, 95% CI = 1.924 – 2.660). These data suggest that while S134E hexa-His hSSB1 bound to the fork substrate with a lower affinity, it does so with greater co-operativity.

Although these data suggest that S134 phosphorylation may alter the affinity of hSSB1 for replication fork junctions, an alternative explanation may include misfolding of the S134E phosphomimetic. To ensure this were not the case, the 1D NMR spectra of this mutant was determined and compared to that of the WT protein (**Figure 4.13 I**). One-dimensional NMR was again performed by Dr Roland Gamsjaeger. The similar spectra observed for WT and S134E hexa-His-hSSB1 however suggests that the difference in DNA-binding observed was not due to misfolding of the mutant. Another alternative explanation that cannot be excluded is the possibility that the unmodified serine residue may be required for fork junction binding and that the reason for suppressed S134E binding is due not to the mimicked phosphorylation of this residue, although simply due to its mutation. Future work may therefore benefit from the included study of S134A hSSB1 in the above assays.

4.2.14 hSSB1 may associate with proteins involved in chromatin remodelling, RNA metabolism, DNA repair and numerous other functions

The data presented in this document indicates that hSSB1 may be phosphorylated at S134 by the DNA-PK kinase and that this modification may be enhanced following replication inhibition. Furthermore, S134 may be required for hSSB1 function under these circumstances, potentially by altering its affinity for replication fork junctions. Irrespective of this, the role of hSSB1 at sites of stalled forks remains relatively unclear. To further elucidate these functions, mass spectrometry was used to detect proteins that may associate with chromatin-bound hSSB1.

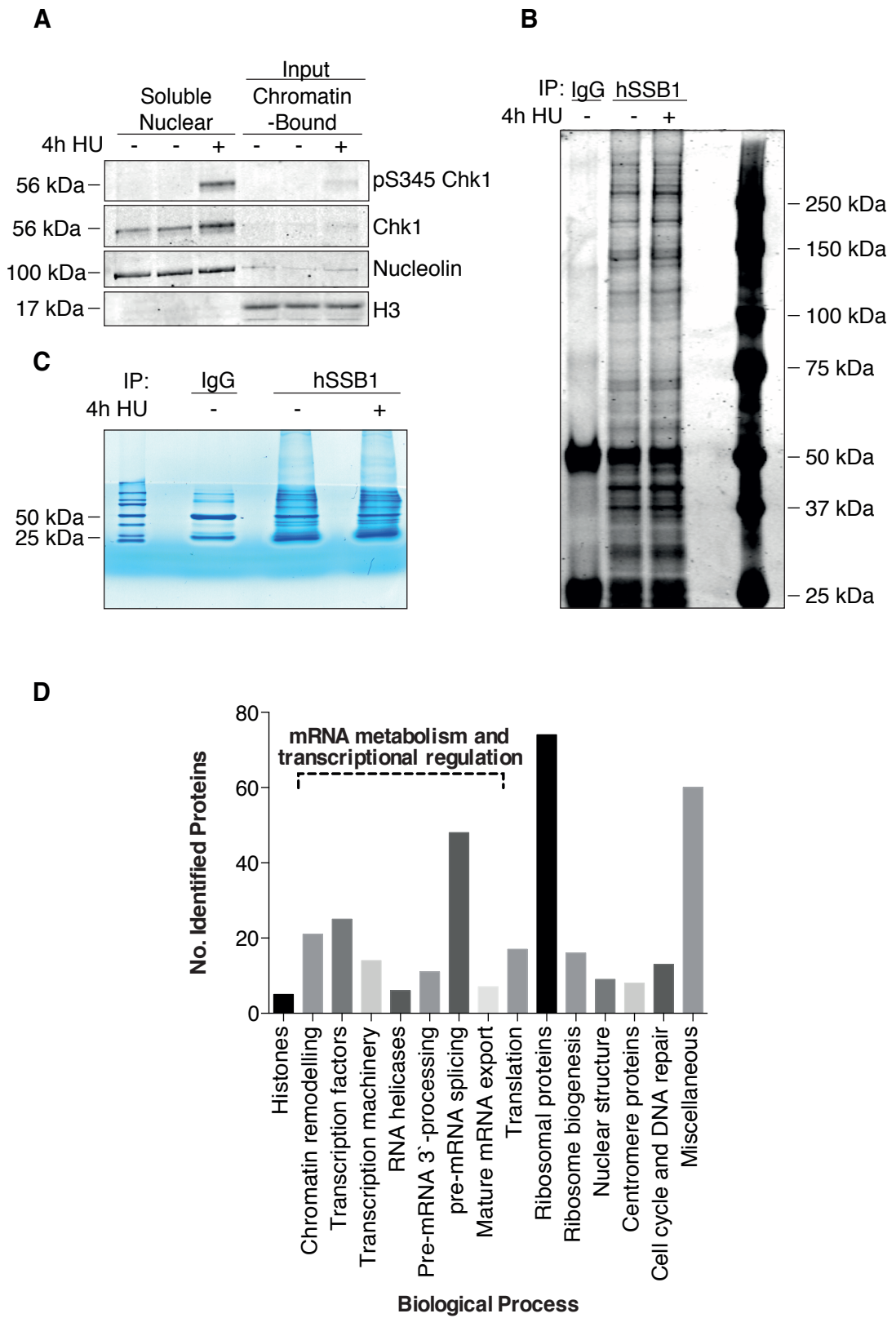
To achieve this, HeLa cells were treated with 3 mM hydroxyurea, or mock treated, for 4 hours prior to enrichment of chromatin-bound proteins by sub-cellular fractionation. Here, cells were resuspended in a hypotonic buffer containing 10 mM KCl and passed 6 times through a 26-gauge needle. Nuclei were then collected by centrifugation and dissolved in a buffer containing 420 mM NaCl. The chromatin-

bound fraction was then collected by further centrifugation and DNA digested with benzonase (a deoxyribonuclease). To assess the purity of this fraction, 10 μ g of the soluble nuclear and chromatin-bound protein fractions were separated by gel electrophoresis and immunoblotted using the indicated antibodies (**Figure 4.14A**). Nucleolin was used as a marker for soluble nuclear protein, while histone H3 was used as a marker for proteins bound to chromatin. As depicted in Figure 4.14A, nucleolin was readily detected in the soluble nuclear fraction, while was greatly reduced in the chromatin fraction. Conversely, histone H3 was detected in the chromatin fraction, while not in the soluble nuclear fraction. Together, these markers suggest that the chromatin fraction is highly enriched for chromatin-bound protein, and contains little contaminating soluble nuclear protein. While much of the soluble nuclear protein was likely removed, it should be noted that the ‘chromatin-bound’ fraction is likely to also contain nucleolar proteins (discussed further below).

hSSB1 was immunoprecipitated from the chromatin fraction using protein G dynabeads bound to a hSSB1 antibody and 10 % of this sample separated by gel electrophoresis; proteins were then stained with colloidal coomassie blue (**Figure 4.14B**). As a number of unique bands were detected in the hSSB1 immunoprecipitated lanes when compared to the IgG lanes, the remaining 90% of the sample was submitted to the Translational Research Institute mass spectrometry facility to allow for identification of co-immunoprecipitating proteins. Here, the samples were electrophoresed briefly on a precast SDS-PAGE, until the dye front had run \sim 1 cm into the gel. This gel was then stained overnight with colloidal coomassie blue (**Figure 4.14C**). Each lane was then excised from the gel and separated into eight individual slices, which were subsequently destained, alkylated, and digested with trypsin. Peptides were then separated and detected by tandem mass spectrometry.

The mass spectrum data was then extracted and searched against the Swiss Prot Human database. This process detected 334 proteins in the hSSB1:IP lanes prior to hydroxyurea treatment and 352 proteins after treatment. These proteins, as well as the number of unique detected peptides, are listed in Appendix 1.

Figure 4.14



Continued over page

Figure 4.14

E

NuRD	WICH-ISWI	SWI/SNF	Tip60 (NuA4)	SIN3
MTA2	BAZ1B	β -actin	ACTL6A	HDAC1
RBBP4	SMARCA5	ACTL6A	HTATIP	HDAC2
RBBP7		BRG1	RUVBL1	RBBP4
HDAC1		DPF2	RUVBL2	RBBP7
HDAC2		PBRM1	TRRAP	SAP18
CHD3		SMARCB1		SIN3A
CHD4		SMARCC1		SAP30
MBD2		SMARCC2		
MBD3		SMARCD1		
		SMARCD2		
		SMARCE1		
		ARID5/A/B/C		
		BCL7		
		BRD7		
		BCL11B		

F

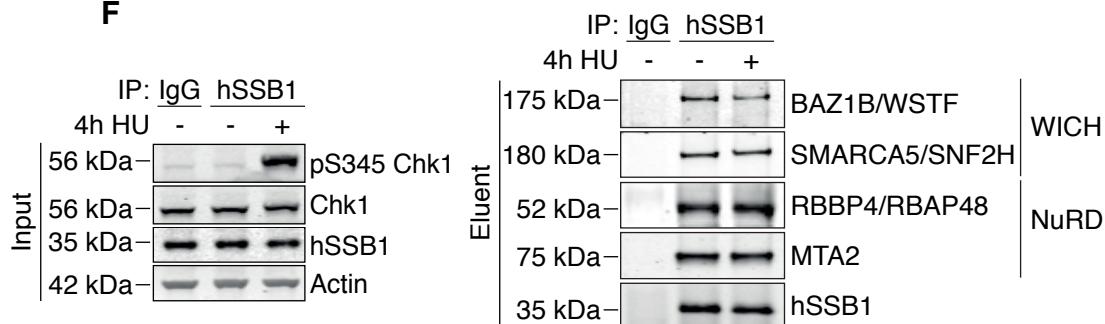


Figure 4.14 hSSB1 may associate with proteins involved in chromatin remodelling, RNA metabolism, DNA repair and numerous other pathways

(A) Subcellular fractionation of HeLa cells. HeLa cells were treated with 3 mM hydroxyurea (HU), or mock treated, and then harvested after 4 hours. Cells were incubated for 10 min at 4 °C in a buffer containing 10 mM KCl and passed through a 26-gauge needle 6 times to lyse cells. The sample was centrifuged and the pellet (containing nuclei) washed once and incubated for 30 min at 4 °C in a buffer containing 420 mM NaCl. The supernatant containing soluble nuclear proteins was then collected and the remaining precipitate incubated in the 420 mM NaCl buffer containing benzonase for 30 min at room temperature. The sample was again centrifuged and the supernatant (‘chromatin-bound’) collected. 10 μ g of the soluble

nuclear and chromatin-bound protein fractions were separated by PAGE and immunoblotted with antibodies against pS345 and total Chk1 (HU treatment positive control) nucleolin (soluble-nuclear marker) and H3 (chromatin marker).

(B) Immunoprecipitation of chromatin-bound hSSB1 500 µg of chromatin-bound protein was incubated overnight at 4 °C with protein G dynabeads bound to a hSSB1 antibody, or a sheep isotype control IgG. Beads were washed five times and protein eluted by heating to 90 °C in SDS loading buffer for 10 minutes. 10% of the eluent was separated by PAGE and stained overnight in colloidal coomassie brilliant blue G-250.

(C) SDS-PAGE separation of immunoprecipitated proteins for in-gel digestion. Upon confirmation of successful immunoprecipitation, the remaining eluent was resolved on a 10% acrylamide SDS-PAGE gel to a depth of 6 mM and stained overnight in colloidal coomassie brilliant blue G-250. The top, fainter section of the image represents the stacking gel.

(D) Proteins involved in numerous pathways were detected by mass spectrometry. The gel-embedded, coomassie blue-stained proteins in (C) were divided into eight 1 mM gel slices, digested with trypsin and extracted. Peptides were separated and detected using an Agilent HPLC CHIP QTOF 6530 system. The mass spectrum data was extracted and searched against the Swiss Prot Human database. Proteins for which corresponding peptides were identified, as well as the number of unique detected peptides, are given in appendix 1. Proteins were manually sorted based on their predominant known biological process as given by UniProt (www.uniprot.org). Proteins identified from either hSSB1:IP sample were pooled and are summarised as the number of unique proteins identified for each biological process.

(E) hSSB1 may associate with proteins composing numerous chromatin-remodelling complexes. From the proteins grouped in the ‘chromatin remodelling’ biological process in appendix 1 and (B), components of numerous chromatin-remodelling complexes were identified. Protein components of each identified

complex are listed in columns and those identified in the hSSB1:IP mass spectrometry shown in **bold** font.

(F) Co-immunoprecipitation of chromatin remodelling proteins with hSSB1.

HeLa cells were treated with 3 mM hydroxyurea (HU), or mock treated, and harvested after 4 hours. Whole cell lysates were prepared and 500 µg incubated for 2 hours at 4 °C with protein G dynabeads bound to a hSSB1 antibody, or a sheep isotype control IgG. Beads were washed five times and protein eluted by heating to 90 °C in SDS loading buffer for 10 minutes. Eluent was immunoblotted with antibodies against BAZ1B, SMARCA5, MTA2, RBBP4 and hSSB1 as indicated. 15 µg whole cell lysate (input) was immunoblotted with antibodies against hSSB1, pS345 and total Chk1 (HU positive control) and actin (loading control). The gel shown here are from an experiment performed concurrently with that in Figure 4.6 E.

10 proteins were detected in the IgG lane and included peptides belonging to three keratin sub-types, two IgG molecules, two histones (one peptide each), Annexin A2, GAPDH and a member of the POTE Ankyrin domain family. The small number of proteins detected in the IgG:IP sample suggests that those identified by hSSB1 immunoprecipitation were so specifically.

Only minor variation in the hSSB1-associating proteins was observed following hydroxyurea treatment. Regardless of this, it was interesting to note that the majority of detected proteins did seem to belong to one of a number of different groups when categorised by their known biological function (**Figure 4.14D**).

Surprisingly, of the proteins identified, only a relatively small number are known to have a direct role in DNA repair or replication. These included the minichromosome maintenance complex subunits 6 and 7 (MCM6 and MCM7) both of which form part of the helicase complex required for unwinding duplex DNA during replication (Bochman and Schwacha, 2009). In addition, numerous peptides were identified which may belong to DNA topoisomerase II alpha or beta. Both of these enzymes function to alter the superhelical state of DNA by cleaving and subsequently re-ligating DNA following helicase winding or unwinding of the DNA and are required

for DNA replication as well as for mRNA transcription (Wendorff et al., 2012). Consistent with the observation that hSSB1 S134 phosphorylation may be regulated by PPP-family phosphatases, the catalytic subunit of PP1 and the regulatory subunit of PP2 was also detected.

The largest group of proteins identified contained 77 ribosomal proteins, either belonging to the 40S or 60S subunit. In addition, 23 proteins involved in ribosome biosynthesis were also detected. As these proteins are not known to bind chromatin, it is likely they were instead identified due to the co-isolation of nucleoli as well as chromatin following the nuclear lysis step of the subcellular fractionation; proteins from these structures were most likely liberated during the subsequent incubation. Interestingly, nucleophosmin, one of the ribosome biogenesis proteins identified, has previously been identified by our group as a direct hSSB1-interacting protein. Although this has previously been considered as evidence that nucleophosmin may have a role in DNA repair, it is tempting to consider that the identification of numerous other ribosomal biogenesis proteins in this study may instead reflect a novel role for hSSB1 in this process. Alternatively, due to the high abundance of ribosomal components in the cell, these proteins are frequent contaminants of mass spectrometry datasets that have been generated from affinity-isolated samples (Mellacheruvu et al 2013). It therefore cannot be excluded that although these proteins were not identified in the IgG sample, their detection may be due to non-specific electrostatic interaction with hSSB1 or other proteins.

RNA metabolism proteins were also highly represented in the data sets, including a number of components of the cleavage and polyadenylation specificity factor complex (CPSF), as well as numerous other ancillary proteins involved in polyadenylation and 3'-end cleavage of mammalian pre-mRNAs (Murthy and Manley, 1995). A number of proteins known to promote pre-mRNA splicing were also detected and were represented by subunits and interacting partners of the U4/U6-U5 tri-snRNP complex, as well as other spliceosome factors. Numerous ATP-dependent RNA helicases were also detected, many of which were of unknown physiological function, although include subunits of the exon junction complex, which marks the position of exon-exon junctions in mature mRNA and promotes mRNA export and translation (Le Hir et al., 2001). Components of heterogeneous

nuclear ribonucleoprotein (hnRNP) complexes were also detected which provide similar pre-mRNA processing functions to those mentioned above (Carpenter et al., 2006).

Numerous proteins involved in chromatin remodelling and modification were also detected in the mass spectrometry data set and represented a number of known protein complexes (**Figure 4.14E**). These included the WICH complex components BAZ1B and SMARCA5, the two proteins for which the greatest number of peptides were detected in the hydroxyurea treated sample. Importantly, while the precise role of this complex remains unclear, both of these proteins have recently been found to associate directly with stalled replication forks (Sirbu et al., 2013). In addition to the WICH complex, peptides corresponding to each component of the NuRD remodelling complex were also observed, with MTA2, RBBP4 and β -actin amongst the highest 'hits' post-damage. The essential role of this complex for replication fork integrity has also been documented (Aranda et al., 2014; Errico et al., 2014; Sims and Wade, 2011). To further validate the association of hSSB1 with WICH and NuRD complex proteins, hSSB1 was immunoprecipitated from whole cell lysate of HeLa cells that had been treated with or without 3 mM hydroxyurea for 4 hours. Proteins were then eluted and immunoblotted with antibodies against BAZ1B, SMARCA5, MTA2 and RBBP4 (**Figure 4.14F**). Consistent with the mass spectrometry data, each of these proteins was specifically immunoprecipitated with hSSB1 both before and after hydroxyurea treatment. These data thereby support that hSSB1 may associated with these chromatin remodelling complexes in cells.

4.4 Discussion

Enzymatically active DNA-PK is a central component of the cellular response to replication fork inhibition (Lin et al., 2014). Indeed, cells depleted of endogenous DNA-PKcs, or expressing an enzymatically deficient kinase mutant, show reduced clonogenic survival when treated with hydroxyurea (Ying et al., 2015). With the notable exception of RPA32 (Liu et al., 2012), as well as auto-phosphorylation (Ying et al., 2015), few relevant DNA-PK substrates have however been identified in the response to replication stress. It was therefore interesting to observe that hSSB1 S134 phosphorylation is required for clonogenic survival of cells treated with the replication stress compounds hydroxyurea and aphidicolin (Figure 4.2) and establish that phosphorylation is primarily a result of DNA-PK activity (Figure 4.4 and 4.7). A decrease in basal and HU-induced hSSB1 S134 phosphorylation was also observed following inhibition, although not depletion, of the ATM and ATR kinases, potentially indicating a secondary role for these enzymes in hSSB1 S134 phosphorylation. Such overlap between the PI3K-like kinases is indeed not uncommon in the phosphorylation of DNA repair proteins and is exemplified by the HU-induced phosphorylation of numerous RPA32 residues by the overlapping activities of ATM, ATR and DNA-PK (Liu et al., 2012). Another example is the phosphorylation of Chk1 S317. Whilst this residue is primarily phosphorylated by the ATR kinase (Zhao and Piwnicka-Worms, 2001), ATM and DNA-PK have recently been implicated in a ‘back-up’ pathway in cells where ATR function is suppressed (Buisson et al., 2015). Although a similar scenario may explain the suppression of hSSB1 S134 phosphorylation observed following ATM and ATR inhibition, an alternative explanation may instead include cross talk between these enzymes and DNA-PK as has been suggested in numerous DNA repair pathways (Chen et al., 2007; Vidal-Eychenié et al., 2013; Yajima et al., 2006). Such an explanation may indeed be more likely than a direct role for ATM and ATR in the phosphorylation of hSSB1 S134, especially given the almost complete reduction in phosphorylation observed following DNA-PK inhibition or depletion (Figure 4.4).

While hSSB1 S134 is also phosphorylated by DNA-PK in undamaged cells, this may be maintained at steady-state levels by the opposing activities of PPP-family protein phosphatases. This family includes numerous members that are inhibited by okadaic

acid in cells, including PP2A, PP4, PP5, and PP6 (Swingle et al., 2007). The increase in hSSB1 phosphorylation observed following treatment of cells with okadaic acid (Figure 4.6) therefore suggests the potential involvement of one of these enzymes in the dephosphorylation of hSSB1. Indeed, each of these enzymes has previously been implicated in the regulation of DNA repair pathways (Lee and Chowdhury, 2011) and may represent plausible regulators of hSSB1. Although an additional increase in hSSB1 phosphorylation was observed when calyculin A was added to cells, a compound that additionally inhibits PP1, it is unclear whether the greater effect observed here with comparison to okadaic acid treatment is due to PP1 involvement. Indeed, calyculin A also shows increased potency towards PP5, another plausible candidate phosphatase of hSSB1, especially considering the involvement of this protein in the regulation of DNA-PK (Wechsler et al., 2004). It was however interesting to note the detection of PP1 and PP2A phosphatase peptides in the mass spectral analysis of hSSB1 interacting proteins (Figure 4.14; as well as the immunoprecipitation of PP2A-C with hSSB1 in Figure 4.6). Although this detection does not necessarily implicate an involvement of these phosphatases in hSSB1 dephosphorylation, a shared role may explain the okadaic acid-induced increase in S134 phosphorylation, as well as the greater effect of calyculin A addition. Further studies will however be required to dissect the individual roles of the PPP-family phosphatases in the regulation of hSSB1 phosphorylation and would most likely require the individual depletion of one or more of the subunits (numerous isozymes of which exist) of each of these phosphatases. Dominant-negative mutants of PP1 (Gallego et al., 2006), PP2A (Kins et al., 2001), PP4 (Zhou et al., 2002), PP5 (Chen et al., 1996) and PP6 (Kajihara et al., 2010) have also been described previously, the exploitation of which may represent another means of assessing the involvement of these phosphatases in hSSB1 dephosphorylation.

It may be useful to consider the reason why hSSB1 phosphorylation could increase following replication inhibition. DNA-PK is stimulated by the interaction with dsDNA that contains short ssDNA overhangs, such as may form at double-strand DNA breaks (Carter et al., 1990; Vidal-Eychenié et al., 2013). As double-strand breaks do occur following hydroxyurea treatment as a result of replication fork collapse (Cobb et al., 2005), the hydroxyurea-induced increase in hSSB1 S134

phosphorylation may therefore be explained by DNA-PK activation as a result of the accumulation of these lesions. Indeed, as replication fork collapse is unlikely to occur immediately after hydroxyurea-induced fork disruption, but instead progressively after a period of fork ‘stalling’, the gradual increase in the number of double-strand breaks may offer an explanation for the time-dependent increase in hSSB1 S134 phosphorylation observed for up to 20 hours post-hydroxyurea treatment (Figure 4.3). This is likely to be compounded by the increase in the number of cells entering S phase over this 20 hour period. The phosphorylation of hSSB1 S134 in response to double-strand DNA break formation is also supported by the increase in phosphorylation observed after the treatment of cells with aphidicolin or camptothecin, compounds which also cause replication fork collapse (Ozeri-Galai et al., 2008). This is especially true of camptothecin treatment, which unlike treatment with hydroxyurea and aphidicolin, induces the formation of double-strand DNA breaks without a lengthy period of fork stalling (Saleh-Gohari et al., 2005). Given that hSSB1 S134 may therefore be phosphorylated in the response to these lesions, it is also interesting to consider the pathway through which this occurs. Indeed, whilst double-strand DNA breaks caused by fork collapse have traditionally been thought to be repaired solely by homologous recombination (HR) (Arnaudeau et al., 2001; Lundin et al., 2002), this has been challenged by the implication of numerous non-homologous end-joining (NHEJ)-related proteins (e.g. DNA-PK, KU, Artmeis, DNA ligase IV) in the replication stress response (Allen et al., 2011). Nevertheless, it is unclear how NHEJ could function in the repair of collapsed forks, as this would produce a ‘one-ended double-strand break’, without providing a second dsDNA end NHEJ could utilise. Furthermore, whilst NHEJ could theoretically function in the re-joining of adjacent collapsed forks, this would result in the loss of genetic material. It therefore seems plausible that if hSSB1 is phosphorylated by DNA-PK at S134 as a result of fork collapse, this is more likely to occur as a result of DNA-PK activity during HR. In this pathway, DNA-PK likely functions through overlap and cross-talk with ATM (Shrivastav et al., 2009), potentially also explaining the involvement of this enzyme as discussed above.

If hSSB1 is indeed phosphorylated at S134 during the repair of collapsed replication forks by HR or NHEJ, it is curious to note that the exposure of HeLa cells to ionising radiation, which causes both direct and indirect double-strand DNA break formation

(Vignard et al., 2013), did not markedly increase the detection of S134 phosphorylation (Figure 4.5). Unlike double-strand DNA breaks that accumulate and persist in cells whilst they are treated with hydroxyurea, conditions under which homologous recombination cannot function, double strand breaks caused by ionising radiation can be freely repaired. Therefore, while hSSB1 S134 may indeed not be phosphorylated during the repair of ionising radiation-induced breaks, it is also possible that it is dynamically phosphorylated and dephosphorylated, such that an increase in phosphorylation was not detected at the time-points chosen. This may be consistent with the observation that, unlike transiently expressed WT 3x FLAG hSSB1, an S134A mutant was not able to rescue cells from the sensitivity to ionising radiation caused by the depletion of endogenous hSSB1.

In the above paragraphs it is suggested that hSSB1 S134 may be phosphorylated following replication fork collapse. Although hydroxyurea does cause the formation of such lesions, the accumulation of which has been detected within 2 - 6 hours of treatment, the vast majority of replication forks are likely to remain stable for greater than 12-18 hours, with many not collapsing for up to 48 hours (Petermann et al., 2010; Saintigny et al., 2001). In addition, whilst replication forks are progressively 'inactivated' following hydroxyurea treatment, many may restart following short disruptions (~ 80% of stalled forks may restart after 2 hours of HU treatment, compared to < 20% after 20 hours) (Petermann et al., 2010). As both hSSB1 and DNA-PK have been suggested to function in the stabilisation and restart of stalled replication forks (Bolderson et al., 2014; Ying et al., 2015), it is therefore also likely that hSSB1 may be phosphorylated during these processes, rather than, or in addition to, in the repair of double-strand DNA breaks caused by fork collapse. Such implications would however require further experimentation. Specifically, DNA fibre analysis could be employed to assess the ability of cells depleted of endogenous hSSB1 and transiently expressing WT or S134A hSSB1 to restart replication following a period of fork disruption. In addition, techniques such as pulse-field gel electrophoresis would allow the monitoring of double-strand DNA break formation in S134A hSSB1-expressing cells following replication inhibition.

In section 4.2.2, clonogenic survival assays were performed, where HeLa cells depleted of endogenous hSSB1 and transiently expressing WT or S134A 3x FLAG hSSB1 were treated with 3 mM hydroxyurea or 6 $\mu\text{g } \mu\text{L}^{-1}$ aphidicolin for 4, 8, 12, 16 or 20 hours. In these assays, cells that were depleted of endogenous hSSB1 were found to be hypersensitive to either drug, which was alleviated by the expression of WT, although not S134A, 3x FLAG hSSB1. Whilst a statistically significant difference in survival was observed between the two groups (siControl and sihSSB1 + WT hSSB1 vs sihSSB1 and sihSSB1 + S134A hSSB1) when treated for 4, 8, 12, or 16 hours, it was interesting to note that similar survival was observed for those cells treated for 20 hours, regardless of hSSB1 status. Although by no means as conclusive as the experiments suggested in the previous paragraph, these observations may provide insight as to how hSSB1 functions following replication disruption. The cell death observed following hydroxyurea treatment is likely to occur through an apoptotic response (Gui et al., 1997), most probably due to the formation of double-strand DNA breaks. Indeed, in a recent publication (Couch et al., 2013), rapid hydroxyurea-induced cell death was observed following inhibition of the ATR kinase, conditions under which double-strand DNA breaks rapidly formed. Whilst the reported hydroxyurea sensitivity observed following ATR inhibition is much greater than observed here for cells depleted of hSSB1, or expressing S134A hSSB1, it is tempting to consider this may occur for a similar reason. Here, S134 phosphorylation may be required for the prevention of double-strand DNA break formation, resulting in reduced cell survival of S134A hSSB1-expressing cells at early time-points. By 20 hours of hydroxyurea treatment, the presence or absence of hSSB1, as well as phosphorylation status, may however be irrelevant due to the increase in fork collapse that is likely to occur in control cells by this time, independently of hSSB1 function (Petermann et al., 2010).

Although DNA-PK is thought to be predominantly activated by binding to ssDNA at double-strand DNA breaks ends, its activity may also be stimulated by binding ssDNA gaps within dsDNA substrates, as well as unbound DNA within structured ssDNA (Vidal-Eychenié et al., 2013). The binding to such substrates within disrupted replication forks is therefore likely to explain the activation of DNA-PK at sites of stalled replication forks, as well as provide a rationale for subsequent hSSB1 S134 phosphorylation. Additionally, the further regulation of hSSB1 phosphorylation

by PPP-family phosphatases may however suggest that, aside from increased DNA-PK activity, hSSB1 S134 phosphorylation may also be stimulated by the suppression of these enzymes. This could, for instance, involve a dissociation of hSSB1 and the PPP-family protein phosphatase, or inactivation of the phosphatase, either as a result of signalling activation or the stimulation of phosphatase inhibitors proteins.

Given the requirement for activated DNA-PK in the phosphorylation of hSSB1 S134, it might be worthwhile to consider that hSSB1 is evidently also phosphorylated in undamaged cells. Indeed, as basal hSSB1 phosphorylation seems to involve DNA-PK function, this scenario suggests that a pool of activated DNA-PK must also exist in non-exogenously damaged cells. This is supported by the similar increase in DNA-PK auto-phosphorylation observed following okadaic acid treatment of cells (Douglas et al., 2002), or depletion of PP5 (Wechsler et al., 2004). It is worth noting that basal phosphorylation of RPA32 S33 was also observed in cells, which increased at a similar rate to hSSB1 S134 phosphorylation following hydroxyurea treatment (Figure 4.3). RPA32 S33 phosphorylation in undamaged cells has previously been found to occur in the late S- and G2 phases of the cell cycle and has been attributed to the persistence of endogenously stalled replication forks (Vassin et al., 2009). A similar scenario may thereby also explain the detection of S134 phosphorylated hSSB1 in undamaged cells. As these experiments were conducted at 21% O₂ and therefore cells were likely to experience significant stress (Jagannathan et al., 2016), the formation of numerous oxidative lesions may also offer an explanation for basal hSSB1 S134 phosphorylation. This could include through the formation of oxidative lesions such as thymine glycol, the most common oxidation product of thymine, which has been found to efficiently block replicative polymerases (Aller et al., 2007). Although such lesions are likely to be rapidly bypassed by translesion synthesis (Kirouac and Ling, 2009; Kusumoto et al., 2002), transient replication fork stalling may represent a stimuli for hSSB1 phosphorylation. In addition, unrepaired oxidative lesions may eventually generate more disruptive species, such as DNA breaks, that could also disrupt replication forks to a substantial degree (Maynard et al., 2009). In addition, hSSB1 has recently been demonstrated to function directly in the repair of oxidised guanine residues (Paquet et al., 2015), a repair process during which hSSB1 could theoretically also be phosphorylated. Further, DNA-PK has been suggested to

also function in the BER pathway (through an as yet unclear mechanism) (Chen et al., 2012), which may explain the DNA-PK-dependency of basal S134 phosphorylation. As detection of S134 phosphorylation predominantly required transient overexpression of hSSB1, it cannot however be ruled out that the high degree of basal hSSB1 phosphorylation observed was due the equilibrium between S134 phosphorylation and dephosphorylation being somewhat altered from endogenous ratios. The deregulation of hSSB1 signalling as a result of transient overexpression may indeed be an appealing explanation, especially considering the hyper-ubiquitination of 3x FLAG hSSB1 described in the previous chapter. Unlike the non-specificity described for poly-ubiquitination, phosphorylation of S134 is however unlikely to be purely an artefact of over-expression, especially considering the detection of endogenous phosphorylated hSSB1 in Figure 4.3, the cell survival defect of S134A-expressing cells in Figure 4.2, as well as the specific nature of DNA-PK and PPP-family phosphatase regulation of this event in Figures 4.4 and 4.6.

A potentially informative finding regarding the regulation of hSSB1 by PPP-family protein phosphatases comes from the observation that while hSSB1 phosphorylation is enhanced following okadaic acid or calyculin A treatment, this is further enhanced by the prior treatment of cells with hydroxyurea (Figure 4.6). While hydroxyurea-induced phosphorylation is not an unexpected finding, it was surprising to note that the relative ratio of phosphorylation in phosphatase inhibitor-treated cells +/- hydroxyurea treatment was similar to that observed for hydroxyurea-treated control cells. This is interesting, as it would be expected that if hSSB1 is stably phosphorylated following hydroxyurea treatment that the same overall increase in hSSB1 phosphorylation would be observed regardless of phosphatase inhibition. Indeed, a similar relative increase in hydroxyurea-induced S134 phosphorylation following phosphatase inhibition instead suggests that a large amount of the hSSB1 that is phosphorylated in response to hydroxyurea treatment is subsequently dephosphorylated, even in the presence of hydroxyurea. These findings may suggest that hSSB1 is both phosphorylated and dephosphorylated in the response to replication inhibition.

Despite the likelihood of S134 phosphorylated hSSB1 functioning at sites of replication fork inhibition, the mutation of hSSB1 DNA or PAR-binding residues did

not markedly alter S134 phosphorylation (Figure 4.8). One possible explanation for this could be that while hSSB1 does at some stage bind to DNA or PAR at disrupted replication forks, this interaction may not be required for its retention at chromatin. Indeed, as hSSB1 is likely to interact directly with numerous other proteins at these sites, it may still be ‘held’ in position to be phosphorylated by these interacting partners, irrespective of substrate binding. A similar situation has previously been demonstrated at sites of double-strand DNA breaks. In these experiments, the PAR-binding mutant WD55AA, which is also likely to be deficient for DNA-binding (our collaborator Dr Roland Gamsjaeger recently calculated a 10-fold difference in K_d for ssDNA-binding of W55A hSSB1 compared to WT), was still recruited to DNA damage sites induced by laser micro-irradiation, albeit at a slower rate (Zhang et al., 2014). Here, PAR-independent chromatin localisation was suggested to require the hSSB1 binding-partner INTS3, a protein the authors found localised to DNA damage sites independently of hSSB1. As INTS3-binding may also be required for hSSB1 function following replication fork inhibition (Figure 4.9), an interaction with this protein may at least partially explain how hSSB1 could be localised to disrupted replication forks and subsequently phosphorylated at S134. Indeed, whilst disruption of INTS3-binding by mutation of residue F98 did not prevent S134 phosphorylation of otherwise WT hSSB1, it is tempting to consider whether disruption of this interaction may prevent phosphorylation of DNA-binding deficient hSSB1. The interaction with numerous other proteins is however of course likely to be important for hSSB1 function following fork disruption, these proteins of which may also mediate chromatin-localisation of DNA-binding deficient hSSB1. It is also possible that non-chromatin bound hSSB1 may be phosphorylated at S134, potentially as a means of regulating soluble pools of the protein. This however would require the activation of DNA-PK independently of DNA-binding, a means of which are not readily apparent.

The interaction of hSSB1 with fork substrates was an unexpected observation (Figure 4.13) as it has previously been shown that hSSB1 is unable to effectively bind dsDNA duplexes (Paquet et al., 2015). Interestingly, a similar observation was recently reported for the annealing helicase SMARCAL1, a protein that also has minimal affinity for dsDNA, although which readily binds model replication forks

lacking exposed ssDNA (Betous et al., 2012). In this work, the authors suggested that SMARCAL1 might capture small amounts of ssDNA that are exposed due to ‘breathing’ of the dsDNA regions adjacent to the fork junction. It is tempting to consider that hSSB1 may bind this structure through a similar means. Indeed, these results are somewhat reminiscent of the finding that hSSB1 is able to bind a dsDNA substrate containing a single 8-oxoguanine modification, potentially due to a similar localised de-stabilisation of the DNA duplex (Paquet et al., 2015). Although the localisation of hSSB1 with disrupted replication forks has previously been demonstrated (Bolderson et al., 2014), the mechanistic consequence of fork-junction binding remains unclear. The decreased affinity of the hSSB1 S134E phosphomimetic for a model fork substrate does however suggest that phosphorylation may act to suppress this function of hSSB1 following replication inhibition. A possible explanation for this may be that while hSSB1 is involved in the initial recruitment and initiation of the replicative stress response (Bolderson et al., 2014), the persistence of hSSB1 at the fork junction may be detrimental to the subsequent restart of the fork. Given that hSSB1 S134 may be both phosphorylated and de-phosphorylated in the response to replication inhibition, it is also tempting to consider that this modification may mediate a dynamic mode of fork junction binding. The increased sensitivity of cells expressing S134A hSSB1 to hydroxyurea and aphidicolin treatment may therefore be explained not only by a need for hSSB1 to bind replication forks junctions, which S134A hSSB1 would be expected to be capable of, but also to be subsequently removed. S134A hSSB1 may therefore be ‘disruptive’ to the replicative stress response, rather than just functionally deficient. In this way, the similar hydroxyurea and aphidicolin sensitivity observed for hSSB1-depleted cells and those transiently expressing S134A hSSB1 may be due to different reasons. Confirmation of this mechanistic role for hSSB1 is however lacking and will require further investigation.

Whilst the above hypothesis may be plausible, it however cannot be discounted that S134 phosphorylation may alter hSSB1 function through a separate means in cells. For instance, while interaction of the S134 phosphorylated peptide with phospho-domain binding proteins was not detected in Section 4.2.10, it cannot be excluded that phosphorylation of S134 may still mediate such an interaction within the context of the full-length protein. Phosphorylation could also mediate an interaction with a

phospho-binding protein that was not included on the microarray, or with another type of protein that does not directly bind the phosphorylated residue, although which may bind S134 phosphorylated hSSB1 due to physical changes in the protein structure. Similarly, whilst S134E hSSB1 did not appear to be less readily degraded than WT hSSB1 (Figure 4.12), it remains possible that glutamic acid is unable to accurately mimic phosphorylation of S134 in cells, such that phosphorylation may indeed have an effect on hSSB1 half-life. A role for S134 phosphorylation in DNA binding may however have informative implications in a phylogenetic context. As demonstrated in Figure 4.11, the presence of serine at residue 134 in mammals is largely restricted to simiiform primates, whilst proline is found at residue 134 in the majority of other species. Although phosphorylation of S134 may alter hSSB1 through electrostatic means, it may be interesting to consider that its affect may instead be exerted through a physical means, similar to what may be expected for a proline residue. It is therefore tempting to speculate that while a proline at residue 134 may similarly prevent binding to fork junctions, the adaptation of a serine at residue 134 in primates may have allowed this type of interaction, which could be regulated by DNA-PK-mediated phosphorylation. The functional analysis of an S134P hSSB1 mutant in future work may therefore be of value and could be tested using similar EMSA assays. Alternatively, as many species other than humans contain a putative phosphorylation site at residue 149, the phosphorylation of S134 may have a compensatory role that is similar to phosphorylation of residue 149. Further investigation will therefore be required to understand these interspecies differences.

Although S134E hSSB1 binds fork substrates with reduced affinity, ssDNA is bound similarly to the WT protein. It is therefore possible that while phosphorylated hSSB1 is displaced from the fork junction, it may still associate with the comparably large quantity of ssDNA exposed by replication inhibition (Sogo et al., 2002). Confirmation of these hypotheses will however require further investigation in cells. Indeed, due to poor specificity of the pS134 hSSB1 antibody in immunofluorescence assays, it has been difficult to assess the localisation of phosphorylated hSSB1 to replication forks using this approach. An assessment of phosphorylated hSSB1 binding to replication forks may therefore be more achievable in future experiments

through employment of a replication fork pull-down assay, such as via the ‘isolation of proteins on nascent DNA’ (iPOND) method. In this assay, cells are pulse labelled with the nucleoside analogue Edu, which in later steps is conjugated to biotin in a click-chemistry reaction. Replication fork DNA, as well as associating proteins, are then isolated by streptavidin purification (Sirbu et al., 2013; Sirbu et al., 2012). Such an approach may therefore allow the specific detection of phosphorylated hSSB1 with replication fork DNA.

Given that hSSB1 seems able to bind replication fork junctions, it is also tempting to consider that hSSB1 might bind other related DNA substrates, such as Holliday junctions. SMARCAL1, for instance, has been found to bind both of these substrates, as well as fork junctions, despite not binding dsDNA (Betous et al., 2012). Each of these substrates is further likely to form during the processing of stalled or collapsed replication forks. Holliday junctions for instance form as an intermediate during helicase-driven fork regression (Machwe et al., 2007; McGlynn et al., 2001), as well as during repair by homologous recombination (Liu and West, 2004). A role for S134 phosphorylation in mediating the interaction of hSSB1 with each of these structures may therefore offer an explanation for the role of this modification in the repair of disrupted replication forks. In addition, the mediation of Holliday junction-binding during homologous recombination-repair may explain the inability of S134A hSSB1 to rescue cells of the hypersensitivity to ionising radiation exposure caused by hSSB1 depletion.

An unexpected observation from this study was the identification of numerous chromatin-remodelling protein complexes by mass spectrometry performed on proteins co-immunoprecipitating with chromatin-bound hSSB1 (Figure 4.14). As each of these complexes have been suggested to function in replication fork integrity and DNA repair, a potential role for hSSB1 with these proteins is an attractive proposition. BAZ1B (WSTF) and SNF2H (SMARCA5) (proteins for which the highest number of peptides were identified), components of the WICH complex, have for instance previously been found to localise with progressing and stalled replication forks, mediated by a direct interaction of BAZ1B with PCNA (Poot et al., 2004; Sirbu et al., 2013). During replication, the WICH complex migrates with PCNA, and by virtue of the SNF2H SWI/SNF2 ATPase domain, is able to disrupt

DNA-histone interactions and maintain an ‘open’ chromatin structure. The depletion of WSTF in cells therefore results in an increase in histone H3 K9 trimethylation and K27 dimethylation, epigenetics marks that have been associated with repressive chromatin structures (Poot et al., 2004). As histone epigenetic changes are also observed following the disruption of other chromatin remodelling complexes, the assessment of these marks in cells may therefore represent one means of indirectly assessing a role for hSSB1 in these processes. Such assessment could for instance be performed either by immunoblotting or immunofluorescence techniques using hSSB1-depleted cells and antibodies against specific histone modifications. In addition, use of the iPond technique to monitor specific modifications at replication forks has previously been described (Sirbu et al., 2013). This technique would also allow for an elegant assessment of such roles for hSSB1 at these sites.

Whilst it is tempting to speculate that the immunoprecipitation of numerous chromatin-remodelling proteins with hSSB1 may suggest a novel pathway through which the hSSB1 functions in the repair of DNA damage, it remains equally plausible that these observations may instead reflect an involvement of hSSB1 in other chromatin remodelling-dependent pathways. This may include processes such as mRNA transcriptional regulation, where chromatin remodelling has an essential role. Indeed, the majority of the chromatin-remodelling proteins immunoprecipitated with hSSB1 are considered transcription factors. A role for hSSB1 in such transactions is supported by a recent publications indicating that hSSB1 (and hSSB2) may function in complex with INTS3 to promote transcription termination at numerous gene targets (Skaar et al., 2015). These data nevertheless provide new information regarding hSSB1 protein associations in cells.

Chapter 5: General Discussion and Concluding Remarks

Evidence provided both here and elsewhere suggest the involvement of hSSB1 in the cellular response to numerous DNA-damaging chemotherapeutics, including exposure to the drugs, etoposide (Kar et al., 2015), hydroxyurea and camptothecin (Bolderson et al., 2014). In addition, hSSB1-depleted cells are hypersensitive to ionising radiation exposure (Richard et al., 2008). It is therefore conceivable that the inactivation or depletion of hSSB1 in combination with such treatments may be of benefit for the treatment of various cancer types. The feasibility of targeting hSSB1 directly in cancer is however unclear, especially considering this protein is neither an enzyme nor a membrane-bound receptor and so means of targeting hSSB1 by classical small molecule-based approaches are less apparent. Indeed, the targeting of protein-protein, or protein-substrate interactions with small-molecules is likely to be applicable only to the disruption of very narrow interaction surfaces (Makley and Gestwicki, 2013), unlike, for instance, the DNA binding groove of the hSSB1 OB-fold. Targeting hSSB1 at the protein level may therefore require the identification of new, high-affinity hSSB1 protein interaction sites, which may represent drugable targets. The effective disruption of the p53-MDM2 E3 ubiquitin ligase interaction by the small molecular inhibitor Nutlin-3 (Poyurovsky et al., 2010; Vassilev et al., 2004), for example, may suggest precedence for the inhibition of proteins through the disrupted binding of modifying enzymes or other major binding partners. The further characterisation of hSSB1 function and regulation may therefore provide a means of targeting hSSB1 in cancer. In addition, the further identification of enzymes involved in the post-translational regulation of hSSB1 may suggest novel anti-cancer targets that may be targetable by classical active site inhibition. For instance, a recent publication found that poly-ubiquitination of hSSB1 occurs predominantly through SCF complexes containing the F-box protein, FBXL5 (Chen et al., 2014). The novel association of this protein with hSSB1 thereby lead the authors to also explore and confirm a role for FBXL5 in the response to the DNA damaging drug etoposide. These data may thereby demonstrate the strength of studying hSSB1 for the identification of new DNA-repair proteins that may be effective anti-cancer targets.

The major aim of this PhD study was to further characterise the post-translational regulation of hSSB1. Data pertaining to this aim have been presented in the preceding two chapters. In the first of these (Chapter 3), the regulation of hSSB1 by poly-ubiquitination was further explored and included the mutation of each hSSB1 lysine residue to arginine, both individually and in combination. The disruption of hSSB1 ubiquitination however required the complete removal of lysine residues from the protein, suggesting that each hSSB1 lysine residue could potentially be modified. Indeed, examination of the hSSB1 crystal structure indicated that each lysine residue side chain may protrude away from the protein and is likely available for modification. The robust poly-ubiquitination of over-expressed hSSB1 may therefore suggest a cellular requirement to degrade excess hSSB1, potentially due to a detrimental effect of de-regulated hSSB1 to the cell. For instance, it seems probable that not all ssDNA-transactions might require hSSB1 and that extensive over-expression may indeed be disruptive to these processes. Furthermore, even in pathways in which hSSB1 is involved, high-level over-expression may prevent proper hSSB1 regulation, which potentially also may be disruptive. Future work into the characterisation of hSSB1 function may therefore benefit from the use of cell lines that express hSSB1 mutants at close-to endogenous levels. Although the generation of cell lines that stably express hSSB1 mutants has been relatively unsuccessful in our group using standard antibiotic selection methods, potentially due to a similar pressure to prevent excess hSSB1 accumulating in the cells as discussed above, it is noted that other groups have had success in generating hSSB1 over-expressing cell lines using a doxycycline-inducible expression system (Ren et al., 2014; Wu et al., 2015). The further employment of this technique may therefore be of benefit for hSSB1 functional assessment in future studies.

In the latter section of chapter 3, mass spectrometry was employed and numerous putative phosphorylation sites detected. One of these, the phosphorylation of serine residue 134 (S134), became the central topic of the second data chapter (Chapter 4). S134 is a component of an SQ motif, numerous of which are phosphorylated in other DNA repair proteins by the P13K-like kinases, ATM, ATR and DNA-PK (Traven and Heierhorst, 2005). Indeed, S134 phosphorylation of hSSB1 was predominantly mediated by DNA-PK and was enhanced following replication fork disruption.

Regulation of hSSB1 by PPP-family protein phosphatases was also observed, allowing for the dynamic mediation of hSSB1 phosphorylation. Here, phosphorylation of S134 is likely required for the proper function of hSSB1, as an S134A hSSB1 mutant was unable to rescue cells from the hydroxyurea and aphidicolin sensitivity observed in hSSB1-depleted cells. Consistent with the above suggestion that further evaluation of hSSB1 post-translational modifications may allow for the identification of anti-cancer targets, the inhibition of DNA-PK has been extensively shown to sensitise cancer cells to DNA damaging chemotherapeutics and radiotherapy (Elliott et al., 2011; Guo et al., 2011; Leahy et al., 2004; Willmore et al., 2004; Zhao et al., 2006). This is also true of the PPP-family protein phosphatases, numerous of which regulate members of the DNA repair pathways and are required for cell survival in response to ionising radiation exposure and replication fork disruption (Ali et al., 2004; Chowdhury et al., 2005; Chowdhury et al., 2008; Keogh et al., 2006; Shen et al., 2011). The targeting of DNA-PK or PPP-family protein phosphatases in cancer treatment has however been problematic due to numerous specificity, stability and pharmacokinetic issues with available inhibitors (Davidson et al., 2013; Swingle et al., 2007), issues that will have to be overcome prior to these enzymes representing viable anti-cancer targets.

As well as providing further insight into the specific regulation of hSSB1 by ubiquitination and S134 phosphorylation, the data provided in this thesis suggests that hSSB1 is likely to be more extensively modified than is currently documented. This is particularly evident based on the detection of numerous putative phosphorylation sites by mass spectrometry, which are likely to be of importance for hSSB1 function. Indeed, whilst a projection of how this may occur is unfeasible, several of these putative phosphorylation sites are particularly intriguing. Residues T53, T76 and T83, for instance, are components of the DNA-binding OB-fold and located in close proximity to the important DNA-binding aromatic residues, W55, Y74-Y78 and Y85A, respectively. It is therefore tempting to speculate that phosphorylation of these sites may affect DNA binding in some way. It was also interesting to observe the putative phosphorylation of S182, as not only does this residue constitute the remaining uncharacterised hSSB1 SQ motif, unlike S134, it is highly conserved amongst animal species. A notable modification not detected by mass spectrometry was the phosphorylation of threonine residue 117. As the

importance of this modification has however previously be suggested in the response to ionising radiation exposure (Richard et al., 2008), detection of this phosphorylation event may therefore require such stimuli. These considerations may also indicate that other additional hSSB1 phosphorylation may also be detected in the response to various forms of DNA damage. This is also likely to be the case with hSSB1 acetylation. Indeed, whilst acetylation of K94 has previously been demonstrated, mutation of this residue was not able to completely prevent the detection of acetylated hSSB1 (Wu et al., 2015). While not yet validated, the acetylation of K15 and K203 has for instance previously been detected by mass spectrometry (Hornbeck et al., 2015). The validation of these modifications may therefore be of value for the further understanding of hSSB1 function.

An interesting finding from the characterisation of hSSB1 S134 phosphorylation was the high level of phosphorylation and dephosphorylation observed in undamaged cells. Whilst the purpose for this dynamic regulation is unclear, these finding do suggest that a pool of phosphorylated hSSB1 exists constitutively in cells. These findings are indeed similar to reports of basal hSSB1 acetylation, which is apparently suppressed by the Sirt4 and HDAC10 deacetylases prior to ionising radiation exposure (Wu et al., 2015). One explanation for the basal phosphorylation and acetylation of hSSB1 may be that by maintaining pools of differentially modified hSSB1, the cell is able to keep hSSB1 in a ‘primed’ state to rapidly respond to various types of DNA lesions. Such an arrangement is indeed consistent with the previous description of hSSB1 as an early responder to DNA damage (Bolderson et al., 2014; Paquet et al., 2015; Richard et al., 2011b). A similar ‘priming’ approach has also been suggested for Chk1, where ATR-mediated phosphorylation is maintained under a suppressive state by PP1 during un-perturbed cell cycles to allow for rapid checkpoint activation in response to replication fork stalling (Leung-Pineda et al., 2006). In future work it may therefore be of interest to determine whether other hSSB1 modifications are similarly suppressed, allowing for the formation of various types of ‘primed’ hSSB1.

In contrast to hSSB1, the post-translational regulation of hSSB2 has remained largely unexplored and to date no modifications have been reported. Further, in the one study to address hSSB2 regulation, it was noted that while acetylation of hSSB1 was readily detected, no such modifications of hSSB2 were found (Wu et al., 2015). The authors therefore concluded the regulation of hSSB2 might be less complex than hSSB1. Consistent with this suggestion, in section 4.2.11 it was noted that unlike hSSB1, hSSB2 does not contain SQ/TQ sequences, the classical phosphorylation motifs of ATM, ATR and DNA-PKcs (Traven and Heierhorst, 2005). It is however unclear whether the lack of information regarding hSSB2 regulation truly does represent that this protein is not modified, or merely that hSSB2 modifications are yet to be thoroughly explored. For example, as hSSB2 has also been suggested to function during double-strand DNA break repair by homologous recombination, most likely by interacting with INTS3 to the mutual exclusion of hSSB1 (Li et al., 2009b), it seems reasonable that hSSB2 could be phosphorylated by one of the numerous DNA repair kinases. A thorough investigation into hSSB2 regulation may thereby also be warranted and may provide further insight into the function of this protein, as well its interplay with hSSB1.

The data presented in this thesis also provide mechanistic insight into hSSB1 function. The finding that hSSB1 is able to bind fork substrates lacking ssDNA *in vitro*, for instance, may point to a role for hSSB1 in processing such substrates in the restart of stalled replication forks in cells. Further, these findings may indicate that hSSB1 can also bind other related substrates, such as Holliday junctions, which equally may direct the dissection of hSSB1 function in replication fork restart and other DNA repair pathways. These and prior findings regarding hSSB1-binding to non-ssDNA substrates (junctions, 8-oxoG (Paquet et al., 2015), poly (ADP)-ribose (Zhang et al., 2014)) may also assist in delineating the role of hSSB1 from other OB-fold containing proteins, such as RPA. Indeed, whilst hSSB1 may be able to compensate for RPA depletion in some circumstances (Kar et al., 2015), it has remained unclear how hSSB1 may compete with the higher affinity, more stable ssDNA binding of RPA in normal cells. The role of hSSB1 in binding a distinct set of substrates that are not bound by RPA may therefore suggest that hSSB1 and RPA function primarily by complementary, non-overlapping means, rather than, or in addition to, by competing for the same substrate. The modulation of hSSB1 substrate

binding by post-translational regulation may also provide a tantalising means through which hSSB1 function is modulated. Such a model is reflected not only by the finding that S134E hSSB1 binds fork junctions with reduced affinity, but also by other recent work from our group (Paquet *et al.* 2016) regarding the binding of hSSB1 to 8-oxo-G lesions. Here, 8-oxo-G-binding was found to require the prior oxidation of hSSB1 and the formation of higher-order oligomers. It therefore seems possible that hSSB1 binding to different substrates may be regulated by distinct post-translational regulation depending on the type of DNA damage that has occurred and the repair pathway that has been activated.

The mass spectrometry data summarised in section 4.2.14 suggests that while hSSB1 has predominantly been thought of in a DNA repair context, it is likely to have roles in many other cellular processes. In particular, the identification of numerous proteins with roles in RNA metabolism and transcriptional transactions may suggest these as important areas of hSSB1 function. These findings were somewhat pre-empted by reports that hSSB1 and hSSB2 may function in the termination of transcription of a wide range of genes (Skaar *et al.*, 2015). Here, both proteins seemingly function as components of the integrator complex, presumably via an interaction with INTS3 (Zhang *et al.*, 2013). In addition, this interaction mediated an association of hSSB1 with RNA polymerase II (Baillat *et al.*, 2005). Consistent with these data, the mass spectrometry data presented in this thesis identified the integrator complex subunits 1, 3, 5 and 6, and as well six subunits of RNA polymerase II, following hSSB1 immunoprecipitation. Components of the cleavage and polyadenylation specificity factor (CPSF) were also identified by mass spectrometry, consistent with the observation of the integrator complex being required for replication-dependent histone mRNA processing (Skaar *et al.*, 2015), one of many functions performed by the CPSF. A role in transcriptional termination may also explain the observed association of hSSB1 with numerous chromatin remodelling complexes, enzymes which are also essential for this process (Alén *et al.*, 2002; Morillon *et al.*, 2003). Aside from a role in transcriptional termination, the identification of numerous proteins with roles earlier and later to transcriptional termination (e.g. transcriptional activation and repression, mRNA splicing, processing and transport) may suggest additional functions in RNA processing in

which hSSB1 may be involved. The further understanding of hSSB1 protein function is therefore likely to benefit not only from the continued study of its role in DNA repair, but also by an investigation into its function in other biological processes.

In summary, the data presented in this thesis provide novel insight into the regulation of hSSB1 by post-translational modifications. This includes data pertaining to the poly-ubiquitination of hSSB1 lysine residues, as well the phosphorylation of S134 in the response to replication inhibition. Numerous other putative sites of modification are also identified, the characterisation of which is likely to be beneficial for the further understanding of hSSB1 function. In addition, findings regarding the mechanistic function of hSSB1 are also provided, which will likely assist in precisely delineating the placement of hSSB1 in DNA repair. The identification of novel protein associations may also suggest new roles for hSSB1 in genome stability maintenance, as well as in other cellular pathways.

References

- Ababou, M., Dutertre, S., Lécluse, Y., Onclercq, R., Chatton, B. and Amor-Guélet, M. (2000). ATM-dependent phosphorylation and accumulation of endogenous BLM protein in response to ionizing radiation. *Oncogene* 19, 5955–5963.
- Acevedo, J., Yan and Michael, W. M. (2016). Direct Binding to RPA-Coated ssDNA Allows Recruitment of the ATR Activator TopBP1 to Sites of DNA Damage. *J. Biol. Chem.* jbc.M116.729194.
- Akan, P., Alexeyenko, A., Costea, P. I., Hedberg, L., Solnestam, B. W., Lundin, S., Hällman, J., Lundberg, E., Uhlen, M. and Lundeberg, J. (2012). Comprehensive analysis of the genome transcriptome and proteome landscapes of three tumor cell lines. *Genome Med* 4, 86.
- Alén, C., Kent, N. A., Jones, H. S., O'Sullivan, J., Aranda, A. and Proudfoot, N. J. (2002). A role for chromatin remodeling in transcriptional termination by RNA polymerase II. *Mol. Cell* 10, 1441–1452.
- Ali, A., Zhang, J., Bao, S., Liu, I., Otterness, D., Dean, N. M., Abraham, R. T. and Wang, X.-F. (2004). Requirement of protein phosphatase 5 in DNA-damage-induced ATM activation. *Genes Dev.* 18, 249–254.
- Allen, C., Ashley, A. K., Hromas, R. and Nickoloff, J. A. (2011). More forks on the road to replication stress recovery. *J Mol Cell Biol* 3, 4–12.
- Aller, P., Rould, M. A., Hogg, M., Wallace, S. S. and Doublé, S. (2007). A structural rationale for stalling of a replicative DNA polymerase at the most common oxidative thymine lesion, thymine glycol. *Proc. Natl. Acad. Sci. U. S. A.* 104, 814–818.
- Anantha, R. W., Vassin, V. M. and Borowiec, J. A. (2007). Sequential and Synergistic Modification of Human RPA Stimulates Chromosomal DNA Repair. *J. Biol. Chem.* 282, 35910–35923.
- Andreeva, A. V. and Kutuzov, M. A. (2001). PPP Family of Protein Ser/Thr Phosphatases: Two Distinct Branches? *Mol Biol Evol* 18, 448–452.

- Arai, T., Kelly, V. P., Minowa, O., Noda, T. and Nishimura, S. (2002). High accumulation of oxidative DNA damage, 8-hydroxyguanine, in Mmh/Ogg1 deficient mice by chronic oxidative stress. *Carcinogenesis* 23, 2005–2010.
- Aranda, S., Rutishauser, D. and Ernfors, P. (2014). Identification of a large protein network involved in epigenetic transmission in replicating DNA of embryonic stem cells. *Nucleic Acids Res.* 42, 6972–6986.
- Arnaudeau, C., Lundin, C. and Helleday, T. (2001). DNA double-strand breaks associated with replication forks are predominantly repaired by homologous recombination involving an exchange mechanism in mammalian cells. *J. Mol. Biol.* 307, 1235–1245.
- Ashley, A. K., Shrivastav, M., Nie, J., Amerin, C., Troksa, K., Glanzer, J. G., Liu, S., Opiyo, S. O., Dimitrova, D. D., Le, P., et al. (2014). DNA-PK phosphorylation of RPA32 Ser4/Ser8 regulates replication stress checkpoint activation, fork restart, homologous recombination and mitotic catastrophe. *DNA Repair* 21, 131–139.
- Bachrati, C. Z. and Hickson, I. D. (2009). Dissolution of double Holliday junctions by the concerted action of BLM and topoisomerase IIIalpha. *Methods Mol. Biol.* 582, 91–102.
- Baillat, D., Hakimi, M. A., Naar, A. M., Shilatifard, A., Cooch, N. and Shiekhattar, R. (2005). Integrator, a multiprotein mediator of small nuclear RNA processing, associates with the C-terminal repeat of RNA polymerase II. *Cell* 123, 265–276.
- Bakkenist, C. J. and Kastan, M. B. (2003). DNA damage activates ATM through intermolecular autophosphorylation and dimer dissociation. *Nature* 421, 499–506.
- Ball, H. L., Myers, J. S. and Cortez, D. (2005). ATRIP binding to replication protein A-single-stranded DNA promotes ATR-ATRIP localization but is dispensable for Chk1 phosphorylation. *Mol. Biol. Cell* 16, 2372–2381.
- Banerjee, A., Yang, W., Karplus, M. and Verdine, G. L. (2005). Structure of a repair enzyme interrogating undamaged DNA elucidates recognition of damaged DNA.

Nature 434, 612–618.

- Bansbach, C. E., Betous, R., Lovejoy, C. A., Glick, G. G. and Cortez, D. (2009). The annealing helicase SMARCAL1 maintains genome integrity at stalled replication forks. *Genes Dev.* 23, 2405–2414.
- Bech-Otschir, D., Helfrich, A., Enenkel, C., Consiglieri, G., Seeger, M., Holzhütter, H.-G., Dahlmann, B. and Kloetzel, P.-M. (2009). Polyubiquitin substrates allosterically activate their own degradation by the 26S proteasome. *Nat. Struct. Mol. Biol.* 16, 219–225.
- Beers, E. P. and Callis, J. (1993). Utility of polyhistidine-tagged ubiquitin in the purification of ubiquitin-protein conjugates and as an affinity ligand for the purification of ubiquitin-specific hydrolases. *J. Biol. Chem.* 268, 21645–21649.
- Bekker-Jensen, S. and Mailand, N. (2010). Assembly and function of DNA double-strand break repair foci in mammalian cells. *DNA Repair (Amst.)* 9, 1219–1228.
- Bell, S. P. and Dutta, A. (2002). DNA replication in eukaryotic cells. *Annu. Rev. Biochem.* 71, 333–374.
- Bermudez, V. P., Lindsey-Boltz, L. A., Cesare, A. J., Maniwa, Y., Griffith, J. D., Hurwitz, J. and Sancar, A. (2003). Loading of the human 9-1-1 checkpoint complex onto DNA by the checkpoint clamp loader hRad17-replication factor C complex in vitro. *Proc. Natl. Acad. Sci. U. S. A.* 100, 1633–1638.
- Berndsen, C. E. and Wolberger, C. (2014). New insights into ubiquitin E3 ligase mechanism. *Nat. Struct. Mol. Biol.* 21, 301–307.
- Bertani, G. (1951). Studies on lysogenesis. I. The mode of phage liberation by lysogenic *Escherichia coli*. *J. Bacteriol.* 62, 293–300.
- Betous, R., Mason, A. C., Rambo, R. P., Bansbach, C. E., Badu-Nkansah, A., Sirbu, B. M., Eichman, B. F. and Cortez, D. (2012). SMARCAL1 catalyzes fork regression and Holliday junction migration to maintain genome stability during DNA replication. *Genes Dev.* 26, 151–162.
- Bignell, G., Micklem, G., Stratton, M. R., Ashworth, A. and Wooster, R. (1997). The

- BRC repeats are conserved in mammalian BRCA2 proteins. *Hum. Mol. Genet.* 6, 53–58.
- Bjorås, M., Luna, L., Johnsen, B., Hoff, E., Haug, T., Rognes, T. and Seeberg, E. (1997). Opposite base-dependent reactions of a human base excision repair enzyme on DNA containing 7,8-dihydro-8-oxoguanine and abasic sites. *EMBO J.* 16, 6314–6322.
- Blainey, P. C., Luo, G., Kou, S. C., Mangel, W. F., Verdine, G. L., Bagchi, B. and Xie, X. S. (2009). Nonspecifically bound proteins spin while diffusing along DNA. *Nat. Struct. Mol. Biol.* 16, 1224–1229.
- Blanco, M. G., Matos, J., Rass, U., Ip, S. C. Y. and West, S. C. (2010). Functional overlap between the structure-specific nucleases Yen1 and Mus81-Mms4 for DNA-damage repair in *S. cerevisiae*. *DNA Repair (Amst.)* 9, 394–402.
- Block, W. D., Yu, Y. and Lees-Miller, S. P. (2004). Phosphatidyl inositol 3-kinase-like serine/threonine protein kinases (PIKKs) are required for DNA damage-induced phosphorylation of the 32 kDa subunit of replication protein A at threonine 21. *Nucleic Acids Res.* 32, 997–1005.
- Bochman, M. L. and Schwacha, A. (2009). The Mcm complex: unwinding the mechanism of a replicative helicase. *Microbiol. Mol. Biol. Rev.* 73, 652–683.
- Bohgaki, M., Bohgaki, T., Ghamrasni, El, S., Srikumar, T., Maire, G., Panier, S., Fradet-Turcotte, A., Stewart, G. S., Raught, B., Hakem, A., et al. (2013). RNF168 ubiquitylates 53BP1 and controls its response to DNA double-strand breaks. *Proc. Natl. Acad. Sci. U. S. A.* 110, 20982–20987.
- Bolderson, E., Petermann, E., Croft, L., Suraweera, A., Pandita, R. K., Pandita, T. K., Helleday, T., Khanna, K. K. and Richard, D. J. (2014). Human single-stranded DNA binding protein 1 (hSSB1/NAPB2) is required for the stability and repair of stalled replication forks. *Nucleic Acids Res.*
- Bolderson, E., Tomimatsu, N., Richard, Boucher, D., Kumar, R., Pandita, T. K., Burma, S. and Khanna, K. K. (2010). Phosphorylation of Exo1 modulates homologous recombination repair of DNA double-strand breaks. *Nucleic Acids*

Res. 38, 1821–1831.

- Bork, P., Blomberg, N. and Nilges, M. (1996). Internal repeats in the BRCA2 protein sequence. *Nat. Genet.* 13, 22–23.
- Branzei, D. and Foiani, M. (2005). The DNA damage response during DNA replication. *Curr. Opin. Cell Biol.* 17, 568–575.
- Breitschopf, K., Bengal, E., Ziv, T., Admon, A. and Ciechanover, A. (1998). A novel site for ubiquitination: the N-terminal residue, and not internal lysines of MyoD, is essential for conjugation and degradation of the protein. *The EMBO Journal* 17, 5964–5973.
- Brooks, S. C., Adhikary, S., Rubinson, E. H. and Eichman, B. F. (2013). Recent advances in the structural mechanisms of DNA glycosylases. *Biochim. Biophys. Acta* 1834, 247–271.
- Bruner, S. D., Norman, D. P. and Verdine, G. L. (2000). Structural basis for recognition and repair of the endogenous mutagen 8-oxoguanine in DNA. *Nature* 403, 859–866.
- Buisson, R., Boisvert, J. L., Benes, C. H. and Zou, L. (2015). Distinct but Concerted Roles of ATR, DNA-PK, and Chk1 in Countering Replication Stress during S Phase. *Mol. Cell* 59, 1011–1024.
- Bujalowski, W., Overman, L. B. and Lohman, T. M. (1988). Binding mode transitions of Escherichia coli single strand binding protein-single-stranded DNA complexes. Cation, anion, pH, and binding density effects. *J. Biol. Chem.* 263, 4629–4640.
- Burgers, P. M. (1988). Mammalian cyclin/PCNA (DNA polymerase delta auxiliary protein) stimulates processive DNA synthesis by yeast DNA polymerase III. *Nucleic Acids Res.* 16, 6297–6307.
- Burgers, P. M. (2009). Polymerase dynamics at the eukaryotic DNA replication fork. *J. Biol. Chem.* 284, 4041–4045.
- Burma, S., Chen, B. P., Murphy, M., Kurimasa, A. and Chen, D. J. (2001). ATM

- phosphorylates histone H2AX in response to DNA double-strand breaks. *J. Biol. Chem.* 276, 42462–42467.
- Burrows and Elledge, S. J. (2008). How ATR turns on: TopBP1 goes on ATRIP with ATR. *Genes Dev.* 22, 1416–1421.
- Burrows and Muller, J. G. (1998). Oxidative nucleobase modifications leading to strand scission. *Chemical reviews.*
- Byun, T. S., Pacek, M., Yee, M.-C., Walter, J. C. and Cimprich, K. A. (2005). Functional uncoupling of MCM helicase and DNA polymerase activities activates the ATR-dependent checkpoint. *Genes Dev.* 19, 1040–1052.
- Canman, C. E., Lim, D. S., Cimprich, K. A., Taya, Y., Tamai, K., Sakaguchi, K., Appella, E., Kastan, M. B. and Siliciano, J. D. (1998). Activation of the ATM kinase by ionizing radiation and phosphorylation of p53. *Science* 281, 1677–1679.
- Carpenter, B., MacKay, C., Alnabulsi, A., MacKay, M., Telfer, C., Melvin, W. T. and Murray, G. I. (2006). The roles of heterogeneous nuclear ribonucleoproteins in tumour development and progression. *Biochim. Biophys. Acta* 1765, 85–100.
- Carreira, A. and Kowalczykowski, S. C. (2011). Two classes of BRC repeats in BRCA2 promote RAD51 nucleoprotein filament function by distinct mechanisms. *Proc. Natl. Acad. Sci. U. S. A.* 108, 10448–10453.
- Carreira, A., Hilario, J., Amitani, I., Baskin, R. J., Shivji, M. K., Venkitaraman, A. R. and Kowalczykowski, S. C. (2009). The BRC repeats of BRCA2 modulate the DNA-binding selectivity of RAD51. *Cell* 136, 1032–1043.
- Carson, C. T., Schwartz, R. A., Stracker, T. H., Lilley, C. E., Lee, D. V. and Weitzman, M. D. (2003). The Mre11 complex is required for ATM activation and the G2/M checkpoint. *EMBO J.* 22, 6610–6620.
- Carter, T., Vancurová, I., Sun, I., Lou, W. and DeLeon, S. (1990). A DNA-activated protein kinase from HeLa cell nuclei. *Mol. Cell. Biol.* 10, 6460–6471.

- Casas-Finet, J. R., Khamis, M. I., Maki, A. H. and Chase, J. W. (1987a). Tryptophan 54 and phenylalanine 60 are involved synergistically in the binding of *E. coli* SSB protein to single-stranded polynucleotides. *FEBS Lett.* 220, 347–352.
- Casas-Finet, J. R., Khamis, M. I., Maki, A. H., Ruvolo, P. P. and Chase, J. W. (1987b). Optically detected magnetic resonance of tryptophan residues in *Escherichia coli* ssb gene product and *E. coli* plasmid-encoded single-stranded DNA-binding proteins and their complexes with poly(deoxythymidylic) acid. *J. Biol. Chem.* 262, 8574–8583.
- Cejka, P., Cannavo, E., Polaczek, P., Masuda-Sasa, T., Pokharel, S., Campbell, J. L. and Kowalczykowski, S. C. (2010). DNA end resection by Dna2-Sgs1-RPA and its stimulation by Top3-Rmi1 and Mre11-Rad50-Xrs2. *Nature* 467, 112–116.
- Chan, Y. W. and West, S. (2015). GEN1 promotes Holliday junction resolution by a coordinated nick and counter-nick mechanism. *Nucleic Acids Res.* 43, 10882–10892.
- Chapman, J. R. and Jackson, S. P. (2008). Phospho-dependent interactions between NBS1 and MDC1 mediate chromatin retention of the MRN complex at sites of DNA damage. *EMBO Rep.* 9, 795–801.
- Chapman, J. R., Barral, P., Vannier, J.-B., Borel, V., Steger, M., Tomas-Loba, A., Sartori, A. A., Adams, I. R., Batista, F. D. and Boulton, S. J. (2013). RIF1 Is Essential for 53BP1-Dependent Nonhomologous End Joining and Suppression of DNA Double-Strand Break Resection. *Mol. Cell* 49, 858–871.
- Chen, B. P. C., Li, M. and Asaithamby, A. (2012). New insights into the roles of ATM and DNA-PKcs in the cellular response to oxidative stress. *Cancer Lett.* 327, 103–110.
- Chen, B. P. C., Uematsu, N., Kobayashi, J., Lerenthal, Y., Krempler, A., Yajima, H., Löbrich, M., Shiloh, Y. and Chen, D. J. (2007). Ataxia telangiectasia mutated (ATM) is essential for DNA-PKcs phosphorylations at the Thr-2609 cluster upon DNA double strand break. *J. Biol. Chem.* 282, 6582–6587.
- Chen, H., Lisby, M. and Symington, L. S. (2013a). RPA coordinates DNA end

- resection and prevents formation of DNA hairpins. *Mol. Cell* 50, 589–600.
- Chen, M. S., Silverstein, A. M., Pratt, W. B. and Chinkers, M. (1996). The tetratricopeptide repeat domain of protein phosphatase 5 mediates binding to glucocorticoid receptor heterocomplexes and acts as a dominant negative mutant. *J. Biol. Chem.* 271, 32315–32320.
- Chen, X., Paudyal, S. C., Chin, R.-I. and You, Z. (2013b). PCNA promotes processive DNA end resection by Exo1. *Nucleic Acids Res.* 41, 9325–9338.
- Chen, Y., Xu, R., Chen, J., Li, X. and He, Q. (2013c). Cleavage of bleomycin hydrolase by caspase-3 during apoptosis. *Oncol. Rep.* 30, 939–944.
- Chen, Z.-W., Liu, B., Tang, N.-W., Xu, Y.-H., Ye, X.-Y., Li, Z.-M., Niu, X.-M., Shen, S.-P., Lu, S. and Xu, L. (2014). FBXL5-mediated degradation of single-stranded DNA-binding protein hSSB1 controls DNA damage response. *Nucleic Acids Res.*
- Cheng, K. C., Cahill, D. S., Kasai, H., Nishimura, S. and Loeb, L. A. (1992). 8-Hydroxyguanine, an abundant form of oxidative DNA damage, causes G----T and A----C substitutions. *J. Biol. Chem.* 267, 166–172.
- Chini, C. C. S. (2003). Human Claspin Is Required for Replication Checkpoint Control. *J. Biol. Chem.* 278, 30057–30062.
- Chini, C. C. S., Wood, J. and Chen, J. (2006). Chk1 is required to maintain claspin stability. *Oncogene* 25, 4165–4171.
- Cho, H. J., Oh, Y. J., Han, S. H., Chung, H. J., Kim, C. H., Lee, N. S., Kim, W.-J., Choi, J.-M. and Kim, H. (2013). Cdk1 protein-mediated phosphorylation of receptor-associated protein 80 (RAP80) serine 677 modulates DNA damage-induced G2/M checkpoint and cell survival. *J. Biol. Chem.* 288, 3768–3776.
- Choi, Harada, J. J., Goldberg, R. B. and Fischer, R. L. (2004). An invariant aspartic acid in the DNA glycosylase domain of DEMETER is necessary for transcriptional activation of the imprinted MEDEA gene. *Proc. Natl. Acad. Sci. U. S. A.* 101, 7481–7486.

- Choi, J.-H., Lindsey-Boltz, L. A., Kemp, M., Mason, A. C., Wold, M. S. and Sancar, A. (2010). Reconstitution of RPA-covered single-stranded DNA-activated ATR-Chk1 signaling. *Proc. Natl. Acad. Sci. U. S. A.* 107, 13660–13665.
- Chou, D. M. and Elledge, S. J. (2006). Tipin and Timeless form a mutually protective complex required for genotoxic stress resistance and checkpoint function. *Proc. Natl. Acad. Sci. U. S. A.* 103, 18143–18147.
- Chowdhury, D., Keogh, M.-C., Ishii, H., Peterson, C. L., Buratowski, S. and Lieberman, J. (2005). gamma-H2AX dephosphorylation by protein phosphatase 2A facilitates DNA double-strand break repair. *Mol. Cell* 20, 801–809.
- Chowdhury, D., Xu, X., Zhong, X., Ahmed, F., Zhong, J., Liao, J., Dykxhoorn, D. M., Weinstock, D. M., Pfeifer, G. P. and Lieberman, J. (2008). A PP4-phosphatase complex dephosphorylates gamma-H2AX generated during DNA replication. *Mol. Cell* 31, 33–46.
- Ciccia, A., Bredemeyer, A. L., Sowa, M. E., Terret, M. E., Jallepalli, P. V., Harper, J. W. and Elledge, S. J. (2009). The SIOD disorder protein SMARCAL1 is an RPA-interacting protein involved in replication fork restart. *Genes Dev.* 23, 2415–2425.
- Cobb, J. A., Schleker, T., Rojas, V., Bjergbaek, L., Tercero, J. A. and Gasser, S. M. (2005). Replisome instability, fork collapse, and gross chromosomal rearrangements arise synergistically from Mec1 kinase and RecQ helicase mutations. *Genes Dev.* 19, 3055–3069.
- Conery, A. R. and Harlow, E. (2010). High-throughput screens in diploid cells identify factors that contribute to the acquisition of chromosomal instability. *Proceedings of the National Academy of Sciences* 107, 15455–15460.
- Constantinou, A., Tarsounas, M., Karow, J. K., Brosh, R. M., Bohr, V. A., Hickson, I. D. and West, S. C. (2000). Werner's syndrome protein (WRN) migrates Holliday junctions and co-localizes with RPA upon replication arrest. *EMBO Rep.* 1, 80–84.
- Couch, F. B., Bansbach, C. E., Driscoll, R., Luzwick, J. W., Glick, G. G., Bétous, R.,

- Carroll, C. M., Jung, S. Y., Qin, J., Cimprich, K. A., et al. (2013). ATR phosphorylates SMARCAL1 to prevent replication fork collapse. *Genes Dev.* 27, 1610–1623.
- Curth, U., Greipel, J., Urbanke, C. and Maass, G. (1993). Multiple binding modes of the single-stranded DNA binding protein from *Escherichia coli* as detected by tryptophan fluorescence and site-directed mutagenesis. *Biochemistry (Mosc.)* 32, 2585–2591.
- David, S. S., O'Shea, V. L. and Kundu, S. (2007). Base-excision repair of oxidative DNA damage. *Nature* 447, 941–950.
- Davidson, D., Amrein, L., Panasci, L. and Aloyz, R. (2013). Small Molecules, Inhibitors of DNA-PK, Targeting DNA Repair, and Beyond. *Front Pharmacol* 4, 5.
- Davies, S. L., North, P. S. and Hickson, I. D. (2007). Role for BLM in replication-fork restart and suppression of origin firing after replicative stress. *Nat. Struct. Mol. Biol.* 14, 677–679.
- De Bont, R. and van Larebeke, N. (2004). Endogenous DNA damage in humans: a review of quantitative data. *Mutagenesis* 19, 169–185.
- de Jager, M., van Noort, J., van Gent, D. C., Dekker, C., Kanaar, R. and Wyman, C. (2001). Human Rad50/Mre11 is a flexible complex that can tether DNA ends. *Mol. Cell* 8, 1129–1135.
- Deans, A. J. and West, S. C. (2011). DNA interstrand crosslink repair and cancer. *Nat. Rev. Cancer* 11, 467–480.
- Delacroix, S., Wagner, J. M., Kobayashi, M., Yamamoto, K. and Karnitz, L. M. (2007). The Rad9-Hus1-Rad1 (9-1-1) clamp activates checkpoint signaling via TopBP1. *Genes Dev.* 21, 1472–1477.
- Dephoure, N., Gould, K. L., Gygi, S. P. and Kellogg, D. R. (2013). Mapping and analysis of phosphorylation sites: a quick guide for cell biologists. *Mol. Biol. Cell* 24, 535–542.

- Di Virgilio, M., Callen, E., Yamane, A., Zhang, W., Jankovic, M., Gitlin, A. D., Feldhahn, N., Resch, W., Oliveira, T. Y., Chait, B. T., et al. (2013). Rif1 Prevents Resection of DNA Breaks and Promotes Immunoglobulin Class Switching. *Science*.
- Dianov, G. L. (1999). Role of DNA Polymerase beta in the Excision Step of Long Patch Mammalian Base Excision Repair. *J. Biol. Chem.* 274, 13741–13743.
- Dianov, G. L. and Hübscher, U. (2013). Mammalian base excision repair: the forgotten archangel. *Nucleic Acids Res.* 41, 3483–3490.
- Difilippantonio, M. J., Zhu, J., Chen, H. T., Meffre, E., Nussenzweig, M. C., Max, E. E., Ried, T. and Nussenzweig, A. (2000). DNA repair protein Ku80 suppresses chromosomal aberrations and malignant transformation. *Nature* 404, 510–514.
- Dodson, M. L., Michaels, M. L. and Lloyd, R. S. (1994). Unified catalytic mechanism for DNA glycosylases. *J. Biol. Chem.* 269, 32709–32712.
- Dornreiter, I., Erdile, L. F., Gilbert, I. U., Winkler, von, D., Kelly, T. J. and Fanning, E. (1992). Interaction of DNA polymerase alpha-primase with cellular replication protein A and SV40 T antigen. *EMBO J.* 11, 769–776.
- Douglas, P., Sapkota, G. P., Morrice, N., Yu, Y., Goodarzi, A. A., Merkle, D., Meek, K., Alessi, D. R. and Lees-Miller, S. P. (2002). Identification of in vitro and in vivo phosphorylation sites in the catalytic subunit of the DNA-dependent protein kinase. *Biochem. J.* 368, 243–251.
- Duursma, A. M., Driscoll, R., Elias, J. E. and Cimprich, K. A. (2013). A role for the MRN complex in ATR activation via TOPBP1 recruitment. *Mol. Cell* 50, 116–122.
- Egglar, A. L., Inman, R. B. and Cox, M. M. (2002). The Rad51-dependent pairing of long DNA substrates is stabilized by replication protein A. *J. Biol. Chem.* 277, 39280–39288.
- Ehrlund, A., Anthonisen, E. H., Gustafsson, N., Venteclef, N., Robertson Remen, K., Damdimopoulos, A. E., Galeeva, A., Pelto-Huikko, M., Lalli, E., Steffensen, K.

- R., et al. (2009). E3 ubiquitin ligase RNF31 cooperates with DAX-1 in transcriptional repression of steroidogenesis. *Mol. Cell. Biol.* 29, 2230–2242.
- Eisele, F. and Wolf, D. H. (2008). Degradation of misfolded protein in the cytoplasm is mediated by the ubiquitin ligase Ubr1. *FEBS Lett.* 582, 4143–4146.
- Elliott, S. L., Crawford, C., Mulligan, E., Summerfield, G., Newton, P., Wallis, J., Mainou-Fowler, T., Evans, P., Bedwell, C., Durkacz, B. W., et al. (2011). Mitoxantrone in combination with an inhibitor of DNA-dependent protein kinase: a potential therapy for high risk B-cell chronic lymphocytic leukaemia. *Br. J. Haematol.* 152, 61–71.
- Ellison, V. and Stillman, B. (2003). Biochemical characterization of DNA damage checkpoint complexes: clamp loader and clamp complexes with specificity for 5' recessed DNA. *PLoS Biol.* 1, E33.
- Errico, A. and Costanzo, V. (2012). Mechanisms of replication fork protection: a safeguard for genome stability. *Crit. Rev. Biochem. Mol. Biol.* 47, 222–235.
- Errico, A., Aze, A. and Costanzo, V. (2014). Mta2 promotes Tipin-dependent maintenance of replication fork integrity. *Cell Cycle* 13, 2120–2128.
- Escribano-Díaz, C., Orthwein, A., Fradet-Turcotte, A., Xing, M., Young, J. T. F., Tkac, J., Cook, M. A., Rosebrock, A. P., Munro, M., Canny, M. D., et al. (2013). A Cell Cycle-Dependent Regulatory Circuit Composed of 53BP1-RIF1 and BRCA1-CtIP Controls DNA Repair Pathway Choice. *Mol. Cell* 49, 872–883.
- Espejo, A., Côté, J., Bednarek, A., Richard, S. and Bedford, M. T. (2002). A protein-domain microarray identifies novel protein-protein interactions. *Biochem. J.* 367, 697–702.
- Fajerman, I., Schwartz, A. L. and Ciechanover, A. (2004). Degradation of the Id2 developmental regulator: targeting via N-terminal ubiquitination. *Biochem. Biophys. Res. Commun.* 314, 505–512.
- Fanning, E., Klimovich, V. and Nager, A. R. (2006). A dynamic model for replication protein A (RPA) function in DNA processing pathways. *Nucleic*

Acids Res. 34, 4126–4137.

- Farber-Katz, S. E., Dippold, H. C., Buschman, M. D., Peterman, M. C., Xing, M., Noakes, C. J., Tat, J., Ng, M. M., Rahajeng, J., Cowan, D. M., et al. (2014). DNA damage triggers Golgi dispersal via DNA-PK and GOLPH3. *Cell* 156, 413–427.
- Favre, B., Turowski, P. and Hemmings, B. A. (1997). Differential inhibition and posttranslational modification of protein phosphatase 1 and 2A in MCF7 cells treated with calyculin-A, okadaic acid, and tautomycin. *J. Biol. Chem.* 272, 13856–13863.
- Feldhahn, N., Ferretti, E., Robbiani, D. F., Callen, E., Deroubaix, S., Selleri, L., Nussenzweig, A., Nussenzweig, M. C., (2012). The *hSSB1* orthologue *Obfc2b* is essential for skeletogenesis but dispensable for the DNA damage response *in vivo*. *EMBO J.* 31 (20), 4045-4056.
- Feng, J., Wakeman, T., Yong, S., Wu, X., Kornbluth, S. and Wang, X. F. (2009). Protein phosphatase 2A-dependent dephosphorylation of replication protein A is required for the repair of DNA breaks induced by replication stress. *Mol. Cell. Biol.* 29, 5696–5709.
- Feng, L., Wang and Chen, J. (2010). The Lys63-specific deubiquitinating enzyme BRCC36 is regulated by two scaffold proteins localizing in different subcellular compartments. *J. Biol. Chem.* 285, 30982–30988.
- Fiedler, K. L. and Cotter, R. J. (2013). Using glycylation, a chemical derivatization technique, for the quantitation of ubiquitinated proteins. *Anal. Chem.* 85, 5827–5834.
- Finley, D. (2009). Recognition and processing of ubiquitin-protein conjugates by the proteasome. *Annu. Rev. Biochem.* 78, 477–513.
- Fradet-Turcotte, A., Canny, M. D., Escribano-Díaz, C., Orthwein, A., Leung, C. C. Y., Huang, H., Landry, M.-C., Kitevski-LeBlanc, J., Noordermeer, S. M., Sicheri, F., et al. (2013). 53BP1 is a reader of the DNA-damage-induced H2A Lys 15 ubiquitin mark. *Nature* 499, 50–54.

- Friedberg, E. C. (2005). Suffering in silence: the tolerance of DNA damage. *Nat. Rev. Mol. Cell Biol.* 6, 943–953.
- Friedman, J. I. and Stivers, J. T. (2010). Detection of damaged DNA bases by DNA glycosylase enzymes. *Biochemistry (Mosc.)* 49, 4957–4967.
- Friedman, J. I., Majumdar, A. and Stivers, J. T. (2009). Nontarget DNA binding shapes the dynamic landscape for enzymatic recognition of DNA damage. *Nucleic Acids Res.* 37, 3493–3500.
- Fromme, J. C., Bruner, S. D., Yang, W., Karplus, M. and Verdine, G. L. (2003). Product-assisted catalysis in base-excision DNA repair. *Nat. Struct. Biol.* 10, 204–211.
- Frosina, G., Fortini, P., Rossi, O., Carrozzino, F., Raspaglio, G., Cox, L. S., Lane, D. P., Abbondandolo, A. and Dogliotti, E. (1996). Two pathways for base excision repair in mammalian cells. *J. Biol. Chem.* 271, 9573–9578.
- Fujisawa, H., Nakajima, N. I., Sunada, S., Lee, Y., Hirakawa, H., Yajima, H., Fujimori, A., Uesaka, M. and Okayasu, R. (2015). VE-821, an ATR inhibitor, causes radiosensitization in human tumor cells irradiated with high LET radiation. *Radiat Oncol* 10, 175.
- Galkin, V. E., Esashi, F., Yu, X., Yang, S., West, S. C. and Egelman, E. H. (2005). BRCA2 BRC motifs bind RAD51-DNA filaments. *Proc. Natl. Acad. Sci. U. S. A.* 102, 8537–8542.
- Gallego, M., Kang, H. and Virshup, D. M. (2006). Protein phosphatase 1 regulates the stability of the circadian protein PER2. *Biochem. J.* 399, 169–175.
- Gamsjaeger, R., Kariawasam, R., Touma, C., Kwan, A. H., White, M. F. and Cubeddu, L. (2013). Backbone and side-chain ¹H, ¹³C and ¹⁵N resonance assignments of the OB domain of the single stranded DNA binding protein from *Sulfolobus solfataricus* and chemical shift mapping of the DNA-binding interface. *Biomol NMR Assign* 1–4.
- Garcia, V., Phelps, S. E., Gray, S. and Neale, M. J. (2011). Bidirectional resection of

- DNA double-strand breaks by Mre11 and Exo1. *Nature* 479, 241–244.
- Gatei, M., Scott, S. P., Filippovitch, I., Soronika, N., Lavin, M. F., Weber, B. and Khanna, K. K. (2000). Role for ATM in DNA damage-induced phosphorylation of BRCA1. *Cancer Res.* 60, 3299–3304.
- Gatti, M., Pinato, S., Maspero, E., Soffientini, P., Polo, S. and Penengo, L. (2012). A novel ubiquitin mark at the N-terminal tail of histone H2As targeted by RNF168 ubiquitin ligase. *Cell Cycle* 11, 2538–2544.
- Gautam, D. and Bridge, E. (2013). The kinase activity of ataxia-telangiectasia mutated interferes with adenovirus E4 mutant DNA replication. *J. Virol.* 87, 8687–8696.
- German, P., Szaniszló, P., Hajas, G., Radak, Z., Bacsí, A., Hazra, T. K., Hegde, M. L., Ba, X. and Boldogh, I. (2013). Activation of cellular signaling by 8-oxoguanine DNA glycosylase-1-initiated DNA base excision repair. *DNA Repair (Amst.)* 12, 856–863.
- Goldberg, A. L. (2012). Development of proteasome inhibitors as research tools and cancer drugs. *J. Cell Biol.* 199, 583–588.
- Goodarzi, A. A., Jonnalagadda, J. C., Douglas, P., Young, D., Ye, R., Moorhead, G. B. G., Lees-Miller, S. P. and Khanna, K. K. (2004). Autophosphorylation of ataxia-telangiectasia mutated is regulated by protein phosphatase 2A. *EMBO J.* 23, 4451–4461.
- Gotter, A. L., Suppa, C. and Emanuel, B. S. (2007). Mammalian TIMELESS and Tipin are evolutionarily conserved replication fork-associated factors. *J. Mol. Biol.* 366, 36–52.
- Gravel, S., Chapman, J. R., Magill, C. and Jackson, S. P. (2008). DNA helicases Sgs1 and BLM promote DNA double-strand break resection. *Genes Dev.* 22, 2767–2772.
- Gu, P., Deng, W., Lei, M. and Chang, S. (2013). Single strand DNA binding proteins 1 and 2 protect newly replicated telomeres. *Cell Res.* 23, 705–719.

- Gui, C. Y., Jiang, C., Xie, H. Y. and Qian, R. L. (1997). The apoptosis of HEL cells induced by hydroxyurea. *Cell Res.* 7, 91–97.
- Guo, Deshpande, R. and Paull, T. T. (2010a). ATM activation in the presence of oxidative stress. *Cell Cycle* 9, 4805–4811.
- Guo, Kozlov, S., Lavin, M. F., Person, M. D. and Paull, T. T. (2010b). ATM Activation by Oxidative Stress. *Science* 330, 517–521.
- Guo, L., Liu, X., Jiang, Y., Nishikawa, K. and Plunkett, W. (2011). DNA-dependent protein kinase and ataxia telangiectasia mutated (ATM) promote cell survival in response to NK314, a topoisomerase II α inhibitor. *Mol. Pharmacol.* 80, 321–327.
- Hanada, K., Budzowska, M., Davies, S. L., van Drunen, E., Onizawa, H., Beverloo, H. B., Maas, A., Essers, J., Hickson, I. D. and Kanaar, R. (2007). The structure-specific endonuclease Mus81 contributes to replication restart by generating double-strand DNA breaks. *Nat. Struct. Mol. Biol.* 14, 1096–1104.
- Hanahan, D., Jessee, J. and Bloom, F. R. (1991). Plasmid transformation of *Escherichia coli* and other bacteria. *Methods Enzymol.* 204, 63–113.
- Heck, J. W., Cheung, S. K. and Hampton, R. Y. (2010). Cytoplasmic protein quality control degradation mediated by parallel actions of the E3 ubiquitin ligases Ubr1 and San1. *Proceedings of the National Academy of Sciences* 107, 1106–1111.
- Hill, J. W., Hazra, T. K., Izumi, T. and Mitra, S. (2001). Stimulation of human 8-oxoguanine-DNA glycosylase by AP-endonuclease: potential coordination of the initial steps in base excision repair. *Nucleic Acids Res.* 29, 430–438.
- Ho, C. K., Mazón, G., Lam, A. F. and Symington, L. S. (2010). Mus81 and Yen1 promote reciprocal exchange during mitotic recombination to maintain genome integrity in budding yeast. *Mol. Cell* 40, 988–1000.
- Honkanen, R. E. and Golden, T. (2002). Regulators of Serine / Threonine Protein Phosphatases at the Dawn of a Clinical Era? *Current medicinal chemistry* 9, 2055–2075.

- Hopfner, K. P., Karcher, A., Craig, L., Woo, T. T., Carney, J. P. and Tainer, J. A. (2001). Structural biochemistry and interaction architecture of the DNA double-strand break repair Mre11 nuclease and Rad50-ATPase. *Cell* 105, 473–485.
- Hopfner, K.-P., Craig, L., Moncalian, G., Zinkel, R. A., Usui, T., Owen, B. A. L., Karcher, A., Henderson, B., Bodmer, J.-L., McMurray, C. T., et al. (2002). The Rad50 zinc-hook is a structure joining Mre11 complexes in DNA recombination and repair. *Nature* 418, 562–566.
- Hornbeck, P. V., Kornhauser, J. M., Tkachev, S., Zhang, B., Skrzypek, E., Murray, B., Latham, V. and Sullivan, M. (2012). PhosphoSitePlus: a comprehensive resource for investigating the structure and function of experimentally determined post-translational modifications in man and mouse. *Nucleic Acids Res.* 40, D261–70.
- Hornbeck, P. V., Zhang, B., Murray, B., Kornhauser, J. M., Latham, V. and Skrzypek, E. (2015). PhosphoSitePlus, 2014: mutations, PTMs and recalibrations. *Nucleic Acids Res.* 43, D512–20.
- Hsu, G. W., Ober, M., Carell, T. and Beese, L. S. (2004). Error-prone replication of oxidatively damaged DNA by a high-fidelity DNA polymerase. *Nature* 431, 217–221.
- Huang, J., Gong, Z., Ghosal, G. and Chen, J. (2009). SOSS complexes participate in the maintenance of genomic stability. *Mol. Cell* 35, 384–393.
- Huff, J. P., Grant, B. J., Penning, C. A. and Sullivan, K. F. (1990). Optimization of routine transformation of *Escherichia coli* with plasmid DNA. *BioTechniques* 9, 570–2– 574– 576–7.
- Husnjak, K., Elsasser, S., Zhang, N., Chen, X., Randles, L., Shi, Y., Hofmann, K., Walters, K. J., Finley, D. and Dikic, I. (2008). Proteasome subunit Rpn13 is a novel ubiquitin receptor. *Nature* 453, 481–488.
- Iftode, C., Daniely, Y. and Borowiec, J. A. (1999). Replication protein A (RPA): the eukaryotic SSB. *Crit. Rev. Biochem. Mol. Biol.* 34, 141–180.

- Ishikura, S., Weissman, A. M. and Bonifacino, J. S. (2010). Serine residues in the cytosolic tail of the T-cell antigen receptor alpha-chain mediate ubiquitination and endoplasmic reticulum-associated degradation of the unassembled protein. *J. Biol. Chem.* 285, 23916–23924.
- Jackson, S. P. and Bartek, J. (2009). The DNA-damage response in human biology and disease. *Nature* 461, 1071–1078.
- Jagannathan, L., Cuddapah, S. and Costa, M. (2016). Oxidative stress under ambient and physiological oxygen tension in tissue culture. *Curr Pharmacol Rep* 2, 64–72.
- Jensen, R. B., Carreira, A. and Kowalczykowski, S. C. (2010). Purified human BRCA2 stimulates RAD51-mediated recombination. *Nature* 467, 678–683.
- Jowsey, P., Morrice, N. A., Hastie, C. J., McLauchlan, H., Toth, R. and Rouse, J. (2007). Characterisation of the sites of DNA damage-induced 53BP1 phosphorylation catalysed by ATM and ATR. *DNA Repair (Amst.)* 6, 1536–1544.
- Jungmichel, S., Clapperton, J. A., Lloyd, J., Hari, F. J., Spycher, C., Pavic, L., Li, J., Haire, L. F., Bonalli, M., Larsen, D. H., et al. (2012). The molecular basis of ATM-dependent dimerization of the Mdc1 DNA damage checkpoint mediator. *Nucleic Acids Res.* 40, 3913–3928.
- Kaidi, A. and Jackson, S. P. (2013). KAT5 tyrosine phosphorylation couples chromatin sensing to ATM signalling. *Nature* 498, 70–74.
- Kajihara, R., Fukushige, S., Shioda, N., Tanabe, K., Fukunaga, K. and Inui, S. (2010). CaMKII phosphorylates serine 10 of p27 and confers apoptosis resistance to HeLa cells. *Biochem. Biophys. Res. Commun.* 401, 350–355.
- Kang, H. S., Beak, J. Y., Kim, Y.-S., Petrovich, R. M., Collins, J. B., Grissom, S. F. and Jetten, A. M. (2006). NABP1, a novel RORgamma-regulated gene encoding a single-stranded nucleic-acid-binding protein. *Biochem. J.* 397, 89–99.
- Kar, A., Kaur, M., Ghosh, T., Khan, M. M., Sharma, A., Shekhar, R., Varshney, A.

- and Saxena, S. (2015). RPA70 depletion induces hSSB1/2-INTS3 complex to initiate ATR signaling. *Nucleic Acids Res.* 43, 4962–4974.
- Kemp, M. G., Akan, Z., Yilmaz, S., Grillo, M., Smith-Roe, S. L., Kang, T. H., Cordeiro-Stone, M., Kaufmann, W. K., Abraham, R. T., Sancar, A., et al. (2010). Tipin-replication protein A interaction mediates Chk1 phosphorylation by ATR in response to genotoxic stress. *J. Biol. Chem.* 285, 16562–16571.
- Keogh, M.-C., Kim, J.-A., Downey, M., Fillingham, J., Chowdhury, D., Harrison, J. C., Onishi, M., Datta, N., Galicia, S., Emili, A., et al. (2006). A phosphatase complex that dephosphorylates gammaH2AX regulates DNA damage checkpoint recovery. *Nature* 439, 497–501.
- Khamis, M. I., Casas-Finet, J. R. and Maki, A. H. (1987a). Stacking interactions of tryptophan residues and nucleotide bases in complexes formed between Escherichia coli single-stranded DNA binding protein and heavy atom-modified poly(uridylic) acid. A study by optically detected magnetic resonance spectroscopy. *J. Biol. Chem.* 262, 1725–1733.
- Khamis, M. I., Casas-Finet, J. R., Maki, A. H., Murphy, J. B. and Chase, J. W. (1987b). Role of tryptophan 54 in the binding of E. coli single-stranded DNA-binding protein to single-stranded polynucleotides. *FEBS Lett.* 211, 155–159.
- Khanna, K. K. and Jackson, S. P. (2001). DNA double-strand breaks: signaling, repair and the cancer connection. *Nat. Genet.* 27, 247–254.
- Kiianitsa, K., Solinger, J. A. and Heyer, W.-D. (2006). Terminal association of Rad54 protein with the Rad51-dsDNA filament. *Proc. Natl. Acad. Sci. U. S. A.* 103, 9767–9772.
- Kim, Biade, S. and Matsumoto (1998). Involvement of flap endonuclease 1 in base excision DNA repair. *J. Biol. Chem.* 273, 8842–8848.
- Kim, W., Bennett, E. J., Huttlin, E. L., Guo, A., Li, J., Possemato, A., Sowa, M. E., Rad, R., Rush, J., Comb, M. J., et al. (2011). Systematic and quantitative assessment of the ubiquitin-modified proteome. *Mol. Cell* 44, 325–340.

- Kins, S., Cramer, A., Evans, D. R., Hemmings, B. A., Nitsch, R. M. and Gotz, J. (2001). Reduced protein phosphatase 2A activity induces hyperphosphorylation and altered compartmentalization of tau in transgenic mice. *J. Biol. Chem.* 276, 38193–38200.
- Kirouac, K. N. and Ling, H. (2009). Structural basis of error-prone replication and stalling at a thymine base by human DNA polymerase ϵ . *EMBO J.* 28, 1644–1654.
- Kirpota, O. O., Endutkin, A. V., Ponomarenko, M. P., Ponomarenko, P. M., Zharkov, D. O. and Nevinsky, G. A. (2011). Thermodynamic and kinetic basis for recognition and repair of 8-oxoguanine in DNA by human 8-oxoguanine-DNA glycosylase. *Nucleic Acids Res.* 39, 4836–4850.
- Koç, A., Wheeler, L. J., Mathews, C. K. and Merrill, G. F. (2004). Hydroxyurea arrests DNA replication by a mechanism that preserves basal dNTP pools. *J. Biol. Chem.* 279, 223–230.
- Komander, D. (2009). The emerging complexity of protein ubiquitination. *Biochem. Soc. Trans.* 37, 937–953.
- Kozlov, S. V., Graham, M. E., Jakob, B., Tobias, F., Kijas, A. W., Tanuji, M., Chen, P., Robinson, P. J., Taucher-Scholz, G., Suzuki, K., et al. (2011). Autophosphorylation and ATM activation: additional sites add to the complexity. *J. Biol. Chem.* 286, 9107–9119.
- Kozlov, S. V., Graham, M. E., Peng, C., Chen, P., Robinson, P. J. and Lavin, M. F. (2006). Involvement of novel autophosphorylation sites in ATM activation. *EMBO J.* 25, 3504–3514.
- Kozlov, S. V., Waardenberg, A. J., Engholm-Keller, K., Arthur, J. W., Graham, M. E. and Lavin, M. F. (2016). Reactive oxygen species (ROS)-activated ATM-dependent phosphorylation of cytoplasmic substrates identified by large-scale phosphoproteomics screen. *Mol Cell Proteomics.* 15, 1032-1047.
- Krokan, H., Wist, E. and Krokan, R. H. (1981). Aphidicolin inhibits DNA synthesis by DNA polymerase α and isolated nuclei by a similar mechanism. *Nucleic*

Acids Res. 9, 4709–4719.

Krokan, Standal, R. and Slupphaug, G. (1997). DNA glycosylases in the base excision repair of DNA. *Biochem. J.* 325 (Pt 1), 1–16.

Kubbutat, M. H. G., Ludwig, R. L., Ashcroft, M. and Vousden, K. H. (1998). Regulation of Mdm2-Directed Degradation by the C Terminus of p53. *Mol. Cell. Biol.* 18, 5690–5698.

Kubota, Y., Nash, R. A., Klungland, A., Schär, P., Barnes, D. E. and Lindahl, T. (1996). Reconstitution of DNA base excision-repair with purified human proteins: interaction between DNA polymerase beta and the XRCC1 protein. *EMBO J.* 15, 6662–6670.

Kuhlbrodt, K., Mouysset, J. and Hoppe, T. (2005). Orchestra for assembly and fate of polyubiquitin chains. *Essays Biochem.* 41, 1–14.

Kumagai, A. and Dunphy, W. G. (2000). Claspin, a Novel Protein Required for the Activation of Chk1 during a DNA Replication Checkpoint Response in Xenopus Egg Extracts. *Mol. Cell* 6, 839–849.

Kumagai, A., Lee, Yoo, H. Y. and Dunphy, W. G. (2006). TopBP1 activates the ATR-ATRIP complex. *Cell* 124, 943–955.

Kunisada, M. (2005). 8-Oxoguanine Formation Induced by Chronic UVB Exposure Makes Ogg1 Knockout Mice Susceptible to Skin Carcinogenesis. *Cancer Res.* 65, 6006–6010.

Kusumoto, R., Masutani, C., Iwai, S. and Hanaoka, F. (2002). Translesion synthesis by human DNA polymerase eta across thymine glycol lesions. *Biochemistry (Mosc.)* 41, 6090–6099.

Lammens, K., Bemeleit, D. J., Mockel, C., Clausing, E., Schele, A., Hartung, S., Schiller, C. B., Lucas, M., Angermuller, C., Soding, J., et al. (2011). The Mre11:Rad50 structure shows an ATP-dependent molecular clamp in DNA double-strand break repair. *Cell* 145, 54–66.

Landry, J. J. M., Pyl, P. T., Rausch, T., Zichner, T., Tekkedil, M. M., Stütz, A. M.,

- Jauch, A., Aiyar, R. S., Pau, G., Delhomme, N., et al. (2013). The genomic and transcriptomic landscape of a HeLa cell line. *G3 (Bethesda)* 3, 1213–1224.
- Le Hir, H., Gatfield, D., Izaurralde, E. and Moore, M. J. (2001). The exon-exon junction complex provides a binding platform for factors involved in mRNA export and nonsense-mediated mRNA decay. *The EMBO Journal* 20, 4987–4997.
- Leahy, J. J. J., Golding, B. T., Griffin, R. J., Hardcastle, I. R., Richardson, C., Rigoreau, L. and Smith, G. C. M. (2004). Identification of a highly potent and selective DNA-dependent protein kinase (DNA-PK) inhibitor (NU7441) by screening of chromenone libraries. *Bioorg. Med. Chem. Lett.* 14, 6083–6087.
- Lee, D.-H. and Chowdhury, D. (2011). What goes on must come off: phosphatases gate-crash the DNA damage response. *Trends Biochem. Sci.* 36, 569–577.
- Lee, J. H. and Paull, T. T. (2005). ATM activation by DNA double-strand breaks through the Mre11-Rad50-Nbs1 complex. *Science* 308, 551–554.
- Lee, J., Kumagai, A. and Dunphy, W. G. (2007). The Rad9-Hus1-Rad1 checkpoint clamp regulates interaction of TopBP1 with ATR. *J. Biol. Chem.* 282, 28036–28044.
- Lee, J.-H., Goodarzi, A. A., Jeggo, P. A. and Paull, T. T. (2010). 53BP1 promotes ATM activity through direct interactions with the MRN complex. *EMBO J.* 29, 574–585.
- Lee, J.-H., Mand, M. R., Deshpande, R. A., Kinoshita, E., Yang, S.-H., Wyman, C. and Paull, T. T. (2013). Ataxia telangiectasia-mutated (ATM) kinase activity is regulated by ATP-driven conformational changes in the Mre11/Rad50/Nbs1 (MRN) complex. *J. Biol. Chem.* 288, 12840–12851.
- Lee, S.-H., Princz, L. N., Klügel, M. F., Habermann, B., Pfander, B. and Biertümpfel, C. (2015). Human Holliday junction resolvase GEN1 uses a chromodomain for efficient DNA recognition and cleavage. *Elife* 4.
- Leung-Pineda, V., Ryan, C. E. and Piwnica-Worms, H. (2006). Phosphorylation of

- Chk1 by ATR is antagonized by a Chk1-regulated protein phosphatase 2A circuit. *Mol. Cell. Biol.* 26, 7529–7538.
- Li, W. and Ye, Y. (2008). Polyubiquitin chains: functions, structures, and mechanisms. *Cell. Mol. Life Sci.* 65, 2397–2406.
- Li, W., Bengtson, M. H., Ulbrich, A., Matsuda, A., Reddy, V. A., Orth, A., Chanda, S. K., Batalov, S. and Joazeiro, C. A. P. (2008). Genome-wide and functional annotation of human E3 ubiquitin ligases identifies MULAN, a mitochondrial E3 that regulates the organelle's dynamics and signaling. *PLoS ONE* 3, e1487.
- Li, X. and Heyer, W.-D. (2008). Homologous recombination in DNA repair and DNA damage tolerance. *Cell Res.* 18, 99–113.
- Li, X. and Heyer, W.-D. (2009). RAD54 controls access to the invading 3'-OH end after RAD51-mediated DNA strand invasion in homologous recombination in *Saccharomyces cerevisiae*. *Nucleic Acids Res.* 37, 638–646.
- Li, X., Stith, C. M., Burgers, P. M. and Heyer, W.-D. (2009a). PCNA Is Required for Initiation of Recombination-Associated DNA Synthesis by DNA Polymerase delta. *Mol. Cell* 36, 704–713.
- Li, Y., Bolderson, E., Kumar, R., Muniandy, P. A., Xue, Y., Richard, Seidman, M., Pandita, T. K., Khanna, K. K. and Wang, W. (2009b). hSSB1 and hSSB2 form similar multiprotein complexes that participate in DNA damage response. *J. Biol. Chem.* 284, 23525–23531.
- Lin, Y.-F., Shih, H.-Y., Shang, Z., Matsunaga, S. and Chen, B. P. (2014). DNA-PKcs is required to maintain stability of Chk1 and Claspin for optimal replication stress response. *Nucleic Acids Res.*
- Lindsey-Boltz, L. A., Serçin, Ö., Choi, J. H. and Sancar, A. (2009). Reconstitution of Human Claspin-mediated Phosphorylation of Chk1 by the ATR (Ataxia Telangiectasia-mutated and Rad3-related) Checkpoint Kinase. *J. Biol. Chem.* 284, 33107–33114.
- Liu, H. and Naismith, J. H. (2008). An efficient one-step site-directed deletion,

- insertion, single and multiple-site plasmid mutagenesis protocol. *BMC Biotechnol.* 8, 91.
- Liu, J., Doty, T., Gibson, B. and Heyer, W. D. (2010). Human BRCA2 protein promotes RAD51 filament formation on RPA-covered single-stranded DNA. *Nat. Struct. Mol. Biol.* 17, 1260–1262.
- Liu, S., Bekker-Jensen, S., Mailand, N., Lukas, C., Bartek, J. and Lukas, J. (2006). Claspin operates downstream of TopBP1 to direct ATR signaling towards Chk1 activation. *Mol. Cell. Biol.* 26, 6056–6064.
- Liu, S., Ho, C. K., Ouyang, J. and Zou, L. (2013). Nek1 kinase associates with ATR-ATRIP and primes ATR for efficient DNA damage signaling. *Proc. Natl. Acad. Sci. U. S. A.* 110, 2175–2180.
- Liu, S., Opiyo, S. O., Manthey, K., Glanzer, J. G., Ashley, A. K., Amerin, C., Troksa, K., Shrivastav, M., Nickoloff, J. A. and Oakley, G. G. (2012). Distinct roles for DNA-PK, ATM and ATR in RPA phosphorylation and checkpoint activation in response to replication stress. *Nucleic Acids Res.* 40, 10780–10794.
- Liu, S., Shiotani, B., Lahiri, M., Maréchal, A., Tse, A., Leung, C. C. Y., Glover, J. N. M., Yang, X. H. and Zou, L. (2011). ATR autophosphorylation as a molecular switch for checkpoint activation. *Mol. Cell* 43, 192–202.
- Liu, Y. and West, S. C. (2004). Happy Hollidays: 40th anniversary of the Holliday junction. *Nat. Rev. Mol. Cell Biol.* 5, 937–944.
- Liu, Y., Beard, W. A., Shock, D. D., Prasad, R., Hou, E. W. and Wilson, S. H. (2005). DNA Polymerase {beta} and Flap Endonuclease 1 Enzymatic Specificities Sustain DNA Synthesis for Long Patch Base Excision Repair. *J. Biol. Chem.* 280, 3665–3674.
- Lohman, T. M., Bujalowski, W., Overman, L. B. and Wei, T. F. (1988). Interactions of the E. coli single strand binding (SSB) protein with ss nucleic acids. Binding mode transitions and equilibrium binding studies. *Biochem. Pharmacol.* 37, 1781–1782.

- Lundin, C., Erixon, K., Arnaudeau, C., Schultz, N., Jenssen, D., Meuth, M. and Helleday, T. (2002). Different roles for nonhomologous end joining and homologous recombination following replication arrest in mammalian cells. *Mol. Cell. Biol.* 22, 5869–5878.
- Lydeard, J. R., Jain, S., Yamaguchi, M. and Haber, J. E. (2007). Break-induced replication and telomerase-independent telomere maintenance require Pol32. *Nature* 448, 820–823.
- Machwe, A., Xiao, L., Groden, J. and Orren, D. K. (2006). The Werner and Bloom syndrome proteins catalyze regression of a model replication fork. *Biochemistry (Mosc.)* 45, 13939–13946.
- Machwe, A., Xiao, L., Lloyd, R. G., Bolt, E. and Orren, D. K. (2007). Replication fork regression in vitro by the Werner syndrome protein (WRN): holliday junction formation, the effect of leading arm structure and a potential role for WRN exonuclease activity. *Nucleic Acids Res.* 35, 5729–5747.
- Madeira, F., Tinti, M., Murugesan, G., Berrett, E., Stafford, M., Toth, R., Cole, C., MacKintosh, C. and Barton, G. J. (2015). 14-3-3-Pred: improved methods to predict 14-3-3-binding phosphopeptides. *Bioinformatics* 31, 2276–2283.
- Maga, G., Villani, G., Crespan, E., Wimmer, U., Ferrari, E., Bertocci, B. and Hubscher, U. (2007). 8-oxo-guanine bypass by human DNA polymerases in the presence of auxiliary proteins. *Nature* 447, 606–608.
- Makley, L. N. and Gestwicki, J. E. (2013). Expanding the number of “druggable” targets: non-enzymes and protein-protein interactions. *Chem Biol Drug Des* 81, 22–32.
- Maloisel, L., Fabre, F. and Gangloff, S. (2008). DNA polymerase delta is preferentially recruited during homologous recombination to promote heteroduplex DNA extension. *Mol. Cell. Biol.* 28, 1373–1382.
- Manthey, K. C., Opiyo, S., Glanzer, J. G., Dimitrova, D., Elliott, J. and Oakley, G. G. (2007). NBS1 mediates ATR-dependent RPA hyperphosphorylation following replication-fork stall and collapse. *J. Cell Sci.* 120, 4221–4229.

- Mao, Z., Bozzella, M., Seluanov, A. and Gorbunova, V. (2008a). DNA repair by nonhomologous end joining and homologous recombination during cell cycle in human cells. *Cell Cycle* 7, 2902–2906.
- Mao, Z., Bozzella, M., Seluanov, A. and Gorbunova, V. (2008b). Comparison of nonhomologous end joining and homologous recombination in human cells. *DNA Repair (Amst.)* 7, 1765–1771.
- Marini, V. and Krejci, L. (2012). Unwinding of synthetic replication and recombination substrates by Srs2. *DNA Repair (Amst.)* 11, 789–798.
- Marnett, L. J. and Plataras, J. P. (2001). Endogenous DNA damage and mutation. *Trends Genet.* 17, 214–221.
- Matos, J. and West, S. C. (2014). Holliday junction resolution: regulation in space and time. *DNA Repair (Amst.)* 19, 176–181.
- Matsumoto, Kim and Bogenhagen, D. F. (1994). Proliferating cell nuclear antigen-dependent abasic site repair in *Xenopus laevis* oocytes: an alternative pathway of base excision DNA repair. *Mol. Cell. Biol.* 14, 6187–6197.
- Mattioli, F., Vissers, J. H. A., van Dijk, W. J., Ikpa, P., Citterio, E., Vermeulen, W., Marteijn, J. A. and Sixma, T. K. (2012). RNF168 Ubiquitinates K13-15 on H2A/H2AX to Drive DNA Damage Signaling. *Cell* 150, 1182–1195.
- Maynard, S., Schurman, S. H., Harboe, C., de Souza-Pinto, N. C. and Bohr, V. A. (2009). Base excision repair of oxidative DNA damage and association with cancer and aging. *Carcinogenesis* 30, 2–10.
- Mazin, A. V., Mazina, O. M., Bugreev, D. V. and Rossi, M. J. (2010). Rad54, the motor of homologous recombination. *DNA Repair* 9, 286–302.
- McGlynn, P. and Lloyd, R. G. (2002). Recombinational repair and restart of damaged replication forks. *Nat. Rev. Mol. Cell Biol.* 3, 859–870.
- McGlynn, P., Lloyd, R. G. and Marians, K. J. (2001). Formation of Holliday junctions by regression of nascent DNA in intermediates containing stalled

replication forks: RecG stimulates regression even when the DNA is negatively supercoiled. *Proc. Natl. Acad. Sci. U. S. A.* 98, 8235–8240.

McNally, R., Bowman, G. D., Goedken, E. R., O'Donnell, M. and Kuriyan, J. (2010). Analysis of the role of PCNA-DNA contacts during clamp loading. *BMC Struct. Biol.* 10, 3.

Mellacheruvu, D., Wright, Z., Couzens, A. L., Lambert, J. P., St-Denis, N. A., Li, T., Miteva, Y. V., Hauri, S., Sardi, ME., Low, T. Y., Halim, V, A., Bagshaw, R, D., Hubner, N. C., al-Hakim, A., Bouchard, A., Faubert, D., Fermin, D., Dunham, W. H., Goudreault, M., Lin, Z., Gonzalez, B., Pawson, T., Durocher, D., Coulombe, B., Aebersold, R., Supeti-Furga, G., Colinge, J., Heck, A, J R., Choi, H., Gstaiger, M., Mohammed, S., Cristea, I. M., Bennet, K. L., Washburn, M. P., Raught, B., Ewing, R. M., Gingras, A., Nesvizhskii, A. I. (2013). The CRAPome: a contaminant repository for affinity purification-mass spectrometry data. *Nat. Methods.* 10, 730-736.

Meng, Z., Capalbo, L., Glover, D. M. and Dunphy, W. G. (2011). Role for casein kinase 1 in the phosphorylation of Claspin on critical residues necessary for the activation of Chk1. *Mol. Biol. Cell* 22, 2834–2847.

Merrill, B. M., Williams, K. R., Chase, J. W. and Konigsberg, W. H. (1984). Photochemical cross-linking of the Escherichia coli single-stranded DNA-binding protein to oligodeoxynucleotides. Identification of phenylalanine 60 as the site of cross-linking. *J. Biol. Chem.* 259, 10850–10856.

Metzger, M. B., Hristova, V. A. and Weissman, A. M. (2012). HECT and RING finger families of E3 ubiquitin ligases at a glance. *J. Cell Sci.* 125, 531–537.

Min, W., Bruhn, C., Grigaravicius, P., Zhou, Z.-W., Li, F., Krüger, A., Siddeek, B., Greulich, K.-O., Popp, O., Meisezahl, C., et al. (2013). Poly(ADP-ribose) binding to Chk1 at stalled replication forks is required for S-phase checkpoint activation. *Nat Commun* 4, 2993.

Mockel, C., Lammens, K., Schele, A. and Hopfner, K. P. (2012). ATP driven structural changes of the bacterial Mre11:Rad50 catalytic head complex. *Nucleic Acids Res.* 40, 914–927.

- Mohammad, D. H. and Yaffe, M. B. (2009). 14-3-3 proteins, FHA domains and BRCT domains in the DNA damage response. *DNA Repair (Amst.)* 8, 1009–1017.
- Mol, C. D., Arvai, A. S., Slupphaug, G., Kavli, B., Alseth, I., Krokan and Tainer, J. A. (1995). Crystal structure and mutational analysis of human uracil-DNA glycosylase: structural basis for specificity and catalysis. *Cell* 80, 869–878.
- Mordes, D. A., Glick, G. G., Zhao, R. and Cortez, D. (2008). TopBP1 activates ATR through ATRIP and a PIKK regulatory domain. *Genes Dev.* 22, 1478–1489.
- Morillon, A., Karabetsov, N., O'Sullivan, J., Kent, N., Proudfoot, N. and Mellor, J. (2003). Isw1 chromatin remodeling ATPase coordinates transcription elongation and termination by RNA polymerase II. *Cell* 115, 425–435.
- Moudry, P., Watanabe, K., Wolanin, K. M., Bartkova, J., Wassing, I. E., Watanabe, S., Strauss, R., Troelsgaard Pedersen, R., Oestergaard, V. H., Lisby, M., et al. (2016). TOPBP1 regulates RAD51 phosphorylation and chromatin loading and determines PARP inhibitor sensitivity. *J. Cell Biol.* 212, 281–288.
- Mu, D., Bessho, T., Nechev, L. V., Chen, D. J., Harris, T. M., Hearst, J. E. and Sancar, A. (2000). DNA interstrand cross-links induce futile repair synthesis in mammalian cell extracts. *Mol. Cell. Biol.* 20, 2446–2454.
- Murphy, A. K., Fitzgerald, M., Ro, T., Kim, J. H., Rabinowitsch, A. I., Chowdhury, D., Schildkraut, C. L. and Borowiec, J. A. (2014). Phosphorylated RPA recruits PALB2 to stalled DNA replication forks to facilitate fork recovery. *J. Cell Biol.* 206, 493–507.
- Murthy, K. G. and Manley, J. L. (1995). The 160-kD subunit of human cleavage-polyadenylation specificity factor coordinates pre-mRNA 3'-end formation. *Genes Dev.* 9, 2672–2683.
- Murzin, A. G. (1993). OB(oligonucleotide/oligosaccharide binding)-fold: common structural and functional solution for non-homologous sequences. *EMBO J.* 12, 861–867.

- Nakada, D., Matsumoto, K. and Sugimoto, K. (2003). ATM-related Tel1 associates with double-strand breaks through an Xrs2-dependent mechanism. *Genes Dev.* 17, 1957–1962.
- Nakano, T., Miyamoto-Matsubara, M., Shoulkamy, M. I., Salem, A. M. H., Pack, S. P., Ishimi, Y. and Ide, H. (2013). Translocation and stability of replicative DNA helicases upon encountering DNA-protein cross-links. *J. Biol. Chem.* 288, 4649–4658.
- Nakata, Y., Tang, X. and Yokoyama, K. K. (1997). Preparation of competent cells for high-efficiency plasmid transformation of *Escherichia coli*. *Methods Mol. Biol.* 69, 129–137.
- Namiki, Y. and Zou, L. (2006). ATRIP associates with replication protein A-coated ssDNA through multiple interactions. *Proc. Natl. Acad. Sci. U. S. A.* 103, 580–585.
- Nash, H. M., Lu, R., Lane, W. S. and Verdine, G. L. (1997). The critical active-site amine of the human 8-oxoguanine DNA glycosylase, hOgg1: direct identification, ablation and chemical reconstitution. *Chem. Biol.* 4, 693–702.
- Nathan, J. A., Kim, H. T., Ting, L., Gygi, S. P. and Goldberg, A. L. (2013). Why do cellular proteins linked to K63-polyubiquitin chains not associate with proteasomes? *EMBO J.* 32, 552–565.
- Nimonkar, A. V., Genschel, J., Kinoshita, E., Polaczek, P., Campbell, J. L., Wyman, C., Modrich, P. and Kowalczykowski, S. C. (2011). BLM-DNA2-RPA-MRN and EXO1-BLM-RPA-MRN constitute two DNA end resection machineries for human DNA break repair. *Genes Dev.* 25, 350–362.
- Nimonkar, A. V., Sica, R. A. and Kowalczykowski, S. C. (2009). Rad52 promotes second-end DNA capture in double-stranded break repair to form complement-stabilized joint molecules. *Proc. Natl. Acad. Sci. U. S. A.* 106, 3077–3082.
- Niu, H., Erdjument-Bromage, H., Pan, Z. Q., Lee, S. H., Tempst, P. and Hurwitz, J. (1997). Mapping of amino acid residues in the p34 subunit of human single-stranded DNA-binding protein phosphorylated by DNA-dependent protein

- kinase and Cdc2 kinase in vitro. *J. Biol. Chem.* 272, 12634–12641.
- Obara, K. and Yabu, H. (1993). Dual effect of phosphatase inhibitors on calcium channels in intestinal smooth muscle cells. *American Journal of Physiology - Cell Physiology* 264, C296–C301.
- Okumoto, K., Misono, S., Miyata, N., Matsumoto, Y., Mukai, S. and Fujiki, Y. (2011). Cysteine ubiquitination of PTS1 receptor Pex5p regulates Pex5p recycling. *Traffic* 12, 1067–1083.
- Olsen, J. V., Ong, S.-E. and Mann, M. (2004). Trypsin cleaves exclusively C-terminal to arginine and lysine residues. *Mol. Cell. Proteomics* 3, 608–614.
- Olson, E., Nievera, C. J., Klimovich, V., Fanning, E. and Wu, X. (2006). RPA2 is a direct downstream target for ATR to regulate the S-phase checkpoint. *J. Biol. Chem.* 281, 39517–39533.
- Overman, L. B. and Lohman, T. M. (1994). Linkage of pH, anion and cation effects in protein-nucleic acid equilibria. Escherichia coli SSB protein-single stranded nucleic acid interactions. *J. Mol. Biol.* 236, 165–178.
- Overman, L. B., Bujalowski, W. and Lohman, T. M. (1988). Equilibrium binding of Escherichia coli single-strand binding protein to single-stranded nucleic acids in the (SSB)₆₅ binding mode. Cation and anion effects and polynucleotide specificity. *Biochemistry (Mosc.)* 27, 456–471.
- Ozeri-Galai, E., Schwartz, M., Rahat, A. and Kerem, B. (2008). Interplay between ATM and ATR in the regulation of common fragile site stability. *Oncogene* 27, 2109–2117.
- Paliwal, S., Kanagaraj, R., Sturzenegger, A., Burdova, K. and Janscak, P. (2013). Human RECQ5 helicase promotes repair of DNA double-strand breaks by synthesis-dependent strand annealing. *Nucleic Acids Res.*
- Palumbo, A. M., Smith, S. A., Kalcic, C. L., Dantus, M., Stemmer, P. M. and Reid, G. E. (2011). Tandem mass spectrometry strategies for phosphoproteome analysis. *Mass Spectrom Rev* 30, 600–625.

- Paquet, N., Adams, M.N., **Ashton, N.W.**, Touma, C., Gamsjaeger, R., Cubeddu, L., Leong, V., Beard, S., Bolderson, E., O'Byrne, K.J., Richard, D.J. (2016) Oxidative hSSB1 (NABP2/OBFC2B) oligomerization regulates its activity in response to oxidative stress. *Scientific Reports* 6, 27446.
- Paquet, N., Adams, M. N., Leong, V., Ashton, N. W., Touma, C., Gamsjaeger, R., Cubeddu, L., Beard, S., Burgess, J. T., Bolderson, E., et al. (2015). hSSB1 (NABP2/ OBFC2B) is required for the repair of 8-oxo-guanine by the hOGG1-mediated base excision repair pathway. *Nucleic Acids Res.* gkv790.
- Paquet, N., Box, J. K., Ashton, N. W., Suraweera, A., Croft, L. V., Urquhart, A. J., Bolderson, E., Zhang, S.-D., O'Byrne, K. J. and Richard, D. J. (2014). Néstor-Guillermo Progeria Syndrome: a biochemical insight into Barrier-to-Autointegration Factor 1, alanine 12 threonine mutation. *BMC Mol. Biol.* 15, 27.
- Parikh, S. S., Mol, C. D., Slupphaug, G., Bharati, S., Krokan and Tainer, J. A. (1998). Base excision repair initiation revealed by crystal structures and binding kinetics of human uracil-DNA glycosylase with DNA. *EMBO J.* 17, 5214–5226.
- Pellegrini, L., Yu, D. S., Lo, T., Anand, S., Lee, M., Blundell, T. L. and Venkitaraman, A. R. (2002). Insights into DNA recombination from the structure of a RAD51-BRCA2 complex. *Nature* 420, 287–293.
- Peng, J., Schwartz, D., Elias, J. E., Thoreen, C. C., Cheng, D., Marsischky, G., Roelofs, J., Finley, D. and Gygi, S. P. (2003). A proteomics approach to understanding protein ubiquitination. *Nat. Biotechnol.* 21, 921–926.
- Petermann, E. and Helleday, T. (2010). Pathways of mammalian replication fork restart. *Nat. Rev. Mol. Cell Biol.* 11, 683–687.
- Petermann, E., Keil, C. and Oei, S. L. (2006). Roles of DNA ligase III and XRCC1 in regulating the switch between short patch and long patch BER. *DNA Repair (Amst.)* 5, 544–555.
- Petermann, E., Orta, M. L., Issaeva, N., Schultz, N. and Helleday, T. (2010). Hydroxyurea-stalled replication forks become progressively inactivated and require two different RAD51-mediated pathways for restart and repair. *Mol. Cell*

37, 492–502.

- Peterson, S. E., Li, Y., Wu-Baer, F., Chait, B. T., Baer, R., Yan, H., Gottesman, M. E. and Gautier, J. (2013). Activation of DSB processing requires phosphorylation of CtIP by ATR. *Mol. Cell* 49, 657–667.
- Peth, A., Uchiki, T. and Goldberg, A. L. (2010). ATP-dependent steps in the binding of ubiquitin conjugates to the 26S proteasome that commit to degradation. *Mol. Cell* 40, 671–681.
- Petroski, M. D. and Deshaies, R. J. (2005). Mechanism of lysine 48-linked ubiquitin-chain synthesis by the cullin-RING ubiquitin-ligase complex SCF-Cdc34. *Cell* 123, 1107–1120.
- Podlutzky, A. J., Dianova, I. I., Podust, V. N., Bohr, V. A. and Dianov, G. L. (2001). Human DNA polymerase beta initiates DNA synthesis during long-patch repair of reduced AP sites in DNA. *EMBO J.* 20, 1477–1482.
- Poirier, M. C. (2004). Chemical-induced DNA damage and human cancer risk. *Nat. Rev. Cancer* 4, 630–637.
- Polo, S. E. and Jackson, S. P. (2011). Dynamics of DNA damage response proteins at DNA breaks: a focus on protein modifications. *Genes Dev.* 25, 409–433.
- Polo, S. E., Blackford, A. N., Chapman, J. R. and Baskcomb, L. (2012). Regulation of DNA-End Resection by hnRNPU-like Proteins Promotes DNA Double-Strand Break Signaling and Repair. *Mol. Cell.*
- Poot, R. A., Bozhenok, L., van den Berg, D. L. C., Steffensen, S., Ferreira, F., Grimaldi, M., Gilbert, N., Ferreira, J. and Varga-Weisz, P. D. (2004). The Williams syndrome transcription factor interacts with PCNA to target chromatin remodelling by ISWI to replication foci. *Nat. Cell Biol.* 6, 1236–1244.
- Poyurovsky, M. V., Katz, C., Laptenko, O., Beckerman, R., Lokshin, M., Ahn, J., Byeon, I.-J. L., Gabizon, R., Mattia, M., Zupnick, A., et al. (2010). The C terminus of p53 binds the N-terminal domain of MDM2. *Nat. Struct. Mol. Biol.* 17, 982–989.

- Prakash, R., Satory, D., Dray, E., Papusha, A., Scheller, J., Kramer, W., Krejci, L., Klein, H., Haber, J. E., Sung, P., et al. (2009). Yeast Mph1 helicase dissociates Rad51-made D-loops: implications for crossover control in mitotic recombination. *Genes Dev.* 23, 67–79.
- Prickett, T. D. and Brautigan, D. L. (2006). The $\alpha 4$ Regulatory Subunit Exerts Opposing Allosteric Effects on Protein Phosphatases PP6 and PP2A. *J. Biol. Chem.* 281, 30503–30511.
- Ragunathan, S., Kozlov, A. G., Lohman, T. M. and Waksman, G. (2000). Structure of the DNA binding domain of E. coli SSB bound to ssDNA. *Nat. Struct. Biol.* 7, 648–652.
- Ramírez-Lugo, J. S., Yoo, H. Y., Yoon, S. J. and Dunphy, W. G. (2011). CtIP interacts with TopBP1 and Nbs1 in the response to double-stranded DNA breaks (DSBs) in *Xenopus* egg extracts. *Cell Cycle* 10, 469–480.
- Ranalli, T. A., Tom, S. and Bambara, R. A. (2002). AP Endonuclease 1 Coordinates Flap Endonuclease 1 and DNA Ligase I Activity in Long Patch Base Excision Repair. *J. Biol. Chem.* 277, 41715–41724.
- Reinhardt, H. C. and Yaffe, M. B. (2013). Phospho-Ser/Thr-binding domains: navigating the cell cycle and DNA damage response. *Nat. Rev. Mol. Cell Biol.* 14, 563–580.
- Ren, W., Chen, H., Sun, Q., Tang, X., Lim, S. C., Huang, J. and Song, H. (2014). Structural Basis of SOSS1 Complex Assembly and Recognition of ssDNA. *Cell Rep* 6, 982–991.
- Resjö, S., Göransson, O., Härndahl, L., Zolnierowicz, S., Manganiello, V. and Degerman, E. (2002). Protein phosphatase 2A is the main phosphatase involved in the regulation of protein kinase B in rat adipocytes. *Cell. Signal.* 14, 231–238.
- Richard, Bolderson, E., Cubeddu, L., Wadsworth, R. I., Savage, K., Sharma, G. G., Nicolette, M. L., Tsvetanov, S., McIlwraith, M. J., Pandita, R. K., et al. (2008). Single-stranded DNA-binding protein hSSB1 is critical for genomic stability. *Nature* 453, 677–681.

- Richard, Cubeddu, L., Urquhart, A. J., Bain, A., Bolderson, E., Menon, D., White, M. F. and Khanna, K. K. (2011a). hSSB1 interacts directly with the MRN complex stimulating its recruitment to DNA double-strand breaks and its endonuclease activity. *Nucleic Acids Res.* 39, 3643–3651.
- Richard, Savage, K., Bolderson, E., Cubeddu, L., So, S., Ghita, M., Chen, D. J., White, M. F., Richard, K., Prise, K. M., et al. (2011b). hSSB1 rapidly binds at the sites of DNA double-strand breaks and is required for the efficient recruitment of the MRN complex. *Nucleic Acids Res.* 39, 1692–1702.
- Robison, J. G., Elliott, J., Dixon, K. and Oakley, G. G. (2004). Replication protein A and the Mre11.Rad50.Nbs1 complex co-localize and interact at sites of stalled replication forks. *J. Biol. Chem.* 279, 34802–34810.
- Rodriguez, M. S., Desterro, J. M. P., Lain, S., Lane, D. P. and Hay, R. T. (2000a). Multiple C-Terminal Lysine Residues Target p53 for Ubiquitin-Proteasome-Mediated Degradation. *Mol. Cell. Biol.* 20, 8458–8467.
- Rodriguez, M. S., Desterro, J. M., Lain, S., Lane, D. P. and Hay, R. T. (2000b). Multiple C-terminal lysine residues target p53 for ubiquitin-proteasome-mediated degradation. *Mol. Cell. Biol.* 20, 8458–8467.
- Roldán-Arjona, T., Wei, Y. F., Carter, K. C., Klungland, A., Anselmino, C., Wang, R. P., Augustus, M. and Lindahl, T. (1997). Molecular cloning and functional expression of a human cDNA encoding the antimutator enzyme 8-hydroxyguanine-DNA glycosylase. *Proc. Natl. Acad. Sci. U. S. A.* 94, 8016–8020.
- Sadowski, M. and Sarcevic, B. (2010). Mechanisms of mono- and poly-ubiquitination: Ubiquitination specificity depends on compatibility between the E2 catalytic core and amino acid residues proximal to the lysine. *Cell Div* 5, 19.
- Saintigny, Y., Delacote, F., Varès, G., Petitot, F., Lambert, S., Averbek, D. and Lopez, B. S. (2001). Characterization of homologous recombination induced by replication inhibition in mammalian cells. *EMBO J.* 20, 3861–3870.
- Saleh-Gohari, N. and Helleday, T. (2004). Conservative homologous recombination

- preferentially repairs DNA double-strand breaks in the S phase of the cell cycle in human cells. *Nucleic Acids Res.* 32, 3683–3688.
- Saleh-Gohari, N., Bryant, H. E., Schultz, N., Parker, K. M., Cassel, T. N. and Helleday, T. (2005). Spontaneous homologous recombination is induced by collapsed replication forks that are caused by endogenous DNA single-strand breaks. *Mol. Cell. Biol.* 25, 7158–7169.
- San Filippo, J., Sung, P. and Klein, H. (2008). Mechanism of eukaryotic homologous recombination. *Annu. Rev. Biochem.* 77, 229–257.
- Sartori, A. A., Lukas, C., Coates, J., Mistrik, M., Fu, S., Bartek, J., Baer, R., Lukas, J. and Jackson, S. P. (2007). Human CtIP promotes DNA end resection. *Nature* 450, 509–514.
- Savvides, S. N., Raghunathan, S., Futterer, K., Kozlov, A. G., Lohman, T. M. and Waksman, G. (2004). The C-terminal domain of full-length E. coli SSB is disordered even when bound to DNA. *Protein Sci.* 13, 1942–1947.
- Schiller, C. B., Lammens, K., Guerini, I., Coordes, B., Feldmann, H., Schlauderer, F., Mockel, C., Schele, A., Strasser, K., Jackson, S. P., et al. (2012). Structure of Mre11-Nbs1 complex yields insights into ataxia-telangiectasia-like disease mutations and DNA damage signaling. *Nat. Struct. Mol. Biol.* 19, 693–700.
- Schneider-Poetsch, T., Ju, J., Eyler, D. E., Dang, Y., Bhat, S., Merrick, W. C., Green, R., Shen, B. and Liu, J. O. (2010). Inhibition of eukaryotic translation elongation by cycloheximide and lactimidomycin. *Nat. Chem. Biol.* 6, 209–217.
- Schreiner, P., Chen, X., Husnjak, K., Randles, L., Zhang, N., Elsassner, S., Finley, D., Dikic, I., Walters, K. J. and Groll, M. (2008). Ubiquitin docking at the proteasome through a novel pleckstrin-homology domain interaction. *Nature* 453, 548–552.
- Schurtenberger, P., Egelhaaf, S. U., Hindges, R., Maga, G., Jonsson, Z. O., May, R. P., Glatter, O. and Hubscher, U. (1998). The solution structure of functionally active human proliferating cell nuclear antigen determined by small-angle neutron scattering. *J. Mol. Biol.* 275, 123–132.

- Sezonov, G., Joseleau-Petit, D. and D'Ari, R. (2007). *Escherichia coli* physiology in Luria-Bertani broth. *J. Bacteriol.* 189, 8746–8749.
- Shao, R. G., Cao, C. X., Zhang, H., Kohn, K. W., Wold, M. S. and Pommier, Y. (1999). Replication-mediated DNA damage by camptothecin induces phosphorylation of RPA by DNA-dependent protein kinase and dissociates RPA:DNA-PK complexes. *EMBO J.* 18, 1397–1406.
- Shen, Y., Wang, Y., Sheng, K., Fei, X., Guo, Q., Larner, J., Kong, X., Qiu, Y. and Mi, J. (2011). Serine/threonine protein phosphatase 6 modulates the radiation sensitivity of glioblastoma. *Cell Death Dis* 2, e241.
- Shi, W., Bain, A. L., Schwer, B., Al-Ejeh, F., Smith, C., Wong, L., Chai, H., Miranda, M. S., Ho, U., Kawaguchi, M., Miura, Y., Finnie, J. W., Wall, M., Heierhorst, J., Wicking, C., Spring, K. J., Alt, F. W., Khanna, K. K. (2013). Essential developmental, genomic stability and tumour suppressor functions of the mouse orthologue of *hSSB1/NABP2*. *Plos Genetics* 9 (2), p. e1003298.
- Shi, W., Feng, Z., Zhang, J., Gonzalez-Suarez, I., Vanderwaal, R. P., Wu, X., Powell, S. N., Roti Roti, J. L. and Gonzalo, S. (2010). The role of RPA2 phosphorylation in homologous recombination in response to replication arrest. *Carcinogenesis* 31, 994–1002.
- Shimura, T., Martin, M. M., Torres, M. J., Gu, C., Pluth, J. M., DeBernardi, M. A., DiBernardi, M. A., McDonald, J. S. and Aladjem, M. I. (2007). DNA-PK is involved in repairing a transient surge of DNA breaks induced by deceleration of DNA replication. *J. Mol. Biol.* 367, 665–680.
- Shrivastav, M., De Haro, L. P. and Nickoloff, J. A. (2008). Regulation of DNA double-strand break repair pathway choice. *Cell Res.* 18, 134–147.
- Shrivastav, M., Miller, C. A., De Haro, L. P., Durant, S. T., Chen, B. P. C., Chen, D. J. and Nickoloff, J. A. (2009). DNA-PKcs and ATM co-regulate DNA double-strand break repair. *DNA Repair (Amst.)* 8, 920–929.
- Sidorova, J. M., Kehrl, K., Mao, F. and Monnat, R. (2013). Distinct functions of human RECQ helicases WRN and BLM in replication fork recovery and

- progression after hydroxyurea-induced stalling. *DNA Repair (Amst.)* 12, 128–139.
- Siedler, S., Stahlhut, S. G., Malla, S., Maury, J. and Neves, A. R. (2014). Novel biosensors based on flavonoid-responsive transcriptional regulators introduced into *Escherichia coli*. *Metab. Eng.* 21, 2–8.
- Sims, J. K. and Wade, P. A. (2011). Mi-2/NuRD complex function is required for normal S phase progression and assembly of pericentric heterochromatin. *Mol. Biol. Cell* 22, 3094–3102.
- Sirbu, B. M., Couch, F. B. and Cortez, D. (2012). Monitoring the spatiotemporal dynamics of proteins at replication forks and in assembled chromatin using isolation of proteins on nascent DNA. *Nat Protoc* 7, 594–605.
- Sirbu, B. M., McDonald, W. H., Dugrawala, H., Badu-Nkansah, A., Kavanaugh, G. M., Chen, Y., Tabb, D. L. and Cortez, D. (2013). Identification of proteins at active, stalled, and collapsed replication forks using isolation of proteins on nascent DNA (iPOND) coupled with mass spectrometry. *J. Biol. Chem.* 288, 31458–31467.
- Skaar, J. R., Ferris, A. L., Wu, X., Saraf, A., Khanna, K. K., Florens, L., Washburn, M. P., Hughes, S. H. and Pagano, M. (2015). The Integrator complex controls the termination of transcription at diverse classes of gene targets. *Cell Res.* 25, 288–305.
- Skaar, J. R., Richard, Saraf, A., Toschi, A., Bolderson, E., Florens, L., Washburn, M. P., Khanna, K. K. and Pagano, M. (2009). INTS3 controls the hSSB1-mediated DNA damage response. *J. Cell Biol.* 187, 25–32.
- Smits, V. A. J., Reaper, P. M. and Jackson, S. P. (2006). Rapid PIKK-dependent release of Chk1 from chromatin promotes the DNA-damage checkpoint response. *Curr. Biol.* 16, 150–159.
- Sogo, J. M., Lopes, M. and Foiani, M. (2002). Fork reversal and ssDNA accumulation at stalled replication forks owing to checkpoint defects. *Science* 297, 599–602.

- Solinger, J. A., Kiiianitsa, K. and Heyer, W.-D. (2002). Rad54, a Swi2/Snf2-like Recombinational Repair Protein, Disassembles Rad51:dsDNA Filaments. *Mol. Cell* 10, 1175–1188.
- Spaulding, M., O'Leary, M. A. and Gatesy, J. (2009). Relationships of Cetacea (Artiodactyla) among mammals: increased taxon sampling alters interpretations of key fossils and character evolution. *PLoS ONE* 4, e7062.
- Spycher, C., Miller, E. S., Townsend, K., Pavic, L., Morrice, N. A., Janscak, P., Stewart, G. S. and Stucki, M. (2008). Constitutive phosphorylation of MDC1 physically links the MRE11-RAD50-NBS1 complex to damaged chromatin. *J. Cell Biol.* 181, 227–240.
- Staker, B. L., Hjerrild, K., Feese, M. D., Behnke, C. A., Burgin, A. B. and Stewart, L. (2002). The mechanism of topoisomerase I poisoning by a camptothecin analog. *Proc. Natl. Acad. Sci. U. S. A.* 99, 15387–15392.
- Stauffer, M. E. and Chazin, W. J. (2004). Physical interaction between replication protein A and Rad51 promotes exchange on single-stranded DNA. *J. Biol. Chem.* 279, 25638–25645.
- Suhasini, A. N. and Brosh, R. M. J. (2012). Fanconi anemia and Bloom's syndrome crosstalk through FANCD1-BLM helicase interaction. *Trends Genet.* 28, 7–13.
- Suhasini, A. N., Rawtani, N. A., Wu, Y., Sommers, J. A., Sharma, S., Mosedale, G., North, P. S., Cantor, S. B., Hickson, I. D. and Brosh, R. M. J. (2011). Interaction between the helicases genetically linked to Fanconi anemia group J and Bloom's syndrome. *EMBO J.* 30, 692–705.
- Suhasini, A. N., Sommers, J. A., Muniandy, P. A., Coulombe, Y., Cantor, S. B., Masson, J.-Y., Seidman, M. M. and Brosh, R. M. (2013). Fanconi anemia group J helicase and MRE11 nuclease interact to facilitate the DNA damage response. *Mol. Cell. Biol.* 33, 2212–2227.
- Sun, Latham, K. A., Dodson, M. L. and Lloyd, R. S. (1995). Studies on the Catalytic Mechanism of Five DNA Glycosylases. *J. Biol. Chem.*

- Sun, Y., Jiang, X., Chen, S., Fernandes, N. and Price, B. D. (2005). A role for the Tip60 histone acetyltransferase in the acetylation and activation of ATM. *Proc. Natl. Acad. Sci. U. S. A.* 102, 13182–13187.
- Sun, Y., Jiang, X., Xu, Y., Ayrapetov, M. K., Moreau, L. A., Whetstine, J. R. and Price, B. D. (2009). Histone H3 methylation links DNA damage detection to activation of the tumour suppressor Tip60. *Nat. Cell Biol.* 11, 1376–1382.
- Sun, Y., Xu, Y., Roy, K. and Price, B. D. (2007). DNA damage-induced acetylation of lysine 3016 of ATM activates ATM kinase activity. *Mol. Cell. Biol.* 27, 8502–8509.
- Sung, P., Krejci, L., Van Komen, S. and Sehorn, M. G. (2003). Rad51 recombinase and recombination mediators. *J. Biol. Chem.* 278, 42729–42732.
- Swingle, M., Ni, L. and Honkanen, R. E. (2007). Small-molecule inhibitors of ser/thr protein phosphatases: specificity, use and common forms of abuse. *Methods Mol. Biol.* 365, 23–38.
- Swuec, P. and Costa, A. (2014). Molecular mechanism of double Holliday junction dissolution. *Cell Biosci* 4, 36.
- Sørensen, C. S., Syljuåsen, R. G., Falck, J., Schroeder, T., Rønnstrand, L., Khanna, K. K., Zhou, B.-B., Bartek, J. and Lukas, J. (2003). Chk1 regulates the S phase checkpoint by coupling the physiological turnover and ionizing radiation-induced accelerated proteolysis of Cdc25A. *Cancer Cell* 3, 247–258.
- Thrower, J. S., Hoffman, L., Rechsteiner, M. and Pickart, C. M. (2000). Recognition of the polyubiquitin proteolytic signal. *The EMBO Journal* 19, 94–102.
- Tokarev, A. A., Munguia, J. and Guatelli, J. C. (2011). Serine-threonine ubiquitination mediates downregulation of BST-2/tetherin and relief of restricted virion release by HIV-1 Vpu. *J. Virol.* 85, 51–63.
- Toledo, L. I., Altmeyer, M., Rask, M.-B., Lukas, C., Larsen, D. H., Povlsen, L. K., Bekker-Jensen, S., Mailand, N., Bartek, J. and Lukas, J. (2013). ATR prohibits replication catastrophe by preventing global exhaustion of RPA. *Cell* 155, 1088–

- Tomimatsu, N., Mukherjee, B., Deland, K., Kurimasa, A., Bolderson, E., Khanna, K. K. and Burma, S. (2012). Exo1 plays a major role in DNA end resection in humans and influences double-strand break repair and damage signaling decisions. *DNA Repair (Amst.)* 11, 441–448.
- Traven, A. and Heierhorst, J. (2005). SQ/TQ cluster domains: concentrated ATM/ATR kinase phosphorylation site regions in DNA-damage-response proteins. *Bioessays* 27, 397–407.
- Treier, M., Staszewski, L. M. and Bohmann, D. (1994). Ubiquitin-dependent c-Jun degradation in vivo is mediated by the delta domain. *Cell* 78, 787–798.
- Udeshi, N. D., Mani, D. R., Eisenhaure, T., Mertins, P., Jaffe, J. D., Clauser, K. R., Hacohen, N. and Carr, S. A. (2012). Methods for quantification of in vivo changes in protein ubiquitination following proteasome and deubiquitinase inhibition. *Mol. Cell. Proteomics* 11, 148–159.
- Udeshi, N. D., Mertins, P., Svinkina, T. and Carr, S. A. (2013a). Large-scale identification of ubiquitination sites by mass spectrometry. *Nat Protoc* 8, 1950–1960.
- Udeshi, N. D., Svinkina, T., Mertins, P., Kuhn, E., Mani, D. R., Qiao, J. W. and Carr, S. A. (2013b). Refined preparation and use of anti-diglycine remnant (K- ϵ -GG) antibody enables routine quantification of 10,000s of ubiquitination sites in single proteomics experiments. *Mol. Cell. Proteomics* 12, 825–831.
- Unsal-Kacmaz, K., Chastain, P. D., Qu, P. P., Minoo, P., Cordeiro-Stone, M., Sancar, A. and Kaufmann, W. K. (2007). The human Tim/Tipin complex coordinates an Intra-S checkpoint response to UV that slows replication fork displacement. *Mol. Cell. Biol.* 27, 3131–3142.
- Uziel, T., Lerenthal, Y., Moyal, L., Andegeko, Y., Mittelman, L. and Shiloh, Y. (2003). Requirement of the MRN complex for ATM activation by DNA damage. *EMBO J.* 22, 5612–5621.

- van Loon, B. and Hubscher, U. (2009). An 8-oxo-guanine repair pathway coordinated by MUTYH glycosylase and DNA polymerase. *Proc. Natl. Acad. Sci. U. S. A.* 106, 18201–18206.
- Vassilev, L. T., Vu, B. T., Graves, B., Carvajal, D., Podlaski, F., Filipovic, Z., Kong, N., Kammlott, U., Lukacs, C., Klein, C., et al. (2004). In vivo activation of the p53 pathway by small-molecule antagonists of MDM2. *Science* 303, 844–848.
- Vassin, V. M., Anantha, R. W., Sokolova, E., Kanner, S. and Borowiec, J. A. (2009). Human RPA phosphorylation by ATR stimulates DNA synthesis and prevents ssDNA accumulation during DNA-replication stress. *J. Cell Sci.* 122, 4070–4080.
- Vidal-Eychenié, S., Décaillet, C., Basbous, J. and Constantinou, A. (2013). DNA structure-specific priming of ATR activation by DNA-PKcs. *J. Cell Biol.* 202, 421–429.
- Vidhyasagar, V., He, Y., Guo, M., Ding, H., Talwar, T., Nguyen, V., Nwosu, J., Katselis, G. and Wu, Y. (2016). C-termini are essential and distinct for nucleic acid binding of human NABP1 and NABP2. *Biochim. Biophys. Acta* 1860, 371–383.
- Vignard, J., Mirey, G. and Salles, B. (2013). Ionizing-radiation induced DNA double-strand breaks: a direct and indirect lighting up. *Radiother Oncol* 108, 362–369.
- Vizcaíno, J. A., Csordas, A., Del-Toro, N., Dianes, J. A., Griss, J., Lavidas, I., Mayer, G., Perez-Riverol, Y., Reisinger, F., Ternent, T., et al. (2016). 2016 update of the PRIDE database and its related tools. *Nucleic Acids Res.* 44, D447–56.
- Waga, S. and Stillman, B. (1998). The DNA replication fork in eukaryotic cells. *Annu. Rev. Biochem.* 67, 721–751.
- Wang, B. and Elledge, S. J. (2007). Ubc13/Rnf8 ubiquitin ligases control foci formation of the Rap80/Abraxas/Brc1/Brcc36 complex in response to DNA damage. *Proc. Natl. Acad. Sci. U. S. A.* 104, 20759–20763.

- Wang, B., Matsuoka, S., Ballif, B. A., Zhang, D., Smogorzewska, A., Gygi, S. P. and Elledge, S. J. (2007). Abraxas and RAP80 form a BRCA1 protein complex required for the DNA damage response. *Science* 316, 1194–1198.
- Wang, Gong, Z. and Chen, J. (2011). MDC1 collaborates with TopBP1 in DNA replication checkpoint control. *J. Cell Biol.* 193, 267–273.
- Ward, I. M., Wu, X. and Chen, J. (2001). Threonine 68 of Chk2 is phosphorylated at sites of DNA strand breaks. *J. Biol. Chem.* 276, 47755–47758.
- Washington, M. T., Carlson, K. D., Freudenthal, B. D. and Pryor, J. M. (2010). Variations on a theme: eukaryotic Y-family DNA polymerases. *Biochim. Biophys. Acta* 1804, 1113–1123.
- Watanabe, S., Watanabe, K., Akimov, V., Bartkova, J., Blagoev, B., Lukas, J. and Bartek, J. (2013). JMJD1C demethylates MDC1 to regulate the RNF8 and BRCA1-mediated chromatin response to DNA breaks. *Nat. Struct. Mol. Biol.* 20, 1425–1433.
- Waters, T. R., Gallinari, P., Jiricny, J. and Swann, P. F. (1999). Human thymine DNA glycosylase binds to apurinic sites in DNA but is displaced by human apurinic endonuclease 1. *J. Biol. Chem.* 274, 67–74.
- Wechsler, T., Chen, B. P. C., Harper, R., Morotomi-Yano, K., Huang, B. C. B., Meek, K., Cleaver, J. E., Chen, D. J. and Wabl, M. (2004). DNA-PKcs function regulated specifically by protein phosphatase 5. *Proc. Natl. Acad. Sci. U. S. A.* 101, 1247–1252.
- Wei, Y. F., Robins, P., Carter, K., Caldecott, K., Pappin, D. J., Yu, G. L., Wang, R. P., Shell, B. K., Nash, R. A. and Schär, P. (1995). Molecular cloning and expression of human cDNAs encoding a novel DNA ligase IV and DNA ligase III, an enzyme active in DNA repair and recombination. *Mol. Cell. Biol.* 15, 3206–3216.
- Weinstock, D. M., Richardson, C. A., Elliott, B. and Jasin, M. (2006). Modeling oncogenic translocations: distinct roles for double-strand break repair pathways in translocation formation in mammalian cells. *DNA Repair (Amst.)* 5, 1065–

1074.

- Wen, J., Cerosaletti, K., Schultz, K. J., Wright, J. A. and Concannon, P. (2012). NBN Phosphorylation regulates the accumulation of MRN and ATM at sites of DNA double-strand breaks. *Oncogene*.
- Wendorff, T. J., Schmidt, B. H., Heslop, P., Austin, C. A. and Berger, J. M. (2012). The structure of DNA-bound human topoisomerase II alpha: conformational mechanisms for coordinating inter-subunit interactions with DNA cleavage. *J. Mol. Biol.* 424, 109–124.
- Willers, H., Dahm-Daphi, J. and Powell, S. N. (2004). Repair of radiation damage to DNA. *Br. J. Cancer* 90, 1297–1301.
- Williams and David, S. S. (1998). Evidence that MutY is a monofunctional glycosylase capable of forming a covalent Schiff base intermediate with substrate DNA. *Nucleic Acids Res.* 26, 5123–5133.
- Williams, C., van den Berg, M., Sprenger, R. R. and Distel, B. (2007). A conserved cysteine is essential for Pex4p-dependent ubiquitination of the peroxisomal import receptor Pex5p. *J. Biol. Chem.* 282, 22534–22543.
- Williams, R. L. and Urbé, S. (2007). The emerging shape of the ESCRT machinery. *Nat. Rev. Mol. Cell Biol.* 8, 355–368.
- Willmore, E., de Caux, S., Sunter, N. J., Tilby, M. J., Jackson, G. H., Austin, C. A. and Durkacz, B. W. (2004). A novel DNA-dependent protein kinase inhibitor, NU7026, potentiates the cytotoxicity of topoisomerase II poisons used in the treatment of leukemia. *Blood* 103, 4659–4665.
- Wilson and Barsky, D. (2001). The major human abasic endonuclease: formation, consequences and repair of abasic lesions in DNA. *Mutat. Res.* 485, 283–307.
- Wilson, M. A., Kwon, Y., Xu, Y., Chung, W.-H., Chi, P., Niu, H., Mayle, R., Chen, X., Malkova, A., Sung, P., et al. (2013). Pif1 helicase and Pol δ promote recombination-coupled DNA synthesis via bubble migration. *Nature* 502, 393–396.

- Wu, Y., Chen, H., Lu, J., Zhang, M., Zhang, R., Duan, T., Wang, X., Huang, J. and Kang, T. (2015). Acetylation-dependent function of human single-stranded DNA binding protein 1. *Nucleic Acids Res.* gkv707.
- Xia, B., Sheng, Q., Nakanishi, K., Ohashi, A., Wu, J., Christ, N., Liu, X., Jasin, M., Couch, F. J. and Livingston, D. M. (2006). Control of BRCA2 cellular and clinical functions by a nuclear partner, PALB2. *Mol. Cell* 22, 719–729.
- Xie, Y. (2010). Structure, assembly and homeostatic regulation of the 26S proteasome. *J Mol Cell Biol* 2, 308–317.
- Xu and Leffak, M. (2010). ATRIP from TopBP1 to ATR--in vitro activation of a DNA damage checkpoint. *Proc. Natl. Acad. Sci. U. S. A.* 107, 13561–13562.
- Xu, D., Muniandy, P., Leo, E., Yin, J., Thangavel, S., Shen, X., Li, M., Agama, K., Guo, R., Fox, D. 3., et al. (2010a). Rif1 provides a new DNA-binding interface for the Bloom syndrome complex to maintain normal replication. *EMBO J.* 29, 3140–3155.
- Xu, G., Paige, J. S. and Jaffrey, S. R. (2010b). Global analysis of lysine ubiquitination by ubiquitin remnant immunoaffinity profiling. *Nat. Biotechnol.* 28, 868–873.
- Xu, P. and Peng, J. (2006). Dissecting the ubiquitin pathway by mass spectrometry. *Biochim. Biophys. Acta* 1764, 1940–1947.
- Xu, Vaithiyalingam, S., Glick, G. G., Mordes, D. A., Chazin, W. J. and Cortez, D. (2008). The basic cleft of RPA70N binds multiple checkpoint proteins, including RAD9, to regulate ATR signaling. *Mol. Cell. Biol.* 28, 7345–7353.
- Yajima, H., Lee, K.-J. and Chen, B. P. C. (2006). ATR-dependent phosphorylation of DNA-dependent protein kinase catalytic subunit in response to UV-induced replication stress. *Mol. Cell. Biol.* 26, 7520–7528.
- Yan and Michael, W. M. (2009a). TopBP1 and DNA polymerase-alpha directly recruit the 9-1-1 complex to stalled DNA replication forks. *J. Cell Biol.* 184, 793–804.

- Yan and Michael, W. M. (2009b). TopBP1 and DNA polymerase alpha-mediated recruitment of the 9-1-1 complex to stalled replication forks: Implications for a replication restart-based mechanism for ATR checkpoint activation. *Cell Cycle* 8, 2877–2884.
- Yan, H., Toczylowski, T., McCane, J., Chen, C. and Liao, S. (2011). Replication protein A promotes 5'→3' end processing during homology-dependent DNA double-strand break repair. *J. Cell Biol.* 192, 251–261.
- Yan, J., Yang, X.-P., Kim, Y.-S. and Jetten, A. M. (2008). RAP80 responds to DNA damage induced by both ionizing radiation and UV irradiation and is phosphorylated at Ser 205. *Cancer Res.* 68, 4269–4276.
- Yang, H., Jeffrey, P. D., Miller, J., Kinnucan, E., Sun, Y., Thoma, N. H., Zheng, N., Chen, P. L., Lee, W. H. and Pavletich, N. P. (2002). BRCA2 function in DNA binding and recombination from a BRCA2-DSS1-ssDNA structure. *Science* 297, 1837–1848.
- Yang, S. H., Zhou, R., Campbell, J., Chen, J., Ha, T. and Paull, T. T. (2012). The SOSS1 single-stranded DNA binding complex promotes DNA end resection in concert with Exo1. *EMBO J.*
- Yata, K., Lloyd, J., Maslen, S., Bleuyard, J.-Y., Skehel, M., Smerdon, S. J. and Esashi, F. (2012). Plk1 and CK2 act in concert to regulate Rad51 during DNA double strand break repair. *Mol. Cell* 45, 371–383.
- Yeeles, J. T. P., Poli, J., Marians, K. J. and Pasero, P. (2013). Rescuing stalled or damaged replication forks. *Cold Spring Harb Perspect Biol* 5, a012815–a012815.
- Ying, S., Chen, Z., Medhurst, A. L., Neal, J. A., Bao, Z., Mortusewicz, O., McGouran, J., Song, X., Shen, H., Hamdy, F. C., et al. (2015). DNA-PKcs and PARP1 bind to unresected stalled DNA replication forks where they recruit XRCC1 to mediate repair. *Cancer Res.* canres.0608.2015.
- Yoo, H. Y., Kumagai, A., Shevchenko, A., Shevchenko, A. and Dunphy, W. G. (2009). The Mre11-Rad50-Nbs1 complex mediates activation of TopBP1 by

- ATM. *Mol. Biol. Cell* 20, 2351–2360.
- Yoshizawa-Sugata, N. and Masai, H. (2007). Human Tim/Timeless-interacting protein, Tipin, is required for efficient progression of S phase and DNA replication checkpoint. *J. Biol. Chem.* 282, 2729–2740.
- You, Z., Chahwan, C., Bailis, J., Hunter, T. and Russell, P. (2005). ATM activation and its recruitment to damaged DNA require binding to the C terminus of Nbs1. *Mol. Cell. Biol.* 25, 5363–5379.
- You, Z., Kong, L. and Newport, J. (2002). The role of single-stranded DNA and polymerase alpha in establishing the ATR, Hus1 DNA replication checkpoint. *J. Biol. Chem.* 277, 27088–27093.
- Yusufzai, T. and Kadonaga, J. T. (2008). HARP is an ATP-driven annealing helicase. *Science* 322, 748–750.
- Yuzhakov, A., Kelman, Z., Hurwitz, J. and O'Donnell, M. (1999). Multiple competition reactions for RPA order the assembly of the DNA polymerase delta holoenzyme. *EMBO J.* 18, 6189–6199.
- Zellweger, R., Dalcher, D., Mutreja, K., Berti, M., Schmid, J. A., Herrador, R., Vindigni, A. and Lopes, M. (2015). Rad51-mediated replication fork reversal is a global response to genotoxic treatments in human cells. *J. Cell Biol.* 208, 563–579.
- Zernik-Kobak, M., Vasunia, K., Connelly, M., Anderson, C. W. and Dixon, K. (1997). Sites of UV-induced phosphorylation of the p34 subunit of replication protein A from HeLa cells. *J. Biol. Chem.* 272, 23896–23904.
- Zhang, F., Chen, Y., Li, M. and Yu, X. (2014). The oligonucleotide/oligosaccharide-binding fold motif is a poly(ADP-ribose)-binding domain that mediates DNA damage response. *Proceedings of the National Academy of Sciences* 111, 7278–7283.
- Zhang, F., Ma, T. and Yu, X. (2013). A core hSSB1-INTS complex participates in DNA damage response. *J. Cell Sci.*

- Zhang, F., Wu, J. and Yu, X. (2009). Integrator3, a partner of single-stranded DNA-binding protein 1, participates in the DNA damage response. *J. Biol. Chem.* 284, 30408–30415.
- Zhao, H. and Piwnica-Worms, H. (2001). ATR-mediated checkpoint pathways regulate phosphorylation and activation of human Chk1. *Mol. Cell. Biol.* 21, 4129–4139.
- Zhao, Y., Thomas, H. D., Batey, M. A., Cowell, I. G., Richardson, C. J., Griffin, R. J., Calvert, A. H., Newell, D. R., Smith, G. C. M. and Curtin, N. J. (2006). Preclinical evaluation of a potent novel DNA-dependent protein kinase inhibitor NU7441. *Cancer Res.* 66, 5354–5362.
- Zharkov, D. O., Rosenquist, T. A., Gerchman, S. E. and Grollman, A. P. (2000). Substrate specificity and reaction mechanism of murine 8-oxoguanine-DNA glycosylase. *J. Biol. Chem.* 275, 28607–28617.
- Zhou, Ahn, J., Wilson, S. H. and Prives, C. (2001). A role for p53 in base excision repair. *The EMBO Journal* 20, 914–923.
- Zhou, G., Mihindukulasuriya, K. A., MacCorkle-Chosnek, R. A., Van Hooser, A., Hu, M. C.-T., Brinkley, B. R. and Tan, T.-H. (2002). Protein phosphatase 4 is involved in tumor necrosis factor-alpha-induced activation of c-Jun N-terminal kinase. *J. Biol. Chem.* 277, 6391–6398.
- Zhou, Y. and Paull, T. T. (2013). DNA-dependent Protein Kinase Regulates DNA End Resection in Concert with Mre11-Rad50-Nbs1 (MRN) and Ataxia Telangiectasia-mutated (ATM). *J. Biol. Chem.* 288, 37112–37125.
- Zimmermann, M., Lottersberger, F., Buonomo, S. B., Sfeir, A. and de Lange, T. (2013). 53BP1 Regulates DSB Repair Using Rif1 to Control 5' End Resection. *Science*.
- Zou, L. (2003). Sensing DNA Damage Through ATRIP Recognition of RPA-ssDNA Complexes. *Science* 300, 1542–1548.

Appendix A

Table 6.1 Numerous hSSB1-associating proteins were identified by mass spectrometry

Proteins for which corresponding peptides were identified in section 4.2.14, as well as the number of unique peptides detected before and after hydroxyurea (HU) treatment, are listed below. Proteins are grouped based on their predominant known biological process as given by UniProt (www.uniprot.org).

Protein	Unique peptides pre HU	Unique peptides post HU	Protein	Unique peptides pre HU	Unique peptides post HU
Histones					
Core histone macro-H2A.1	14	15	Histone H3.2	5	7
Histone H2A type 2-A	6	5	Histone H4	9	10
Histone H2B type 1-B	6	0	Putative histone H2B type 2-C	0	3
Histone H2B type 1-M	0	7			
Chromatin Remodelling/Modifying					
Actin-like protein 6A	2	4	Polycomb protein SUZ12	1	1
Actin, beta	20	19	Protein AATF	0	1
Chromodomain-helicase-DNA-binding protein 4	3	4	Protein polybromo-1	2	0
Histone acetyltransferase KAT7	1	1	Protein Wiz	1	5
Histone deacetylase 1	0	10	Remodeling and spacing factor 1	1	0
Histone deacetylase 2	9	0	RuvB-like 1	5	7
Histone deacetylase complex subunit SAP18	0	2	RuvB-like 2	0	2
Histone-binding protein RBBP4	14	16	SWI/SNF complex subunit SMARCC1	3	4
Histone-lysine N-methyltransferase EHMT1	2	4	SWI/SNF-related matrix-associated actin-dependent regulator of chromatin subfamily A member 5	16	26
Histone-lysine N-methyltransferase EHMT2	1	3	SWI/SNF-related matrix-associated actin-dependent regulator of chromatin subfamily D member 1	0	1

Histone-lysine N-methyltransferase SUV39H1	0	2	SWI/SNF-related matrix-associated actin-dependent regulator of chromatin subfamily D member 2	1	3
Metastasis-associated protein MTA2	16	18	SWI/SNF-related matrix-associated actin-dependent regulator of chromatin subfamily E member 1	2	2
Methyl-CpG-binding domain protein 2	0	5	Transcription activator BRG1	3	4
Methyl-CpG-binding domain protein 3	1	3	Tyrosine-protein kinase BAZ1B	17	28
Transcription Factors, Activators and Repressors					
Activity-dependent neuroprotector homeobox protein	10	14	Parafibromin	0	2
Alpha-actinin-4	1	0	Periphilin-1	1	4
ATPase family AAA domain-containing protein 2	6	10	PHD finger protein 14	1	2
Bcl-2-associated transcription factor 1	4	4	Polymerase I and transcript release factor	2	2
Catenin delta-1	1	1	Proline-, glutamic acid- and leucine-rich protein 1	15	15
Cell division cycle 5-like protein	2	3	Protein C3orf33	1	0
Chromobox protein homolog 3	8	9	RNA-binding protein 14	2	3
Chromobox protein homolog 8	0	2	SAFB-like transcription modulator	2	0
Chromodomain Y-like protein	1	1	Scaffold attachment factor B1	12	12
Deoxynucleotidyltransferase terminal-interacting protein 2	0	2	Serrate RNA effector molecule homolog	2	5
F-box-like/WD repeat-containing protein TBLXR1	0	1	Testis-expressed sequence 10 protein	10	12
General transcription factor 3C polypeptide 2	0	1	Transcription factor ETV6	1	1
General transcription factor 3C polypeptide 3	0	1	Transcription intermediary factor 1-alpha	10	2
High mobility group protein 20A	3	2	Transcription intermediary factor 1-beta	0	16
M-phase phosphoprotein 8	2	2	Transcriptional repressor p66-beta	7	11
Nuclear receptor coactivator 5	4	4	Unconventional myosin-Ic	0	1
Paired amphipathic helix protein Sin3a	3	2	Zinc finger protein ubiquitin-binding domain 4	0	2
Transcription					

CTD small phosphatase-like protein 2	0	1	Integrator complex subunit 5	1	3
DBIRD complex subunit ZNF326	2	4	Integrator complex subunit 6	0	1
DNA-directed RNA polymerase II subunit RPB1	2	0	Regulation of nuclear pre-mRNA domain-containing protein 1B	0	2
DNA-directed RNA polymerase II subunit RPB2	5	6	Regulation of nuclear pre-mRNA domain-containing protein 2	4	3
DNA-directed RNA polymerase II subunit RPB3	3	4	RNA polymerase-associated protein CTR9 homolog	0	1
DNA-directed RNA polymerase II subunit RPB9	1	1	TATA-binding protein-associated factor 2N	0	1
DNA-directed RNA polymerases I, II, and III subunit RPABC1	1	1	Transcription elongation factor SPT6	5	0
DNA-directed RNA polymerases I, II, and III subunit RPABC3	0	2	Zinc finger CCCH domain-containing protein 14	2	2
Integrator complex subunit 1	1	0	Zinc finger CCCH domain-containing protein 18	1	1
Integrator complex subunit 3	5	12			
RNA Helicases					
ATP-dependent RNA helicase DDX18	2	2	Probable ATP-dependent RNA helicase DDX17	0	11
ATP-dependent RNA helicase DDX24	0	2	Probable ATP-dependent RNA helicase DDX5	14	0
ATP-dependent RNA helicase DDX39A	0	1	Eukaryotic initiation factor 4A-III	8	10
ATP-dependent RNA helicase DDX3X	0	5	Putative ATP-dependent RNA helicase DHX30	0	1
ATP-dependent RNA helicase DDX50	1	1	U5 small nuclear ribonucleoprotein 200 kDa helicase	5	0
Putative pre-mRNA-splicing factor ATP-dependent RNA helicase DHX15	12	8			
Pre-mRNA 3'-Processing					
Cleavage and polyadenylation specificity factor subunit 2	2	1	WD repeat-containing protein 18	3	4
Cleavage and polyadenylation specificity factor subunit 5	2	1	WD repeat-containing protein 43	1	0

Cleavage and polyadenylation specificity factor subunit 6	2	2	Pre-mRNA 3'-end-processing factor FIP1	2	1
Cleavage and polyadenylation specificity factor subunit 7	1	0	Protein virilizer homolog	4	1
Cleavage stimulation factor subunit 2	1	1	Symplekin	6	2
ELAV-like protein 1	1	0			
Pre-mRNA Splicing					
116 kDa U5 small nuclear ribonucleoprotein component	15	20	Serine/arginine-rich splicing factor 10	4	4
Apoptotic chromatin condensation inducer in the nucleus	14	9	Serine/arginine-rich splicing factor 7	5	5
Double-stranded RNA-specific adenosine deaminase	1	0	Serine/arginine-rich splicing factor 9	7	8
Heat shock cognate 71 kDa protein	12	13	Small nuclear ribonucleoprotein Sm D1	2	2
Heterogeneous nuclear ribonucleoprotein A3	5	5	Small nuclear ribonucleoprotein Sm D2	2	2
Heterogeneous nuclear ribonucleoprotein H	7	10	Small nuclear ribonucleoprotein Sm D3	0	3
Heterogeneous nuclear ribonucleoprotein H3	4	3	Small nuclear ribonucleoprotein-associated protein N	2	2
Heterogeneous nuclear ribonucleoprotein K	8	12	SNW domain-containing protein 1	4	3
Heterogeneous nuclear ribonucleoprotein L	2	4	Splicing factor 3A subunit 1	2	5
Heterogeneous nuclear ribonucleoprotein M	10	8	Splicing factor 3A subunit 3	2	4
Heterogeneous nuclear ribonucleoprotein U-like protein 1	1	0	Splicing factor 3B subunit 1	16	15
Heterogeneous nuclear ribonucleoprotein U-like protein 2	13	16	Splicing factor 3B subunit 2	7	7
Heterogeneous nuclear ribonucleoproteins C1/C2	12	10	Splicing factor 3B subunit 3	1	0
Intron-binding protein aquarius	1	0	Splicing factor 3B subunit 4	1	2
KH domain-containing, RNA-binding, signal transduction-associated protein 1	1	0	Splicing factor U2AF 65 kDa subunit	6	5
Matrin-3	14	14	Splicing factor, proline- and glutamine-rich	2	2

Non-POU domain-containing octamer-binding protein	1	2	TAR DNA-binding protein 43	0	2
Nuclease-sensitive element-binding protein 1	1	2	Thyroid hormone receptor-associated protein 3	0	2
Pre-mRNA-processing factor 6	1	0	Transformer-2 protein homolog alpha	2	3
Pre-mRNA-processing-splicing factor 8	1	0	Transformer-2 protein homolog beta	2	6
Pre-mRNA-splicing regulator WTAP	1	0	U2 snRNP-associated SURP motif-containing protein	2	2
Protein mago nashi homolog 2	4	4	U4/U6 small nuclear ribonucleoprotein Prp31	2	1
RNA-binding motif protein, X chromosome	9	8	U4/U6 small nuclear ribonucleoprotein Prp4	0	1
RNA-binding protein 12B	2	2	U4/U6.U5 tri-snRNP-associated protein 1	1	3
RNA-binding protein Raly	6	7	U5 small nuclear ribonucleoprotein 40 kDa protein	4	3
Serine/arginine-rich splicing factor 1	10	10			
Mature mRNA Export					
Ataxin-2-like protein	3	0	RNA-binding protein 8A	2	2
Caprin-1	1	1	THO complex subunit 2	0	3
Nuclear cap-binding protein subunit 1	4	2	THO complex subunit 5 homolog	1	0
Plasminogen activator inhibitor 1 RNA-binding protein	1	1	THO complex subunit 6 homolog	1	1
Translation					
Elongation factor 1-alpha 1	1	2	Eukaryotic translation initiation factor 3 subunit I	1	1
Elongation factor 1-delta	0	1	Eukaryotic translation initiation factor 3 subunit L	6	3
Elongation factor 1-gamma	1	1	Eukaryotic translation initiation factor 3 subunit M	3	2
Eukaryotic translation initiation factor 3 subunit A	11	9	Eukaryotic translation initiation factor 4B	1	2
Eukaryotic translation initiation factor 3 subunit B	1	4	Fragile X mental retardation protein 1	2	2
Eukaryotic translation initiation factor 3 subunit C-like protein	1	3	Fragile X mental retardation syndrome-related protein 1	2	2
Eukaryotic translation initiation factor 3 subunit D	0	2	La-related protein 1	4	4

Eukaryotic translation initiation factor 3 subunit E	2	5	Polyadenylate-binding protein 1	5	7
Eukaryotic translation initiation factor 3 subunit F	3	6	Polypyrimidine tract-binding protein 1	1	1
Eukaryotic translation initiation factor 3 subunit G	3	5			
Ribosomal Proteins					
28S ribosomal protein S27, mitochondrial	1	0	60S ribosomal protein L11	2	2
28S ribosomal protein S30, mitochondrial	0	1	60S ribosomal protein L12	5	5
39S ribosomal protein L38, mitochondrial	1	0	60S ribosomal protein L13	6	8
40S ribosomal protein S10	2	4	60S ribosomal protein L13a	5	5
40S ribosomal protein S11	2	6	60S ribosomal protein L14	3	4
40S ribosomal protein S12	5	4	60S ribosomal protein L15	5	5
40S ribosomal protein S13	4	4	60S ribosomal protein L17	5	5
40S ribosomal protein S14	4	4	60S ribosomal protein L18	5	4
40S ribosomal protein S15	1	4	60S ribosomal protein L18a	5	5
40S ribosomal protein S15a	2	2	60S ribosomal protein L19	3	2
40S ribosomal protein S16	5	4	60S ribosomal protein L21	1	2
40S ribosomal protein S17	6	5	60S ribosomal protein L22	3	2
40S ribosomal protein S18	8	7	60S ribosomal protein L23	1	1
40S ribosomal protein S19	4	5	60S ribosomal protein L23a	3	3
40S ribosomal protein S2	10	11	60S ribosomal protein L24	3	3
40S ribosomal protein S20	1	2	60S ribosomal protein L26	2	2
40S ribosomal protein S21	1	2	60S ribosomal protein L27	3	4
40S ribosomal protein S23	1	1	60S ribosomal protein L27a	4	4
40S ribosomal protein S24	3	3	60S ribosomal protein L28	2	2
40S ribosomal protein S25	3	4	60S ribosomal protein L29	1	2
40S ribosomal protein S26	3	4	60S ribosomal protein L3	11	14
40S ribosomal protein S27-like	1	2	60S ribosomal protein L30	3	5
40S ribosomal protein S28	2	2	60S ribosomal protein L31	1	1

40S ribosomal protein S29	0	1	60S ribosomal protein L32	1	4
40S ribosomal protein S3	13	14	60S ribosomal protein L34	2	2
40S ribosomal protein S3a	6	7	60S ribosomal protein L35	1	3
40S ribosomal protein S4, X isoform	10	12	60S ribosomal protein L35a	2	1
40S ribosomal protein S5	2	4	60S ribosomal protein L36	2	3
40S ribosomal protein S6	5	4	60S ribosomal protein L36a-like	1	1
40S ribosomal protein S7	7	8	60S ribosomal protein L37a	1	0
40S ribosomal protein S8	7	7	60S ribosomal protein L38	0	1
40S ribosomal protein S9	7	10	60S ribosomal protein L4	14	17
40S ribosomal protein SA	13	14	60S ribosomal protein L5	7	7
60S acidic ribosomal protein P0	13	13	60S ribosomal protein L6	9	10
60S acidic ribosomal protein P1	2	2	60S ribosomal protein L7	12	13
60S acidic ribosomal protein P2	4	5	60S ribosomal protein L7a	7	9
60S ribosomal protein L10	6	5	60S ribosomal protein L8	6	8
60S ribosomal protein L10a	5	4	60S ribosomal protein L9	3	4
Ribosome Biogenesis					
Bystin	1	1	Ribosomal biogenesis protein LAS1L	2	6
Nucleolar complex protein 2 homolog	2	1	Ribosomal L1 domain-containing protein 1	6	9
Nucleolar complex protein 4 homolog	0	1	Ribosomal RNA-processing protein 7 homolog A	0	1
Nucleolar GTP-binding protein 1	4	5	Ribosome biogenesis protein BRX1 homolog	9	8
Nucleolar GTP-binding protein 2	2	1	Ribosome biogenesis regulatory protein homolog	1	1
Nucleolar protein 58	1	1	Ribosome production factor 2 homolog	0	1
Nucleolar protein 6	2	5	rRNA 2'-O-methyltransferase fibrillarin	1	2
Nucleophosmin	4	6	Sentrin-specific protease 3	1	0
Polynucleotide 5'-hydroxyl-kinase NOL9	3	4	Superkiller viralicidic activity 2-like 2	3	4
Probable 28S rRNA (cytosine(4447)-C(5))-methyltransferase	0	1	U3 small nucleolar ribonucleoprotein protein MPP10	0	1
Probable rRNA-processing protein EBP2	7	9			

Cell Cycle and DNA Repair					
Cullin-4A	6	5	Serine/threonine-protein phosphatase 2A 65 kDa regulatory subunit A beta isoform	0	1
DNA damage-binding protein 1	4	4	Serine/threonine-protein phosphatase PP1-beta catalytic subunit	2	5
DNA replication licensing factor MCM6	1	0	Cyclin-dependent kinase inhibitor 2A, isoform 4	2	1
DNA replication licensing factor MCM7	1	1	Tyrosine-protein kinase Yes	1	0
DNA topoisomerase 2-alpha	14	16	Enhancer of rudimentary homolog	2	3
E3 ubiquitin-protein ligase RING1	1	2	NEDD8	2	2
Serine/threonine-protein kinase mTOR	1	1	Transitional endoplasmic reticulum ATPase	3	0
Centromere Proteins and Regulation					
Aurora kinase B	2	3	Kinesin-like protein KIF23	1	1
Borealin	2	5	Major centromere autoantigen B	0	1
Centromere protein V	1	2	MAU2 chromatid cohesion factor homolog	3	4
Condensin-2 complex subunit G2	0	2	Microfibrillar-associated protein 1	0	1
Emerin	2	3	Mitotic interactor and substrate of PLK1	1	1
Inner centromere protein	0	3	Structural maintenance of chromosomes protein 1A	1	0
Kinesin-like protein KIF20A	0	3	Ubiquitin carboxyl-terminal hydrolase 10	0	1
Nuclear Structure and Scaffolding Proteins					

A-kinase anchor protein 8	1	1	Lamin-B1	1	0
Actin-related protein 3	0	1	LIM domain and actin-binding protein 1	1	0
Barrier-to-autointegration factor	2	2	Nuclear mitotic apparatus protein 1	1	0
Flotillin-1	4	0	Prelamin-A/C	8	7
Flotillin-2	2	2	Vimentin	1	4
Miscellaneous					
1-phosphatidylinositol 4,5-bisphosphate phosphodiesterase eta-2	0	1	Importin subunit alpha-3	2	6
4F2 cell-surface antigen heavy chain	3	3	Junction plakoglobin	1	2
60 kDa heat shock protein, mitochondrial	1	2	Kelch repeat and BTB domain-containing protein 3	0	0
Alkaline phosphatase, tissue-nonspecific isozyme	2	0	Kelch-like protein 35	1	1
Annexin A2	6	9	Keratin, type I cytoskeletal 10	10	1
ATP synthase subunit alpha, mitochondrial	2	1	Keratin, type I cytoskeletal 9	5	14
ATP synthase subunit beta, mitochondrial	1	2	Keratin, type II cytoskeletal 1	13	9
ATP-binding cassette sub-family E member 1	1	1	Keratin, type II cytoskeletal 7	1	16
BAG family molecular chaperone regulator 2	1	1	Latrophilin-3	0	1
Bone marrow stromal antigen 2	0	1	Microsomal glutathione S-transferase 1	0	1
Brain acid soluble protein 1	3	5	Mitochondrial carrier homolog 2	1	2
Cadherin-13	0	1	Myb-binding protein 1A	3	1

Calcium homeostasis endoplasmic reticulum protein	0	2	Myosin light polypeptide 6	0	2
Caveolin-1	2	2	Myosin-9	4	0
CD109 antigen	4	4	Nebulin	1	0
CD44 antigen	2	2	Peroxiredoxin-1	1	0
CD59 glycoprotein	2	4	Peroxiredoxin-2	1	3
Coiled-coil domain-containing protein 25	1	0	PH-interacting protein	1	1
Complement component 1 Q subcomponent-binding protein, mitochondrial	2	4	Protein FAM208A	5	4
Complement decay-accelerating factor	3	3	Protein Hook homolog 3	0	1
CSC1-like protein 2	0	1	Protein kinase C and casein kinase substrate in neurons protein 3	1	1
Desmoglein-2	3	1	Protein Red	1	0
Dihydrolipoyllysine-residue succinyltransferase component of 2-oxoglutarate dehydrogenase complex, mitochondrial	2	1	PWWP domain-containing protein MUMIL1	1	1
DnaJ homolog subfamily A member 1	0	3	Ras GTPase-activating protein-binding protein 2	2	3
Dolichyl-diphosphooligosaccharide--protein glycosyltransferase 48 kDa subunit	2	1	Regulator of microtubule dynamics protein 3	0	1
Drebrin	2	5	Solute carrier family 12 member 2	1	1
Dynein light chain 1, cytoplasmic	0	2	Stomatin-like protein 2, mitochondrial	2	1
Erlin-1	1	0	SUN domain-containing protein 2	1	0

Erythrocyte band 7 integral membrane protein	5	0	Thy-1 membrane glycoprotein	1	0
Erythrocyte band 7 integral membrane protein	0	6	Titin	1	0
Glioma tumor suppressor candidate region gene 2 protein	1	1	tRNA-splicing ligase RtcB homolog	1	1
Glyceraldehyde-3-phosphate dehydrogenase	1	4	Tubulin alpha-1B chain	1	2
Glypican-1	1	0	Ubiquitin-associated protein 2-like	0	1
GRAM domain-containing protein 1B	0	1	V-type proton ATPase subunit d 1	1	0
Guanine nucleotide-binding protein G(i) subunit alpha-2	6	6	V-type proton ATPase subunit E 1	1	0
Guanine nucleotide-binding protein G(I)/G(S)/G(T) subunit beta-1	3	4	Very-long-chain enoyl-CoA reductase	0	1
Guanine nucleotide-binding protein subunit beta-2-like 1	0	15	Vesicle-associated membrane protein-associated protein B/C	1	0
Guanine nucleotide-binding protein-like 3	2	1	Voltage-dependent anion-selective channel protein 1	2	3
Importin subunit alpha-1	2	4	Voltage-dependent anion-selective channel protein 2	2	4